Development of Control techniques for Direct AC-AC Matrix Converter fed Multi-phase Multi-motor Drive System

Mohammed Ahmed Saleh

Electrical & Electronics Engineering
College of Engineering & Science
Victoria University, Melbourne, Australia

Submitted in fulfilment of the requirements of the degree of PhD

September 2013

ABSTRACT

There are numerous industrial applications, such as paper mills, locomotive traction, oil and gas, mining and machine tools, which require high performance control of more than one electric motor simultaneously. When more than one electric motors are employed in an electric drive, it is called, 'multi-motor drive'. These multi-motor drives are generally available in two configurations. The first one consists of a number of three-phase voltage source inverters connected in parallel to a common DC link, each inverter feeding a three-phase AC motor. This configuration allows independent control of all machines by means of their own three-phase voltage source inverters (VSIs). Nevertheless, this configuration needs *n* number of voltage source inverters for supplying *n* number of AC machines. The second configuration comprises one inverter, which feeds multiple parallel-connected three-phase motors. However, the later configuration does not allow independent control of each motor and is suitable only for traction application. The power converter supplying the drive system, are conventionally, voltage source inverters. However, alternative solution could be a direct AC-AC converter that can supply the electric drive system. Exploring this alternative solution is the subject of this thesis.

Thus for decoupled dynamic control of AC machines working in a group (multi-motor drive) is possible by employing multi-phase (more than three-phase) motors, where their stator windings are connected in either series or in parallel and the combination is supplied from a single multi-phase power converter.

This thesis explores the control techniques of multi-phase direct AC-AC converter for such specific series and parallel-connected multi-phase motor drives. The research presented here utilises additional degrees of freedom available in a multi-phase system to control a number of machines independently. The concept is based on the fact that independent flux and torque control of any AC machine, regardless of the number of stator phases requires control of only two stator current components. This leaves the remaining current components free to control other machines within the group.

The multi-phase multi-motor drive system fed using multi-phase direct AC-AC converter need precise Pulse Width Modulation (PWM) technique to independently control the drive system. The subject of this research is to propose PWM techniques for such configurations. The thesis focuses on four different cases; five-phase, six-phase (symmetrical and asymmetrical), and seven-phase system. Five-phase and six-phase drive systems consists of two motors, and seven-phase drive system controls three motors. The thesis presents various PWM techniques aimed at these drive configuration. Carrier-based, carrier-based with harmonic injection and direct duty ratio based PWM techniques are presented in the thesis. The independence of control of various motors are shown by simulation and experimentation. Although, the proposed techniques are equally applicable to series-connected drives and parallel-connected drives, the thesis focuses on the former drive configuration. Analytical, simulation and experimental approach is used throughout the thesis.

Declaration

"I, Mohammed Ahmed Saleh, declare that the PhD thesis entitled "*Development of Control techniques for Direct AC-AC Matrix Converter fed Multi-phase Multi-motor Drive System*" is no more than 100,000 words in length including quotes and exclusive of tables, figures, appendices, bibliography, references and footnotes. This thesis contains no material that has been submitted previously, in whole or in part, for the award of any other academic degree or diploma. Except where otherwise indicated, this thesis is my own work".

Signature **Date**

ACKNOWLEDGEMENT

The research work presented in this thesis has been carried out under the invaluable and expert guidance of Professor Akhtar Kalam, Dr. Atif Iqbal and Prof. Haitham Abu-Rub. I consider it a privilege to have been associated with them for carrying out the research work towards my PhD degree. I have greatly benefited from their deep insight into the subject and constant support during numerous fruitful discussions. It is with a deep sense of my affection and gratitude that I wish to express my sincere thanks to them.

It is my duty to thanks the Head of the Departments, Department of Electrical Engineering, Qatar University and Department of Electrical & Computer Engineering, Texas A&M University at Qatar for their help in completing the experimental work at their laboratory.

My sincere thanks are due to Mr. SK. Moin Ahmed, Research Associate, Department of Electrical & Computer Engineering, Texas A&M University at Qatar, Qatar, for his endless support in commissioning the experimental set up used in this work.

I must also acknowledge here the fruitful discussions that I had time and again with my colleagues, Mr. Moidu Thavot, Mr. Khaleequr Rahman and Mr. Ahmad Anad of Qatar University, Doha, Qatar.

I also sincerely thanks Qatar Foundation for providing fund for the research work through the NPRP 4-152-02-053.

I would like to thank my parents, my wife's parents and my relatives for their moral support for pursuing this work. Without their constant assurances and assistance, completion of this project would have not been possible.

Finally, the patience, understanding and co-operation provided throughout the work by my wife Mona and children Abdullah, Reema and Nour, who had to bear the constraints of my long working hours during the last three years, are greatly appreciated.

List of Publications

1. Iqbal, A., Payami, S., **Saleh. M.**, Ahmad, A.A., Moinuddin, S., (2013), "Five-phase AC/DC/AC converter with PWM rectifier", *Australian journal of Electrical & Electronics Engineering (Accepted).*
2. **Saleh, M,**Iqbal, A., Ahmed, Sk. M., Abu-Rub. H., Kalam, A., (2013) "Direct Duty ratio based PWM control of a five-phase Matrix Converter supplying five-phase two-motor drive system", *Australian Journal of Electrical & Electronics Engg.,* vol. 9, issue 3, pp. 283-293, Feb. 2013
3. Ahmed, SK.M., Iqbal, A**.,** Abu-Rub, H., Rodriguez, J., **Saleh, M.**, (2011), "Simple carrier-based PWM technique for a three to nine-phase Matrix Converter", *IEEE Trans. On Ind. Elect.,* vol. 58, no. 11, pp. 5014-5023, Nov. 2011.
4. Iqbal, A., **Saleh, M.,** Ahmed, Sk. M., Abu-Rub. H., Kalam, A., (2013) "Simple carrier-based PWM technique for a three to quasi six-phase Matrix Converter", *Australian Journal of Electrical & Electronics Engg.,* vol. 9, issue 3, pp. 295-304, Feb. 2013.
5. Ahmed, M. SK, Iqbal A., Abu-Rub, H., **Saleh, M.**, Kalam. A., (2013), "Vector Control of a Five-phase induction motor supplied by a Non-square 3X5 phase Matrix Converter", *Australian Journal of Electrical Engineering,* vol. 10, no. 1, March 2013, pp. 55-63.
6. **Saleh, M.**, Iqbal, A., Thavot, M., Kalam, A., (2013), "Modeling of seven-phase series-connected three-motor drive system", *7th IEEE GCC COnf.,* Doha, Qatar, Nov. 2013 (review).
7. **Saleh, M.**, Khan, M.A., Iqbal, A., Moin, SK., Kalam, A., (2013) "Three to seven phase Matrix Converter supplied seven-phase three-motor drive", *Journal of Innovation in Electronics and Communication,* vol. 2, Issue 3, pp. 6-13. July-Dec. 2013.
8. Ahmad, R., Iqbal, A., **Saleh, M.,** Kalam, A. (2013), "Performance Analysis of Soft Starter Based Control of Five-phase Induction Motor", *2013 IEEE PES General Meeting, 21 - 25 July 2013, Vancouver, BC, Canada.* CD-ROM paper.
9. Islam, S., Bakhs, Ilahi, Iqbal, A., **Saleh, M.**, Kalam, A. (2013), "Stability Analysis of a Series-Connected Five-phase Induction Motor Drive System using Flux-linkage model" Paper 4604, 8th IEEE Int. conf. on Industrail electronics and applications, 19-21 June, 2013, Melbourne, Australia, CD-ROM paper.
10. Iqbal, A., Pyami, S., **Saleh, M.**, Anad, A., Kalam, A., (2012), "Analysis of Five-phase AC/DC/AC active front end converter", *Australian Universities Power Engineering Conf (AUPEC),* 26-29 Sept., Bali, Indonesia, CD-ROM paper.
11. **Saleh, M.,**Iqbal, A., Moin, SK., Kalam, A., (2012), "Matrix Converter based Five-phase series-connected induction motor drive", *Australian Universities Power Engineering Conf (AUPEC),* 26-29 Sept., Bali, Indonesia CD-ROM paper.
12. **Saleh. M.,** Iqbal, A., Ahmed, SK.M, Abu-Rub, H., Akhtar, K., (2011), "Carrier-based PWM technique for a three to six phase Matrix Converter supplying six-phase two-motor drives", *IEEE IECON,* 7-10 Nov, Melbourne, Australia pp. 3347-3352.

Table of Contents

LIST OF FIGURES

LIST OF TABLES

LIST OF ABBREVIATIONS

VSI	Voltage Source Inverter
CSI	Current Source Inverter
PWM	Pulse Width Modulation
MC	Matrix Converter
DDPWM	Direct Duty Ratio Pulse Width Modulation
DC	Direct current
AC	Alternating Current
THD	Total Harmonic Distortion
DSP	Digital Signal Processors
FPGA	Field Programmable Gate Arrays
PC	Personal Computer
HVDC	High Voltage DC
FFT	Fast Fourier Transform
RMS	Root Mean Square
IGBT	Insulated Gate Bi-polar Transistor
LC	Inductor Capacitor
WTHD	Weighted Total Harmonic Distortion
DMC	Direct Matrix Converter
Mmf	Magneto motive force

LIST OF SYMBOLS

V	Voltage	Volt (V)
I	Current	Ampere (A)
R	Resistance	Ohms (Ω)
α_0	Output current space vector	-
β_0	Output voltage space vector	-
α_i	Input current space vector	-
β_i	Input voltage space vector	-
ω	Angular Velocity	rad/sec
L_{aa}	Self Inductance between phase a and a	Henry (H)
L_{ab}	Self Inductance between phase a and b	Henry (H)
M	Mutual inductance	Henry (H)
T_e	Electromagnetic torque	Newton-meter (Nm)

Chapter 1
Introduction

1.1 Preliminary Remark

Variable speed motor drive system is required in numerous industrial applications as they offer significant advantages compared to a fixed speed drive system. The major advantages include higher efficiency, better power factor, reduced thermal loading and thus reduced overall operational costs. Three-phase motor drives are traditionally used in industrial drives due to readily available three-phase supply and off-the-shelf motor availability. Power electronic converters are used as interface between three-phase grid supply and the driving motor. The power converter has no limitation in number of legs being used and thus there is no restriction in the number of phases of the converters. With the advancement in power semiconductor technology this additional degree of freedom in power electronic converter is now exploited by developing multi-phase supply options. Hence multi-phase (more than three-phase) electric drives have attracted much attention in recent years due to some inherent advantages that they offer compared to their three-phase counterpart such as lower motor torque pulsation, less DC link current harmonics, higher redundancy and hence better fault tolerant characteristics and lower per phase converter ratings etc. The major applications of multi-phase drives are assumed in safety critical applications such as ship propulsion, ‘more electric aircraft’ applications, electric and hybrid-electric vehicles, traction, mining, oil & gas and in general purpose applications in high power range as presented in reference [1.1] - [1.4].

A block diagram of a variable frequency drive system is shown in Fig. 1.1 The major components of a variable drive system are: power source (grid supply), power converter for power processing, controller that can be digital signal processor/micro-controller/field programmable gate arrays, electric motor, sensors (voltage, current and speed) for feedback signals. The controller can be programmed using PC.

The power supply to a variable speed drive system is obtained from power electronic converter that is capable of providing variable voltage and variable frequency. There are four types of power electronic converters:

i) AC/DC/AC converter with diode based rectifier,

ii) AC/DC/AC converter with PWM rectifier also called back-to-back converter,

iii) AC/AC converter called cyclo converter, and

iv) AC/AC converter called Matrix Converter.

This thesis developed control techniques for direct AC/AC converter, i.e. a Matrix Converter.

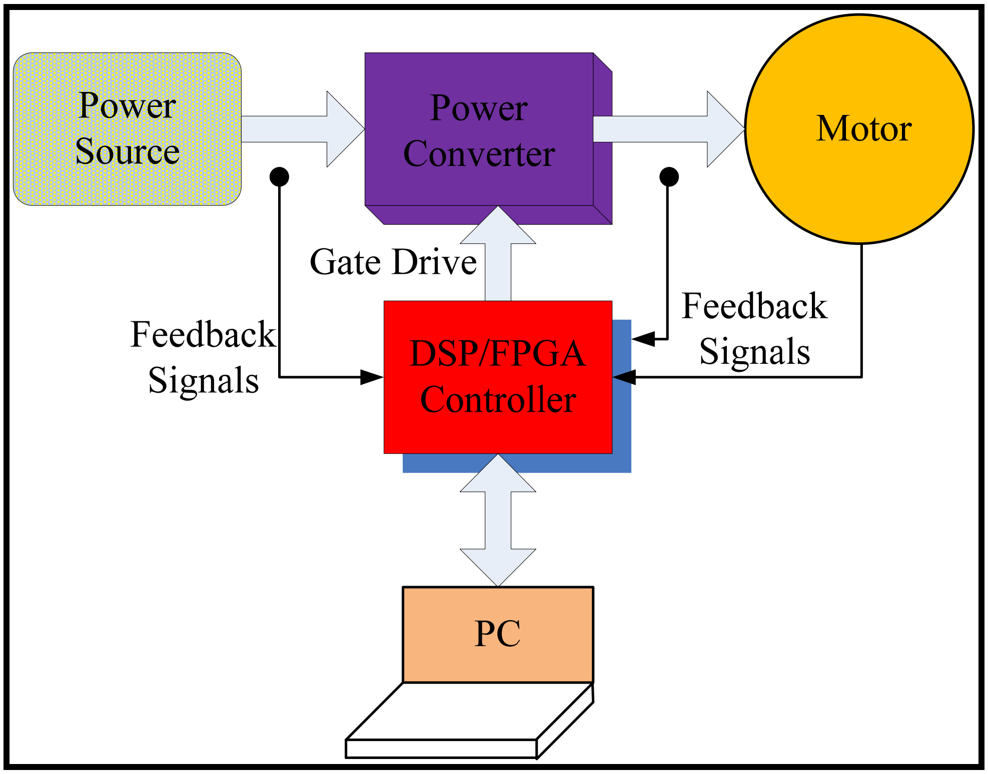

Fig. 1.1 General block diagram of a variable speed drive

1.2 Power Electronic Converters

The power electronic converter is the heart of a variable speed drive system. It is used to process the electrical power of utility grid and supply to the electric motor. This will act as an interface between the utility grids and the electric motor. Huge research effort is put to develop technically feasible and commercially viable power electronic converters. The rapid growth in the semiconductor material and switching devices has led to significant improvement in the power converters and also has helped in developing their several variants. Mainly classified, the power electronic converters used in variable speed drive applications are as presented in reference [1.5];

i) AC Voltage Regulator

ii) Cyclo converters

iii) AC-DC-AC converter with diode based rectifier called an inverter

iv) AC-DC-AC converter with active rectifier or PWM rectifier called back-to-back converter

v) AC-AC converter called Matrix Converter.

AC voltage regulators have limited use since they can only vary the voltage while the output side frequency is same as the input side frequency. The power semiconductor switching device used should have bi-directional power flow characteristics. Bi-directional switching can be obtained by connecting anti-parallel BJTs, or MOSFETs, or IGBTs. In some applications Triacs and Thyristor based voltage regulators are also used. Other ways of obtaining bi-directional power flow is shown in Fig. 1.2. This is further elaborated in Chapter 3. The output voltage in AC voltage regulator varies from 0 to input voltage magnitude. Hence the maximum voltage transfer ratio is 1.

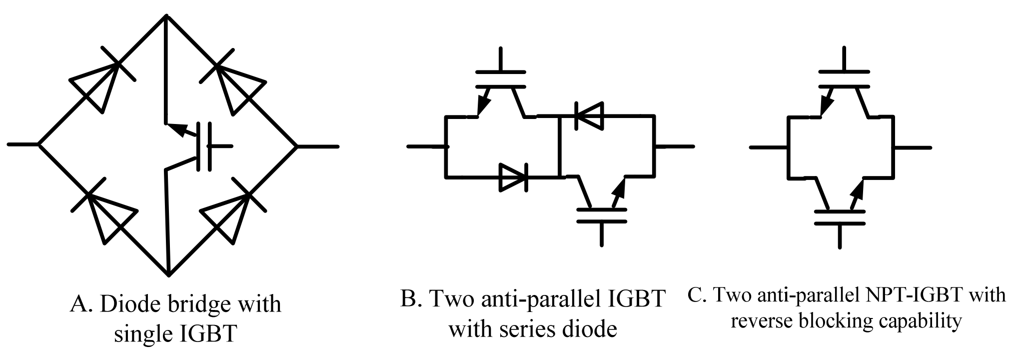

Fig. 1.2. Possible discrete implementations of a bi-directional switch.

Cyclo converter is fully controlled direct AC-AC conversion. Both output voltage magnitude and frequency are controllable. The maximum output voltage magnitude is same as input voltage magnitude while the output frequency is limited to 33% of the input frequency. Hence the application of cyclo converter is also limited but they are used where small speed control range is needed and is mostly used in high power drive system.

AC-DC-AC converter with diode based rectifier is most commonly employed in variable speed drive system because of its simplicity and low cost. Several types of diode based rectifiers are in practice but mostly three-phase bridge type rectifiers are the most common. The output of rectifier contains ripple that can be minimized by using a filter. The output of a rectifier is used to feed inverter system through DC link capacitor. Large values of DC link capacitors are usually used to offer constant voltage to the inverter. Rectifiers are uncontrolled but the inverter is controlled using different types of pulse width modulation.

AC-DC-AC converter with controlled rectifier or active rectifier called back-to-back converter is also employed where bi-directional power flow is required. The rectifier is controllable and the power factor can be controlled and can be even made unity. The source side current is sinusoidal. In case of regeneration of drive system, power can flow back to the utility grid and this is only possible when active rectifier is used. The output voltage magnitude is limited by the amount of DC link voltage and the type of PWM method employed.

Direct AC-AC converter system mostly called Matrix Converter consist of arrays of bi-directional power semiconductor switches (bi-directional switches are shown in Fig. 1.2). Three-phase utility grid system is connected to the output through the matrix arrays. Each leg has three bi-directional switches and any output can be connected to any input line through the switching action of bi-directional power switches. The voltage of input side appears at the output side and the current in any phase of the load can be drawn from any phase of the utility grid. A small LC filter is connected at the source side to remove the current ripple (Which appears due to switching action). Matrix Converter has the following major advantages:

- Sinusoidal input and output currents
- Controllable input side power factor
- No bulky DC link capacitor is needed
- Bi-directional power flow.

The major disadvantage with the Matrix Converter is the low output voltage, in case of three-phase configuration the output is 15% less than the input side. In case of five-phase output the output is almost 20% lower than the input side. Higher the output number of phases, lower the output voltage magnitude. To enhance the output voltage, over-modulation is required and also AC chopper can be used in conjunction with the Matrix Converter. Additional shortcoming of a Matrix Converter is its complex control.

1.3 Features of Multi-phase Motor Drive

An obvious question arises, why the thesis topic is chosen on multi-phase motor drive when three-phase drive is being successfully used in industries for decades? The simple answer lies in the inherent advantages that a multi-phase drive offers compared to their three-phase counterpart. Some of the known advantages of multi-phase motor drives are given in reference [1.1]:

a. Reducing the amplitude of torque pulsation and increasing the frequency of torque pulsation in inverter fed multi-phase drive system when inverter is operating in square wave mode. The frequency of torque pulsation is 2n*fundamental frequency, where n is the number of phases. Thus for instance in a five-phase machine the torque pulsation occurs at 10 times the fundamental frequency while in three-phase case it is 6 times the fundamental.

b. .Higher efficiency compared to the three-phase counterpart. This is attributed to the fact that the stator excitation produces a field with lower space harmonic in case of multi-phase machine when compared to three-phase machines.

c. Higher torque density in multi-phase machines compared to the three-phase machines. The reason behind this is that apart from fundamental, higher current harmonic contribute towards the torque development in concentrated winding machines. For instance in case of a five-phase machine, third harmonic along with the fundamental may be injected to enhance the torque production and similarly in case of a seven-phase machine, 3rd and 5th harmonics may be utilised. Thus in general harmonics lower than the phase number may be utilised effectively to enhance the torque production. This is a special characteristic of multi-phase machines and is not available in a three-phase machine.

d. Greater fault tolerance than their three-phase counterpart and offers more reliable solution. If one phase of a three-phase opens, the machine may continue to run but it requires special arrangement for starting (i.e. a divided DC bus with a neutral point) and the machine has to be heavily de-rated to avoid excessive heating. In contrast in case of five-phase machine, the machine will start, accelerated, reject load transient and continue to run normally with minimal de-rating even with a loss of one phase. In case of a seven-phase machine unnoticeable change occurs even with a loss of up to two phases. This trend continues with higher phase number. Thus multi-phase machine drive is suited ideally for safety critical applications such as ship propulsion, air craft applications & defence and emergency services applications.

e. Less volume to weight ratio

f. Better noise and vibration characteristics

g. Lower DC link current harmonics

h. Reducing rotor current harmonics

i. Reducing current per-phase without increasing voltage per-phase. This reduction in power per-phase translates into the reduction in the rating per converter leg. Thus the series/parallel combination of power semiconductor switches may be avoided and consequently avoiding the associated static and dynamic voltage sharing problems. This is one of the driving forces behind the accelerated use of multi-phase machines in high power drive applications.

1.4 Analyzed Drive Topologies

In this thesis, multi-phase multi-motor drive system is analyzed. The focus of the research is on the development of control schemes for multi-phase Matrix Converter feeding multi-phase multi-motor drive system. When referring to multi-motor drive system, means more than one machine are controlled simultaneously either independently or under identical operational conditions. In three-phase multi-motor drive system, two topologies are possible:

i) X number of three-phase motors with independent vector control, which is fed using X number of three-phase inverters with 3X legs. Motor/inverter sets connected in parallel, with common DC link. This configuration is shown in Fig. 1.3a.

ii) X number of three-phase motors which is fed using one three-phase inverter. In this structure motors have to be identical and to operate under the same load torque with the same angular speed. This is shown in Fig. 1.3b.

Both these drive topologies do not offer independent control of connected three-phase motors.

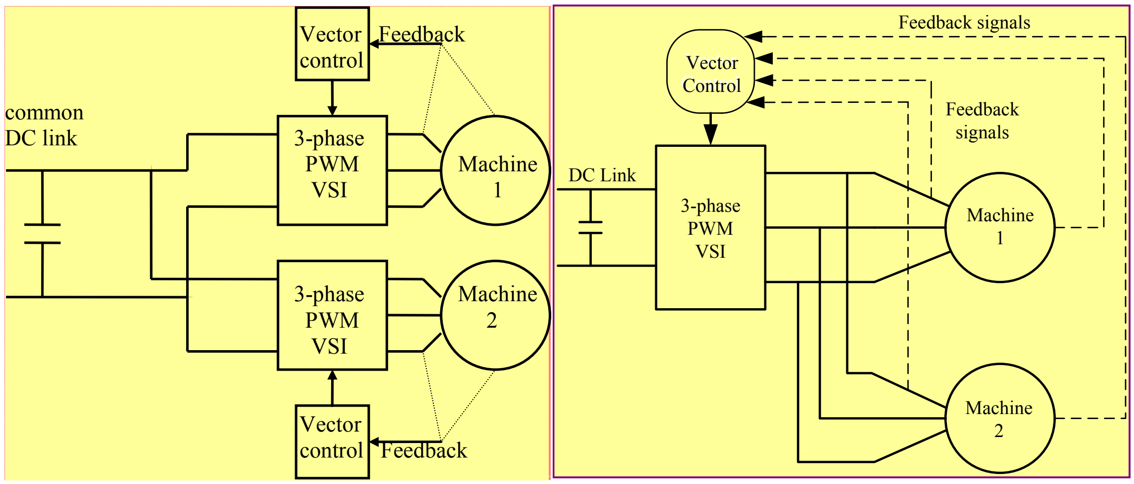

a b

Fig. 1.3. Three-phase multi-motor drive system.

Multi-phase drive system can however, offer independent control of more than one machine when supplied from a single variable voltage and variable frequency power source and field oriented control is employed as shown in reference [1.6].

This is a generalized concept where multi-phase machine's stator can be either connected in series or in parallel while supply is given from only one power source and all the machines can be controlled independently both in transient and steady state conditions. The topologies investigated in this thesis are:

- Five-phase series-connected two-motor drive system
- Six-phase series-connected two-motor drive system
- Seven-phase series-connected three-motor drive system.

It is important to mention here that the main purpose of the thesis is to develop pulse width modulation techniques for three-phase input and multi-phase (5-phase, 6-phase, 7-phase) output to produce appropriate fundamental frequencies. Further to note, that the developed PWM are equally applicable to series-connected drive and parallel-connected drive systems. Series-connected or parallel-connected refers to stator winding connection and rotors are independent.

It is evident from the dynamic model of multi-phase machine in given reference [1.7], that only two orthogonal current components namely d-q is responsible for torque production and rest of the components do not contribute to the torque production rather they are loss producing and they are limited only by leakage inductances. This finding is important as the field oriented control principle of a three-phase machine can be extended very easily to the multi-phase machine as shown in reference [1.6]. The extra non-torque current components are further utilized recently to control other machine in series/parallel-connected multi-motor drive system presented in references [1.8] - [1.12]. This is a general concept where *n* number of multi-phase machine's stator windings can be connected either in series or parallel and the supply is given from a single multi-phase voltage source inverter and all the machines in the group can be controlled independently using field oriented control principle. The number of connectable machines depends upon the phase number and if the phase number is even or odd for instance in a five-phase and six-phase system two machines can be connected, in seven and eight-phase system three machines can be connected and controlled independently. The specific case of five-phase system is presented in reference [1.10-1.11], six-phase system is presented in reference [1.8-1.9] and seven-phase system is presented in reference [1.12]. The basic principle of control lies in the fact that the d-q component (torque producing) one machine becomes the x-y (non-torque producing) component of the other and vice versa. This is possible by appropriate phase transposition in the connection of the two or more stator windings. The major advantage of such concept is reduction in the number of power converters used, e.g. in case of a five-phase machine, instead of using two separate converters just one converter is sufficient. The major disadvantage of this concept is increase in the losses because current of all machines is carried by all the stator winding of the machines. This is worst in case of five- and seven-phase systems but it is marginally better in case of a six-phase system where a six-phase machine and three-phase is connected in series. The six-phase machine's stator current cancels out at the point of interconnection of three-phase machine. Thus the losses of six-phase machine will increase marginally if small three-phase motors are used and three-phase motor's losses will not alter. The application of a five-phase two-motor drive system is identified in a winder drive where the winding and unwinding machines can be the two series-connected machines. In this special application, situation never arises when both the machines are loaded to rated condition. When load on one machine increases, the load on the other machine decreases. The application of six-phase two-motor drive system is identified in a situation where six-phase machine can be used as main driving motor such as in ship propulsion and three-phase machine can be used for auxiliary function such as for pumping. The basic structure of five-phase series-connected two motor drives, six-phase series-connected two motor drives and seven-phase three-motor drive are shown in Fig. 1.4. These three drive system topologies are used in the present thesis for developing their control using direct AC-AC multi-phase Matrix Converter.

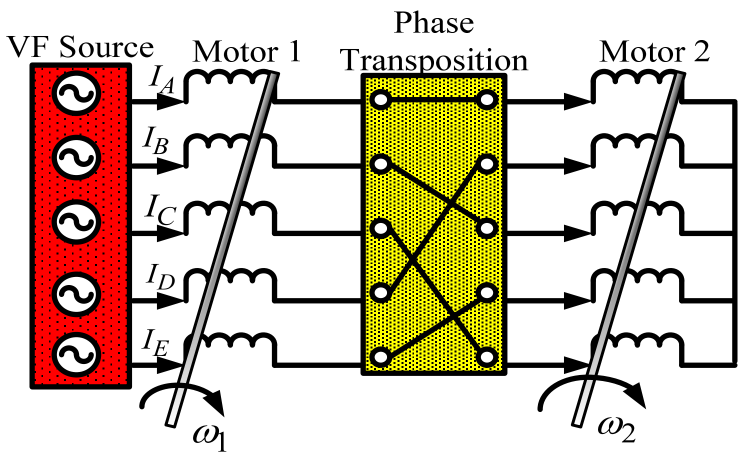

Fig. 1.4a. Five-phase series-connected two-motor drive structure.

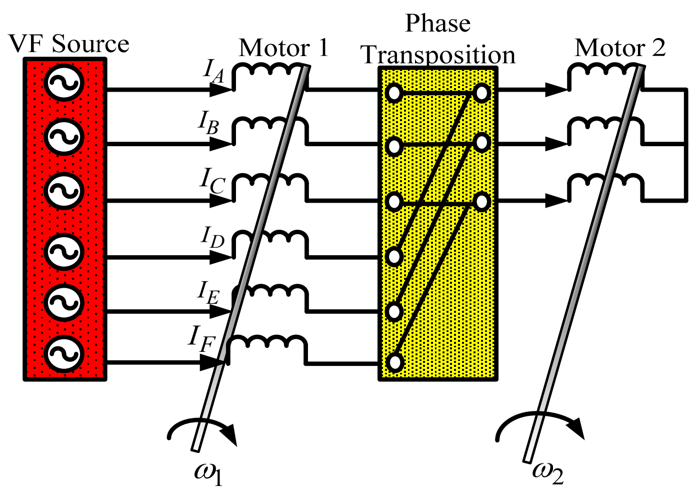

Fig. 1.4b. Six-phase series-connected two-motor drive system.

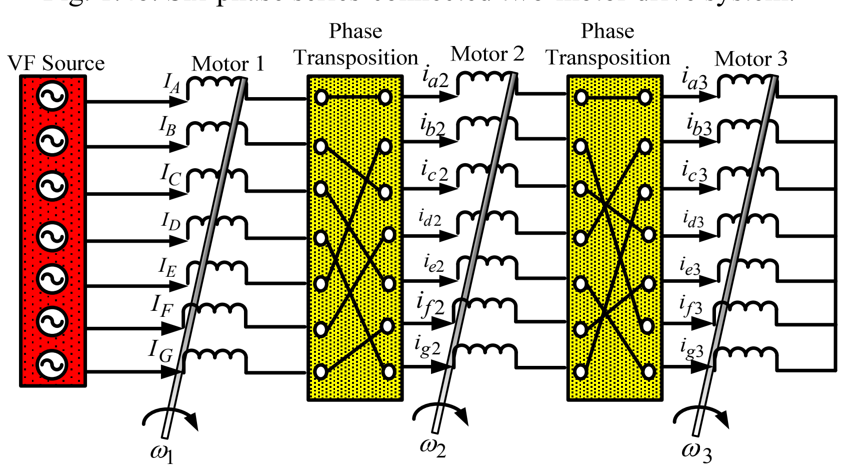

Fig. 1.4c. Seven-phase series-connected three-motor drive system.

Since the thesis explores the Pulse Width Modulation (PWM) of AC-AC Matrix Converter for controlling multi-phase multi-motor drive system, it is important to present state-of-the-art in the PWM techniques of such converter. A review on the state-of-the-art in the Matrix Converter is presented in references [1.13] - [1.16]. Power circuit of a general three-phase to *n*-phase Matrix Converter is shown in Fig. 1.5. The determination of appropriate PWM method for complex Matrix Converter topology especially for multi-phase output is a key issue. The restriction imposed on the PWM strategies are: the input phases must not be short circuited and the output phase should not be open circuited.

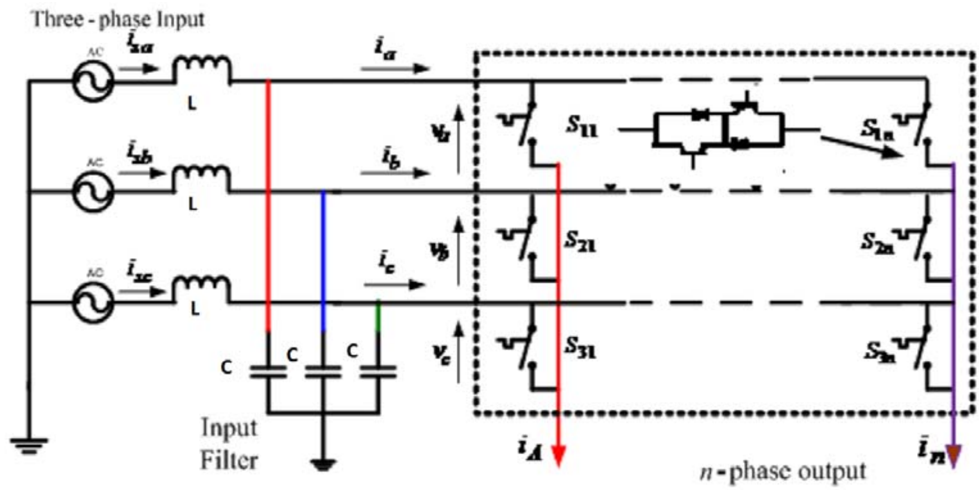

Fig. 1.5. Outlay of a three-phase to n-phase direct Matrix Converter.

The early modulation method proposed by Alesina and Venturuni [1.17] - [1.18] for three-to three-phase Matrix Converter may still be extended for multi-phase Matrix Converter topology with some modifications, but the output voltage magnitude will once again be limited to 50% of the input voltage magnitude. Thus it is not practical to use this method due to small output voltage magnitude. Similar concept is put forth in reference [1.19], where the outputs are dealt independently and PWM method is presented focusing on three-to single-phase and three-to three-phase Matrix Converter. This thesis describes the application of optimum control theory to N-input K-output Matrix Converters based on the transformation of actual converter topology into a suitable equivalent structure. The topologies and control properties of the most common Matrix Converters are analyzed by developing the general anti-transformation criteria.

Space vector PWM approach used for three-to three-phase Matrix Converter, offering higher output voltage magnitude as references [1.20]-[1.21], although can be extended to multi-phase topology as presented in references [1.22]-[1.24], is highly complex due to large number of space vectors available. For instance in a three-to five-phase Matrix Converter total number of space vector generated are 2^{15} = 32768, nevertheless, due to constraints imposed by switching actions, 3^5 =243 vectors are useful. Following the analogy with five-phase three-level voltage source inverter, the number of space vectors that can be used to generated sinusoidal output is further limited to 93 as in reference [1.22]. Nevertheless, space vectors PWM for real time processing still poses a challenge. The output voltage magnitude with space vector PWM in a three to five-phase Matrix Converter is limited to 78.86% of the input magnitude for linear modulation range. This limit can further be raised by exploiting over-modulation region. No work has so far been reported on over-modulation of the multi-phase Matrix Converter and also this is not the subject of this thesis.

Carrier-based PWM scheme is the simplest approach for controlling a Matrix Converter. Carrier based PWM is one of the recently developed modulation strategies for the Matrix Converter in three-to three-phase topology. As in the traditional sinusoidal PWM used in voltage source inverters, it employs the carrier and reference signals. The implementation of this scheme is simpler compared to the space vector PWM by using conventional UP/DOWN counters, which are embedded in most of the single chip microcontrollers. However, the carrier signal employed in this PWM is discontinuous and thus the method is intuitively difficult to understand. In addition, increasing the limit of modulation is a trivial task. Since, offset is added in this PWM, it is not suitable for topology where input and output neutral needs connection.

Another simpler and modular modulation approach, compared to the space vector PWM was developed called 'direct duty ratio PWM', which offers the advantages of simpler real time implementation as shown in reference [1.25]. This approach is modular in nature and it is seen that this can be employed for any phase number or switch number of the Matrix Converter. The major advantage of this modulation scheme is that it is highly intuitive and flexible, and can be applied to any topology of the Matrix Converter as the concept is based on 'per output phase'.

This thesis focuses on direct AC-AC three-phase to *n*-phase Matrix Converter fed series/parallel-connected multi-motor drive system. The emphasis is placed on the development of appropriate PWM techniques for five-phase, six-phase two-motor drive and seven-phase three-motor drive (Fig. 1.4). The major aim is to develop two fundamental frequency output for two-motor drive and three fundamental frequencies output for three-motor drive from multi-phase Matrix Converter. The pulse width modulation techniques developed in this thesis are:

- Carrier-based PWM
- Direct duty ratio based PWM.

1.5 Research Objectives

The present research is based on the development of mathematical model of three-phase input and multi-phase output direct AC-AC Matrix Converter and exploring their control algorithm for the multi motor drive system. The principle set objectives of the proposed research are:

i) To investigate the current state-of-the art in multi-phase motor drive research area by carrying out comprehensive literature review from available data bases.

ii) To review the modelling procedure of a five-phase series-connected two-motor drive, a six-phase and three-phase series-connected two-motor drive and a seven-phase three-motor drive using general machine modelling approach.

iii) To review the modelling procedure of a three-phase to five-phase Matrix Converter, a three-phase to six-phase Matrix Converter and three-phase to seven-phase Matrix Converter using space vector concept.

iv) To investigate the operation of a three-phase input and five-phase output Matrix Converter for producing two independent fundamental frequency components using; i) carrier-based PWM, ii) direct duty ratio based PWM assuming series-connected/parallel-connected two motor drive system being fed using this power source.

v) To investigate the operation of a three-phase input and six-phase output Matrix Converter for producing two independent fundamental frequency components using carrier-based PWM, assuming series-connected/parallel-connected two motor drive system being fed using this power source.

vi) To investigate the operation of a three-phase input and seven-phase output Matrix Converter for producing three independent fundamental frequency components using carrier-based PWM, assuming series-connected/parallel-connected three motor drive system being fed using this power source.

1.6 Layout of the Thesis

The complete thesis is organized into eight different chapters. Chapter 1 starts with the introductory remark and provides a review of basic literature available on the specific topic of multi-phase motor drives. An overview on the existing power electronic converter topologies is presented. A question is raised as to why at all the proposed research is looking into the multi-phase motor drives and in support a number of existing advantages are highlighted. An overview of the drive configuration investigated in the thesis is elaborated. Brief introduction to the Matrix Converter is elaborated. The objectives of the research are set and are discussed.

Chapter 2 presents literature review in the multi-phase multi-motor drive control research. At first state-of-the art in multi-phase drive system is discussed. This is followed by the description on conventional Matrix Converter topology and its control is elaborated. Finally multi-phase Matrix Converter topology is discussed along with its control and work done so far in the literature.

Chapter 3 is dedicated to the existing control technique of conventional three-phase to three-phase direct Matrix Converter. The control can be divided into scalar and vector control approaches. The limitation of lower output voltage is rectified by harmonic injection. Theoretical maximum limit of output voltage is achieved and elaborated.

Chapter 4 is dedicated to the modelling of a multi-phase series-connected multi-motor drive system. Three configurations are taken up for discussion: five-phase series-connected two-motor, six-phase two-motor and seven-phase three-motor. Modelling is done assuming multi-phase induction machines. Although this concept of series connection is independent of type of machines, but only one type of machine is considered to show the viability of the approach. Phase variable modelling approach is used with general assumption of sinusoidally distributed mmf. This is followed by transformation of the model in the rotational reference frame and then in the stationary reference frame. The developed model is validated using MATLAB/SIMULINK approach assuming ideal sinusoidal supply.

Chapter 5 elaborate the space vector model of multi-phase Matrix Converter. Three different topologies are discussed: three-phase to five-phase, three-phase to six-phase and three-phase to seven-phase. For n-phase input and m-phase output, the number of switching states is 2^{nxm} and after imposing the constraints, the remaining switching states are elaborated in this chapter.

The PWM approaches of multi-phase Matrix Converter are complex and challenging due to their circuit configuration and AC signals at both input side and output side. Hence, simpler approach of carrier-based PWM is discussed in Chapter 6. At first carrier-based scheme for single-motor drive is elaborated followed by multi-phase multi-motor drive system. Five-phase single-and two-motor drive, six-phase single and two-motor drive and seven-phase single-and three-motor drive topologies are discussed. Simulation and experimental results are included to validate the PWM schemes.

Chapter 7 elaborate another PWM technique based on direct duty ratio calculation. This is a simple approach that is highly modular in nature since the computation is done one per-leg basis. Five-phase single-motor and two-motor drive system is discussed. Simulation and experimental results are included.

Chapter 8 is the final chapter, and provides a summary of the thesis and the salient points from each chapter. Conclusions are made as to the viability of the series-connected/parallel-connected multi-phase multi-motor drive fed using three-phase input multi-phase output direct Matrix Converter. Future research work possible related to this area is suggested and reported in this chapter.

References used in each chapter are given at the end of each chapter itself and hence no separate references chapter is given. List of publications out of this thesis is provided at the end.

1.7 Novelty and Contribution of Thesis

The major contributions of the thesis are as follows:

- Development of mathematical model of multi-phase multi-motor drive system. Mathematical model of a five-phase two-motor drive and a six-phase two-motor drive is obtained from the literature and is further developed in and reported in the thesis. Mathematical model of seven-phase three-motor drive system is not reported in the literature and is developed in this thesis based on phase variable concept. The developed model is then transformed into three orthogonal planes using general transformation matrix. The mathematical model developed is verified using simulation approach. The developed mathematical model helps in developing decoupled control scheme.
- Development of simple control algorithms for decoupled dynamic control of five-phase two-motor drive, six-phase two-motor drive and seven-phase three-motor drive. Control algorithm is developed based on sinusoidal carrier-based PWM scheme and direct duty ratio based PWM scheme.

References:

[1.1] E. Levi, “Multi-phase Machines for Variable speed applications” *IEEE Trans. Ind. Elect.,* vol. 55, no. 5, May 2008, pp. 1893-1909.

[1.2] G.K. Singh “Multi-phase induction machine drive research – a survey”, *Electric Power System Research,* vol. 61, 2002, pp. 139-147.

[1.3] R. Bojoi, F. Farina, F. Profumo, Tenconi,“Dual three induction machine drives control-A survey”, *IEEE Tran. On Ind. Appl.,*vol. 126, no. 4, pp. 420-429, 2006.

[1.4] E. Levi, R. Bojoi, F. Profumo, H.A. Toliyat, S. Williamson, “Multi-phase induction motor drives-A technology status review”, *IET Elect. Power Appl.* Vol. 1, no. 4, pp. 489-516, July 2007.

[1.5] H. Abu-Rub, A. Iqbal, J. Guzinski, “*High Performance Control of AC Drives with MATLAB/SIMULINK Models”,* Wiley, UK, 2012.

[1.6] A. Iqbal, “Modelling and control of series-connected five-phase and six-phase two-motor drives,” *PhD Thesis,* Liverpool John Moores University, Liverpool, UK, 2006.

[1.7] E. Levi, M .Jones, S.N. Vukosavic, H.A. Toliyat, “A novel concept of a multi-phase, multi-motor vector controlled drive system supplied from a single voltage source inverter,” *IEEE Trans. on Power Electronics,* vol. 19, no. 2, 2004, pp. 320-335.

[1.8] E. Levi, S.N. Vukosavic, M. Jones, “Vector control schemes for series-connected six-phase two-motor drive systems,” *IEE Proc. – Electric Power Applications,* vol. 152, no. 2, 2005, pp. 226-238.

[1.9] M. Jones, S.N. Vukosavic, E.Levi, A.Iqbal, “A six-phase series-connected two-motor drive with decoupled dynamic control,” *IEEE Trans. on Industry Applications,* vol. 41, no. 4, 2005, pp. 1056-1066.

[1.10] E. Levi, M. Jones, A. Iqbal, S.N. Vukosavic, H.A. Toliyat, “An induction machine / Syn-Rel two-motor five-phase series-connected drive,” *IEEE Trans. on Energy Conversion,* vol. 22, no. 2, 2007, pp. 281-289.

[1.11] E. Levi, M. Jones, S.N. Vukosavic, A. Iqbal, H.A. Toliyat, “Modelling, control and experimental investigation of a five-phase series-connected two-motor drive with single inverter supply,” *IEEE Trans. on Industrial Electronics,* vol. 54, no. 3, 2007, pp. 1504-1516.

[1.12] M. Jone, E. Levi, S.N. Vukosavic, H.A. Toliyat, “Independent vector control of a seven-phase three-motor drive system supplied from a single voltage source inverter”, *Proc. 34th IEEE PESC*, 2003, vol. 4, pp. 1865-1870.

[1.13] P.W. Wheeler, J. Rodriguez, Jon C. Clare, L. Empringham, A. Weinstein, “Matrix Converters: A Technology Review”, *IEEE Trans. On Ind. Elect.* vol. 49, no. 2, April, 2002, pp. 276-288.

[1.14] P. Wheeler, L. Xu, M. Y.Lee, L. Empringham, C. Klumpner, J.Clare, “A review of multi-level Matrix Converter topologies,” *Proc. IET Power Electronics, Machines and Drives Conf.*, York, UK, 2008, pp. 286-290.

[1.15] L. Empringham, J. Kolar, J. Rodriguez, P. W. Wheeler, J. C. Clare, "Technological issues and industrial application of Matrix Converters: A review," *IEEE Trans. on Ind. Elec.*, 2013 (d.o.i.10.1109/TIE.2012.2216231).

[1.16] J. Rodriguez, M. Rivera, J. W. Kolar, P. W. Wheeler, "A review of control and modulation methods for Matrix Converters," *IEEE Trans. On Ind. Elec.*, vol. 59, no. 1, pp. 58-70, 2012.

[1.17] A. Alesina, M. Venturini, “Solid state power conversion: A Fourier analysis approach to generalised transformer synthesis” *IEEE Trans. Circuit System,* vol. 28, no. CS-4, pp. 319-330, April 1981.

[1.18] A. Alesina, M. Venturini, “Analysis and design of optimum amplitude nine-switch direct AC-AC converters”, *IEEE Trans. Power Elect.* vol. PE-4, no. 1, pp. 101-112, 1989.

[1.19] P. Tenti, L. Malesani, L. Rossetto, “Optimum control of *N*-input *K*-output Matrix Converters,” *IEEE Trans. on Power Electronics,* vol. 7, no. 4, 1992, pp. 707-713.

[1.20] D. Casadei, G. Grandi, G. Serra, A. Tani, “Space vector control of Matrix Converters with unity power factor and sinusoidal input/output waveforms”, *Proc. EPE Conf.,* vol. 7, pp. 170-175, 1993.

[1.21] L. Huber, D. Borojevic, “Space vector modulated three-phase to three-phase Matrix Converter with input power factor correction”, *IEEE Trans. Ind. Appl.* Vol. 31, no. 6, pp. 1234-1246, Nov./Dec. 1995.

[1.22] Sk. M. Ahmed, A. Iqbal, H. Abu-Rub, M.R. Khan, “Space vector PWM technique for a novel three-to-five phase Matrix Converter,” *IEEE Energy Conversion Conf. and Exhibition,* Atlanta, GA, 2010, pp. 1875-1880.

[1.23] Sk. M. Ahmed, A. Iqbal, H. Abu-rub, M.R. Khan, “Carrier based PWM technique for a novel three-to-seven phase Matrix Converter,” *Int. Conf. on Electrical Machines ICEM*, Rome, Italy, 2010, CD-ROM.\

[1.24] A. Iqbal, Sk.M. Ahmed, H. Abu-Rub, M.R. Khan, “Carrier based PWM technique for a novel three-to-five phase Matrix Converter,” *Power Conversion and Intelligent Motion PCIM*, Nuremberg, Germany, 2010, pp. 998-1003.

[1.25] Y. Li, N.-S. Choi, B.-M. Han, K. M. Kim, B. Lee, J.-H. Park, "Direct duty ratio pulse width modulation method for Matrix Converters, "*Int. Journal of Control, Automation, and Systems*, vol. 6, no. 5, pp.660-669, 2008.

Chapter 2
Literature Review

2.1 Introduction

Traditionally, variable-speed electric drives are based on three-phase configuration of an electric machine and a power electronic converter. Such a situation is the relic of a bygone era, when machines were supplied from the grid. Since the power electronic converter can be viewed as an interface that decouples three-phase mains from the machine, the number of machine's phases does not have to be limited to three in variable-speed drives as shown reference [2.1]. Nevertheless, three-phase machines are still customarily adopted for variable speed applications due to the wide off-the-shelf availability of both machines and converters. However, in all applications where a machine is not readily available, multi-phase machines (machines with more than three phases on stator) offer a number of advantages as shown in reference [2.2]. These include (but are not limited to): i) possibility of splitting the required per-phase power rating across more than three phases, thus reducing current rating of the semiconductor components (of exceptional importance in high-power and high-current applications), ii) a significant improvement in fault tolerance of the drive, since any AC machines (regardless of the number of phases) requires only two currents for independent flux and torque control of the machine (in a three-phase machine open-circuit fault in one phase means that there are not two independent currents available for control anymore; however, an n-phase machine can continue to operate with a rotating field in post-fault operation as long as no more than (n-3) phases are faulted), and, iii) a potentially better efficiency due to reduced space harmonic content of the magneto-motive force.

Although the multi-phase variable-speed drive systems have been a subject of research interest for the last 50 years, it is the last ten years that have seen an enormous growth of the quantum of knowledge in the area as presented in reference [2.1]. This has been initiated by numerous specific application areas, such as high power industrial applications, electric ship propulsion, locomotive traction, electric and hybrid electric vehicles, etc., where advantages of multi-phase systems outweigh the initial higher cost of the development.

In general, the conversion of an input ac power at a given frequency to an output power at a different frequency can be obtained with different systems, employing rotating electrical machinery, non-linear magnetic devices or static circuits containing controllable power electronic switches. Restricting the discussion of AC/AC power frequency conversion to static circuits, the available structures can be divided in “direct” and “indirect” power conversion schemes. Indirect schemes consist of two or more stages of power conversion and an intermediate DC-link stage is always present. A typical example of two stage indirect AC/DC/AC power frequency conversion is the diode-bridge rectifier-inverter structure, in which an AC power is firstly converted to a DC power (diode rectifier), and then converted back to an AC power at variable frequency (inverter). In direct conversion schemes a single stage carries out the AC/AC power frequency conversion. This is the subject of the research.

2.2 Multi-phase Motor Drive Systems

Multi-phase ac machine can be either induction or synchronous. The induction machine can be either a wound or cage type, it is the later design which has been extensively discussed in the literature. In synchronous category it can either be a permanent magnet, with field winding or reluctance type. The stator of a multi-phase can be designed with sinusoidal winding or with concentrated winding. Both machines differ in properties due to different distribution of their mmf waves. Some of the properties of multi-phase machines which are independent of their type and are highlighted in references [2.3]-[2.10].

MMF produced by stator excitation have lower space harmonics and this affect a number of characteristics of a multi-phase machine such as their efficiency and power factor.

- The frequency of torque ripple in a multi-phase machine fed using a multi-phase inverter operating in square wave mode is $2n$, where n being phase number, thus increasing phase number correspondingly increases the frequency of torque ripple.
- Only two current components are required for the torque/flux control of an ac machine irrespective of number of phases thus the extra current components available in multi-phase machines can be utilised for other purposes.
- Due to sharing of power among large number of phases the power per phase gets reduced for handling same amount of power as that of a three-phase machine. The power sharing by each inverter leg also reduces and thus lower rating power semiconductor can be used.

- Due to availability of large number of phases a multi-phase machine is more fault tolerant compared to their three-phase counterpart. Since only two current components are required for torque/flux control a multi-phase machine do not pose any problem in the event of occurrence of fault unless there is a loss of more than *n-3* phases occurs.

The consequence of mmf with lower space harmonic in multi-phase machine is their higher efficiency and lower acoustic noise. Higher frequency of torque ripple once again put less stress on the driving load and quieter operation of the machine. Higher efficiency of multi-phase machine compared to three-phase machine may be explained as follows: consider two machines of identical design with different phase numbers. If both machines have to develop same amount of torque at same speed, then they must have same rotor copper losses, same air-gap mmf and same fundamental component of stator current. The higher efficiency is attributed to lower stator copper losses. The stator copper losses will reduce with increasing phase number as given in Table [2.1].

Table 2.1. Reduction in stator copper loss vs phase number of machine.

Phase Number	5	6	9	12	15
Reduction in stator C_u. Loss	5.6%	6.7%	7.9%	8.3%	8.5%

It is important to note here that the rotor copper losses and iron losses (since air gap mmf is unchanged) will remain unchanged with the change in machine phase number. The reduction in stator copper losses is due to that fact that the stator current lower order harmonic changes. The use of higher phase number increases the pole number of the harmonic components and thus reducing their magnitude and consequently reducing the stator copper losses due to these harmonic components.

Reduction in the magnitude of torque pulsation and the increase in the frequency of torque pulsation in an inverter (operating in 180° conduction mode) fed multi-phase is their another salient feature. as in reference [2.11], it is demonstrated that the air gap field produced by q^{th} harmonic component of excitation current in a 2*P* pole machine with *n* balanced phases will have pole-pair numbers given by:

$$\beta = P(q - 2kn) \qquad k = 0, \pm 1, \pm 2, \pm 3, \ldots\ldots \tag{2.1}$$

Positive values of β correspond to forward rotating fields and negative values represents backward rotating field. For fields of the same pole number to be produced by two distinct excitation components , with frequencies f_1 and f_2, (2.1) shows that there must be solution to the equation:

$$P(q_1 - 2k_1 n) = P(q_2 - 2k_2 n) \tag{2.2}$$

from which one gets:

$$(q_1 - q_2) = (2k_1 n - 2k_2 n) = 2n(k_1 - k_2) \tag{2.3}$$

Thus the frequency of torque pulsation is:

$$(q_1 - q_2)f = 2nf(k_1 - k_2) \tag{2.4}$$

where k_1 and k_2 are integers. Equation (2.4) reveals that the frequency of torque pulsation in a balanced n-phase machine is produced at all even multiples of the product of the phase number and the fundamental frequency of the supply. For instance in a three-phase machine the torque ripple frequency exist at multiple of 300 Hz, in a five-phase machine it shifts to 500 Hz . Thus higher the phase number higher will be the torque pulsation frequency.

One important property of a multi-phase machine with concentrated stator winding is enhancement in average torque produced by the machine by injecting higher order harmonic currents [2.12-2.15]. This is a special characteristic of a multi-phase machine which is not available in a three-phase machine. All harmonic current of the order between fundamental and *n* can be injected along with fundamental to improve the torque production. For instance in a five-phase machine 3rd harmonic can be added and in a seven-phase machine 3rd and 5th can be added with the fundamental as presented in reference [2.1]. In even phase number machine only quasi six-phase configuration is utilised for torque enhancement by injecting 3rd harmonic as shown in reference [2.16].

Assuming an odd phase number machine with one neutral point, there exist *n-3* additional current components and thus the same number of additional degree of freedom. This additional degree of freedom may be used for various purposes, such as:

- Enhancement of torque production by injecting higher order current harmonics in concentrated winding machines as above mentioned.
- Fault mitigation and providing fault tolerant operation. A number of publications are available in this regard, some of them are given in reference [2.17-2.27]. In the event of a fault (one phase out) in a three-phase drive with

star-connected stator winding and isolated neutral point, the two available healthy phase currents become identical with 180° phase shift. Hence it is no more possible to independently control the remaining two phase currents unless a divided DC bus along with a neutral point is provided as demonstrated in reference [2.28]. In contrast to this, multi-phase machine may still generate rotating mmf with the loss of upto *n-3* phases. The phase redundancy concept was developed by Jahns in reference [2.29] for multi-phase machine and it was shown that machine normal operation of a multi-phase machine is possible with appropriate post fault strategy. The simplest post fault strategy can be adopted for a machine with $n=pk$ phases (p = 3,4,5…., k = 2,3,4,…) and the complete winding is configured as k windings with a phase each, with k isolated neutral points and k independent p-phase inverters. In the event of a fault in any phase of p set, then the complete set of p-phases is taken out of the service. For instance in case of quasi six-phase machine with two set of three-phase windings one set is completely taken out of the service rendering the supply to only one set and thus the complete drive operate with half torque and power. In case of a 15-phase motor with three set of 5-phase windings, one or more complete 5-phase windings may be taken out of the service to keep the drive running with reduced rating. This simple strategy is although easy to implement and no change is required in the software but this may not be suitable for safety critical applications as there is a huge loss in developed torque. In such situations, machine with one neutral point is better suited. This is so since the currents of all the remaining healthy phases are regulated to offer an optimum solution. The post fault strategy is application dependent and three different situations may occur as highlighted in reference [2.25]. Assuming loss of one phase, strategy 1 could be to maintain the same torque level as that of the pre fault conditions without any pulsation. In this case the increase in currents in healthy phases are inevitable and the currents increase by a factor $\frac{n}{(n-1)}$ and correspondingly the stator copper losses will also increase but there will be no change in the rotor copper losses. The second strategy is based on the keeping the stator copper loss under post-fault condition to the same level as that of the pre-fault condition. The stator current has to be increased to $\sqrt{\frac{n}{(n-1)}}$ in the remaining healthy phases. The torque and power reduces and the rotor copper loss increases. The third strategy keeps the stator current during post fault at the same level as that of pre fault condition. In this scheme the stator copper losses reduced by a factor of $\frac{n}{(n-1)}$, however, the torque level and power is reduced with corresponding increase in the rotor copper loss. All three scheme discussed in reference [2.25] assumes load whose torque varies as square of speed. All these strategies require configuring the software in post-fault operation.

- Another useful purpose of additional degree of freedom in terms of extra current components is the independent control of two or more multi-phase machine whose stator windings are connected in series or parallel. A number of published work is available on this issue which is taken up in detail in next section

It is important to emphasize here that the additional degree of freedom available in multi-phase motor drive can be utilised for one purpose at one time as given in reference [2.1].

2.3 Three-phase input and three-phase output Matrix Converter

A direct AC-AC converter is proposed in reference [2.30] called 'Matrix Converter' has been the focus of an intensive on-going research. Several aspects of the Matrix Converter has been investigated in the literature. Most commonly the control techniques have been explored, and comprehensive review is presented in references [2.31-2.32]. From the literature review, it is seen that the control characteristics of a direct AC-AC Matrix Converter when used in variable speed drives application, are:

- The output voltage magnitude and frequency should be controlled independently;
- The source side (utility grid side) current should be completely sinusoidal and the power factor angle of the source side should be fully controllable
- The output voltage to input voltage ratio should be maximum
- The Matrix Converter should satisfy the conflicting requirements of minimum low order harmonics distortion and minimum switching losses
- The Matrix Converter input side is connected to the utility grid and hence prone to unbalancing and distortion. The control should compensate for such operational conditions
- The control should be computationally efficient.

The control scheme originally proposed in reference [2.33], although characterized by better performance than naturally commutated cyclo-converters, it had significant output voltage limitations and serious output voltage waveforms distortion with high total harmonic distortion.

An alternative high switching frequency control technique was proposed in reference [2.34] which was more effective than traditional control techniques, but still can generate a maximum output voltage equal to half of the input voltage magnitude. This is a scalar control approach and had serious limitation of reduced output voltage and practically had no attraction. Further to the this, other limitation is the poor factor control at the source side.

Another control approach was proposed in references [2.35-2.37], where a Matrix Converter is considered as composed of two stages i.e. rectification and inversion. Hence the input voltages are first “rectified” to create a fictitious DC bus and then “inverted” to obtain variable voltage and variable frequency waveform. However, the limitation of output voltage magnitude and uncontrolled source side power factor was still un resolved.

The direct PWM method developed by Alesina and Venturini [2.34] limits the output to half the input voltage. This limit was subsequently raised to 0.866 by taking advantage of third harmonic injection as shown in reference [2.38] and it was realized that this is maximum output that can be obtained from a three-to-three phase Matrix Converter. Indirect method assumes a Matrix Converter as a cascaded virtual three-phase rectifier and a virtual voltage source inverter with imaginary DC link. With this representation, space vector PWM method of VSI is extended to a Matrix Converter as given in references [2.39]-[2.40]. Although the space vector PWM method is suited to three-phase system but the complexity of implementation increases with the increase in the number of switches/phases. Motivated from the simple implementation, carrier-based PWM scheme has been introduced for Matrix Converter as shown in reference [2.41-2.43]. Carrier based PWM is the latest modulation strategy for the Matrix Converter. As in the traditional sinusoidal PWM used in voltage source inverters, it employs the carrier and reference signals. The implementation of this scheme is simpler using conventional UP/DOWN counter which are embedded in a single chip microcontrollers. This chapter focuses on different Matrix Converter modulation strategies based on space vector modulation.

2.4 Multi-phase Matrix Converter

The power circuit topology of a three-phase to k-phase Matrix Converter is illustrated in Fig. 2.1. There are k legs with each leg having three bi-directional power switches connected in series. Each power switch is bi-directional in nature with anti-parallel connected Insulated Gate Bi-polar Transistors (IGBTs) and diodes. The input is similar to a three-phase to three-phase Matrix Converter having LC filters.

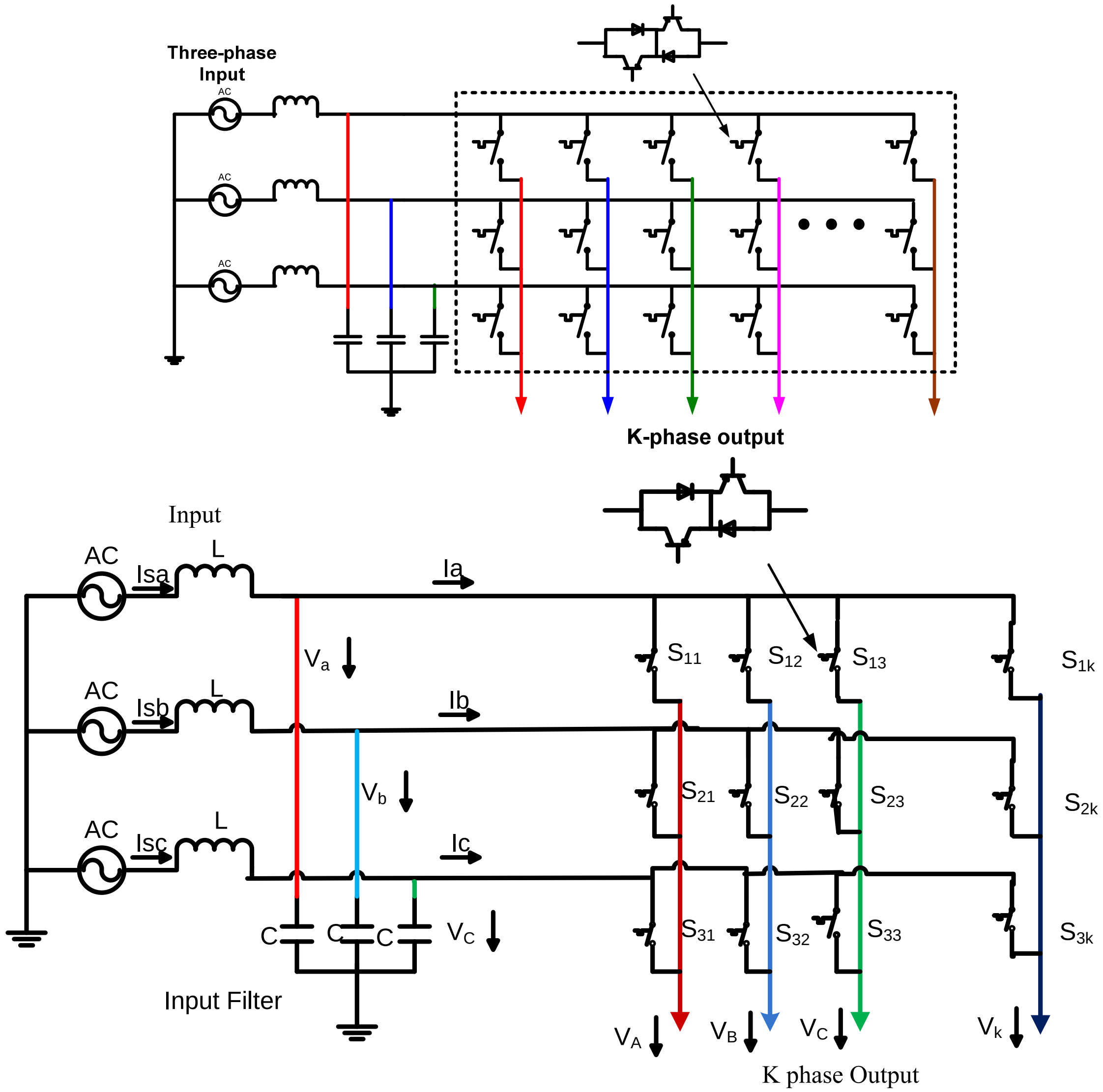

Fig. 2.1. Power Circuit topology of Three-phase to k-phase Matrix Converter.

The load to the Matrix Converter could be a star-connected R or R-L or an AC machine. As far as the research on multi-phase output AC-AC converters is concerned, there has been relatively little development until recently. Theoretical principles of such a converter have been established in reference [2.44]. Probably the first considerations of a real world application of a three to *n*-phase Matrix Converter application, in more-electric aircraft, have been reported as shown in reference [2.45]. During the last four years or so, Matrix Converter with multi-phase output have quickly gained in importance, with a significant number of papers dealing with the subject as discussed in references [2.46]-[2.54]. This is a consequence of accelerated pace of developments in the multi-phase drive area in general.

The determination of appropriate PWM method for complex Matrix Converter topology, especially for multi-phase output, is a key issue. The restrictions imposed on the PWM strategies are that the input phases must not be short circuited and none of the output phases should be open circuited.

The early modulation method, proposed by Alesina and Venturini as shown in reference [2.34] for three-phase to three-phase Matrix Converter, may still be extended for multi-phase Matrix Converter topology with little modifications, but the output voltage magnitude will once again be limited to 50% of the input voltage magnitude. Thus it is not practical to use this method due to the restricted output voltage magnitude. Space vector PWM approach used for three-phase to three-phase Matrix Converter, offering higher output voltage magnitude as given in reference [2.34], although extendable to multi-phase topology as presented in reference [2.52], is highly complex due to large number of space vectors available. For instance, in a three-phase to five-phase Matrix Converter total number of space vectors generated is $2^{15} = 32768$. Nevertheless, due to constraints imposed by the switching actions, only $3^5 = 243$ vectors are useful. Following the analogy with five-phase three-level voltage source inverter, the number of space vectors that can be used to generate sinusoidal output is further limited to 93 as discussed in reference [2.52]. Nevertheless, space vector PWM for real time processing still poses a challenge. The output voltage magnitude with space vector PWM in a three-phase to five-phase Matrix Converter is limited to 78.86% of the input magnitude for linear modulation range. This limit can further be raised by exploiting the over-modulation region. No work has so far been reported on over-modulation of the multi-phase Matrix Converter.

Carrier-based PWM scheme has been introduced for three-phase to multi-phase Matrix Converter as discussed in references [2.50] - [2.51]. Carrier based PWM is one of the recently developed modulation strategies for the Matrix Converter in three-phase to three-phase topology. As in the traditional sinusoidal PWM, used in voltage source inverters, it employs the carrier and reference signals. The implementation of this scheme is simpler compared to the space vector PWM due to the use of conventional UP/DOWN counters, which are embedded in most of the single chip microcontrollers. However, the carrier signal employed in this PWM is discontinuous and thus the method is intuitively difficult to understand. In addition, increasing the limit of modulation is not a trivial task. Since an offset is added in this PWM, it is not suitable for topology where input and output neutrals needs connection.

Another simpler, compared to the space vector PWM, and modular modulation approach was developed recently and is called 'direct duty ratio PWM' (DPWM). It offers the advantages of simpler real time implementation as presented in reference [2.54]. This approach is modular in nature and it is shown that this can be employed for any phase number or switch number of the Matrix Converter. The major advantage of this modulation scheme is that it is highly intuitive and flexible, and can be applied to any topology of the Matrix Converter, since the concept is based on 'per output phase'.

Multi-phase Matrix Converter is suitable for application in renewable energy system. In multi-phase wind generation, a multi-phase Matrix Converter is used as an interface between the generator and utility grid. The input side of multi-phase Matrix Converter is n-phase and output is 3-phase since this is to be connected to utility grid as given in reference [2.55]. Simulation results are presented in reference [2.55] for the concept of higher phase input and lower phase output. For the same Matrix Converter configuration, space vector PWM is elaborated and five-phase is successfully transformed to three-phase and connected to the utility grid in reference [2.56]. The major advantage of this configuration is high voltage transfer ratio which can go up-to 104% of the input as given in reference [2.56]. Multi-phase electric generators (that can be used in wind turbine driven configuration) possess all the listed advantages of a multi-phase machine. The multi-phase to three-phase Matrix Converter can give finer resolution and higher magnitude output voltages and hence better performing overall multi-phase generation system. A dual three-phase Permanent Magnet Synchronous Machine (two stator windings with 30° phase displacement) is considered as a possible solution for electric ship propulsion, in conjunction with a Matrix Converter driven by a modified direct torque control as presented in reference [2.57]. The Matrix Converter is controlled using space vector pulse width modulation as shown in reference [2.57]. The machine is supplied by two sets of transformers, each one providing six-phase secondary by phase shifting the three-phase primary voltages. Each of these secondary six-phase voltages is then applied to a separate Matrix Converter that gives a three-phase output. There are two alternatives to the original Matrix Converter topology; called single-sided Matrix Converter and indirect Matrix Converter, as shown in Fig. (2.2.)

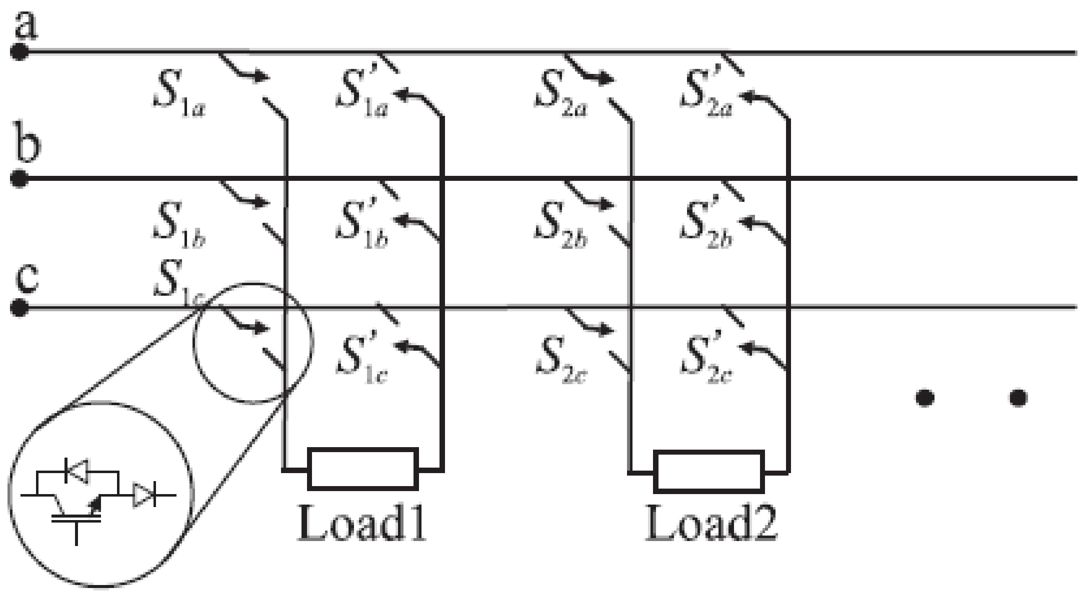

Fig. 2.2. Single-sided Matrix Converter with unidirectional power switches as shown in reference [2.58].

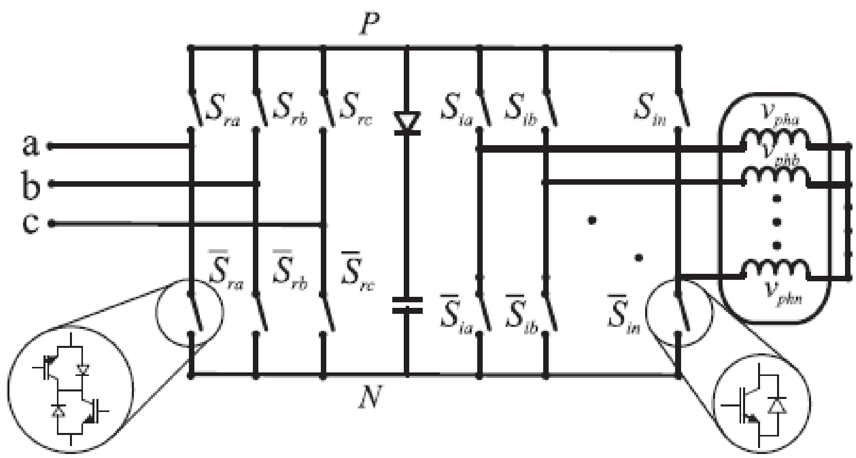

Fig. 2.3. Indirect Matrix Converter with rectifier and inversion stage as shown in reference [2.58].

A single-sided multi-phase Matrix Converter that supplies unidirectional current to run a switched reluctance motor is proposed in reference [2.59]. The topology do not use bi-directional power switches. The converter essentially consists of a controlled rectifier applied separately to each one of the load phases. Therefore, by adding more rectifiers, more phases can be supplied. In essence, the topology provides easier commutation, modulation and higher fault tolerance and modular structure.

A single sided Matrix Converter supplying brushless DC motor with fault tolerant property is proposed in reference [2.60]. High fault tolerance and power density are claimed and results are provided for a five-phase BLDC machine supplied by single sided Matrix Converter.

Application of a single-sided Matrix Converter supplying a five-phase brushless DC drive for applications in the more electric aircraft is proposed in reference [2.61]. The real time implementation is done using a field programmable gate array (FPGA) and hysteresis control is employed. Hysteresis control is employed in order to maximize the system robustness and remove the elements imposing the highest risk of failure. Experimental results are provided for a range of operating conditions including field weakening region and single-phase open-circuit fault.

The indirect Matrix Converter, discussed in reference [2.62], is a topology which employed active rectifier instead of diode based rectifier. The topology uses a fully controllable rectifier with bi-directional switches. Contrary to conventional Voltage Source Inverter, this topology does not include a large bulky capacitor in the DC-bus, to increase the system robustness. The clamping circuit, consisting of a diode and a smaller capacitor, use to protect from overvoltage in the DC-link if the inductive load continues to draw current when the inverter stage is turned off. The two stages, rectifier and inverter, are controlled independently but are synchronized. The rectifier control aims to create maximal DC-bus voltage and minimal distortion to the source side current, which is controlled to be in phase with the input voltage for unity power factor operation. The inverter part of indirect Matrix Converter control relies on accepted modulation techniques for multi-phase VSIs [2.1].

2.5 Summary

This chapter present the state-of-the art in the development of multi-phase motor drive system. Advantages of multi-phase motor drive over three-phase drive system are investigated and the literatures are cited where such advantages are highlighted. The developments in the control algorithms of multi-phase power converters are addressed. The multi-phase power converters can be AC-DC, DC-AC and AC-AC. The focus of the research is AC-AC converter and hence literature related to AC-AC converter is mostly cited. At first conventional three-phase input to three-phase output Matrix Converter is taken up for discussion and the relevant literature are cited. This is followed by the discussion on three-phase input and multi-phase output Matrix Converter is elaborated. Some recent works are reported in the literature and the findings are summarized.

References:

[2.1] E. Levi, "Multi-phase electric machines for variable-speed applications," IEEE Trans. on Industrial Electronics, vol. 55, no. 5, 2008, pp. 1893-1909.

[2.2] E. Levi, R. Bojoi, F. Profumo, H.A. Toliyat, S. Williamson, "Multi-phase induction motor drives – A technology status review," IET – Electric Power Applications, vol. 1, no. 4, 2007, pp. 489-516.

[2.3] J.W. Kelly, E.G. Strangas, J.M. Miller, "Multi-phase inverter analysis," Proc. IEEE Int. Electric Machines and Drives Conf. IEMDC, Cambridge, MA, 2001, pp. 147-155.

[2.4] O. Ojo, G. Dong, "Generalized discontinuous carrier-based PWM modulation scheme for multi-phase converter-machine systems," Proc. IEEE Ind. Appl. Soc. Annual Meeting IAS, Hong Kong, 2005, CD-ROM paper 38P3.

[2.5] A. Iqbal, E. Levi, M. Jones, S.N. Vukosavic, "Generalised sinusoidal PWM with harmonic injection for multi-phase VSIs," Proc. IEEE Power Elec. Spec. Conf. PESC, Jeju, Korea, 2006, pp. 2871-2877.

[2.6] M.J. Duran, E. Levi, "Multi-dimensional approach to multi-phase space vector pulse width modulation," Proc. IEEE Ind. Elec. Soc. Annual Meeting IECON, Paris, France, 2006, pp. 2103-2108.

[2.7] A. Iqbal, E. Levi, "Space vector PWM techniques for sinusoidal output voltage generation with a five-phase voltage source inverter," Electric Power Components and Systems, vol. 34, no. 2, 2006, pp. 119-140.

[2.8] J.W. Kelly, E.G. Strangas, J.M. Miller, "Multi-phase space vector pulse width modulation," IEEE Trans. on Energy Conversion, vol. 18, no. 2, 2003, pp. 259-264.

[2.9] H.M. Ryu, J.H. Kim, S.K. Sul, "Analysis of multi-phase space vector pulse-width modulation based on multiple d-q spaces concept," IEEE Trans. on Power Electronics, vol. 20, no. 6, 2005, pp. 1364-1371.

[2.10] S. Williamson, A.C. Smith, "Pulsating torque and losses in multi-phase induction machines," IEEE Trans. Ind. Appl., vol. 39, no. 4, Jul./Aug. 2003, pp. 986–993.

[2.11] H. Weh, U. Schroder, "Static inverter concepts for multi-phase machines with square-wave current-field distribution," in *Proc. EPE*, Brussels, Belgium, 1985, pp. 1.147–1.152.

[2.12] H.A. Toliyat, M.M. Rahimian, T.A. Lipo, "Analysis and modeling of five phase converters for adjustable speed drive applications," in Proc. EPE, Brighton, U.K., 1993, pp. 194–199.

[2.13] H. A. Toliyat, T.A Lipo, "Analysis of concentrated winding induction machines for adjustable speed drive applications-experimental results," IEEE Trans. Energy Conv., vol. 9, Dec. 1994, pp. 695–700.

[2.14] H.A. Toliyat, S.P. Waikar, T.A. Lipo, "Analysis and simulation of five-phase synchronous reluctance machines including third harmonic of air gap MMF," IEEE Trans. Ind. Appl., vol. 34, no. 2, Mar./Apr. 1998, pp. 332–339.

[2.15] R.O.C. Lyra, T.A. Lipo, "Torque density improvement in a six-phase induction motor with third harmonic current injection," *IEEE Trans. Ind. Appl.*, vol. 38, no. 5, Sep./Oct. 2002, pp. 1351–1360.

[2.16] L. Lillo, L. Emprimgham, P.W. Wheeler, S. Khwan-on, C. Gereda, M.N. Othman, X. Huang, "Multi-phase power converter drive for fault-tolerant machine development in Aerospace applications", *IEEE Transaction on Industrial Electronics,* vol. 57, no. 2, pp. 575-583, 2010.

[2.17] X. L. Alberti, N. bianchi, "Experimental test of Dual Three-Phase Induction Motor Under Faulty Operation Condition," IEEE Transactions On Industrial Electronics, Vol. 59, no. 5,PP. 2041-2048, 2012.
[2.18] X. hang , A. Goodman, C. Gerada, Y. Fang, Q. Lu, "Design Of a Five Phase Brushless DC Motor For a Safety Critical Aerospace Application," IEEE Transactions On Industrial Electronics, Vol. 59, no. 9,PP. 3532-3541, 2012.
[2.19] A. Mohammedpour, L. Parsa. "A Unified Fault tolerant current control Approach For Five Phase PM Motors with Trapezoidal Back EMF Under Different Stator Winding Connections," IEEE Transactions On Power Electronics, Vol. 28, no. 7,PP. 3517-3527, 2013.
[2.20] Y. Zhao, T.A. Lipo. "Modelling And Control of a Multi Phase Induction Machine with Structural Unbalance Part I, Machine Modelling and Multi-dimensional Current Regulation," IEEE Transactions On Energy Conversion, Vol. 11, no. 3,PP. 578-584, 1996.
[2.21] J-P. Martin, F. Meibody-Tabar, B. Davat. "Multi-phase Permanente Magnet Synchronous Machine Supplied By VSIs, Working Under Fault Conditions," IEEE Industry Application Conferences, Vol. 3,PP. 1710-1717, 2000.
[2.22] R. Kaininezhad, B. Nahed-Mobarakeh, L. Baghli, F. Betin, G.A Capolino, "Modelling And Control Of Six Phase Symmetrical Induction Machine Under Fault Condition Due to Open Phase," IEEE Transactions On Industrial Electronics, Vol. 55, no.5,PP. 1966-1977, 2008.
[2.23] J.R. Fu, T.A. Lipo, "Disturbance Free Operations Of a Multi-Phase current Regulated Motor Drive With An Opened Phase." IEEE Transaction on Industry Applications, Vol. 30, no.5. PP. 1267-1274, 1994.
[2.24] H.M Ryu, J.W. Kim, S.K. Sul, "Synchronous-Frame Current Control of Multi Phase Synchronous Motor Under Asymmetric Fault Condition Due To Open Phases." ." IEEE Transaction on Industry Applications, Vol. 42, no.4. PP. 1062-1274, 1994.
[2.25] A. Tani, M. Mengoni, L. Zarrii, G. Serra, D. Cassadei, "Control of Multi-phase Induction Motor with an Odd Number of Phases Under Open circuit Phase Faults." IEEE Transactions On Power Electronics, Vol. 27, no. 2,PP. 565-572, 2012.
[2.26] S. Dwari, L. Parsa, "Fault tolerant Control of Five Phase Permanent Magnet Motors with Trapezoidal Back EMF." IEEE Transactions on Industrial Electronics, Vol. 58, no. 2, PP. 476-485, 2012.
[2.27] F. Barrero , J. Prieto, E. Levi, R, Gregor , S. Toral , M. Duran, M. Jones "An Enhanced Predictive Current Control Method for Asymmetrical Six Phase Motor Drives." IEEE Transactions On Industrial Electronics, Vol. 58, no. 8, PP. 3242-3252, 2011.
[2.28] J.R. Fu, T.A. Lipo, "Disturbance-free operation of a multi-phase current-regulated motor drive with an opened phase," IEEE Trans. Ind. Appl., vol. 30, no. 5, Sep./Oct. 1994, pp. 1267–1274.
[2.29] T.M. Jahns, "Improved reliability in solid-state AC drives by means of multiple independent phase-drive units," IEEE Trans. Ind. Appl., vol. IA-16, no. 3, May/Jun. 1980, pp. 321–331.
[2.30] M.P. Kazmierkowski, R. Krishnan, F. Blaabjerg, "*Control in Power Electronics-Selected Problems*", Academic Press, UK, ISSN: 0-12-402772-5.
[2.31] P.W. Wheeler, J. Rodriguez, Jon C. Clare, L. Empringham, A. Weinstein, "Matrix Converters: A Technology Review", IEEE Trans. On Ind. Elect. vol. 49, no. 2, April, 2002, pp. 276-288.

[2.32] J. Rodriguez, M. Rivera, J. W. Kolar, P. W. Wheeler, "A review of control and modulation methods for Matrix Converters," IEEE Trans. On Ind. Elec., vol. 59, no. 1, pp. 58-70, 2012.
[2.33] M. Venturini, "A new sine wave in, sine wave out, conversion technique eliminates reactive elements," in Proceedings of Power-con 7, San Diego, CA, 1980, pp. E3-1-E3-15.
[2.34] A. Alesina, M. Venturini, "Solid state power conversion: A Fourier analysis approach to generalised transformer synthesis" *IEEE Trans. Circuit System,* vol. 28, no. CS-4, pp. 319-330, April 1981.
[2.35] P.D. Ziogas, S.I. Khan, M.H. Rashid, "Some Improved Forced Commutated Cyclo-converters Structure", IEEE Transactions on Industry Applications, vol. IA-21, No 5,Sept./Oct. 1985, pp. 1242-1253.
[2.36] P.D. Ziogas, S.I. Khan, M.H. Rashid, "Analysis and Design of Forced Commutated Cyclo-converter Structures with Improved Transfer Characteristics," IEEE Transactions on Industry Applications, vol. IE-33, No. 3, August 1986, pp. 271-280.
[2.37] A. Alesina, M. Venturnin, "Analysis and design of optimum amplitude nine-switch direct AC-AC converters", *IEEE Trans. Power Elect.* vol. PE-4, no. 1, pp. 101-112, 1989.
[2.38] D. Casadei, G. Grandi, G. Serra, A. Tani, "Space vector control of Matrix Converters with unity power factor and sinusoidal input/output waveforms", Proc. EPE Conf., vol. 7, pp. 170-175, 1993.
[2.39] L.Huber, D. Borojevic, "Space vector modulated three-phase to three-phase Matrix Converter with input power factor correction", IEEE Trans. Ind. Appl. Vol. 31, no. 6, pp. 1234-1246, Nov./Dec. 1995.
[2.40] B. Wang, G. Venkataramanan, "A carrier-based PWM algorithm for indirect Matrix Converters," in Proc. IEEE-PESC 2006, pp. 2780–2787, 2006.
[2.41] Young-Doo Yoon and Seung-Ki Sul, "Carrier-based modulation technique for Matrix Converter," IEEE Trans. Power Elect., vol. 21, no. 6, pp. 1691–1703, November 2006.
[2.42] Poh C. Loh, R. Rong, F. Blaabjerg, P. Wang, "Digital carrier Modulation and Sampling Issues of Matrix Converter", IEEE Trans. On Power Elect., vol. 24, no. 7, July 2009.
[2.43] P. Tenti, L. Malesani, L. Rossetto, "Optimum control of *N*-input *K*-output Matrix Converters," IEEE Trans. on Power Electronics, vol. 7, no. 4, 1992, pp. 707-713.
[2.44] X. Huang, K. Bradley, A. Goodman, C. Gerada, P. Wheeler, J. Clare, C. Whitley, "Fault-tolerant brushless DC motor drive for electro-hydrostatic actuation system in aerospace application," IEEE Industry Application Society Annual Meeting IAS, Tampa, FL, 2006, pp. 473-480.
[2.45] J. Szczepanik, "Multi-phase Matrix Converter for power systems application," Proc. Int. Symp. on Power Electronics, Electrical Drives, Automation and Motion SPEEDAM, Ischia, Italy, 2008, pp. 772-777.
[2.46] J. Szczepanik, T. Sienko, "New control strategy for multi-phase Matrix Converter," IEEE Int. Conf. on Systems Engineering, Las Vegas, Nevada, 2008, pp. 121-126.
[2.47] J. Szczepanik, T. Sienko, "A new concept of application of multi-phase Matrix Converter in power systems," IEEE EUROCON – The Int. Conf. on "Computer as a Tool", Warsaw, Poland, 2007, pp. 1535-1540.
[2.48] J. Szczepanik, T. Sienko, "Control scheme for a multi-phase Matrix Converter," IEEE EUROCON, Saint-Petersburg, Russia, 2009, pp. 545-551.

[2.49] X. Huang, K. Bradley, A. Goodman, C. Gerada, P. Wheeler, J. Clare, C. Whitley, “Fault-tolerant analysis of multi-phase single sided matrix converter for brushless DC drives,” IEEE Int. Symp. on Industrial Electronics, Vigo, Spain, 2007, pp. 3168-3173.
[2.50] Sk. M. Ahmed, A. Iqbal, H. Abu-rub, M.R. Khan, “Carrier based PWM technique for a novel three-to-seven phase Matrix Converter,” Int. Conf. on Electrical Machines ICEM, Rome, Italy, 2010, CD-ROM.
[2.51] A. Iqbal, Sk. M. Ahmed, H. Abu-Rub, M.R. Khan, “Carrier based PWM technique for a novel three-to-five phase Matrix Converter,” Power Conversion and Intelligent Motion PCIM, Nuremberg, Germany, 2010, pp. 998-1003.
[2.52] Sk. M. Ahmed, A. Iqbal, H. Abu-Rub, M.R. Khan, “Space vector PWM technique for a novel three-to-five phase Matrix Converter,” IEEE Energy Conversion Conf. and Exhibition, Atlanta, GA, 2010, pp. 1875-1880.
[2.53] M. Mihret, M. Abreham, O. Ojo, S. Karugaba, “Modulation schemes for five-phase to three-phase AC-AC Matrix Converter,” IEEE Energy Conversion Conf. and Exhibition, Atlanta, GA, 2010, pp. 1887-1893.
[2.54] A. Iqbal, Sk. M. Ahmed, H. Abu-Rub, “Generalised duty ratio based pulse width modulation technique for a three-to-k phase Matrix Converter, IEEE Trans. on Industrial Electronics, under publication.
[2.55] O. Ojo, M. Abreham, S. Karugaba, O. A. Komolafe, "Carrier-based modulation of non-square multi-phase AC-AC Matrix Converters," in Proc. IEEE Int. Symp. on Ind. Elec. ISIE, Bari, Italy, pp. 2141-2146, 2010.
[2.56] O. Abdel-Rahim, H. Abu-Rub, A. Iqbal, “Five-to-Three Phase Direct Matrix Converter with Model Predictive Control”, 4th Int. conf. on Power Engineering, Energy and Electrical drives, CD-ROM paper, 13-17 May, 2013, Istanbul, Turkey.
[2.57] G. Yi, Y. Xuekui, "Research on Matrix Converter control multi-phase PMSM for all electric ship," in Proc. Int. Conf. on Electrical and Control Engineering ICECE, Yichang, China, pp. 3120-3123, 2011.
[2.58] E. Levi, N. Bodo, O. Dordevic, M. Jones, “Recent advances in power electronic converter control for multi-phase drive system”, Proc. WEMDCD, 2013.
[2.59] A. S. Goodman, K. J. Bradley, P. W. Wheeler, “Evaluation of the single sided Matrix Converter driven switched reluctance motor,” in Proc. IEEE Ind. Appl. Annual Meeting IAS, Seattle, WA, pp. 1847-1851, 2004.
[2.60] H. Xiaoyan, K. Bradley, A. Goodman, C. Gerada, P. Wheeler, J. Clare, C. Whitley, "Fault-tolerance analysis of multi-phase single sided Matrix Converter for brushless DC drives," in Proc. IEEE Int. Symp. On Ind. Elec. ISIE, Vigo, Spain, pp. 3168-3173, 2007.
[2.61] H. Xiaoyan, A. Goodman, C. Gerada, F. Youtong, L. Qinfen, "A single sided Matrix Converter drive for a brushless DC motor in aero-space applications," IEEE Trans. on Ind. Elec., vol. 59, no. 9, pp.3542-3552, 2012.
[2.62] Li Gang, “PWM Algorithams for indeirect Matrix Converter”, Proc. 7th international power electronics and motion control conference (IPEMC) , vol.3, pp. 1713-1717, 2012

Chapter 3
Over-View of Modelling and Control of three-phase by three-phase Matrix-Converter

3.1 Introduction

In general, conventional Matrix Converter topologies consist of three phase input to single-or three-phase output. The complexity of the Matrix Converter circuit configuration makes the phase control and the determination of suitable modulation strategies a difficult task. Two different mathematical approaches have been considered in the past to face this problem, namely the Modulation Duty-Cycle Matrix(MDCM) or Alesina-Venturuni approach (scalar method) and the Space Vector Modulation (SVM) approach. In recent literature two different latest modulation techniques are introduced namely-Carrier based PWM technique and Direct Duty-ratio based PWM technique (DDPWM). This chapter discusses the conventional Matrix Converter topology (three-phase input and three-phase output) and different modulation techniques for the control of Matrix Converter.

3.2 Control Algorithms for Matrix Converter

There are several different open-loop and closed-loop control methods suitable for Matrix Converters. The open-loop methods can be considered as pure modulation strategies if load control strategies are ignored. In addition, a closed-loop control system does not usually control the converter itself, but rather the load, so that they also contain a modulator. Thus modulation is one of the key issues with Matrix Converters (MC). Before the modulation techniques are discussed in detail, the basic connection of Matrix Converter is explained.

In Fig. 3.1 subscripts d and r in the IGBTs label stand for direct and reverse respectively and they refer to the output current flow direction, which is assumed to be direct or positive when it is from the input to the output. With reference to Fig. 3.1, when the output phase, accordingly to the main control algorithm, has to be commutated from one input phase to another, two rules must be respected by any commutation strategy:

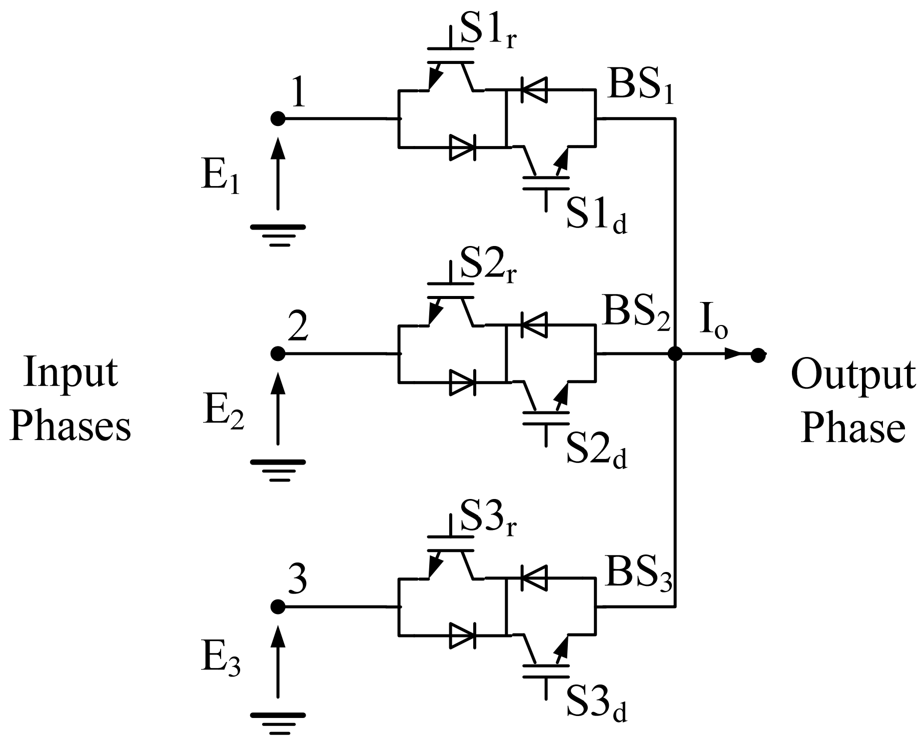

Fig. 3.1. Three phase (input) to single phase (output) basic connection.

i) The commutation does not have to cause a short circuit between the two input phases, because the consequent high circulating current might destroy the switches;

ii) The commutation does not have to cause an interruption of the output current because the consequent overvoltage might likely destroy the switches.

To fulfil these requirements some knowledge of the commutation conditions is mandatory.

In order to carry out a safe commutation, the voltage between the involved bi-directional switches or the output current must be measured.

These information are required in order to determine the proper sequence of the devices switching state combinations that does not lead to the hazard either of a short circuit or of an overvoltage and provides the safe commutation of the output current. This is the common operating principle of all the commutation strategies that have been proposed in literature.

3.3 Modulation Duty Cycle Matrix Approach

The basic scheme of three-phase Matrix Converters has been represented in Fig. 3.2. The switching behaviour of the converter generates discontinuous output voltage waveforms. Assuming inductive loads connected at the output side leads to continuous output current waveforms. In these operating conditions, the instantaneous power balance equation, applied at the input and output side of an ideal converter, leads to discontinuous input currents. The presence of capacitors at the input side is required to ensure continuous input voltage waveforms. In order to analyse the modulation strategies, an opportune converter model is introduced, which is valid considering ideal switches and a switching frequency much higher than input and output frequencies. Under these assumptions, the higher frequency components of the variables can be neglected, and the input/output quantities are represented by their average values over a cycle period T_C .

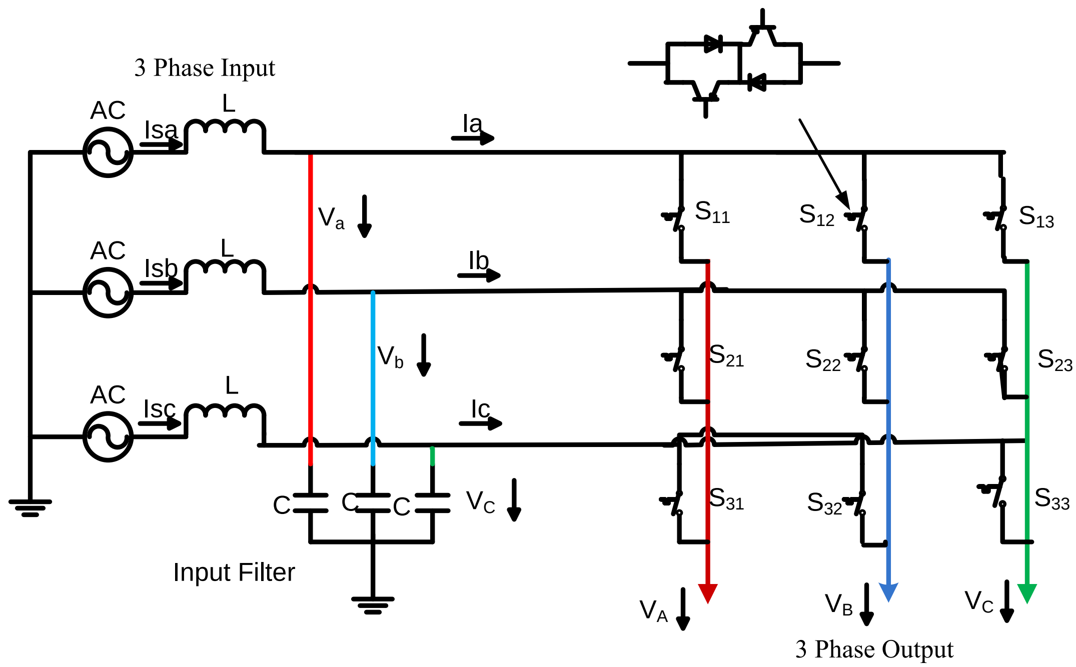

Fig. 3.2. General topology of three phase to three phase Matrix Converter.

The input/output relationships of voltages and currents are related to the states of the nine switches, and can be written in matrix form as shown in reference [3.1]

$$\begin{bmatrix} v_{o1} \\ v_{o2} \\ v_{o3} \end{bmatrix} = \begin{bmatrix} m_{11} & m_{12} & m_{13} \\ m_{21} & m_{22} & m_{23} \\ m_{31} & m_{32} & m_{33} \end{bmatrix} \begin{bmatrix} v_{i1} \\ v_{i2} \\ v_{i3} \end{bmatrix} \tag{3.1}$$

$$\begin{bmatrix} i_{i1} \\ i_{i2} \\ i_{i3} \end{bmatrix} = \begin{bmatrix} m_{11} & m_{12} & m_{13} \\ m_{21} & m_{22} & m_{23} \\ m_{31} & m_{32} & m_{33} \end{bmatrix} \begin{bmatrix} i_{o1} \\ i_{o2} \\ i_{o3} \end{bmatrix} \tag{3.2}$$

with $0 \le m_{hk} \le 1$, h=1,2,3 k=1,2,3. (3.3)

The variables m_{hk} are the duty-cycles of the nine switches S_{hk} and can be represented by the duty-cycle matrix m_x. In order to prevent short-circuit on the input side and ensure uninterrupted load current flow, these duty-cycles must satisfy the three following constraint conditions:

$$\begin{aligned} m_{11} + m_{12} + m_{13} &= 1 \\ m_{21} + m_{22} + m_{23} &= 1 \\ m_{31} + m_{32} + m_{33} &= 1 \end{aligned} \tag{3.4}$$

The determination of any modulation strategy for the Matrix Converter, can be formulated as the problem of determining, in each cycle period, the duty-cycle matrix that satisfies the input-output voltage relationships of equation (3.1),the required instantaneous input power factor, and the constraint conditions from the equations (3.3)-(3.4). The solution of this problem represents a hard task and is not unique, as documented by the different solutions proposed in literature. It should be noted that in order to completely determine the modulation strategy it is necessary to define the switching pattern, which is the commutation sequence of the nine switches. The use of different switching patterns for the same duty-cycle matrix leads to a different behaviour in terms of number of switch commutations and ripple of input and output quantities.

A. Alesina-Venturini 1981 (AV method)

A first solution, obtained by using the duty-cycle matrix approach, has been proposed in reference [3.2]. This strategy allows the control of the output voltages and input power factor, and can be summarized in the following equation, valid for unity input power factor ($\alpha_i = \beta_i$).

$$m_{hk} = \frac{1}{3}\left\{1 + 2q\cos\left[\alpha_o - (h-1)\frac{2\pi}{3}\right]\cos\left[\beta_o - (k-1)\frac{2\pi}{3}\right]\right\} \tag{3.5}$$

Assuming balanced supply voltages and balanced output conditions, the maximum value of the voltage transfer ratio q is 0.5. This low value represents the major drawback of this modulation strategy. The allocation of the switch states within a cycle period is not unique and different switching patterns lead to different input-output ripple performance. A typical double-sided switching pattern usually adopted is represented schematically in Fig. 3.3. It is possible to see by using this modulation technique, 12 switch commutations occur in each cycle period (a commutation takes place when the value of h or k in m_{hk} changes).

B. Alesina-Venturini 1989 (Optimum AV method)

In order to improve the performance of the previous modulation strategy in terms of maximum voltage transfer ratio, a second solution has been presented in reference [3.3]. In this case the modulation law can be described by the following relationship:

$$m_{hk} = \frac{1}{3}\left[\begin{array}{l} 1+2q\cos\left[\beta_i - \dfrac{2\pi(k-1)}{3}\right] \\ \cdot\left[\cos\left(\alpha_o - \dfrac{2\pi(h-1)}{3}\right) - \dfrac{\cos(3\alpha_o)}{6} + \dfrac{\cos(3\beta_i)}{2\sqrt{3}}\right] - \\ \dfrac{2}{3\sqrt{3}}q\left[\cos\left(4\beta_i - (k-1)\dfrac{2\pi}{3}\right) - \cos\left(2\beta_i + (k-1)\dfrac{2\pi}{3}\right)\right] \end{array}\right] \quad (3.6)$$

In particular, the solution given in equation (3.6) is valid for unity input power factor.

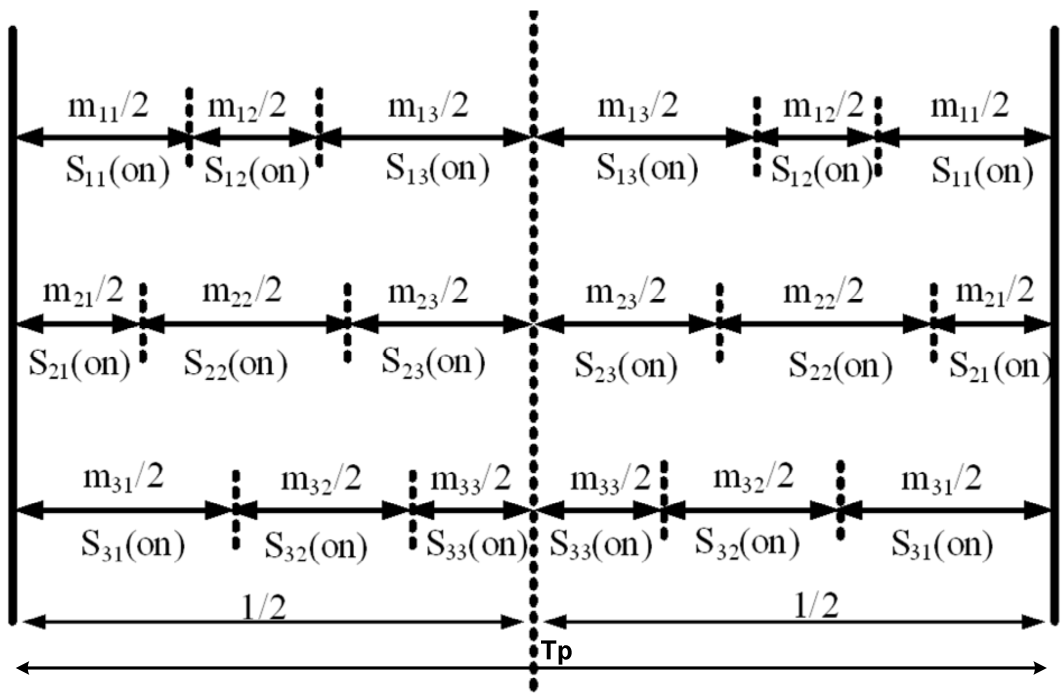

Fig. 3.3. Double-sided switching pattern in a cycle period Tp.

For unity power. factor ($\alpha_i = \beta_i$), and the maximum voltage transfer ratio q is 0.866. It should be noted that in a complete solution, valid for values of the input power factor different from unity, has been derived. The corresponding expressions for m_{hk} are very complex and require the knowledge of the output power factor.

3.4 Space Vector Control Approach

The Space Vector Approach is based on the instantaneous space vector representation of input and output voltages and currents. Among the 27 possible switching configurations available in three-phase Matrix Converters, 21 only can be usefully employed in the SVM algorithm, and can be represented as shown in Tab. 3.1.The first 18 switching configurations determine an output voltage vector $\overline{v_o}$ and an input current vector $\overline{i_i}$, having fixed directions, as represented in Figs. 3.4(a) and (b), and is referred to as "active configurations". The magnitude of these vectors depends upon the instantaneous values of the input line-to-line voltages and output line currents respectively. The last 3 switching configurations determine zero input current and output voltage vectors and is referred to as "zero configurations". The remaining 6 switching configurations have each output phase connected to a different input phase. In this case the output voltage and input current vectors have variable directions and cannot be usefully used to synthesize the reference vectors as shown in references [3.4-3.6].

A. SVM Technique

The SVM algorithm for Matrix Converters presented in this paragraph has the inherent capability to achieve the full control of both output voltage vector and instantaneous input current displacement angle as presented in reference [3.1]. At any sampling instant, the output voltage vector $\overline{v_o}$ and the input current displacement angle ϕ_i are known as reference quantities (Figs. 3.4 (a) and 3.4 (b)). The input line-to-neutral voltage vector $\overline{v_i}$ is imposed by the source voltages and is known by measurements. Then, the control of ϕ_i can be achieved controlling the phase angle β_i of the input current vector. In principle, the SVM algorithm is based on the selection of 4 active configurations that are applied for suitable time intervals within each cycle period T_p . The zero configurations are applied to complete T_p .

In order to explain the modulation algorithm, reference will be made to Figs. 3.5 (a) and (b), where $\overline{v_o}$ and $\overline{i_i}$ are assumed both lying in sector 1, without missing the generality of the analysis. The reference voltage vector $\overline{v_o}$ is resolved into the components $\overline{v_o}'$ and $\overline{v_o}''$ along the two adjacent vector directions. The $\overline{v_o}'$ component can be synthesised using two voltage vectors having the same direction of $\overline{v_o}'$. Among the six possible switching configurations

(±7, ±8, ±9), the ones that allow also the modulation of the input current direction must be selected. It is verified that this constraint allows the elimination of two switching configurations (+8 and -8 in this case). The remaining four, can be assumed to apply the positive switching configurations (+7 and +9). The meaning of this assumption will be discussed later in this paragraph. With similar considerations the switching configurations required to synthesize the $\overline{v_o}''$ component can be selected (+1 and +3).

Table 3.1. SWITCHING CONFIGURATIONS USED IN THE SVM ALGORITHM.

Switch configuration	Switches On			v_o	α_o	i_i	β_i
+1	S_{11}	S_{22}	S_{32}	$2/3\ v_{12i}$	0	$2/\sqrt{3}\ i_{o1}$	$-\pi/6$
−1	S_{12}	S_{21}	S_{31}	$-2/3\ v_{12i}$	0	$-2/\sqrt{3}\ i_{o1}$	$-\pi/6$
+2	S_{12}	S_{23}	S_{33}	$2/3\ v_{23i}$	0	$2/\sqrt{3}\ i_{o1}$	$\pi/2$
−2	S_{13}	S_{22}	S_{32}	$-2/3\ v_{23i}$	0	$-2/\sqrt{3}\ i_{o1}$	$\pi/2$
+3	S_{13}	S_{21}	S_{31}	$2/3\ v_{31i}$	0	$2/\sqrt{3}\ i_{o1}$	$7\pi/6$
−3	S_{11}	S_{23}	S_{33}	$-2/3\ v_{31i}$	0	$-2/\sqrt{3}\ i_{o1}$	$7\pi/6$
+4	S_{12}	S_{21}	S_{32}	$2/3\ v_{12i}$	$2\pi/3$	$2/\sqrt{3}\ i_{o2}$	$-\pi/6$
−4	S_{11}	S_{22}	S_{31}	$-2/3\ v_{12i}$	$2\pi/3$	$-2/\sqrt{3}\ i_{o2}$	$-\pi/6$
+5	S_{13}	S_{22}	S_{33}	$2/3\ v_{23i}$	$2\pi/3$	$2/\sqrt{3}\ i_{o2}$	$\pi/2$
−5	S_{12}	S_{23}	S_{32}	$-2/3\ v_{23i}$	$2\pi/3$	$-2/\sqrt{3}\ i_{o2}$	$\pi/2$
+6	S_{11}	S_{23}	S_{31}	$2/3\ v_{31i}$	$2\pi/3$	$2/\sqrt{3}\ i_{o2}$	$7\pi/6$
−6	S_{13}	S_{21}	S_{33}	$-2/3\ v_{31i}$	$2\pi/3$	$-2/\sqrt{3}\ i_{o2}$	$7\pi/6$
+7	S_{12}	S_{22}	S_{31}	$2/3\ v_{12i}$	$4\pi/3$	$2/\sqrt{3}\ i_{o3}$	$-\pi/6$
−7	S_{11}	S_{21}	S_{32}	$-2/3\ v_{12i}$	$4\pi/3$	$-2/\sqrt{3}\ i_{o3}$	$-\pi/6$
+8	S_{13}	S_{23}	S_{32}	$2/3\ v_{23i}$	$4\pi/3$	$2/\sqrt{3}\ i_{o3}$	$\pi/2$
−8	S_{12}	S_{22}	S_{33}	$-2/3\ v_{23i}$	$4\pi/3$	$-2/\sqrt{3}\ i_{o3}$	$\pi/2$
+9	S_{11}	S_{21}	S_{33}	$2/3\ v_{31i}$	$4\pi/3$	$2/\sqrt{3}\ i_{o3}$	$7\pi/6$
−9	S_{13}	S_{23}	S_{31}	$-2/3\ v_{31i}$	$4\pi/3$	$-2/\sqrt{3}\ i_{o3}$	$7\pi/6$
0_1	S_{11}	S_{21}	S_{31}	0	-	0	-
0_2	S_{12}	S_{22}	S_{32}	0	-	0	-
0_3	S_{13}	S_{23}	S_{33}	0	-	0	-

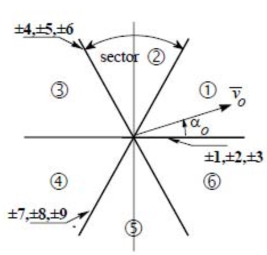

a.

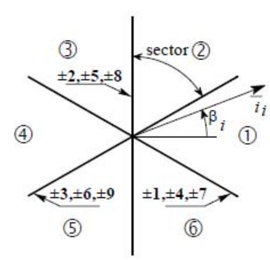

b.

Fig. 3.4. Direction of the output line-to neutral voltage vectors generated by the active configurations.

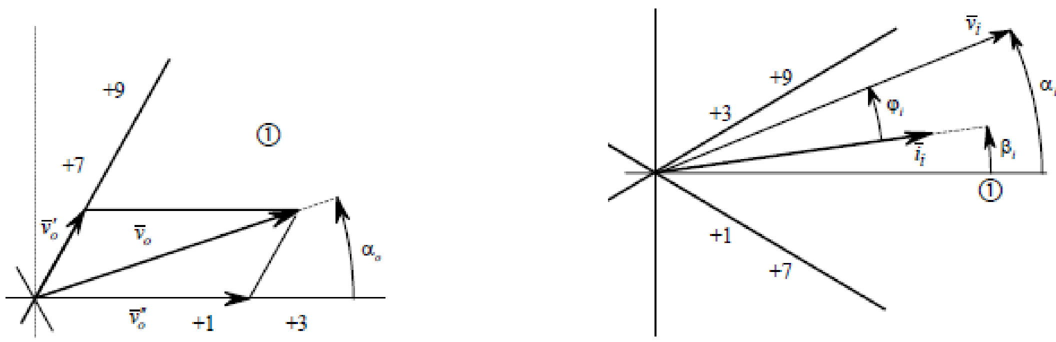

a. b.

Fig. 3.4a. Output voltage vectors modulation principle. Fig. 3.4(b) - Input current vectors modulation principle.

Using the same procedure, it is possible to determine the four switching configurations related to any possible combination of output voltage and input current sectors, leading to the results summarized in Tab. 3.2. Four symbols (I, II, III, IV) are also introduced in the last row of Table. 3.2 to identify the four general switching configurations, valid for any combination of input and output sectors. Now it is possible to write, in a general form, the four basic equations of the SVM algorithm, which satisfy, at the same time, the requirements of the reference output voltage vector and input current displacement angle. With reference to the output voltage vector, the two following equations can be written:

Table 3.2. Selection of the switching configurations for each combination of output voltage and input current sectors.

		Sector of the output voltage vector											
		1 or 4				2 or 5				3 or 6			
Sector of the input current vector	1 or 4	+9	+7	+3	+1	+6	+4	+9	+7	+3	+1	+6	+4
	2 or 5	+8	+9	+2	+3	+5	+6	+8	+9	+2	+3	+5	+6
	3 or 6	+7	+8	+1	+2	+4	+5	+7	+8	+1	+2	+4	+5
		I	II	III	IV	I	II	III	IV	I	II	III	IV

$$\overline{v_o}' = \overline{v_o{}^I}\delta^I + \overline{v_o{}^{II}}\delta^{II} = \frac{2}{\sqrt{3}} v_o \cos\left(\hat{\alpha}_o - \frac{\pi}{3}\right) e^{j\left[(K_v-1)\pi/3+\pi/3\right]} \tag{3.7}$$

$$\overline{v_o}'' = \overline{v_o{}^{III}}\delta^{III} + \overline{v_o{}^{IV}}\delta^{IV} = \frac{2}{\sqrt{3}} v_o \cos\left(\hat{\alpha}_o + \frac{\pi}{3}\right) e^{j\left[(K_v-1)\pi/3\right]} \tag{3.8}$$

With reference to the input current displacement angle, two equations are obtained by imposing to the vectors $\overline{v_o{}^I}\delta^I + \overline{v_o{}^{II}}\delta^{II}$ and $\overline{v_o{}^{III}}\delta^{III} + \overline{v_o{}^{IV}}\delta^{IV}$ to have the direction defined by β_i. This can be achieved by imposing a null-value to the two vectors component along the direction perpendicular to $e^{j\beta_i}$ (i.e. $je^{j\beta_i}$), leading to

$$\left(\overline{v_o{}^I}\delta^I + \overline{v_o{}^{II}}\delta^{II}\right).je^{j\beta_i} e^{j(K_i-1)\pi/3} = 0 \tag{3.9}$$

$$\left(\overline{v_o{}^{III}}\delta^{III} + \overline{v_o{}^{IV}}\delta^{IV}\right).je^{j\beta_i} e^{j(K_i-1)\pi/3} = 0 \tag{3.10}$$

In equations (3.7)-(3.10) $\hat{\alpha}_o$ and $\hat{\beta}_i$ are the output voltage and input current phase angle measured with respect to the bisecting line of the corresponding sector, and differ from $\hat{\alpha}_o$ and $\hat{\beta}_i$ according to the output voltage and input current sectors. In these equations the following angle limits apply

$$-\frac{\pi}{6} \le \hat{\alpha}_o \le +\frac{\pi}{6}, \qquad -\frac{\pi}{6} \le \hat{\beta}_i \le +\frac{\pi}{6} \tag{3.11}$$

$\delta^I, \delta^{II}, \delta^{III}, \delta^{IV}$ are the duty-cycles (i.e. $\delta^I = t^I / T_p$) of the 4 switching configurations, K_v=1,2,..,6 represents the output voltage sector and K_i=1,2,…,6 represents the input current sector. v_0^I , v_0^{II} , v_0^{III} , v_0^{IV} are the output voltage vectors associated respectively with the switching configurations I, II, III, IV given in Tab. 3.2. The same formalism is used for the input current vectors.

Solving equations (3.7)-(3.10) with respect to the duty-cycles, after some tedious manipulations, leads to the following relationships as seen from reference [3.7]:

$$\delta^I = (-1)^{K_v+K_i} \frac{2}{\sqrt{3}} q. \frac{\cos\left(\widehat{\alpha}_o - \frac{\pi}{3}\right)\cos\left(\widehat{\beta}_o - \frac{\pi}{3}\right)}{\cos\phi_i} \tag{3.12}$$

$$\delta^{II} = (-1)^{K_v+K_i+1} \frac{2}{\sqrt{3}} q. \frac{\cos\left(\widehat{\alpha}_o - \frac{\pi}{3}\right)\cos\left(\widehat{\beta}_o + \frac{\pi}{3}\right)}{\cos\phi_i} \tag{3.13}$$

$$\delta^{III} = (-1)^{K_v+K_i+1} \frac{2}{\sqrt{3}} q. \frac{\cos\left(\widehat{\alpha}_o + \frac{\pi}{3}\right)\cos\left(\widehat{\beta}_o - \frac{\pi}{3}\right)}{\cos\phi_i} \tag{3.14}$$

$$\delta^{IV} = (-1)^{K_v+K_i} \frac{2}{\sqrt{3}} q. \frac{\cos\left(\widehat{\alpha}_o + \frac{\pi}{3}\right)\cos\left(\widehat{\beta}_o + \frac{\pi}{3}\right)}{\cos\phi_i} \tag{3.15}$$

Equations (3.12) - (3.15) have a general validity and can be applied for any combination of output voltage sector K_v and input current sector K_i.It should be noted that, for any sector combinations, two of the duty cycles calculated by equations (3.12)-(3.15) assume negative values. This is due to the assumption made of using only the positive switching configurations in writing the basic equations (3.7)-(3.10). A negative value of the duty-cycle means that the corresponding negative switching configuration has to be selected instead of the positive one. Furthermore, for the feasibility of the control strategy, the sum of the absolute values of the four duty-cycles must be lower than unity.

$$\left|\delta^I\right| + \left|\delta^{II}\right| + \left|\delta^{III}\right| + \left|\delta^{IV}\right| \le 1 \tag{3.16}$$

The zero configurations are applied to complete the cycle period. By introducing equations (3.12)-(3.15) in equation (3.16), after some manipulations, leads to the following equation.

$$q \le \frac{\sqrt{3}}{2} \frac{|\cos\phi_i|}{\cos\widehat{\alpha}_o \cos\widehat{\beta}_i} \tag{3.17}$$

Equation (3.17) represents, at any instant, the theoretical maximum voltage transfer ratio, which is dependent on the output voltage and input current phase angles and the displacement angle of the input current vector. It is useful to note that, in the particular case of balanced supply voltages and balanced output voltages, the maximum voltage transfer ratio occurs when equation (3.17) is a minimum (i.e. when $\cos\widehat{\beta}_i$ and $\cos\widehat{\alpha}_o$ are equal to 1), leading to

$$q \le \frac{\sqrt{3}}{2} |\cos\phi_i| \tag{3.18}$$

Assuming unity input power factor, equation (3.18) gives the well-known maximum voltage transfer ratio of Matrix Converters 0.866.Using the SVM technique, the switching pattern is defined by the switching configuration sequence. With reference to the particular case of output voltage vector lying in sector 1 and input current vector lying in sector 1, the switching configurations selected are, in general, 0_1, 0_2, 0_3, +1, -3, -7, +9. It can be verified that there is only one switching configuration sequence characterized by only one switch commutation for each switching configuration change, that is 0_3, -3, +9, 01, -7, +1, 02. The corresponding general double-sided switching pattern is shown in Fig. 3.5.

The use of the three zero configuration leads to 12 switch commutations in each cycle period. It should be noted that the possibility to select the duty-cycles of three zero configurations gives two degree of freedom, being $\delta_{01} + \delta_{02} + \delta_{03} = 1 - \delta_1 - \delta_7 - \delta_3 - \delta_9$. These two degree of freedom can be utilized to define different switching patterns, characterized by different behaviour in terms of ripple of the input and output quantities. In particular, the two degree of freedom might be utilized to eliminate one or two zero configurations, affecting also the number of commutations in each cycle period.

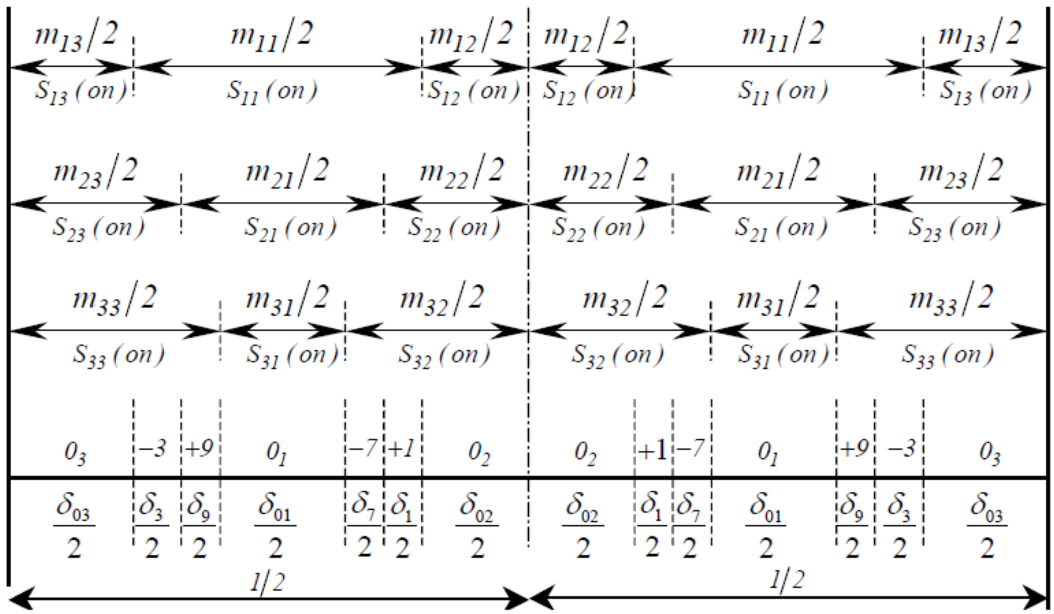

Fig. 3.5. Double-sided switching pattern in a cycle period Tp [3.7].

3.7 Carrier-Based PWM Approach

A. Carrier Based Control Strategy

Considering a balanced three-phase system, the input voltages can be given as

$$
\begin{aligned}
v_a &= |V|\cos(\omega t) \\
v_b &= |V|\cos(\omega t - 2\pi/3) \\
v_b &= |V|\cos(\omega t - 4\pi/3)
\end{aligned}
\tag{3.19}
$$

The duty ratios should be so chosen that the output voltage remains independent of input frequency. In other words the three-phase balanced input voltages can be considered to be in stationary reference frame and the output voltage can be considered to be in synchronous reference frame, so the that input frequency term will be absent in the output voltage as shown in references [3.8-3.10]. Hence the duty ratios d_{aA}, d_{bA} *and* d_{cA} are chosen as

$$
\begin{aligned}
d_{aA} &= k\cos(\omega t - \rho), \\
d_{bA} &= k\cos(\omega t - 2\pi/3 - \rho), \\
d_{cA} &= k\cos(\omega t - 4\pi/3 - \rho)
\end{aligned}
\tag{3.20}
$$

Therefore the phase A output voltage can be obtained by using the above duty ratios as

$$v_A = k_A\widehat{V}[\cos(\omega t)\bullet\cos(\omega t-\rho)+\cos(\omega t-2\pi/3)\bullet\cos(\omega t-2\pi/3-\rho)$$
$$+\cos(\omega t-4\pi/3)\bullet\cos(\omega t-4\pi/3-\rho)] \tag{3.21}$$

In general equation (3.21) can be written as:

$$v_A = \frac{3}{2}k_A\widehat{V}\cos(\rho) \tag{3.22}$$

In equation (3.22), $\cos(\rho)$ term indicates that the output voltage is affected by the choice of ρ and later it will be explained that the input power factor depends on ρ. Thus, the output voltage V_A is independent of the input frequency and only depends on the amplitude $\widehat{V}$ of the input voltage and k_A is a time-varying signal with the desired output frequency ω_o. The 3-phase reference output voltages can be represented as:

$$\begin{aligned} k_A &= m\cos(\omega_o t), \\ k_B &= m\cos(\omega_o t-2\pi/3), \\ k_C &= m\cos(\omega_o t-4\pi/3) \end{aligned} \tag{3.23}$$

Where k_B and k_C are the reference output voltage modulating signals for the output phases *B* and *C* respectively. Therefore, from equation (3.22), the output voltage in phase-*A* is:

$$v_A = \left[\frac{3}{2}k_A\widehat{V}\cos(\rho)\right]\cos(\omega_o t) \tag{3.24}$$

B. Application of Offset Duty Ratios

In the discussions, mentioned in the section (3.7. A), duty-ratios become negative which are not practically realizable. For the switches connected to output phase-A, at any instant, the condition $0 \le d_{aA}, d_{bA}, d_{cA} \le 1$ should be valid. Therefore, offset duty ratios should to be added to the existing duty-ratios, so that the net resultant duty-ratios of individual switches are always positive. Furthermore, the offset duty-ratios should be added equally to all the output phases to ensure that the resultant output voltage vector produced by the offset duty ratios is null in the load. That is, the offset duty-ratios can only add the common-mode voltages in the output. Considering the case of output phase-A as shown in reference [3.9]:

$$d_{aA}+d_{bA},+d_{cA} = k_A\cos(\omega t-\rho)+k_A\cos(\omega t-2\pi/3-\rho)+k_A\cos(\omega t-4\pi/3-\rho)=0 \tag{3.25}$$

To cancel the negative components from individual duty ratios absolute value of the duty-ratios are added. Thus the minimum individual offset duty ratios should be $D_a(t)=|0.5\cos(\omega t-\rho)|, D_b(t)=|0.5\cos(\omega t-2\pi/3-\rho)| and \ldots D_c(t)=|0.5\cos(\omega t-4\pi/3-\rho)|$ respectively. The effective duty ratios are $d_{aA}+D_a(t), d_{bA}+D_b(t), d_{cA}+D_c(t)$. The same holds good for the input phases b and c. The net duty ratio $d_{aA}+D_a(t)$ should be accommodated within a range of 0 to 1.

Thus $0\le d_{aA}+D_a(t)\le 1$, i.e $0\le k_A\cos(\omega t-\rho)+|k_A\cos(\omega t-\rho)|\le 1$. This implies that in the worst case $0\le 2.|k_A|\le 1$ The maximum value of $|k_A|$ or in other words '*m*' in equation (3.23) is equal to 0.5. Hence the offset duty-ratios (Fig. 3.5) corresponding to the three input phases are chosen as

$$\begin{aligned}
D_a(t)&=|0.5\cos(\omega_o t)|,\\
D_b(t)&=|0.5\cos(\omega_o t-2\pi/3)|,\\
D_c(t)&=|0.5\cos(\omega_o t-4\pi/3)|
\end{aligned} \tag{3.26}$$

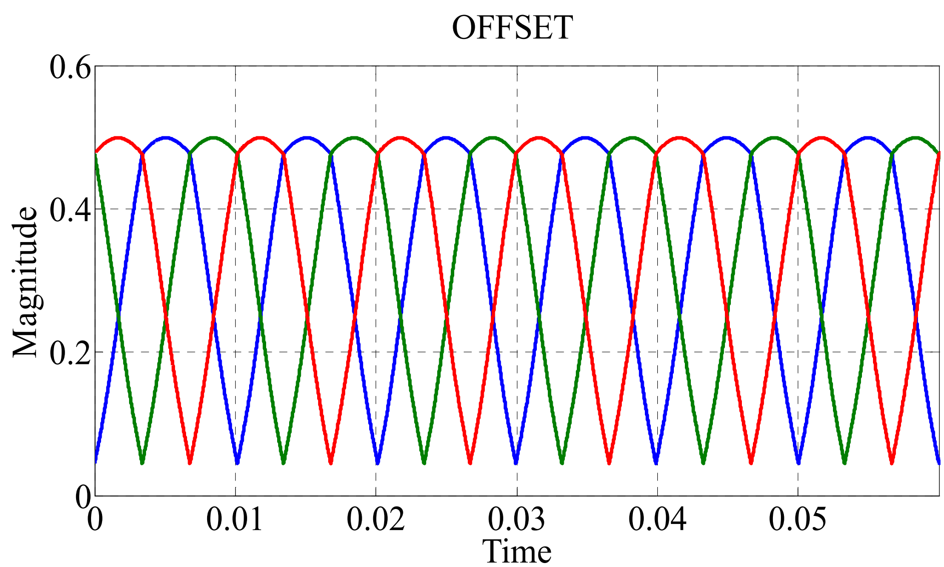

Fig. 3.6. Modified offset duty ratios for all input phases.

Thus the modified duty ratios for output phase-*A* are

$$\begin{aligned}
d_{aA}&=D_a(t)+m\cos(\omega_o t),\\
d_{bA}&=D_b(t)+m\cos(\omega_o t-2\pi/3),\\
d_{cA}&=D_c(t)+m\cos(\omega_o t-4\pi/3)
\end{aligned} \tag{3.27}$$

In any switching cycle the output phase has to be connected to any of the input phases. The summation of the duty ratios in equation (3.27) must equal to unity. But the summation $\{D_a(t)+D_b(t)+D_c(t)\}$ is less than or equal to unity as shown in Fig. 3.5. Hence another offset duty-ratio $(1-\{D_a(t)+D_b(t)+D_c(t)\})/3$ is added $D_a(t), D_b(t) and D_c(t)$ in equation (3.27). The addition of this offset duty-ratio in all switches will maintain the output voltages and input currents unaffected. Similarly, the duty-ratios are calculated for the output phases *B* and *C*.

If k_A, k_B and k_C are chosen to be 3-phase sinusoidal references as given in Equation (3.23), the input voltage capability is not fully utilized for output voltage generation. To overcome this, an additional common mode term equal to $[-\{\max(k_A,k_B,k_C)+\min(k_A,k_B,k_C)\}/2]$ is added as in the carrier-based space-vector PWM principle as implemented in two-level inverters. Thus the amplitude of k_A, k_B and k_C can be enhanced from 0.5 to 0.57.

Thus the duty-ratios for output phase-A are modified as:

$$\begin{aligned}
d_{aA} &= D_a(t)+(1-\{D_a(t)+D_b(t)+D_c(t)\})/3+[k_A-\{\max(k_A,k_B,k_C)+\\
&\min(k_A,k_B,k_C)\}/2]\times\cos(\omega t-\rho)\\
d_{bA} &= D_a(t)+(1-\{D_a(t)+D_b(t)+D_c(t)\})/3+[k_A-\{\max(k_A,k_B,k_C)+\\
&\min(k_A,k_B,k_C)\}/2]\times\cos(\omega t-2\pi/3-\rho)\\
d_{cA} &= D_a(t)+(1-\{D_a(t)+D_b(t)+D_c(t)\})/3+[k_A-\{\max(k_A,k_B,k_C)+\\
&\min(k_A,k_B,k_C)\}/2]\times\cos(\omega t-4\pi/3-\rho)
\end{aligned} \tag{3.28}$$

3.8 Direct Duty Ratio Based PWM approach

In this section, the pulse width modulation technique is discussed based on duty ratio calculation in conjunction with the generalised three-to three-phase topology of the proposed Matrix Converter. The duty ratio based PWM (DPWM) is developed by using the concept of per-phase output average over one switching period as discussed in references [3.10-3.11]. The developed scheme is modular in nature and is thus applicable to the generalised converter circuit topology.

It is assumed that a switching period T_S of the carrier wave consist of two sub-periods, T_1 (rising slope of the triangular carrier) and T_2 (falling slope of the triangular carrier). When the carrier changes from zero to the peak value, the sub-period is called $T_{1,}$ and when the carrier changes from peak to the zero value it is termed as sub-interval T_2. The input three-phase sinusoidal waveform can assume different values at different instants of times. The maximum among the three input signals is termed as *Max*, the medium amplitude among three input signals is termed as *Mid* and the smallest magnitude is represented as *Min.* During interval T_1 (positive slope of the carrier), the line-to-line voltage between *Max* and *Min* ($Max\{v_A, v_B, v_C\} - Min\{v_A, v_B, v_C\}$) phases is used for the calculation of duty ratio and no consideration is given to the medium amplitude of input signal. The output voltage should initially follow the *Max* signal of the input and then should follow the *Min* signal of the input. During interval T_2, two line voltages between *Max* and *Mid* ($Max\{v_A, v_B, v_C\} - Mid\{v_A, v_B, v_C\}$) and *Mid* and *Min* ($Mid\{v_A, v_B, v_C\} - Min\{v_A, v_B, v_C\}$) is calculated first, and the largest among the two is used for the calculation of the duty ratio. This is done to balance the volt-second principle. Two different cases can arise in time period T_2 depending upon the relative magnitude of the input voltages. If *(Max-Mid)* > *(Mid-Min)*, the output should follow *Max* for certain time period and then follow *Mid* for certain time period. This situation is termed as Case I. This is further explained in the next section. Similarly, if *Max-Mid* <*Mid-Min*, the output should follow at first *Mid* of the input signal and then *Min* of the input signal and this is termed as Case II. Thus DPWM approach uses two out of three of the line-to-line input voltages to synthesis output voltages, and all the three input phases are utilized to conduct current during each switching period. Case I and Case II and the generation of gating signals are further elaborated in the next section.

i) *Case-I*: For condition *(Max-Mid)* ≥ *(Mid-Min),* the generation of gating pattern for k^{th} output phase is illustrated in Fig. 3.6 for one switching period. To generate the pattern, at first the duty ratio $D_{k1}, k \in a, b \,\&\, c$, is calculated and then compared with high frequency triangular carrier signal to generate the k^{th} output phase pattern. The gating pattern for the k^{th} leg of the Matrix Converter is directly derived from the output pattern. The switching pattern is drawn assuming that the *Max* is the phase 'A' of the input, *Mid* is the phase 'B' and *Min* is the phase 'C'. The switching pattern changes in accordance with the variation in the relative magnitude of the input phases. The output follows *Min* of the input signal if the magnitude of the duty ratio is more than the magnitude of the carrier and the slope of the carrier is positive. The output follows the *Max* of the input signal if the magnitude of the carrier is more than the magnitude of the duty ratio irrespective of the slope of the carrier. Finally, the output tracks *Mid* if the magnitude of the carrier signal is smaller compared to the magnitude of the duty ratio and the slope of the carrier is negative. Thus, the resulting output phase voltage changes like *Min→Max→Max→Mid*. These transition periods are termed as, t_{k1}, t_{k2}, t_{k3} and t_{k4} and these four sub-intervals can be expressed presented in references [3.10-3.12]:

$$\begin{aligned}
&t_{k1} = D_{k1}\delta T_s \\
&t_{k2} = (1 - D_{k1})\delta T_s \\
&t_{k3} = (1 - D_{k1})(1 - \delta)T_s \\
&t_{k4} = D_{k1}(1 - \delta)T_s \\
&T_s = t_{k1} + t_{k2} + t_{k3} + t_{k4}
\end{aligned} \tag{3.29}$$

Where D_{k1} is the k^{th} phase duty ratio value, when Case I is under consideration and δ is defined by $\delta = \frac{T_1}{T_s}$, which refers to the fraction of the slope of the carrier. Now, by using the volt-second principle of PWM control, the following equation can be written:

$$v_{ok}^{*}T_s = \int_{0}^{T_s} v_{ok}\,dt = Min\{v_A, v_B, v_C\}.t_{k1} + Max\{v_A, v_B, v_C\}.\left(t_{k2} + t_{k3}\right) + Mid\{v_A, v_B, v_C\}.t_{k4} \tag{3.30}$$

Substituting the time intervals expressions from equation (3.29) into equation (3.30), yield

$$v_{ok}^{*} = \frac{1}{T_s}\int_{0}^{T_s} v_{ok}\,dt = D_{k1}\begin{pmatrix} \delta.Min\{v_A, v_B, v_C\} - \delta.Mid\{v_A, v_B, v_C\} + \\ Mid\{v_A, v_B, v_C\} - Max\{v_A, v_B, v_C\} \end{pmatrix} + Max\{v_A, v_B, v_C\} \tag{3.31}$$

Where T_s is the sampling period, v_{ok}^{*}, v_{ok} are the reference and actual average output voltage of phase '*k*', respectively and v_A, v_B, v_C are the input side three-phase voltages. *Max, Mid* and *Min* refer to the maximum, medium and minimum values, D_k represents the duty ratio of the power switch.

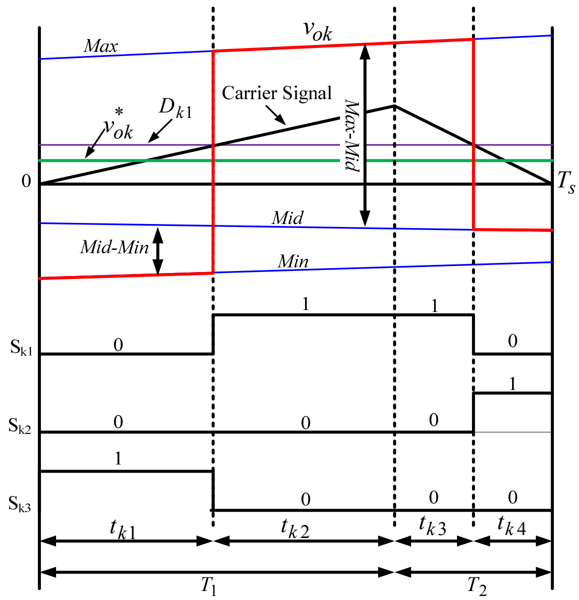

Fig. 3.7. Output and Switching pattern for kth phase in the Case I.

The duty ratio is obtained from equation (3.31) as:

$$D_{k1} = \frac{Max\{v_A, v_B, v_C\} - v_{ok}^*}{\Delta + \delta\left(Mid\{v_A, v_B, v_C\} - Min\{v_A, v_B, v_C\}\right)} \tag{3.32}$$

Where $\Delta = \left(Max\{v_A, v_B, v_C\} - Mid\{v_A, v_B, v_C\}\right)$

Similarly, the duty ratios of other output phases can be obtained which can subsequently be used for implementation of the PWM scheme.

ii) *Case-II*: Now considering another situation of *Max-Mid* <*Mid-Min.* The output and the switching patterns can be derived once again following the same principle laid down in the previous sub section. Fig. 3.7 shows the output and switching pattern for the k^{th} output phase. Here once again a high frequency triangular carrier wave is compared with the duty ratio value, D_{k2} to generate the switching pattern. The only difference in this case when compared to the previous one is the interval when the magnitude of the carrier signal is greater than the magnitude of the duty ratio and the slope is negative. Then, the output should follow *Mid* instead of *Max*. Contrary to Case I, for this situation the output must follow *Max* of the input. The time intervals t_{k1}, t_{k2}, t_{k3} and t_{k4} are the same as in equation (3.29) and now the output phase voltage is changed with the sequence of *Min→Max→Mid→Min*. The volt-second principle is now applied to derive the equation for the duty ratio. The volt-second principle equation can be written as:

$$v_{ok}^{*}T_s = \int_0^{T_s} v_{ok}dt = Min\{v_A, v_B, v_C\}.(t_{k1} + t_{k4}) + Max\{v_A, v_B, v_C\}.t_{k2} + Mid\{v_A, v_B, v_C\}.t_{k3} \tag{3.33}$$

Now once again substituting the time expression from equation (3.29) into equation (3.33), one obtains:

$$\begin{aligned} v_{ok}^{*} = \frac{1}{T_s}\int_0^{T_s} v_{ok}dt = D_{k2}&\begin{pmatrix} Min\{v_A, v_B, v_C\} - \delta.Max\{v_A, v_B, v_C\} - \\ Mid\{v_A, v_B, v_C\} + \delta.Mid\{v_A, v_B, v_C\} \end{pmatrix} + \\ \delta.Max\{v_A, v_B, v_C\} - \delta.Mid\{v_A, v_B, v_C\} &+ Mid\{v_A, v_B, v_C\} \end{aligned} \tag{3.34}$$

The duty ratio can now be obtained as:

$$D_{K2} = \frac{\delta.\Delta + \left(Mid\{v_A, v_B, v_C\} - v_{ok}^{*}\right)}{\delta.\Delta + \left(Mid\{v_A, v_B, v_C\} - Min\{v_A, v_B, v_C\}\right)} \tag{3.35}$$

The switching signals for the bi-directional power switching devices can be generated by considering the switching states of Fig. (3.6) and of Fig. (3.7.) Depending upon the output pattern, the gating signals are derived. If the output pattern of phase "*k*" is *Max* (or *Mid*, *Min*), the output phase "*k*" is connected to the input phase whose voltage is *Max* (or *Mid*, *Min*).

The input voltages are at first examined for their relative magnitudes and the phases with maximum, medium, and minimum values are determined. The information about their relative magnitudes are given to the next computation block along with the commanded output phase voltages. The computation block either uses equation (3.32) or equation (3.35) to generate the duty ratios depending upon the relative magnitude of the input voltages. The duty ratio obtained goes to the PWM block. The PWM block calculates the time sub-interval using equation (3.29). The gating pattern is then derived accordingly and given to the Matrix Converter.

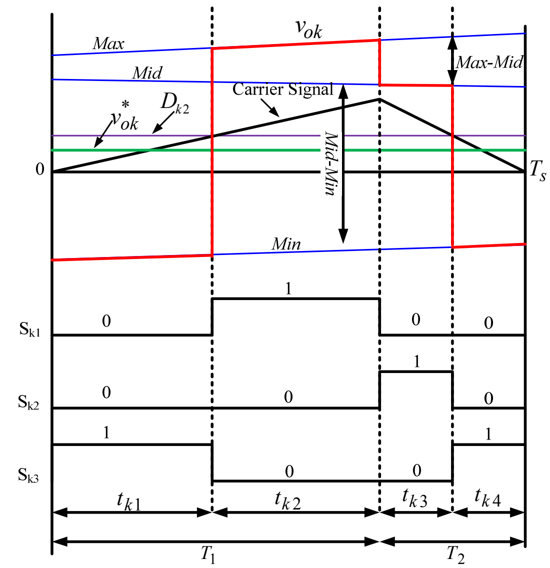

Fig. 3.8. Output and Switching pattern for k^{th} phase in the Case II.

3.9 Summary

This chapter encompasses the modelling and control issues of a three-phase input and three-phase output Matrix Converter. Modelling based on space vector approach is elaborated in several literature which is summarized in this chapter. Control issues are also discussed in this chapter. It is seen that the first PWM reported in the literature, called 'scalar control' produces only 50% output, in other words, the maximum obtainable output voltage is only 50% that of input voltage. The control approach is improved by injecting harmonic components and the output is raised to 86% of the input value. The quality of output voltage is further enhanced by employing space vector PWM technique. The implementation of space vector PWM is quite complex. This is followed by the discussion on Carrier-based PWM and direct duty ratio based PWM.

References:

[3.1] M.P. Kazmierkowski, R. Krishnan, F. Blaabjerg, "*Control in Power Electronics-Selected Problems",* Academic Press, UK, 2002.

[3.2] A. Alesina, M. Venturini, "Solid state power conversion: A Fourier analysis approach to generalised transformer synthesis," IEEE Trans. Circuit System*,* vol. 28, no. CS-4, pp. 319-330, April 1981.

[3.3] A. Alesina, M. Venturini, "Analysis and design of optimum-amplitude nine-switch direct AC-AC converters," IEEE Transactions on Power Electronics., vol. 4, no. 1, pp. 101–12, Jan 1989.

[3.4] L. Huber, D. Borojevic, “Space vector modulator for forced commutated cycloconverters,” in Conference Record of the IEEE Industry Applications Society Annual Meeting, 1989, vol. 1, pp. 871–6.
[3.5] L. Huber, D. Borojevic, N. Burany, “Voltage space vector based pwmcontrol of forced commutated cycloconverters,” in IECON ’89. 15th Annual Conference of IEEE Industrial Electronics Society, 1989, vol. 1, pp. 106–11.
[3.6] L. Huber, D. Borojevic, “Space vector modulation with unity input power factor for forced commutated cyclo-converters,” in Conference Record of the 1991 IEEE Industry Applications Society Annual Meeting,1991, vol. 1, pp. 1032–41.
[3.7] R.A. Petrocelli, “New Modulation methods for Matrix Converters”, *PhD Thesis, Manchester University,* May 2002.
[3.8] Y. D. Yoon, S. K. Sul, “Carrier-Based Modulation Technique for Matrix Converter.” IEEE Trans. Power Electron*,* vol. 21, no. 6, pp 1691-1703, Nov. 2006.
[3.9] P. Satish, K.K. Mohapatra, N. Mohan, “Carrier-based control of Matrix Converter in linear and over-modulation region,” SCSC 2007, pp. 98-105.
[3.10] Yulong Li, Nam-Sup Choi, "Carrier Based Pulse Width Modulation for Matrix Converters," proceeding of IEEE APEC Conf., Washington DC, February, 2009.
[3.11] L. Yulong, C. Nam-Sup , H. Byung-Moon, N. Eui-Cheol, “Fault-tolerant modulation strategy with direct duty-ratio PWM for Matrix Converter-fed motor drives”, IEEE 8th International Conference on Power Electronics and ECCE Asia (ICPE & ECCE), 2011, pp. 2891 – 2898.
[3.12] Yulong Li, Nam-Sup Choi, Byung-Moon Han, Kyoung Min Kim, Buhm Lee, Jun-Hyub Park, “Direct Duty Ratio Pulse Width Modulation Method for Matrix Converter,” International Journal of Control, Automation, and Systems, vol. 6, no. 5, Oct. 2008, pp. 660-669.

Chapter 4
Modelling of Multi-phase Multi-motor Drive System

4.1 Introduction

Concept for multi-motor drive systems, based on utilization of multi-phase machines and multi-phase power converters, have been proposed almost a decade ago as specified in reference [4.1]. Since field oriented control of any multi-phase machine requires only two stator current components, the additional stator current components available in multi-phase machine can be used to control other machines. It has been shown that, by connecting multi-phase stator windings in series/parallel with an appropriate phase transposition, it is possible to control independently all the machines with supply coming from a single multi-phase power converter. One specific drive system, covered by this general concept, is the five-phase series-connected two-motor drive, consisting of two five-phase machines and supplied from a single five-phase voltage source inverter. Such topology has been analysed in a considerable depth as discussed in references [4.1]-[4.2] and experimental verification of the existence of control decoupling in this two-motor drive has been provided in references [4.3]-[4.6]. The studies are based on inverter current control in the stationary reference frame, using phase current control in conjunction with hysteresis or ramp-comparison current controllers. The experimental rig utilizes ramp-comparison current control as shown in reference [4.3].

The control techniques developed so far for the five-phase voltage source inverter feeding five-phase series-connected two-motor drive, once again are based on pulse width modulation. Carrier-based sinusoidal PWM are used in reference [4.4]. A modification in the scheme is suggested in reference [4.4] where fifth harmonic is injected in the reference voltages. With the harmonic injection the output voltage magnitude is increased, similar to single-motor drive. A number of space vector PWM techniques have been reported for a multi-phase VSI (five, six, seven and nine phases) for single motor drive in references [4.7-4.25] where attempts have been made to generate sinusoidal waveform. Considering five-phase system there exist two orthogonal planes namely *d-q* and *x-y*. Unwanted low-order harmonics are generated in the output of a five-phase VSI when the space vectors of *x-y* plane are not eliminated completely and they result in distortion in stator current and losses in the machine having sinusoidal mmf distribution. In case of concentrated winding machine, low order harmonic currents are injected along with the fundamental to enhance the torque production. In such cases it is desirable to produce low-order harmonic along with the fundamental as illustrated in reference [4.27].

The use of other types of power converters such as direct AC-AC converter, back-to-back converter is rarely used in the literature to control the multi-phase multi-motor drive system. Use of direct Matrix Converter is elaborated further in Chapters 5-7.

A specific case of, six-phase two-motor drive is presented in reference [4.6] where a symmetrical six-phase machine (60˚ phase displacement with single neutral point) connected in series with a three-phase machine is described. Similar to series connection of multi-phase machines, parallel connection are also possible with independent control of each machine and supplied from one inverter as shown in reference [4.26]. The series-connected multi-motor drive increases the copper losses of both machines and thus lowers the efficiency. However, it is suggested that for special applications where the load requirement is such that all the motors are not fully loaded simultaneously, this technique is beneficial. One such application is identified as winder drive.

Another drive system, covered by the general concept of series and parallel connection, is the seven-phase series-connected three-motor drive, consisting of three seven-phase machines and supplied from a single seven-phase voltage source inverter. This drive system is reported in references [4.27-4.28]. However, no mathematical model of the overall drive structure is presented in the literature. The modelling of seven-phase series-connected drive system is covered in this chapter.

A number of space vector PWM techniques have been reported for a seven-phase VSI for single motor drive references [4.28-4.30] where attempts have been made to generate sinusoidal waveform.

Considering a seven-phase system there exist three orthogonal planes namely *d-q, x1-y1* and *x2-y2*. Unwanted low-order harmonics are generated in the output of a seven-phase VSI when the space vectors of *x1-y1* and *x2-y2* plane are not eliminated completely and they result in distortion in stator current and losses in the machine having sinusoidal mmf distribution. In case of concentrated winding machine, low order harmonic currents are injected along with the fundamental to enhance the torque production. In such cases it is desirable to produce low-order harmonic along with the fundamental.

This chapter elaborate the modelling of three different drive structures;

- Five-phase series-connected two-motor drive

- Six-phase series-connected two-motor drive, and
- Seven-phase series-connected three-motor drive.

4.2 Modelling of five-phase series-connected two-motordrives

Block diagram of the two-motor drive systems is illustrated in Fig. 4.1.

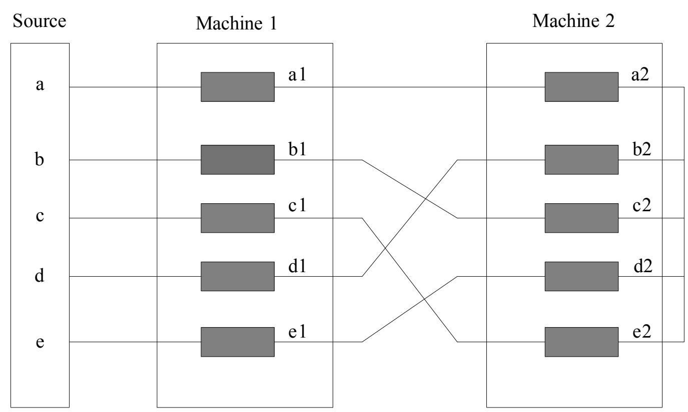

Fig. 4.1. Five-phase series-connected two-motor drive structure.

In Fig. 4.1, the source is a five-phase power converter that can be either a direct AC-AC converter (Matrix Converter) or a voltage source inverter, which directly feed a five-phase machine. The five-phase machine has open-end windings, the second end of the first machine windings are connected with appropriate phase transposition to the second five-phase machine. The second end of the windings is shorted to form the star point. The connection scheme is given in Table 4.1.

Table 4.1. Connectivity matrix for five-phase two motor drive as shown in reference [4.3].

Machine number	a	b	C	d	e
1	a1	b1	c1	d1	e1
2	a2	c2	e2	b2	d2

A. Modelling of series-connected five-phase two-motor drive

Due to the series connection of two stator windings according to Fig. 4.1 the following voltage and current relations can be written as shown in reference [4.9].

$$
\begin{aligned}
v_A &= v_{as1} + v_{as2} \\
v_B &= v_{bs1} + v_{cs2} \\
v_C &= v_{cs1} + v_{es2} \\
v_D &= v_{ds1} + v_{bs2} \\
v_E &= v_{es1} + v_{ds2}
\end{aligned}
\tag{4.1}
$$

$$
\begin{aligned}
i_A &= i_{as1} = i_{as2} \\
i_B &= i_{bs1} = i_{cs2} \\
i_C &= i_{cs1} = i_{es2} \\
i_D &= i_{ds1} = i_{bs2} \\
i_E &= i_{es1} = i_{ds2}
\end{aligned}
\tag{4.2}
$$

In a general case the two machines, although both five-phase, may be different types i.e. induction machine or permanent magnet synchronous machine or synchronous reluctance machine etc, and therefore, may be with different parameters. Let the index '1' denote machine 1 that is directly connected to the five-phase source (note that the source can be any power electronic converter such as inverter or Matrix Converter) and let the index '2' stand for the second machine 2, connected after the first machine through phase transposition. It is important to note that the modelling of the two-motor drive system is independent of the type of power converter being used as source. MC denotes the Matrix Converter.

Voltage balance equation for the complete system can be written in a compact matrix form as

$$
\underline{v} = \underline{R}\,\underline{i} + \frac{d\left(\underline{L}\,\underline{i}\right)}{dt}
\tag{4.3}
$$

where the system is of the 15$^{\text{th}}$ order and:

$$
\underline{v} = \begin{bmatrix} \underline{v}^{MC} \\ \underline{0} \\ \underline{0} \end{bmatrix} \qquad \underline{i} = \begin{bmatrix} \underline{i}^{MC} \\ \underline{i}_{r1} \\ \underline{i}_{r2} \end{bmatrix}
\tag{4.4}
$$

$$
\begin{aligned}
\underline{v}^{MC} &= \begin{bmatrix} v_A & v_B & v_C & v_D & v_E \end{bmatrix}^T \\
\underline{i}^{MC} &= \begin{bmatrix} i_A & i_B & i_C & i_D & i_E \end{bmatrix}^T
\end{aligned}
\tag{4.5}
$$

$$
\begin{aligned}
\underline{i}_{r1} &= \begin{bmatrix} i_{ar1} & i_{br1} & i_{cr1} & i_{dr1} & i_{er1} \end{bmatrix}^T \\
\underline{i}_{r2} &= \begin{bmatrix} i_{ar2} & i_{br2} & i_{cr2} & i_{dr2} & i_{er2} \end{bmatrix}^T
\end{aligned}
\tag{4.6}
$$

The resistance and inductance matrices of equation (4.3) can be written as:

$$\underline{R} = \begin{bmatrix} \underline{R}_{s1} + \underline{R}_{s2} & \underline{0} & \underline{0} \\ \underline{0} & \underline{R}_{r1} & \underline{0} \\ \underline{0} & \underline{0} & \underline{R}_{r2} \end{bmatrix} \tag{4.7}$$

$$\underline{L} = \begin{bmatrix} \underline{L}_{s1} + \underline{L}_{s2}\,' & \underline{L}_{sr1} & \underline{L}_{sr2}\,' \\ \underline{L}_{rs1} & \underline{L}_{r1} & \underline{0} \\ \underline{L}_{rs2}\,' & \underline{0} & \underline{L}_{r2} \end{bmatrix} \tag{4.8}$$

Super script' in equation (4.8) denotes sub-matrices of machine 2 that have been modified through the phase transposition operation, compared to their original form. The sub-matrices of equations (4.7)-(4.8) are all five by five matrices and are given with the following expressions $\left(\alpha = 2\pi/5\right)$:

$$\begin{aligned} \underline{R}_{s1} &= diag(R_{s1} \quad R_{s1} \quad R_{s1} \quad R_{s1} \quad R_{s1}) \\ \underline{R}_{s2} &= diag\left(R_{s2} \quad R_{s2} \quad R_{s2} \quad R_{s2} \quad R_{s2}\right) \\ \underline{R}_{r1} &= diag(R_{r1} \quad R_{r1} \quad R_{r1} \quad R_{r1} \quad R_{r1}) \\ \underline{R}_{r2} &= diag\left(R_{r2} \quad R_{r2} \quad R_{r2} \quad R_{r2} \quad R_{r2}\right) \end{aligned} \tag{4.9}$$

$$\underline{L}_{s1} = \begin{bmatrix} L_{ls1} + M_1 & M_1 \cos\alpha & M_1 \cos 2\alpha & M_1 \cos 2\alpha & M_1 \cos\alpha \\ M_1 \cos\alpha & L_{ls1} + M_1 & M_1 \cos\alpha & M_1 \cos 2\alpha & M_1 \cos 2\alpha \\ M_1 \cos 2\alpha & M_1 \cos\alpha & L_{ls1} + M_1 & M_1 \cos\alpha & M_1 \cos 2\alpha \\ M_1 \cos 2\alpha & M_1 \cos 2\alpha & M_1 \cos\alpha & L_{ls1} + M_1 & M_1 \cos\alpha \\ M_1 \cos\alpha & M_1 \cos 2\alpha & M_1 \cos 2\alpha & M_1 \cos\alpha & L_{ls1} + M_1 \end{bmatrix} \tag{4.10}$$

$$\underline{L}_{s2}\,' = \begin{bmatrix} L_{ls2} + M_2 & M_2 \cos 2\alpha & M_2 \cos\alpha & M_2 \cos\alpha & M_2 \cos 2\alpha \\ M_2 \cos 2\alpha & L_{ls2} + M_2 & M_2 \cos 2\alpha & M_2 \cos\alpha & M_2 \cos\alpha \\ M_2 \cos\alpha & M_2 \cos 2\alpha & L_{ls2} + M_2 & M_2 \cos 2\alpha & M_2 \cos\alpha \\ M_2 \cos\alpha & M_2 \cos\alpha & M_2 \cos 2\alpha & L_{ls2} + M_2 & M_2 \cos 2\alpha \\ M_2 \cos 2\alpha & M_2 \cos\alpha & M_2 \cos\alpha & M_2 \cos 2\alpha & L_{ls2} + M_2 \end{bmatrix} \tag{4.11}$$

$$\underline{L}_{r1} = \begin{bmatrix} L_{lr1} + M_1 & M_1 \cos\alpha & M_1 \cos 2\alpha & M_1 \cos 2\alpha & M_1 \cos\alpha \\ M_1 \cos\alpha & L_{lr1} + M_1 & M_1 \cos\alpha & M_1 \cos 2\alpha & M_1 \cos 2\alpha \\ M_1 \cos 2\alpha & M_1 \cos\alpha & L_{lr1} + M_1 & M_1 \cos\alpha & M_1 \cos 2\alpha \\ M_1 \cos 2\alpha & M_1 \cos 2\alpha & M_1 \cos\alpha & L_{lr1} + M_1 & M_1 \cos\alpha \\ M_1 \cos\alpha & M_1 \cos 2\alpha & M_1 \cos 2\alpha & M_1 \cos\alpha & L_{lr1} + M_1 \end{bmatrix} \tag{4.12}$$

$$\underline{L}_{r2} = \begin{bmatrix} L_{lr2} + M_2 & M_2 \cos\alpha & M_2 \cos 2\alpha & M_2 \cos 2\alpha & M_2 \cos\alpha \\ M_2 \cos\alpha & L_{lr2} + M_2 & M_2 \cos\alpha & M_2 \cos 2\alpha & M_2 \cos 2\alpha \\ M_2 \cos 2\alpha & M_2 \cos\alpha & L_{lr2} + M_2 & M_2 \cos\alpha & M_2 \cos 2\alpha \\ M_2 \cos 2\alpha & M_2 \cos 2\alpha & M_2 \cos\alpha & L_{lr2} + M_2 & M_2 \cos\alpha \\ M_2 \cos\alpha & M_2 \cos 2\alpha & M_2 \cos 2\alpha & M_2 \cos\alpha & L_{lr2} + M_2 \end{bmatrix} \tag{4.13}$$

$$\underline{L}_{sr1} = M_1 \begin{bmatrix} \cos\theta_1 & \cos(\theta_1+\alpha) & \cos(\theta_1+2\alpha) & \cos(\theta_1-2\alpha) & \cos(\theta_1-\alpha) \\ \cos(\theta_1-\alpha) & \cos\theta_1 & \cos(\theta_1+\alpha) & \cos(\theta_1+2\alpha) & \cos(\theta_1-2\alpha) \\ \cos(\theta_1-2\alpha) & \cos(\theta_1-\alpha) & \cos\theta_1 & \cos(\theta_1+\alpha) & \cos(\theta_1+2\alpha) \\ \cos(\theta_1+2\alpha) & \cos(\theta_1-2\alpha) & \cos(\theta_1-\alpha) & \cos\theta_1 & \cos(\theta_1+\alpha) \\ \cos(\theta_1+\alpha) & \cos(\theta_1+2\alpha) & \cos(\theta_1-2\alpha) & \cos(\theta_1-\alpha) & \cos\theta_1 \end{bmatrix} \tag{4.14}$$

$$\underline{L}_{rs1} = \underline{L}_{sr1}^T$$

$$\underline{L}_{sr2}' = M_2 \begin{bmatrix} \cos\theta_2 & \cos(\theta_2+\alpha) & \cos(\theta_2+2\alpha) & \cos(\theta_2-2\alpha) & \cos(\theta_2-\alpha) \\ \cos(\theta_2-2\alpha) & \cos(\theta_2-\alpha) & \cos\theta_2 & \cos(\theta_2+\alpha) & \cos(\theta_2+2\alpha) \\ \cos(\theta_2+\alpha) & \cos(\theta_2+2\alpha) & \cos(\theta_2-2\alpha) & \cos(\theta_2-\alpha) & \cos\theta_2 \\ \cos(\theta_2-\alpha) & \cos\theta_2 & \cos(\theta_2+\alpha) & \cos(\theta_2+2\alpha) & \cos(\theta_2-2\alpha) \\ \cos(\theta_2+2\alpha) & \cos(\theta_2-2\alpha) & \cos(\theta_2-\alpha) & \cos\theta_2 & \cos(\theta_2+\alpha) \end{bmatrix} \tag{4.15}$$

$$\underline{L}_{rs2}' = \underline{L}_{sr2}^T{}'$$

Expansion of equation (4.3) produces the following:

$$\underline{v} = \begin{bmatrix} \underline{v}^{MC} \\ \underline{0} \\ \underline{0} \end{bmatrix} = \begin{bmatrix} \underline{R}_{s1}+\underline{R}_{s2} & \underline{0} & \underline{0} \\ \underline{0} & \underline{R}_{r1} & \underline{0} \\ \underline{0} & \underline{0} & \underline{R}_{r2} \end{bmatrix} \begin{bmatrix} \underline{i}^{MC} \\ \underline{i}_{r1} \\ \underline{i}_{r2} \end{bmatrix} + \begin{bmatrix} \underline{L}_{s1}+\underline{L}_{s2}' & \underline{L}_{sr1} & \underline{L}_{sr2}' \\ \underline{L}_{rs1} & \underline{L}_{r1} & \underline{0} \\ \underline{L}_{rs2}' & \underline{0} & \underline{L}_{r2} \end{bmatrix} \frac{d}{dt} \begin{bmatrix} \underline{i}^{MC} \\ \underline{i}_{r1} \\ \underline{i}_{r2} \end{bmatrix} +$$

$$\begin{bmatrix} \underline{0} & \frac{d}{dt}\underline{L}_{sr1} & \frac{d}{dt}\underline{L}_{sr2}' \\ \frac{d}{dt}\underline{L}_{rs1} & \underline{0} & \underline{0} \\ \frac{d}{dt}\underline{L}_{rs2}' & \underline{0} & \underline{0} \end{bmatrix} \begin{bmatrix} \underline{i}^{MC} \\ \underline{i}_{r1} \\ \underline{i}_{r2} \end{bmatrix} \tag{4.16}$$

where:

$$\frac{d}{dt}\underline{L}_{sr1} = -\omega_1 M_1 \begin{bmatrix} \sin\theta_1 & \sin(\theta_1+\alpha) & \sin(\theta_1+2\alpha) & \sin(\theta_1-2\alpha) & \sin(\theta_1-\alpha) \\ \sin(\theta_1-\alpha) & \sin\theta_1 & \sin(\theta_1+\alpha) & \sin(\theta_1+2\alpha) & \sin(\theta_1-2\alpha) \\ \sin(\theta_1-2\alpha) & \sin(\theta_1-\alpha) & \sin\theta_1 & \sin(\theta_1+\alpha) & \sin(\theta_1+2\alpha) \\ \sin(\theta_1+2\alpha) & \sin(\theta_1-2\alpha) & \sin(\theta_1-\alpha) & \sin\theta_1 & \sin(\theta_1+\alpha) \\ \sin(\theta_1+\alpha) & \sin(\theta_1+2\alpha) & \sin(\theta_1-2\alpha) & \sin(\theta_1-\alpha) & \sin\theta_1 \end{bmatrix} \tag{4.17}$$

$$\frac{d}{dt}\underline{L}_{rs1} = \frac{d}{dt}\underline{L}_{sr1}^T$$

and

$$\frac{d}{dt}\underline{L}_{sr2}' = -\omega_2 M_2 \begin{bmatrix} \sin\theta_2 & \sin(\theta_2+\alpha) & \sin(\theta_2+2\alpha) & \sin(\theta_2-2\alpha) & \sin(\theta_2-\alpha) \\ \sin(\theta_2-2\alpha) & \sin(\theta_2-\alpha) & \sin\theta_2 & \sin(\theta_2+\alpha) & \sin(\theta_2+2\alpha) \\ \sin(\theta_2+\alpha) & \sin(\theta_2+2\alpha) & \sin(\theta_2-2\alpha) & \sin(\theta_2-\alpha) & \sin\theta_2 \\ \sin(\theta_2-\alpha) & \sin\theta_2 & \sin(\theta_2+\alpha) & \sin(\theta_2+2\alpha) & \sin(\theta_2-2\alpha) \\ \sin(\theta_2+2\alpha) & \sin(\theta_2-2\alpha) & \sin(\theta_2-\alpha) & \sin\theta_2 & \sin(\theta_2+\alpha) \end{bmatrix} \quad (4.18)$$

$$\frac{d}{dt}\underline{L}_{rs2}' = \frac{d}{dt}\underline{L}_{sr2}^{T}'$$

Torque equations of the two machines in terms of source currents and their respective rotor currents and rotor positions are obtained as:

$$T_{e1} = -P_1 M_1 \begin{Bmatrix} (i_A i_{ar1} + i_B i_{br1} + i_C i_{cr1} + i_D i_{dr1} + i_E i_{er1})\sin\theta_1 + (i_E i_{ar1} + i_A i_{br1} + i_B i_{cr1} + i_C i_{dr1} + i_D i_{er1})\sin(\theta_1+\alpha) + \\ (i_D i_{ar1} + i_E i_{br1} + i_A i_{cr1} + i_B i_{dr1} + i_C i_{er1})\sin(\theta_1+2\alpha) + (i_C i_{ar1} + i_D i_{br1} + i_E i_{cr1} + i_A i_{dr1} + i_B i_{er1}) \\ \sin(\theta_1-2\alpha) + (i_B i_{ar1} + i_C i_{br1} + i_D i_{cr1} + i_E i_{dr1} + i_A i_{er1})\sin(\theta_1-\alpha) \end{Bmatrix}$$

$$T_{e2} = -P_2 M_2 \begin{Bmatrix} (i_A i_{ar2} + i_D i_{br2} + i_B i_{cr2} + i_E i_{dr2} + i_C i_{er2})\sin\theta_2 + (i_C i_{ar2} + i_A i_{br2} + i_D i_{cr2} + i_B i_{dr2} + i_E i_{er2})\sin(\theta_2+\alpha) + \\ (i_E i_{ar2} + i_C i_{br2} + i_A i_{cr2} + i_D i_{dr2} + i_B i_{er2})\sin(\theta_2+2\alpha) + (i_B i_{ar2} + i_E i_{br2} + i_C i_{cr2} + i_A i_{dr2} + i_D i_{er2}) \\ \sin(\theta_2-2\alpha) + (i_D i_{ar2} + i_B i_{br2} + i_E i_{cr2} + i_C i_{dr2} + i_A i_{er2})\sin(\theta_2-\alpha) \end{Bmatrix} \quad (4.19)$$

The model given with equation (4.16) and (4.19) together with equations (4.7)-(4.15) and equations (4.17)-(4.18) constitutes the 15[th] order model of the complete two-motor drive with phase transposition in the series connection of stator windings in phase-variable form. The equations of motion are:

$$\frac{d\omega_1}{dt} = \frac{P_1}{J_1}\left(T_{e1} - T_{L1}\right)$$

$$\frac{d\omega_2}{dt} = \frac{P_2}{J_2}\left(T_{e2} - T_{L2}\right) \quad (4.20)$$

4.2b Model in the Rotating Reference Frame

In order to simplify the phase-domain model of Section 4.2a, the decoupling transformation is applied. The Clark's decoupling transformation matrixin power invarient form given in reference [4.2] is:

$$\underline{C} = \sqrt{\frac{2}{5}} \begin{array}{c} \alpha \\ \beta \\ x \\ y \\ 0 \end{array} \begin{bmatrix} 1 & \cos\alpha & \cos 2\alpha & \cos 3\alpha & \cos 4\alpha \\ 0 & \sin\alpha & \sin 2\alpha & \sin 3\alpha & \sin 4\alpha \\ 1 & \cos 2\alpha & \cos 4\alpha & \cos 6\alpha & \cos 8\alpha \\ 0 & \sin 2\alpha & \sin 4\alpha & \sin 6\alpha & \sin 8\alpha \\ 1/\sqrt{2} & 1/\sqrt{2} & 1/\sqrt{2} & 1/\sqrt{2} & 1/\sqrt{2} \end{bmatrix} \quad (4.21)$$

The new variables are defined as:

$$\underline{f}_{\alpha\beta}^{MC} = \underline{C}\,\underline{f}^{MC}\,, \qquad f = v, i \tag{4.22}$$

Application of equation (4.22) in conjunction with equation (4.3) can be written as follows (the notation $L_{m1} = 2.5M_1$ and $L_{m2} = 2.5M_2$ applies further on):

Matrix Converter/stator voltage equations:

$$v_\alpha^{MC} = (R_{s1}+R_{s2})i_\alpha^{MC} + (L_{ls1}+L_{ls2}+L_{m1})pi_\alpha^{MC} + L_{m1}\cos(\theta_1)pi_{\alpha r1} - L_{m1}\sin(\theta_1)pi_{\beta r1} - \omega_1 L_{m1}\left(\sin(\theta_1)i_{\alpha r1} + \cos(\theta_1)i_{\beta r1}\right)$$

$$v_\beta^{MC} = (R_{s1}+R_{s2})i_\beta^{MC} + (L_{ls1}+L_{ls2}+L_{m1})pi_\beta^{MC} + L_{m1}\cos(\theta_1)pi_{\alpha r1} - L_{m1}\sin(\theta_1)pi_{\beta r1} - \omega_1 L_{m1}\left(\sin(\theta_1)i_{\alpha r1} + \cos(\theta_1)i_{\beta r1}\right)$$

$$v_x^{MC} = (R_{s1}+R_{s2})i_x^{MC} + (L_{ls1}+L_{ls2}+L_{m1})pi_x^{MC} + L_{m2}\cos(\theta_2)pi_{\alpha r2} - L_{m2}\sin(\theta_2)pi_{\beta r2} - \omega_2 L_{m2}\left(\sin(\theta_2)i_{\alpha r2} + \cos(\theta_2)i_{\beta r2}\right)$$

(4.23a)

$$v_y^{MC} = (R_{s1}+R_{s2})i_y^{MC} + (L_{ls1}+L_{ls2}+L_{m1})pi_y^{MC} + L_{m2}\sin(\theta_2)pi_{\alpha r2} + L_{m2}\cos(\theta_2)pi_{\beta r2} + \omega_2 L_{m2}\left(\cos(\theta_2)i_{\alpha r2} - \sin(\theta_2)i_{\beta r2}\right)$$

$$v_o^{MC} = (R_{s1}+R_{s2})i_o^{MC} + (L_{ls1}+L_{ls2})pi_o^{MC} \tag{4.23b}$$

where, $p = \frac{d}{dt}$

Rotor voltage equations of machine 1:

$$v_{\alpha r1} = 0 = R_{r1}i_{\alpha r1} + L_{m1}\cos(\theta_1)pi_\alpha^{MC} + L_{m1}\sin(\theta_1)pi_\beta^{MC} + (L_{lr1}+L_{m1})pi_{\alpha r1} - \omega_1 L_{m1}\left(\sin(\theta_1)i_\alpha^{MC} - \cos(\theta_1)i_\beta^{MC}\right)$$

$$v_{\beta r1} = 0 = R_{r1}i_{\beta r1} - L_{m1}\sin(\theta_1)pi_\alpha^{MC} + L_{m1}\cos(\theta_1)pi_\beta^{MC} + (L_{lr1}+L_{m1})pi_{\beta r1} - \omega_1 L_{m1}\left(\cos(\theta_1)i_\alpha^{MC} + \sin(\theta_1)i_\beta^{MC}\right)$$

(4.24a)

$$v_{xr1} = 0 = R_{r1}i_{xr1} + L_{lr1}pi_{xr1}$$

$$v_{yr1} = 0 = R_{r1} i_{yr1} + L_{lr1} p i_{yr1}$$

$$v_{or1} = 0 = R_{r1} i_{or1} + L_{lr1} p i_{or1}$$

Rotor voltage equations of machine 2:

$$v_{\alpha r2} = 0 = R_{r2} i_{\alpha r2} + L_{m2}\cos(\theta_2) p i_x^{MC} + L_{m2}\sin(\theta_2) p i_y^{MC} + (L_{lr2} + L_{m2}) p i_{\alpha r2} - \omega_2 L_{m2}\left(\sin(\theta_2) i_x^{MC} - \cos(\theta_2) i_y^{MC}\right)$$

$$v_{\beta r2} = 0 = R_{r2} i_{\beta r2} - L_{m2}\sin(\theta_2) p i_x^{MC} + L_{m2}\cos(\theta_2) p i_y^{MC} + (L_{lr2} + L_{m2}) p i_{\beta r2} - \omega_2 L_{m2}\left(\cos(\theta_2) i_x^{MC} + \sin(\theta_2) i_y^{MC}\right)$$

$$v_{xr2} = 0 = R_{r2} i_{xr2} + L_{lr2} p i_{xr2} \tag{4.24b}$$

$$v_{yr2} = 0 = R_{r1} i_{yr2} + L_{lr2} p i_{yr2}$$

$$v_{or2} = 0 = R_{r2} i_{or2} + L_{lr2} p i_{or2}$$

Electromagnetic torque equations of two machines are obtained as:

$$\begin{aligned} T_{e1} &= P_1 L_{m1}\left[\cos(\theta_1)\left(i_{\alpha r1} i_\beta^{MC} - i_{\beta r1} i_\alpha^{MC}\right) - \sin(\theta_1)\left(i_{\alpha r1} i_\alpha^{MC} + i_{\beta r1} i_\beta^{MC}\right)\right] \\ T_{e2} &= P_2 L_{m2}\left[\cos(\theta_2)\left(i_{\alpha r2} i_y^{MC} - i_{\beta r2} i_x^{MC}\right) - \sin(\theta_2)\left(i_{\alpha r2} i_x^{MC} + i_{\beta r2} i_y^{MC}\right)\right] \end{aligned} \tag{4.25}$$

The torque equations of the two machines show that the torque of machine 1 entirely depends upon the α-axis and β-axis components of source current (Matrix Converter), while the torque developed by machine 2 is due to x-axis and y-axis components of source current (Matrix Converter). This implies that torque of machine 1 can be controlled by controlling α-axis and β-axis components of source current while torque of machine 2 can be controlled by controlling x-axis and y-axis components of source current. Thus an independent control of two machine is possible. It can be seen from equations (4.23)-(4.24) that the x-axis, y-axis current and o-axis components of the two rotors are completely decoupled from the rest of the system. Hence they can be omitted from further consideration. The zero-sequence component current of stator will be zero for isolated neutral system. Hence the equation for inverter zero-sequence component can be omitted as well. Rotor *x, y,* and zero-sequence component equations, as well as the stator zero-sequence component equations are nevertheless retained for the time being, for the sake of completeness.

4.2c Model in the stationary reference frame

Rotational transformation is applied to the rotor equations of both machines 1 and 2 of the two-motor system model, to obtain the model in the stationary common reference frame. The rotational transformation matrix of equation (4.26) is applied to the rotor of machine 1 and equation (4.27) is applied to the rotor of machine 2. Since all the *x-y* components and zero-sequence components are decoupled, rotational transformation needs to be applied to the α-axis and β-axis components only.

$$\underline{D}_1 = \begin{bmatrix} \cos(\beta_1) & \sin(\beta_1) & 0 & 0 & 0 \\ -\sin(\beta_1) & \cos(\beta_1) & 0 & 0 & 0 \\ 0 & 0 & 1 & 0 & 0 \\ 0 & 0 & 0 & 1 & 0 \\ 0 & 0 & 0 & 0 & 1 \end{bmatrix} \tag{4.26}$$

$$\underline{D}_2 = \begin{bmatrix} \cos(\beta_2) & \sin(\beta_2) & 0 & 0 & 0 \\ -\sin(\beta_2) & \cos(\beta_2) & 0 & 0 & 0 \\ 0 & 0 & 1 & 0 & 0 \\ 0 & 0 & 0 & 1 & 0 \\ 0 & 0 & 0 & 0 & 1 \end{bmatrix} \tag{4.27}$$

The angles of transformations are $\beta_1 = -\theta_1$ and $\beta_2 = -\theta_2$ $\left(\theta_1 = \int \omega_1 dt, \theta_2 = \int \omega_2 dt\right)$ (the instantaneous angular positions of the d-axis of the common reference frame with respect to the phases 'a' magnetic axes of the rotors) and ω_1, ω_2 are the electrical angular speeds of rotation of the machine 1 and machine 2, respectively.

By omitting the x-y and zero-sequence equation for rotor windings and the zero-sequence equation of the power source (Matrix Converter), the complete d-q model in stationary reference frame for the two five-phase series-connected machines can be written in developed form as:

Stator Equations:

$$\begin{aligned}
v_d^{MC} &= R_{s1} i_d^{MC} + (L_{ls1} + L_{m1}) p i_d^{MC} + L_{m1} p i_{dr1} + R_{s2} i_d^{MC} + L_{ls2} p i_d^{MC} \\
v_q^{MC} &= R_{s1} i_q^{MC} + (L_{ls1} + L_{m1}) p i_q^{INV} + L_{m1} p i_{qr1} + R_{s2} i_q^{MC} + L_{ls2} p i_q^{MC} \\
v_x^{INV} &= R_{s1} i_x^{INV} + L_{ls1} \frac{di_x^{INV}}{dt} + R_{s2} i_x^{INV} + (L_{ls2} + L_{m2}) \frac{di_x^{INV}}{dt} + L_{m2} \frac{di_{dr2}}{dt} \\
v_y^{INV} &= R_{s1} i_y^{INV} + L_{ls1} \frac{di_y^{INV}}{dt} + R_{s2} i_y^{INV} + (L_{ls2} + L_{m2}) \frac{di_y^{INV}}{dt} + L_{m2} \frac{di_{qr2}}{dt}
\end{aligned} \tag{4.28}$$

Rotor Equations:

Of machine-1

$$\begin{aligned} v_{dr1} &= 0 = R_{r1} i_{dr1} + L_{m1} p i_d^{MC} + (L_{lr1} + L_{m1}) p i_{dr1} + \omega_1 \left(L_{m1} i_q^{MC} + (L_{lr1} + L_{m1}) i_{qr1} \right) \\ v_{qr1} &= 0 = R_{r1} i_{qr1} + L_{m1} p i_q^{MC} + (L_{lr1} + L_{m1}) p i_{qr1} - \omega_1 \left(L_{m1} i_d^{MC} + (L_{lr1} + L_{m1}) i_{dr1} \right) \end{aligned} \tag{4.29}$$

Of machine-2

$$\begin{aligned} v_{dr2} &= 0 = R_{r2} i_{dr1} + L_{m2} p i_x^{MC} + (L_{lr2} + L_{m2}) p i_{dr2} + \omega_2 \left(L_{m2} i_y^{MC} + (L_{lr2} + L_{m2}) i_{qr2} \right) \\ v_{qr2} &= 0 = R_{r1} i_{qr2} + L_{m2} p i_y^{MC} + (L_{lr2} + L_{m2}) p i_{qr2} - \omega_2 \left(L_{m2} i_x^{MC} + (L_{lr2} + L_{m2}) i_{dr2} \right) \end{aligned} \tag{4.30}$$

In addition, the individual stator voltage equations can be derived as;

$$\begin{aligned} v_{ds1} &= R_{s1} i_d^{MC} + (L_{ls1} + L_{m1}) p i_d^{MC} + L_{m1} p i_{dr1} \\ v_{qs1} &= R_{s1} i_q^{MC} + (L_{ls1} + L_{m1}) p i_q^{MC} + L_{m1} p i_{qr1} \\ v_{xs1} &= R_{s1} i_x^{MC} + L_{ls1} p i_x^{MC} \\ v_{ys1} &= R_{s1} i_y^{MC} + L_{ls1} p i_y^{MC} \\ v_{ds2} &= R_{s2} i_x^{MC} + (L_{ls2} + L_{m2}) p i_x^{MC} + L_{m2} i_{dr2} \\ v_{qs2} &= R_{s2} i_y^{MC} + (L_{ls2} + L_{m2}) p i_y^{MC} + L_{m2} i_{qr2} \\ v_{xs2} &= R_{s2} i_d^{MC} + L_{ls2} p i_d^{MC} \\ -v_{ys2} &= R_{s2} i_q^{MC} + L_{ls2} i_q^{MC} \end{aligned} \tag{4.31}$$

Torque equations of the two machines become:

$$\begin{aligned} T_{e1} &= P_1 L_{m1} \left(i_{dr1} i_q^{MC} - i_d^{MC} i_{qr1} \right) \\ T_{e2} &= P_2 L_{m2} \left(i_{dr2} i_y^{MC} - i_x^{MC} i_{qr2} \right) \end{aligned} \tag{4.32}$$

When the phase variable equations are transformed using decoupling matrix, three sets of equations are obtained, namely *d-q, x-y* and zero sequence. In single five-phase motor drives, the *d-q* components are involved in actual electromagnetic energy conversion while the *x-y* components increase the thermal loading of the machine. However, the extra set of current components (*x-y*) available in a five-phase system is effectively utilised in independently controlling an additional five-phase machine when the stator windings of two five-phase machines are connected in series and are supplied from a single five-phase power source. Reference currents generated by two independent vector controllers, are summed up as per the transposition rules and are supplied to the series-connected five-phase machines.

4.2d Simulation Results

Simulation is done for one five-phase IM fed using ideal voltage source , one machine is run at 40 Hz and second machine run at 30 Hz with constant *v/f*. The results are shown in Fig. 4.2. The independence of control is seen from the simulation results. The results also validate the model of derived in the previous section.

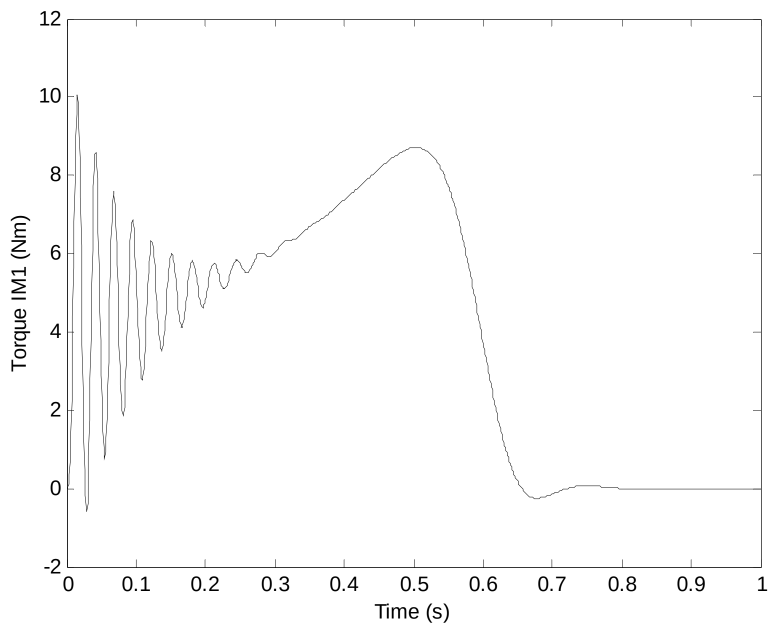

a.

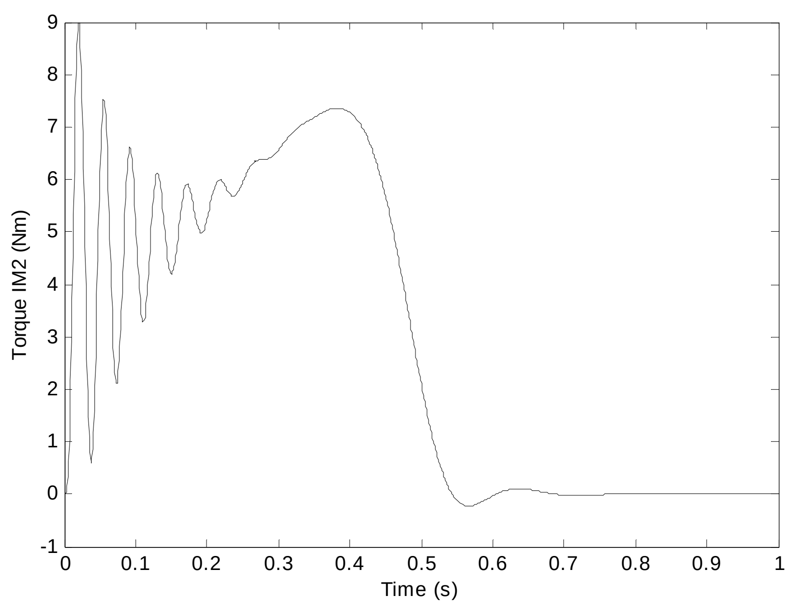

b.

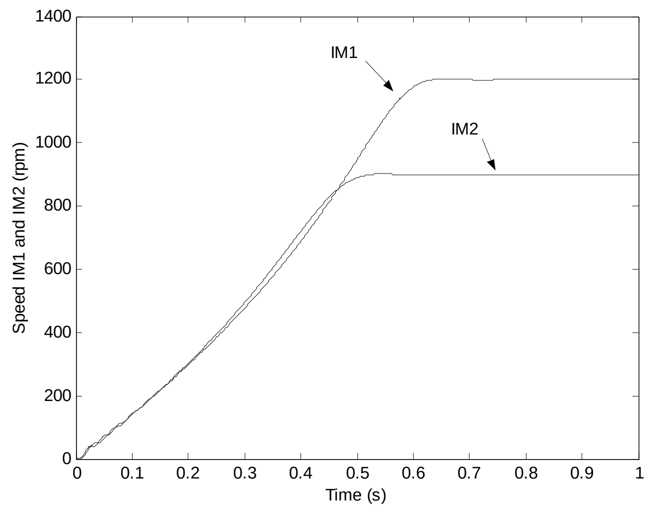

c.

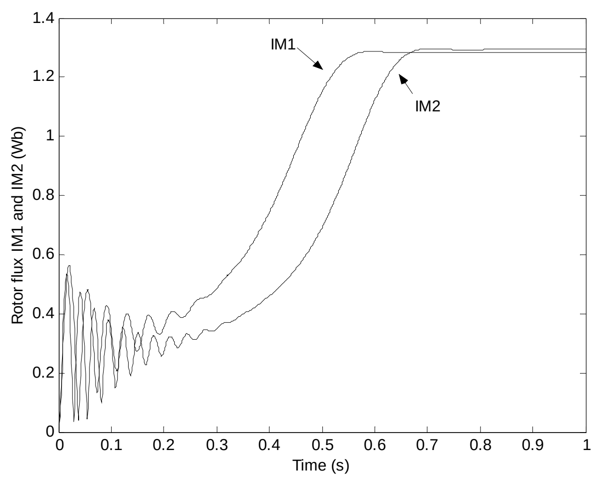

d.

Fig. 4.2. Response of Five-phase Two-motor drive supplied by ideal voltage source, a. Torque of machine 1, b. Torque of machine 2, Speeds of machine 1 and 2, d. Rotor fluxes for machine 1 and 2.

4.3 Modeling of a Six-phase Series-connected Two-motor Drive System

Connection diagram for series connection of stator windings of a six-phase and a three-phase machine is shown in Fig. 4.3 as presented in reference [4.3].

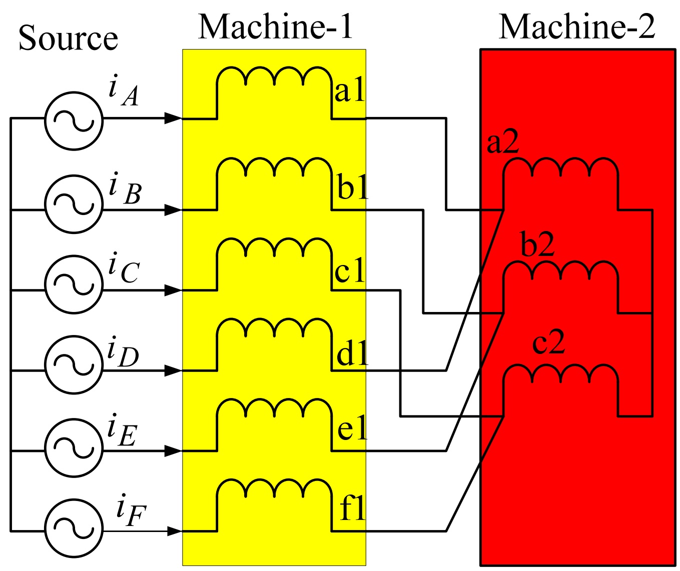

Fig. 4.3. Connection diagram for series connection of a six-phase and a three-phase machine.

4.3a Phase Variable Model

This section develops the model of the complete six-phase two-motor drive system by considering the three-phase machine as a virtual six-phase machine. Let the parameters and variables of the six-phase machine be identified with index 1, while index 2 applies to the three-phase machine. Since the system of Fig. 4.3 is six-phase, it is convenient to represent the three-phase machine as a 'virtual' six-phase machine, meaning that the spatial displacement α stays at 60° and the phases *a2, b2, c2* of the three-phase machine are actually phases *a2, c2, e2* of the virtual six-phase machine with spatial displacements of 120°. Hence the three-phase machine can be represented as a virtual six-phase machine with the following set of equations:

$$\begin{aligned} \underline{v}_{s2} &= \underline{R}_{s2}\underline{i}_{s2} + \frac{d\underline{\psi}_{s2}}{dt} \\ \underline{\psi}_{s2} &= \underline{L}_{s2}\underline{i}_{s2} + \underline{L}_{sr2}\underline{i}_{r2} \end{aligned} \tag{4.33}$$

$$\begin{aligned} \underline{v}_{r2} &= \underline{R}_{r2}\underline{i}_{r2} + \frac{d\underline{\psi}_{r2}}{dt} \\ \underline{\psi}_{r2} &= \underline{L}_{r2}\underline{i}_{r2} + \underline{L}_{rs2}\underline{i}_{s2} \end{aligned} \tag{4.34}$$

where

$$
\begin{aligned}
\underline{v}_{s2} &= \begin{bmatrix} v_{as2} & 0 & v_{cs2} & 0 & v_{es2} & 0 \end{bmatrix}^T \\
\underline{i}_{s2} &= \begin{bmatrix} i_{as2} & 0 & i_{cs2} & 0 & i_{es2} & 0 \end{bmatrix}^T \\
\underline{\psi}_{s2} &= \begin{bmatrix} \psi_{as2} & 0 & \psi_{cs2} & 0 & \psi_{es2} & 0 \end{bmatrix}^T
\end{aligned}
\tag{4.35}
$$

$$
\begin{aligned}
\underline{v}_{r2} &= \begin{bmatrix} v_{ar2} & 0 & v_{cr2} & 0 & v_{er2} & 0 \end{bmatrix}^T \\
\underline{i}_{r2} &= \begin{bmatrix} i_{ar2} & 0 & i_{cr2} & 0 & i_{er2} & 0 \end{bmatrix}^T \\
\underline{\psi}_{r2} &= \begin{bmatrix} \psi_{ar2} & 0 & \psi_{cr2} & 0 & \psi_{er2} & 0 \end{bmatrix}^T
\end{aligned}
\tag{4.36}
$$

The matrices of stator and rotor inductances are given with ($\alpha = 2\pi/6$):

$$
\underline{L}_{s2} = \begin{bmatrix}
L_{ls2} + M_2 & 0 & M_2 \cos 2\alpha & 0 & M_2 \cos 4\alpha & 0 \\
0 & 0 & 0 & 0 & 0 & 0 \\
M_2 \cos 4\alpha & 0 & L_{ls2} + M_2 & 0 & M_2 \cos 2\alpha & 0 \\
0 & 0 & 0 & 0 & 0 & 0 \\
M_2 \cos 2\alpha & 0 & M_2 \cos 4\alpha & 0 & L_{ls2} + M_2 & 0 \\
0 & 0 & 0 & 0 & 0 & 0
\end{bmatrix}
\tag{4.37}
$$

$$
\underline{L}_{r2} = \begin{bmatrix}
L_{lr2} + M_2 & 0 & M_2 \cos 2\alpha & 0 & M_2 \cos 4\alpha & 0 \\
0 & 0 & 0 & 0 & 0 & 0 \\
M_2 \cos 4\alpha & 0 & L_{lr2} + M_2 & 0 & M_2 \cos 2\alpha & 0 \\
0 & 0 & 0 & 0 & 0 & 0 \\
M_2 \cos 2\alpha & 0 & M_2 \cos 4\alpha & 0 & L_{lr2} + M_2 & 0 \\
0 & 0 & 0 & 0 & 0 & 0
\end{bmatrix}
\tag{4.38}
$$

while mutual inductance matrices between stator and rotor windings are:

$$
\begin{aligned}
\underline{L}_{sr2} &= M_2 \begin{bmatrix}
\cos(\theta_2) & 0 & \cos(\theta_2 - 4\alpha) & 0 & \cos(\theta_2 - 2\alpha) & 0 \\
0 & 0 & 0 & 0 & 0 & 0 \\
\cos(\theta_2 - 2\alpha) & 0 & \cos(\theta_2) & 0 & \cos(\theta_2 - 4\alpha) & 0 \\
0 & 0 & 0 & 0 & 0 & 0 \\
\cos(\theta_2 - 4\alpha) & 0 & \cos(\theta_2 - 2\alpha) & 0 & \cos(\theta_2) & 0 \\
0 & 0 & 0 & 0 & 0 & 0
\end{bmatrix} \\
\underline{L}_{rs2} &= \underline{L}_{sr2}^T
\end{aligned}
\tag{4.39}
$$

Resistance matrices are:

$$
\begin{aligned}
\underline{R}_{s2} &= diag(R_{s2} \quad 0 \quad R_{s2} \quad 0 \quad R_{s2} \quad 0) \\
\underline{R}_{r2} &= diag(R_{r2} \quad 0 \quad R_{r2} \quad 0 \quad R_{r2} \quad 0)
\end{aligned}
\tag{4.40}
$$

and the machine torque is:

$$
T_{e2} = -P_2 M_2 \begin{Bmatrix}
\left(i_{as2} i_{ar2} + i_{cs2} i_{cr2} + i_{es2} i_{er2}\right) \sin\theta_2 + \left(i_{es2} i_{ar2} + i_{as2} i_{cr2} + i_{cs2} i_{er2}\right) \sin(\theta_2 - 4\alpha) + \\
+ \left(i_{cs2} i_{ar2} + i_{es2} i_{cr2} + i_{as2} i_{er2}\right) \sin(\theta_2 - 2\alpha)
\end{Bmatrix}
\tag{4.41}
$$

Correlation between machine voltages and source voltages is given with Fig. 4.3, where the phases of the three-phase machine are now labelled as *a2, c2, e2*. Hence

$$\begin{array}{lll} v_A = v_{a1} + v_{a2} & v_B = v_{b1} + v_{c2} & v_C = v_{c1} + v_{e2} \\ v_D = v_{d1} + v_{a2} & v_E = v_{e1} + v_{c2} & v_F = v_{f1} + v_{e2} \end{array} \tag{4.42}$$

Correlation between machine currents and source currents is the following:

$$\underline{i}_{s1} = \begin{bmatrix} i_{as1} \\ i_{bs1} \\ i_{cs1} \\ i_{ds1} \\ i_{es1} \\ i_{fs1} \end{bmatrix} = \begin{bmatrix} i_A \\ i_B \\ i_C \\ i_D \\ i_E \\ i_F \end{bmatrix} = \underline{i}^{MC} \tag{4.43}$$

$$\underline{i}_{s2} = \begin{bmatrix} i_{as2} \\ i_{bs2} \\ i_{cs2} \\ i_{ds2} \\ i_{es2} \\ i_{fs2} \end{bmatrix} = \begin{bmatrix} i_A + i_D \\ 0 \\ i_B + i_E \\ 0 \\ i_C + i_F \\ 0 \end{bmatrix} \tag{4.44}$$

Voltage equations of the complete two-motor system are formulated in terms of source currents and voltages. The system is of the 18th order, since the three-phase machine is represented as a virtual six-phase machine. However, three rotor equations will be redundant (equations for rotor phases *b, d, f*). The complete set of voltage equations can be written as:

$$\begin{bmatrix} \underline{v}^{MC} \\ \underline{0} \\ \underline{0} \end{bmatrix} = \begin{bmatrix} \underline{R}_{s1} + \underline{R}'_{s2} & \underline{0} & \underline{0} \\ \underline{0} & \underline{R}_{r1} & \underline{0} \\ \underline{0} & \underline{0} & \underline{R}_{r2} \end{bmatrix} \begin{bmatrix} \underline{i}^{MC} \\ \underline{i}_{r1} \\ \underline{i}_{r2} \end{bmatrix} + p \left(\begin{bmatrix} \underline{L}_{s1} + \underline{L}'_{s2} & \underline{L}_{s1} & \underline{L}'_{sr} \\ \underline{L}_{rs1} & \underline{L}_{r1} & \underline{0} \\ \underline{L}'_{rs} & \underline{0} & \underline{L}_{r2} \end{bmatrix} \begin{bmatrix} \underline{i}^{INV} \\ \underline{i}_{r1} \\ \underline{i}_{r2} \end{bmatrix} \right) \tag{4.45}$$

All the inductance, resistance and null sub-matrices are of six by six order. Primed sub-matrices are those that have been modified, with respect to their original form as equation (4.45), in the process of series connection of two machines through the phase transposition operation. These sub-matrices are equal to:

$$\underline{R}_{s2}' = \begin{bmatrix} R_{s2} & 0 & 0 & R_{s2} & 0 & 0 \\ 0 & R_{s2} & 0 & 0 & R_{s2} & 0 \\ 0 & 0 & R_{s2} & 0 & 0 & R_{s2} \\ R_{s2} & 0 & 0 & R_{s2} & 0 & 0 \\ 0 & R_{s2} & 0 & 0 & R_{s2} & 0 \\ 0 & 0 & R_{s2} & 0 & 0 & R_{s2} \end{bmatrix} \tag{4.46}$$

$$\underline{L}_{s2}' = \begin{bmatrix} L_{ls2}+M_2 & M_2\cos 2\alpha & M_2\cos 4\alpha & L_{ls2}+M_2 & M_2\cos 2\alpha & M_2\cos 4\alpha \\ M_2\cos 4\alpha & L_{ls2}+M_2 & M_2\cos 2\alpha & M_2\cos 4\alpha & L_{ls2}+M_2 & M_2\cos 2\alpha \\ M_2\cos 2\alpha & M_2\cos 4\alpha & L_{ls2}+M_2 & M_2\cos 2\alpha & M_2\cos 4\alpha & L_{ls2}+M_2 \\ L_{ls2}+M_2 & M_2\cos 2\alpha & M_2\cos 4\alpha & L_{ls2}+M_2 & M_2\cos 2\alpha & M_2\cos 4\alpha \\ M_2\cos 4\alpha & L_{ls2}+M_2 & M_2\cos 2\alpha & M_2\cos 4\alpha & L_{ls2}+M_2 & M_2\cos 2\alpha \\ M_2\cos 2\alpha & M_2\cos 4\alpha & L_{ls2}+M_2 & M_2\cos 2\alpha & M_2\cos 4\alpha & L_{ls2}+M_2 \end{bmatrix} \tag{4.47}$$

$$\underline{L}_{sr2}' = M_2 \begin{bmatrix} \cos\theta_2 & 0 & \cos(\theta_2-4\alpha) & 0 & \cos(\theta_2-2\alpha) & 0 \\ \cos(\theta_2-2\alpha) & 0 & \cos\theta_2 & 0 & \cos(\theta_2-4\alpha) & 0 \\ \cos(\theta_2-4\alpha) & 0 & \cos(\theta_2-2\alpha) & 0 & \cos\theta_2 & 0 \\ \cos\theta_2 & 0 & \cos(\theta_2-4\alpha) & 0 & \cos(\theta_2-2\alpha) & 0 \\ \cos(\theta_2-2\alpha) & 0 & \cos\theta_2 & 0 & \cos(\theta_2-4\alpha) & 0 \\ \cos(\theta_2-4\alpha) & 0 & \cos(\theta_2-2\alpha) & 0 & \cos\theta_2 & 0 \end{bmatrix} \tag{4.48}$$

$$\underline{L}_{rs2}' = \left(\underline{L}_{sr2}'\right)^T$$

Torque equations of the two machines can be given in terms of inverter currents as:

$$T_{e2} = -P_2 M_2 \left\{ \begin{array}{l} \left((i_A+i_D)i_{ar2} + (i_B+i_E)i_{cr2} + (i_C+i_F)i_{er2}\right)\sin\theta_2 + \\ +\left((i_C+i_F)i_{ar2} + (i_A+i_D)i_{cr2} + (i_B+i_E)i_{er2}\right)\sin(\theta_2-4\alpha) + \\ +\left((i_B+i_E)i_{ar2} + (i_C+i_F)i_{cr2} + (i_A+i_D)i_{er2}\right)\sin(\theta_2-2\alpha) \end{array} \right\} \tag{4.49a}$$

$$T_{e1} = -P_1 M_1 \left\{ \begin{array}{l} \left(i_A i_{ar1} + i_B i_{br1} + i_C i_{cr1} + i_D i_{dr1} + i_E i_{er1} + i_F i_{fr1}\right)\sin\theta_1 + \\ \left(i_F i_{ar1} + i_A i_{br1} + i_B i_{cr1} + i_C i_{dr1} + i_D i_{er1} + i_E i_{fr1}\right)\sin(\theta_1-5\alpha) + \\ \left(i_E i_{ar1} + i_F i_{br1} + i_A i_{cr1} + i_B i_{dr1} + i_C i_{er1} + i_D i_{fr1}\right)\sin(\theta_1-4\alpha) + \\ \left(i_D i_{ar1} + i_E i_{br1} + i_F i_{cr1} + i_A i_{dr1} + i_B i_{er1} + i_C i_{fr1}\right)\sin(\theta_1-3\alpha) + \\ \left(i_C i_{ar1} + i_D i_{br1} + i_E i_{cr1} + i_F i_{dr1} + i_A i_{er1} + i_B i_{fr1}\right)\sin(\theta_1-2\alpha) + \\ \left(i_B i_{ar1} + i_C i_{br1} + i_D i_{cr1} + i_E i_{dr1} + i_F i_{er1} + i_A i_{fr1}\right)\sin(\theta_1-\alpha) \end{array} \right\} \tag{4.49b}$$

4.3b Model in the Rotating reference frame

To obtain orthogonal form of the model, the following Clark's decoupling transformation matrices in power invariant form are applied to the phase variable model:

$$\underline{C}_{(6)} = \sqrt{\frac{2}{6}}\begin{array}{c} \alpha \\ \beta \\ x \\ y \\ 0_+ \\ 0_- \end{array}\begin{bmatrix} 1 & \cos\alpha & \cos 2\alpha & \cos 3\alpha & \cos 4\alpha & \cos 5\alpha \\ 0 & \sin\alpha & \sin 2\alpha & \sin 3\alpha & \sin 4\alpha & \sin 5\alpha \\ 1 & \cos 2\alpha & \cos 4\alpha & \cos 6\alpha & \cos 8\alpha & \cos 10\alpha \\ 0 & \sin 2\alpha & \sin 4\alpha & \sin 6\alpha & \sin 8\alpha & \sin 10\alpha \\ 1/\sqrt{2} & 1/\sqrt{2} & 1/\sqrt{2} & 1/\sqrt{2} & 1/\sqrt{2} & 1/\sqrt{2} \\ 1/\sqrt{2} & -1/\sqrt{2} & 1/\sqrt{2} & -1/\sqrt{2} & 1/\sqrt{2} & -1/\sqrt{2} \end{bmatrix} \tag{4.50a}$$

$$\underline{C}_{(3)} = \sqrt{\frac{2}{3}}\begin{bmatrix} 1 & \cos 2\alpha & \cos 4\alpha \\ 0 & \sin 2\alpha & \sin 4\alpha \\ 1/\sqrt{2} & 1/\sqrt{2} & 1/\sqrt{2} \end{bmatrix} \tag{4.50b}$$

Axis components of source output phase voltages are:

$$\underline{v}_{\alpha\beta}^{MC} = \begin{bmatrix} v_\alpha^{MC} \\ v_\beta^{MC} \\ v_x^{MC} \\ v_y^{MC} \\ v_{0+}^{MC} \\ v_{0-}^{MC} \end{bmatrix} = \underline{C}(6)\begin{bmatrix} v_A \\ v_B \\ v_C \\ v_D \\ v_E \\ v_F \end{bmatrix} \tag{4.51}$$

Application of equation (4.50a) - (4.50b) in conjunction with equation (4.42) produces:

$$\underline{v}_{\alpha\beta}^{MC} = \begin{bmatrix} v_\alpha^{MC} \\ v_\beta^{MC} \\ v_x^{MC} \\ v_y^{MC} \\ v_{0+}^{MC} \\ v_{0-}^{MC} \end{bmatrix} = \underline{C}(6)\begin{bmatrix} v_{a1}+v_{a2} \\ v_{b1}+v_{c2} \\ v_{c1}+v_{e2} \\ v_{d1}+v_{a2} \\ v_{e1}+v_{c2} \\ v_{f1}+v_{e2} \end{bmatrix} = \begin{bmatrix} v_{\alpha s1} \\ v_{\beta s1} \\ v_{xs1}+\sqrt{2}v_{\alpha s2} \\ v_{ys1}+\sqrt{2}v_{\beta s2} \\ v_{0+s1}+\sqrt{2}v_{0s2} \\ v_{0-s1} \end{bmatrix} \tag{4.52}$$

The complete decoupled model of the six-phase two-motor drive system. Matrix Converter-stator voltage equations are obtained as:

$$v_\alpha^{MC} = R_{s1}i_\alpha^{MC} + L_{s1}pi_\alpha^{MC} + pL_{m1}\left(\cos\theta_1 i_{\alpha r1} - \sin\theta_1 i_{\beta r1}\right)$$

$$v_\beta^{MC} = R_{s1}i_\beta^{MC} + L_{s1}pi_\beta^{MC} + pL_{m1}\left(\sin\theta_1 i_{\alpha r1} - \cos\theta_1 i_{\beta r1}\right)$$

$$v_x^{MC} = R_{s1}i_x^{MC} + L_{ls1}pi_x^{MC} + \sqrt{2}\left(R_{s2}\sqrt{2}i_x^{MC} + L_{s2}p\sqrt{2}i_x^{MC} + L_{m2}p\left(\cos\theta_2 i_{\alpha r2} - \sin\theta_2 i_{\beta r2}\right)\right)$$
$$v_y^{MC} = R_{s1}i_y^{MC} + L_{ls1}pi_y^{INV} + \sqrt{2}\left(R_{s2}\sqrt{2}i_y^{MC} + L_{s2}p\sqrt{2}i_y^{MC} + L_{m2}p\left(\sin\theta_2 i_{\alpha r2} + \cos\theta_2 i_{\beta r2}\right)\right)$$
$$v_{0+}^{MC} = R_{s1}i_{0+}^{MC} + L_{ls1}pi_{0+}^{MC} + \sqrt{2}\left(R_{s2}\sqrt{2}i_{0+}^{MC} + L_{ls2}p\sqrt{2}i_{0+}^{MC}\right)$$

$$v_{0-}^{MC} = R_{s1}i_{0-}^{MC} + L_{ls1}pi_{0-}^{MC} \quad \text{(4.53}$$

where $L_{m1} = 3M_1$, $L_{m2} = 1.5M_2$. Relationship between inverter current axis components and axis components of stator currents of the two machines is found in the following form:

$$
\begin{aligned}
i_\alpha^{MC} &= i_{\alpha s1} \\
i_\beta^{MC} &= i_{\beta s1} \\
i_x^{MC} &= i_{xs1} = i_{\alpha s2} \big/ \sqrt{2} \\
i_y^{MC} &= i_{ys1} = i_{\beta s2} \big/ \sqrt{2} \\
i_{0+}^{MC} &= i_{0+s1} = i_{0s2} \big/ \sqrt{2} \\
i_{0-}^{MC} &= i_{0-s1}
\end{aligned} \tag{4.54}
$$

Rotor voltage equations of the six-phase machine result in the form:

$$
\begin{aligned}
&0 = R_{r1} i_{\alpha r1} + L_{r1} p i_{\alpha r1} + pL_{m1} \left(\cos\theta_1 i_\alpha^{IMC} + \sin\theta_1 i_\beta^{MC} \right) \\
&0 = R_{r1} i_{\beta r1} + L_{r1} p i_{\beta r1} + pL_{m1} \left(-\sin\theta_1 i_\alpha^{MC} + \cos\theta_1 i_\beta^{MC} \right) \\
&0 = R_{r1} i_k + L_{lr1} \mathrm{p} i_k \qquad k = xr1,\ yr1,\ 0+r1,\ 0-r1
\end{aligned} \tag{4.55}
$$

While rotor voltage equations of the three-phase machine become:

$$
\begin{aligned}
&0 = R_{r2} i_{\alpha r2} + L_{r2} p i_{\alpha r2} + p\sqrt{2} L_{m2} \left(\cos\theta_2 i_x^{MC} + \sin\theta_2 i_y^{MC} \right) \\
&0 = R_{r2} i_{\beta r2} + L_{r2} p i_{\beta r2} + p\sqrt{2} L_{m2} \left(-\sin\theta_2 i_x^{MC} + \cos\theta_2 i_y^{MC} \right) \\
&0 = R_{r2} i_{0r2} + L_{lr2} p i_{0r2}
\end{aligned} \tag{4.56}
$$

Torque equations of the two machines are:

$$
\begin{aligned}
T_{e1} &= P_1 L_{m1} \left[\cos(\theta_1) \left(i_{\alpha r1} i_\beta^{MC} - i_{\beta r1} i_\alpha^{MC} \right) - \sin(\theta_1) \left(i_{\alpha r1} i_\alpha^{MC} + i_{\beta r1} i_\beta^{MC} \right) \right] \\
T_{e2} &= \sqrt{2} P_2 L_{m2} \left[\cos(\theta_2) \left(i_{\alpha r2} i_y^{MC} - i_{\beta r2} i_x^{MC} \right) - \sin(\theta_2) \left(i_{\alpha r2} i_x^{MC} + i_{\beta r2} i_y^{MC} \right) \right]
\end{aligned} \tag{4.57}
$$

4.3c Transformation of the model into the stationary common reference frame

Rotational transformation is applied to rotor equations of the two machines. The obtained model in the stationary common reference frame is described as following. Since the x-y and zero-sequence components of the rotor voltages and currents are zero, the complete model in the stationary reference frame for the six-phase and the three-phase series connected machines consists of ten differential equations. The developed form of inverter voltage equations is:

$$
\begin{aligned}
v_\alpha^{MC} &= R_{s1} i_\alpha^{MC} + (L_{ls1} + L_{m1}) p i_\alpha^{MC} + L_{m1} p i_{dr1} \\
v_\beta^{MC} &= R_{s1} i_\beta^{MC} + (L_{ls1} + L_{m1}) p i_\beta^{MC} + L_{m1} p i_{qr1} \\
v_x^{MC} &= R_{s1} i_x^{MC} + L_{ls1} p i_x^{MC} + \sqrt{2}\left\{ R_{s2}\sqrt{2} i_x^{MC} + (L_{ls2} + L_{m2}) p \sqrt{2} i_x^{MC} + L_{m2} p i_{dr2} \right\} \\
v_y^{MC} &= R_{s1} i_y^{IMC} + L_{ls1} p i_y^{MC} + \sqrt{2}\left\{ R_{s2}\sqrt{2} i_y^{MC} + (L_{ls2} + L_{m2}) p \sqrt{2} i_y^{MC} + L_{m2} p i_{qr2} \right\} \\
v_{0+}^{MC} &= R_{s1} i_{0+}^{MC} + L_{ls1} p i_{0+}^{MC} + \sqrt{2}\left\{ R_{s2}\sqrt{2} i_{0+}^{MC} + L_{ls2} p \sqrt{2} i_{0+}^{MC} \right\} \\
v_{0-}^{MC} &= R_{s1} i_{0-}^{MC} + L_{ls1} p i_{0-}^{MC}
\end{aligned} \tag{4.58}
$$

Rotor voltage equations of the six-phase machine are:

$$
\begin{aligned}
0 &= R_{r1} i_{dr1} + L_{m1} p i_\alpha^{MC} + \left(L_{lr1} + L_{m1}\right) p i_{dr1} + \omega_1 \left(L_{m1} i_\beta^{MC} + \left(L_{lr1} + L_{m1}\right) i_{qr1} \right) \\
0 &= R_{r1} i_{qr1} + L_{m1} p i_\beta^{MC} + \left(L_{lr1} + L_{m1}\right) p i_{qr1} - \omega_1 \left(L_{m1} i_\alpha^{MC} + \left(L_{lr1} + L_{m1}\right) i_{dr1} \right)
\end{aligned} \tag{4.59}
$$

and rotor voltage equations of the three-phase machine are:

$$
\begin{aligned}
0 &= R_{r2} i_{dr2} + \sqrt{2} L_{m2} p i_x^{MC} \left(L_{lr2} + L_{m2}\right) p i_{dr2} + \omega_2 \left(L_{m2} \sqrt{2} i_y^{MC} + \left(L_{lr2} + L_{m2}\right) i_{qr2} \right) \\
0 &= R_{r2} i_{qr2} + \sqrt{2} L_{m2} p i_y^{MC} + \left(L_{lr2} + L_{m2}\right) p i_{qr2} - \omega_2 \left(L_{m2} \sqrt{2} i_x^{MC} + \left(L_{lr2} + L_{m2}\right) i_{dr2} \right)
\end{aligned} \tag{4.60}
$$

Torque equations of the two machines are

$$
\begin{aligned}
T_{e1} &= P_1 L_{m1} \left[i_{dr1} i_q^{MC} - i_d^{MC} i_{qr1} \right] \\
T_{e2} &= \sqrt{2} P_2 L_{m2} \left[i_{dr2} i_y^{MC} - i_x^{MC} i_{qr2} \right]
\end{aligned} \tag{4.61}
$$

The mathemetical equations developed in this section is verified assuming ideal sinusoidal source. The independence of control is observed from the Fig. 4.4.

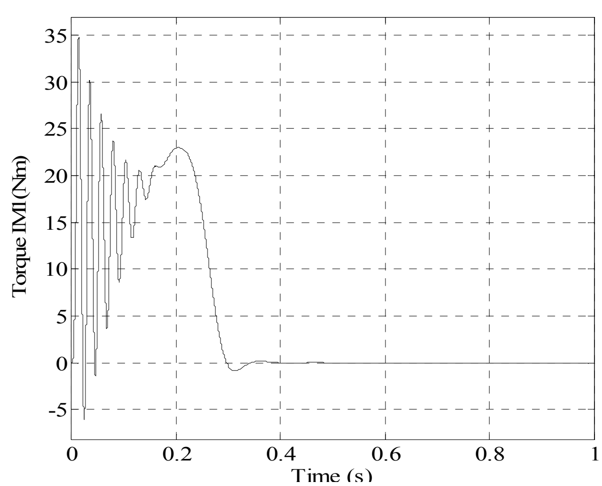

a.

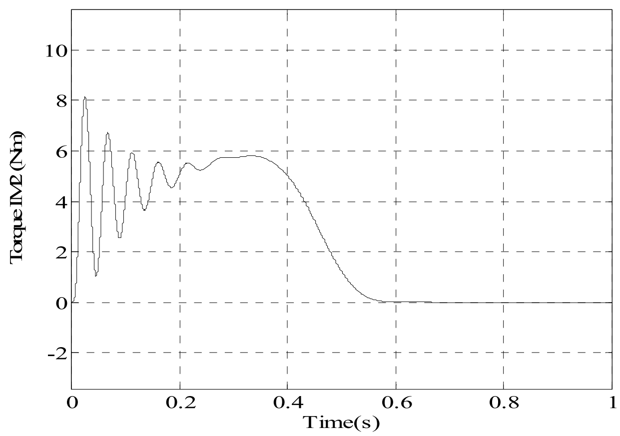

b.

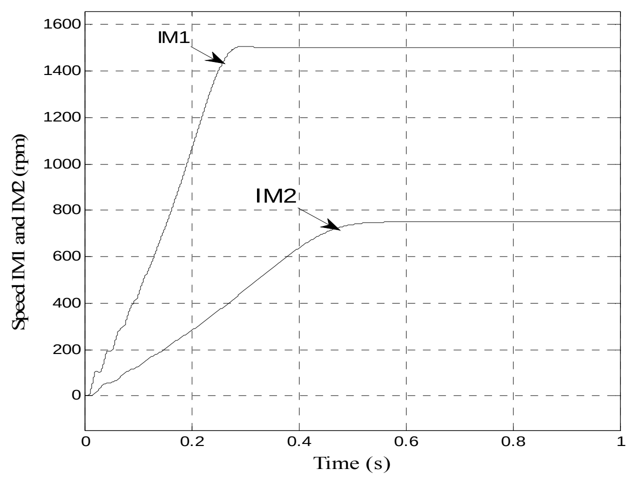

c.

Fig. 4.4. Response of Six-phase Two-motor drive supplied by ideal voltage source.

4.4 Modelling of A Seven-Phase Series-connected Three-Motor Drive System

A seven-phase system, when transformed, has four orthogonal components in a seven dimensional space. However, for field oriented control only two components are needed (component with 90° phase shift).Hence in a seven-phase system, at least three orthogonal pairs are available to control realizable three field oriented controllers. Thus, if the stator windings of three seven-phase machines are connected in series (without any change in the rotor part), all these three machines can be controlled independently as presented in reference [4.6]. To obtain decoupled control of all the three machines, it is important that the d-q current of one machine becomes the x-y of the other two machines. Similarly, the x-y of the first machine becomes the d-q of the others. With such arrangement, the component that will produce the rotating magnetic field in one machine will not produce any rotating magnetic field in the other two machines. This component is then responsible for the torque production while the other component will be limited by the leakage impedance, will not produce any torque. This is achieved by proper phase transposition, between the stator winding connections.

The power supply to three series-connected machine is given by a seven-phase voltage or current controlled PWM inverters or Matrix Converter. In other words, it is possible to independently implement field oriented control of three seven-phase series-connected machines using a single power converter source. In this chapter seven-phase induction machines with spatial displacement of 2π/7 between the phases are considered. Although the concept of independence of control of series-connected machine do not pose any constraints on the type of machine being used. The connection diagram showing three seven-phase machines with stator winding connected in series and supplied by a single power source is given in Fig. 4.5. The stator winding of the three machines are connected in series while the three rotors can independently take three different loads. The three series-connected machines can run under identical loading conditions or they are independent of taking up any loads.

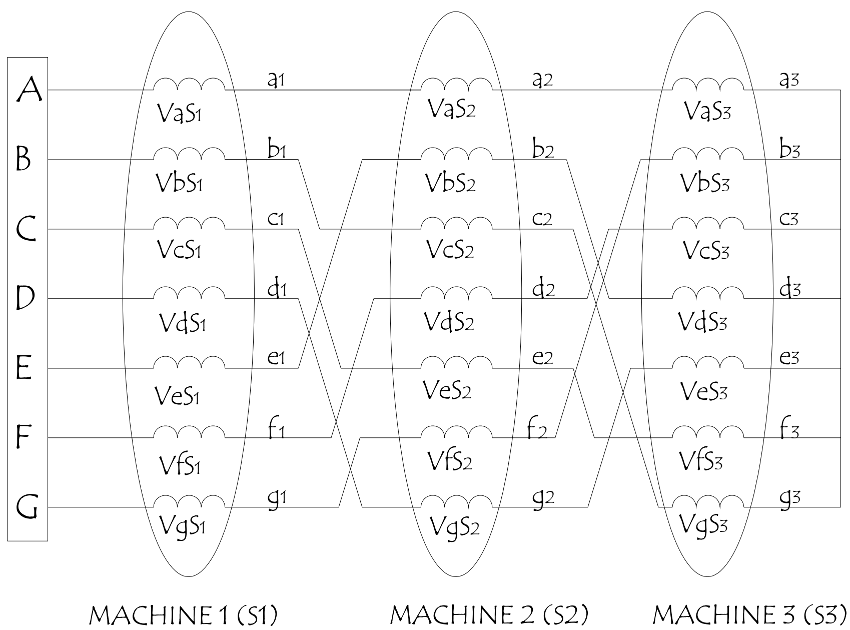

Fig. 4.5. Seven Phase Series-Connected Three-Motor system.

The phase transposition rule of three machine connections is given in Table 4.2. The machines are labelled as M1, M2 and M3 (in column), the phases of the power source are shown in the rows.

Table 4.2. Connectivity Matrix.

Machines	**A**	**B**	**C**	**D**	**E**	**F**	**G**
M1	a_1	b_1	C_1	d_1	e_1	f_1	g_1
M2	a_2	c_2	e_2	g_2	b_2	d_2	f_2
M3	a_3	g_3	f_3	e_3	d_3	c_3	b_3

4.4a Phase Variable Model

Phase variable model of two seven-phase induction machines connected in series according to Fig. 4.5 is developed in state space form. Power source (Matrix Converter) voltage of each phase after series connection as shown in Fig 4.5 can be as they are determined in an appropriate summation of stator phase voltages of individual machine with respect to the stator phase connection.

$$\begin{aligned}
V_A &= V_{aS1} + V_{aS2} + V_{aS3} \\
V_B &= V_{bS1} + V_{cS2} + V_{dS3} \\
V_C &= V_{cS1} + V_{eS2} + V_{gS3} \\
V_D &= V_{dS1} + V_{gS2} + V_{cS3} \\
V_E &= V_{eS1} + V_{bS2} + V_{fS3} \\
V_F &= V_{fS1} + V_{dS2} + V_{bS3} \\
V_G &= V_{gS1} + V_{fS2} + V_{eS3}
\end{aligned} \tag{4.62}$$

The current through each phase winding is:

$$\begin{aligned}
I_A &= I_{aS1} = I_{aS2} = I_{aS3} \\
I_B &= I_{bS1} = I_{cS2} = I_{dS3} \\
I_C &= I_{cS1} = I_{eS2} = I_{gS3} \\
I_D &= I_{dS1} = I_{gS2} = I_{cS3} \\
I_E &= I_{eS1} = I_{bS2} = I_{fS3} \\
I_F &= I_{fS1} = I_{dS2} = I_{bS3} \\
I_G &= I_{gS1} + I_{fS2} + I_{eS3}
\end{aligned} \tag{4.63}$$

After adding angular displacement of frequency, the supply voltage will become:

$$
\begin{aligned}
V_A &= V_1 Sin(2\pi f_1(t)) + V_2 Sin(2\pi f_2(t)) + V_3 Sin(2\pi f_3(t)) \\
V_B &= V_1 Sin(2\pi f_1(t) + 2\pi/7) + V_2 Sin(2\pi f_2(t) + 4\pi/7) + V_3 Sin(2\pi f_3(t) + 6\pi/7) \\
V_C &= V_1 Sin(2\pi f_1(t) + 4\pi/7) + V_2 Sin(2\pi f_2(t) + 8\pi/7) + V_3 Sin(2\pi f_3(t) + 12\pi/7) \\
V_D &= V_1 Sin(2\pi f_1(t) + 6\pi/7) + V_2 Sin(2\pi f_2(t) + 12\pi/7) + V_3 Sin(2\pi f_3(t) + 4\pi/7) \\
V_E &= V_1 Sin(2\pi f_1(t) + 8\pi/7) + V_2 Sin(2\pi f_2(t) + 2\pi/7) + V_3 Sin(2\pi f_3(t) + 10\pi/7) \\
V_F &= V_1 Sin(2\pi f_1(t) + 10\pi/7) + V_2 Sin(2\pi f_2(t) + 6\pi/7) + V_3 Sin(2\pi f_3(t) + 2\pi/7) \\
V_G &= V_1 Sin(2\pi f_1(t) + 12\pi/7) + V_2 Sin(2\pi f_2(t) + 10\pi/7) + V_3 Sin(2\pi f_3(t) + 8\pi/7)
\end{aligned}
\tag{4.64}
$$

Each phase to neutral voltage of power source is indicated with capital letters. The connected three seven phase machines all parameters may be different. The denomination 1 indicates the first machines parameters 2 and 3 for other two. First machine is directly connected to seven phase inverter and phase transposed voltage is supplied to next machines.

The voltage equation in matrix form for the complete system can be represented as:

$$
\underline{V} = \underline{R}\underline{i} + \frac{d\underline{\psi}}{dt} \quad \text{or} \quad \underline{V} = \underline{R}\underline{i} + \underline{L}\frac{d\underline{i}}{dt} \tag{4.65}
$$

where :

$$
\underline{V} = \begin{bmatrix} \underline{v}^{MC} \\ \underline{v}_{r1} \\ \underline{v}_{r2} \\ \underline{v}_{r3} \end{bmatrix} \tag{4.66}
$$

$$
\underline{R} = \begin{bmatrix} \underline{R}_{s1} + \underline{R}_{s2} + \underline{R}_{s3} & 0 & 0 & 0 \\ 0 & \underline{R}_{r1} & 0 & 0 \\ 0 & 0 & \underline{R}_{r2} & 0 \\ 0 & 0 & 0 & \underline{R}_{r3} \end{bmatrix} \tag{4.67a}
$$

$$
\underline{i} = \begin{bmatrix} \underline{i}^{MC} \\ \underline{i}_{r1} \\ \underline{i}_{r2} \\ \underline{i}_{r3} \end{bmatrix} \tag{4.67b}
$$

$$\underline{L} = \begin{bmatrix} \underline{L}_{s1} + \underline{L}^1_{s2} + \underline{L}^1_{s3} & \underline{L}_{sr1} & \underline{L}^1_{sr2} & \underline{L}^1_{sr3} \\ \underline{L}_{rs1} & \underline{L}_{r1} & 0 & 0 \\ \underline{L}^1_{rs2} & 0 & \underline{L}_{r2} & 0 \\ \underline{L}^1_{rs3} & 0 & 0 & \underline{L}_{r3} \end{bmatrix} \tag{4.68}$$

The superscript 1 indicates the modified inductance matrices according to the phase transportation rule. The sub inductance matrix for the inductance of stator and rotor can be represent in seven by seven matrix format as:

$$\underline{L}_s = \begin{bmatrix} L_{aas} & L_{abs} & L_{acs} & L_{ads} & L_{aes} & L_{afs} & L_{ags} \\ L_{bas} & L_{bbs} & L_{bcs} & L_{bds} & L_{bes} & L_{bfs} & L_{bgs} \\ L_{cas} & L_{cbs} & L_{ccs} & L_{cds} & L_{ces} & L_{cfs} & L_{cgs} \\ L_{das} & L_{dbs} & L_{dcs} & L_{dds} & L_{des} & L_{dfs} & L_{dgs} \\ L_{eas} & L_{ebs} & L_{ecs} & L_{eds} & L_{ees} & L_{efs} & L_{egs} \\ L_{fas} & L_{fbs} & L_{fcs} & L_{fds} & L_{fes} & L_{ffs} & L_{fgs} \\ L_{gas} & L_{gbs} & L_{gcs} & L_{gds} & L_{ges} & L_{gfs} & L_{ggs} \end{bmatrix} \tag{4.69}$$

$$L_r = \begin{bmatrix} L_{aar} & L_{abr} & L_{acr} & L_{adr} & L_{aer} & L_{afr} & L_{agr} \\ L_{bar} & L_{bbr} & L_{bcr} & L_{bdr} & L_{ber} & L_{bfr} & L_{bgr} \\ L_{car} & L_{cbr} & L_{ccr} & L_{cdr} & L_{cer} & L_{cfr} & L_{cgr} \\ L_{dar} & L_{dbr} & L_{dcr} & L_{ddr} & L_{der} & L_{dfr} & L_{dgr} \\ L_{ear} & L_{ebr} & L_{ecr} & L_{edr} & L_{eer} & L_{efr} & L_{egr} \\ L_{far} & L_{fbr} & L_{fcr} & L_{fdr} & L_{fer} & L_{ffr} & L_{fgr} \\ L_{gar} & L_{gbr} & L_{gcr} & L_{gdr} & L_{ger} & L_{gfr} & L_{ggr} \end{bmatrix} \tag{4.70}$$

The phase difference between each phase is denoted as $\alpha = {}^{2\pi}\!/_{7}$ and 'M' is mutual inductance between windings. After adding this values for all three stator and rotor windings

$$\underline{L}_s = \begin{bmatrix} L_{ls}+M & MCos\alpha & MCos2\alpha & MCos3\alpha & MCos3\alpha & MCos2\alpha & MCos\alpha \\ MCos\alpha & L_{ls}+M & MCos\alpha & MCos2\alpha & MCos3\alpha & MCos3\alpha & MCos2\alpha \\ MCos2\alpha & MCos\alpha & L_{ls}+M & MCos\alpha & MCos2\alpha & MCos3\alpha & MCos3\alpha \\ MCos3\alpha & MCos2\alpha & MCos\alpha & L_{ls}+M & MCos\alpha & MCos2\alpha & MCos3\alpha \\ MCos3\alpha & MCos3\alpha & MCos2\alpha & MCos\alpha & L_{ls}+M & MCos\alpha & MCos2\alpha \\ MCos2\alpha & MCos3\alpha & MCos3\alpha & MCos2\alpha & MCos\alpha & L_{ls}+M & MCos\alpha \\ MCos\alpha & MCos2\alpha & MCos3\alpha & MCos3\alpha & MCos2\alpha & MCos\alpha & L_{ls}+M \end{bmatrix} \tag{4.70a}$$

$$\underline{L}_{s1} = \begin{bmatrix} L_{ls1}+M1 & M_1Cos\alpha & M_1Cos2\alpha & M_1Cos3\alpha & M_1Cos3\alpha & M_1Cos2\alpha & M_1Cos\alpha \\ M_1Cos\alpha & L_{ls1}+M_1 & M_1Cos\alpha & M_1Cos2\alpha & M_1Cos3\alpha & M_1Cos3\alpha & M_1Cos2\alpha \\ M_1Cos2\alpha & M_1Cos\alpha & L_{ls1}+M_1 & M_1Cos\alpha & M_1Cos2\alpha & M_1Cos3\alpha & M_1Cos3\alpha \\ M_1Cos3\alpha & M_1Cos2\alpha & M_1Cos\alpha & L_{ls1}+M_1 & M_1Cos\alpha & M_1Cos2\alpha & M_1Cos3\alpha \\ M_1Cos3\alpha & M_1Cos3\alpha & M_1Cos2\alpha & M_1Cos\alpha & L_{ls1}+M_1 & M_1Cos\alpha & M_1Cos2\alpha \\ M_1Cos2\alpha & M_1Cos3\alpha & M_1Cos3\alpha & M_1Cos2\alpha & M_1Cos\alpha & L_{ls1}+M_1 & M_1Cos\alpha \\ M_1Cos\alpha & M_1Cos2\alpha & M_1Cos3\alpha & M_1Cos3\alpha & M_1Cos2\alpha & M_1Cos\alpha & L_{ls1}+M_1 \end{bmatrix}$$

(4.70b)

$$\underline{L}_{s2} = \begin{bmatrix} L_{ls2}+M_2 & M_2Cos2\alpha & M_2Cos3\alpha & M_2Cos\alpha & M_2Cos\alpha & M_2Cos3\alpha & M_2Cos2\alpha \\ M_2Cos2\alpha & L_{ls2}+M_2 & M_2Cos2\alpha & M_2Cos3\alpha & M_2Cos\alpha & M_2Cos\alpha & M_2Cos3\alpha \\ M_2Cos3\alpha & M_2Cos2\alpha & L_{ls2}+M_2 & M_2Cos2\alpha & M_2Cos3\alpha & M_2Cos\alpha & M_2Cos\alpha \\ M_2Cos\alpha & M_2Cos3\alpha & M_2Cos2\alpha & L_{ls2}+M_2 & M_2Cos2\alpha & M_2Cos3\alpha & M_2Cos\alpha \\ M_2Cos\alpha & M_2Cos\alpha & M_2Cos3\alpha & M_2Cos2\alpha & L_{ls2}+M_2 & M_2Cos2\alpha & M_2Cos3\alpha \\ M_2Cos3\alpha & M_2Cos\alpha & M_2Cos\alpha & M_2Cos3\alpha & M_2Cos2\alpha & L_{ls2}+M_2 & M_2Cos2\alpha \\ M_2Cos2\alpha & M_2Cos3\alpha & M_2Cos\alpha & M_2Cos\alpha & M_2Cos3\alpha & M_2Cos2\alpha & L_{ls2}+M_2 \end{bmatrix}$$

(4.70c)

$$\underline{L}_{s3} = \begin{bmatrix} L_{ls3}+M_3 & M_3Cos2\alpha & M_3Cos3\alpha & M_3Cos\alpha & M_3Cos\alpha & M_3Cos3\alpha & M_3Cos2\alpha \\ M_3Cos2\alpha & L_{ls3}+M_3 & M_3Cos2\alpha & M_3Cos3\alpha & M_3Cos\alpha & M_3Cos\alpha & M_3Cos3\alpha \\ M_3Cos3\alpha & M_3Cos2\alpha & L_{ls3}+M_3 & M_3Cos2\alpha & M_3Cos3\alpha & M_3Cos\alpha & M_3Cos\alpha \\ M_3Cos\alpha & M_3Cos3\alpha & M_3Cos2\alpha & L_{ls3}+M_3 & M_3Cos2\alpha & M_3Cos3\alpha & M_3Cos\alpha \\ M_3Cos\alpha & M_3Cos\alpha & M_3Cos3\alpha & M_3Cos2\alpha & L_{ls3}+M_3 & M_3Cos2\alpha & M_3Cos3\alpha \\ M_3Cos3\alpha & M_3Cos\alpha & M_3Cos\alpha & M_3Cos3\alpha & M_3Cos2\alpha & L_{ls3}+M_3 & M_3Cos2\alpha \\ M_3Cos2\alpha & M_3Cos3\alpha & M_3Cos\alpha & M_3Cos\alpha & M_3Cos3\alpha & M_3Cos2\alpha & L_{ls3}+M_3 \end{bmatrix}$$

(4.70d)

$$\underline{L}_{r1} = \begin{bmatrix} L_{lr1}+M1 & M_1Cos\alpha & M_1Cos2\alpha & M_1Cos3\alpha & M_1Cos3\alpha & M_1Cos2\alpha & M_1Cos\alpha \\ M_1Cos\alpha & L_{lr1}+M_1 & M_1Cos\alpha & M_1Cos2\alpha & M_1Cos3\alpha & M_1Cos3\alpha & M_1Cos2\alpha \\ M_1Cos2\alpha & M_1Cos\alpha & L_{lr1}+M_1 & M_1Cos\alpha & M_1Cos2\alpha & M_1Cos3\alpha & M_1Cos3\alpha \\ M_1Cos3\alpha & M_1Cos2\alpha & M_1Cos\alpha & L_{lr1}+M_1 & M_1Cos\alpha & M_1Cos2\alpha & M_1Cos3\alpha \\ M_1Cos3\alpha & M_1Cos3\alpha & M_1Cos2\alpha & M_1Cos\alpha & L_{lr1}+M_1 & M_1Cos\alpha & M_1Cos2\alpha \\ M_1Cos2\alpha & M_1Cos3\alpha & M_1Cos3\alpha & M_1Cos2\alpha & M_1Cos\alpha & L_{lr1}+M_1 & M_1Cos\alpha \\ M_1Cos\alpha & M_1Cos2\alpha & M_1Cos3\alpha & M_1Cos3\alpha & M_1Cos2\alpha & M_1Cos\alpha & L_{lr1}+M_1 \end{bmatrix}$$

(4.70e)

$$
\underline{L}_{r2} = \begin{bmatrix} L_{lr2}+M_2 & M_2Cos\alpha & M_2Cos2\alpha & M_2Cos3\alpha & M_2Cos3\alpha & M_2Cos2\alpha & M_2Cos\alpha \\ M_2Cos\alpha & L_{lr2}+M_2 & M_2Cos\alpha & M_2Cos2\alpha & M_2Cos3\alpha & M_2Cos3\alpha & M_2Cos2\alpha \\ M_2Cos2\alpha & M_2Cos\alpha & L_{lr2}+M_2 & M_2Cos\alpha & M_2Cos2\alpha & M_2Cos3\alpha & M_2Cos3\alpha \\ M_2Cos3\alpha & M_2Cos2\alpha & M_2Cos\alpha & L_{lr2}+M_2 & M_2Cos\alpha & M_2Cos2\alpha & M_2Cos3\alpha \\ M_2Cos3\alpha & M_2Cos3\alpha & M_2Cos2\alpha & M_2Cos\alpha & L_{lr2}+M_2 & M_2Cos\alpha & M_2Cos2\alpha \\ M_2Cos2\alpha & M_2Cos3\alpha & M_2Cos3\alpha & M_2Cos2\alpha & M_2Cos\alpha & L_{lr2}+M_2 & M_2Cos\alpha \\ M_2Cos\alpha & M_2Cos2\alpha & M_2Cos3\alpha & M_2Cos3\alpha & M_2Cos2\alpha & M_2Cos\alpha & L_{lr2}+M_2 \end{bmatrix} \tag{4.70f}
$$

$$
\underline{L}_{r3} = \begin{bmatrix} L_{lr3}+M_3 & M_3Cos\alpha & M_3Cos2\alpha & M_3Cos3\alpha & M_3Cos3\alpha & M_3Cos2\alpha & M_3Cos\alpha \\ M_3Cos\alpha & L_{lr3}+M_3 & M_3Cos\alpha & M_3Cos2\alpha & M_3Cos3\alpha & M_3Cos3\alpha & M_3Cos2\alpha \\ M_3Cos2\alpha & M_3Cos\alpha & L_{lr3}+M_3 & M_3Cos\alpha & M_3Cos2\alpha & M_3Cos3\alpha & M_3Cos3\alpha \\ M_3Cos3\alpha & M_3Cos2\alpha & M_3Cos\alpha & L_{lr3}+M_3 & M_3Cos\alpha & M_3Cos2\alpha & M_3Cos3\alpha \\ M_3Cos3\alpha & M_3Cos3\alpha & M_3Cos2\alpha & M_3Cos\alpha & L_{lr3}+M_3 & M_3Cos\alpha & M_3Cos2\alpha \\ M_3Cos2\alpha & M_3Cos3\alpha & M_3Cos3\alpha & M_3Cos2\alpha & M_3Cos\alpha & L_{lr3}+M_3 & M_3Cos\alpha \\ M_3Cos\alpha & M_3Cos2\alpha & M_3Cos3\alpha & M_3Cos3\alpha & M_3Cos2\alpha & M_3Cos\alpha & L_{lr3}+M_3 \end{bmatrix} \tag{4.70g}
$$

$$
\underline{L}_{sr1} = M_1 \begin{bmatrix} Cos\,\theta_1 & Cos(\theta_1+\alpha) & Cos(\theta_1+2\alpha) & Cos(\theta_1+3\alpha) & Cos(\theta_1-3\alpha) & Cos(\theta_1-2\alpha) & Cos(\theta_1-\alpha) \\ Cos(\theta_1-\alpha) & Cos\,\theta_1 & Cos(\theta_1+\alpha) & Cos(\theta_1+2\alpha) & Cos(\theta_1+3\alpha) & Cos(\theta_1-3\alpha) & Cos(\theta_1-2\alpha) \\ Cos(\theta_1-2\alpha) & Cos(\theta_1-\alpha) & Cos\,\theta_1 & Cos(\theta_1+\alpha) & Cos(\theta_1+2\alpha) & Cos(\theta_1+3\alpha) & Cos(\theta_1-3\alpha) \\ Cos(\theta_1-3\alpha) & Cos(\theta_1-2\alpha) & Cos(\theta_1-\alpha) & Cos\,\theta_1 & Cos(\theta_1+\alpha) & Cos(\theta_1+2\alpha) & Cos(\theta_1+3\alpha) \\ Cos(\theta_1+3\alpha) & Cos(\theta_1-3\alpha) & Cos(\theta_1-2\alpha) & Cos(\theta_1-\alpha) & Cos\,\theta_1 & Cos(\theta_1+\alpha) & Cos(\theta_1+2\alpha) \\ Cos(\theta_1+2\alpha) & Cos(\theta_1+3\alpha) & Cos(\theta_1-3\alpha) & Cos(\theta_1-2\alpha) & Cos(\theta_1-\alpha) & Cos\,\theta_1 & Cos(\theta_1+\alpha) \\ Cos(\theta_1+\alpha) & Cos(\theta_1+2\alpha) & Cos(\theta_1+3\alpha) & Cos(\theta_1-3\alpha) & Cos(\theta_1-2\alpha) & Cos(\theta_1-\alpha) & Cos\,\theta_1 \end{bmatrix} \tag{4.70h}
$$

$$
\underline{L}^1_{sr2} = M_2 \begin{bmatrix} Cos\,\theta_2 & Cos\,(\theta_2+\alpha) & Cos\,(\theta_2+2\alpha) & Cos\,(\theta_2+3\alpha) & Cos\,(\theta_1-3\alpha) & Cos\,(\theta_1-2\alpha) & Cos\,(\theta_1-\alpha) \\ Cos\,(\theta_2-2\alpha) & Cos\,(\theta_2-\alpha) & Cos\,\theta_2 & Cos\,(\theta_2+\alpha) & Cos\,(\theta_2+2\alpha) & Cos\,(\theta_2+3\alpha) & Cos\,(\theta_2-3\alpha) \\ Cos\,(\theta_2+3\alpha) & Cos\,(\theta_2-3\alpha) & Cos\,(\theta_2-2\alpha) & Cos\,(\theta_2-\alpha) & Cos\,\theta_2 & Cos\,(\theta_2+\alpha) & Cos\,(\theta_2+2\alpha) \\ Cos\,(\theta_2+\alpha) & Cos\,(\theta_2+2\alpha) & Cos\,(\theta_2+3\alpha) & Cos\,(\theta_2-2\alpha) & Cos\,(\theta_2-\alpha) & Cos\,(\theta_2-\alpha) & Cos\,\theta_2 \\ Cos\,(\theta_2-\alpha) & Cos\,\theta_2 & Cos\,(\theta_2+\alpha) & Cos\,(\theta_2+2\alpha) & Cos\,(\theta_2+3\alpha) & Cos\,(\theta_2-3\alpha) & Cos\,(\theta_2-\alpha) \\ Cos\,(\theta_2-3\alpha) & Cos\,(\theta_2-2\alpha) & Cos\,(\theta_2-\alpha) & Cos\,\theta_2 & Cos\,(\theta_2+\alpha) & Cos\,(\theta_2+2\alpha) & Cos\,(\theta_2+3\alpha) \\ Cos\,(\theta_2+2\alpha) & Cos\,(\theta_2+3\alpha) & Cos\,(\theta_2-3\alpha) & Cos\,(\theta_2-2\alpha) & Cos\,(\theta_2-\alpha) & Cos\,\theta_2 & Cos\,(\theta_2+\alpha) \end{bmatrix} \tag{4.70i}
$$

$$
\underline{L}^1_{sr3} = M_3 \begin{bmatrix} Cos\,\theta_3 & Cos\,(\theta_3+\alpha) & Cos\,(\theta_3+2\alpha) & Cos\,(\theta_3+3\alpha) & Cos\,(\theta_3-3\alpha) & Cos\,(\theta_3-2\alpha) & Cos\,(\theta_3-\alpha) \\ Cos\,(\theta_3-3\alpha) & Cos\,(\theta_3-2\alpha) & Cos\,(\theta_3-\alpha) & Cos\,\theta_3 & Cos\,(\theta_3+\alpha) & Cos\,(\theta_3+2\alpha) & Cos\,(\theta_2+3\alpha) \\ Cos\,(\theta_3+\alpha) & Cos\,(\theta_3+3\alpha) & Cos\,(\theta_3+3\alpha) & Cos\,(\theta_3-2\alpha) & Cos\,(\theta_3-\alpha) & Cos\,(\theta_3-3\alpha) & Cos\,\theta_3 \\ Cos\,(\theta_3-2\alpha) & Cos\,(\theta_3-\alpha) & Cos\,\theta_3 & Cos\,(\theta_3+\alpha) & Cos\,(\theta_3+2\alpha) & Cos\,(\theta_3+3\alpha) & Cos\,(\theta_3-3\alpha) \\ Cos\,(\theta_3+2\alpha) & Cos\,(\theta_3+3\alpha) & Cos\,(\theta_3-3\alpha) & Cos\,(\theta_3-2\alpha) & Cos\,(\theta_2-\alpha) & Cos\,\theta_3 & Cos\,(\theta_3+\alpha) \\ Cos\,(\theta_3-\alpha) & Cos\,\theta_2 & Cos\,(\theta_3+\alpha) & Cos\,(\theta_3+2\alpha) & Cos\,(\theta_3+3\alpha) & Cos\,(\theta_3-3\alpha) & Cos\,(\theta_3-\alpha) \\ Cos\,(\theta_2+3\alpha) & Cos\,(\theta_3-3\alpha) & Cos\,(\theta_3-2\alpha) & Cos\,(\theta_3-\alpha) & Cos\,\theta_3 & Cos\,(\theta_3+\alpha) & Cos\,(\theta_3-3\alpha) \end{bmatrix} \tag{4.70j}
$$

While putting all the matrices in the equation (4.65), the following is obtained:

$$
\begin{bmatrix} \underline{V}^{MC} \\ 0 \\ 0 \\ 0 \end{bmatrix} = \begin{bmatrix} \underline{R}_{s1}+\underline{R}_{s2}+\underline{R}_{s3} & 0 & 0 & 0 \\ 0 & \underline{R}_{r1} & 0 & 0 \\ 0 & 0 & \underline{R}_{r2} & 0 \\ 0 & 0 & 0 & \underline{R}_{r3} \end{bmatrix} \begin{bmatrix} \underline{i}^{MC} \\ \underline{i}_{r1} \\ \underline{i}_{r2} \\ \underline{i}_{r3} \end{bmatrix} + \begin{bmatrix} \underline{L}_{s1}+\underline{L}^{1}_{s2}+\underline{L}^{1}_{s3} & \underline{L}_{sr1} & \underline{L}^{1}_{sr2} & \underline{L}^{1}_{sr3} \\ \underline{L}_{rs1} & \underline{L}_{r1} & 0 & 0 \\ \underline{L}^{1}_{rs2} & 0 & \underline{L}_{r2} & 0 \\ \underline{L}^{1}_{rs3} & 0 & 0 & \underline{L}_{r3} \end{bmatrix} \frac{d}{dt} \begin{bmatrix} \underline{i}^{MC} \\ \underline{i}_{r1} \\ \underline{i}_{r2} \\ \underline{i}_{r3} \end{bmatrix} +
$$

$$
\begin{bmatrix} 0 & \frac{d}{dt}\underline{L}_{sr1} & \frac{d}{dt}\underline{L}^{1}_{sr2} & \frac{d}{dt}\underline{L}^{1}_{sr3} \\ \frac{d}{dt}\underline{L}_{rs1} & 0 & 0 & 0 \\ \frac{d}{dt}\underline{L}^{1}_{rs2} & 0 & 0 & 0 \\ \frac{d}{dt}\underline{L}^{1}_{rs3} & 0 & 0 & 0 \end{bmatrix} \begin{bmatrix} \underline{i}^{MC} \\ \underline{i}_{r1} \\ \underline{i}_{r2} \\ \underline{i}_{r3} \end{bmatrix} \tag{4.71}
$$

where:

$$
{}^{d}\!/_{dt}\,\underline{L}_{sr1} = -\omega_1 M_1 \begin{bmatrix}
Sin\theta_1 & Sin(\theta_1+\alpha) & Sin(\theta_1+2\alpha) & Sin(\theta_1+3\alpha) & Sin(\theta_1-3\alpha) & Sin(\theta_1-2\alpha) & Sin(\theta_1-\alpha) \\
Sin(\theta_1-\alpha) & Sin\theta_1 & Sin(\theta_1+\alpha) & Sin(\theta_1+2\alpha) & Sin(\theta_1+3\alpha) & Sin(\theta_1-3\alpha) & Sin(\theta_1-2\alpha) \\
Sin(\theta_1-2\alpha) & Sin(\theta_1-\alpha) & Sin\theta_1 & Sin(\theta_1+\alpha) & Sin(\theta_1+2\alpha) & Sin(\theta_1+3\alpha) & Sin(\theta_1-3\alpha) \\
Sin(\theta_1-3\alpha) & Sin(\theta_1-2\alpha) & Sin(\theta_1-\alpha) & Sin\theta_1 & Sin(\theta_1+\alpha) & Sin(\theta_1+2\alpha) & Sin(\theta_1+3\alpha) \\
Sin(\theta_1+3\alpha) & Sin(\theta_1-3\alpha) & Sin(\theta_1-2\alpha) & Sin(\theta_1-\alpha) & Sin\theta_1 & Sin(\theta_1+\alpha) & Sin(\theta_1+2\alpha) \\
Sin(\theta_1+2\alpha) & Sin(\theta_1+3\alpha) & Sin(\theta_1-3\alpha) & Sin(\theta_1-2\alpha) & Sin(\theta_1-\alpha) & Sin\theta_1 & Sin(\theta_1+\alpha) \\
Sin(\theta_1+\alpha) & Sin(\theta_1+2\alpha) & Sin(\theta_1+3\alpha) & Sin(\theta_1-3\alpha) & Sin(\theta_1-2\alpha) & Sin(\theta_1-\alpha) & Sin\theta_1
\end{bmatrix} \tag{4.71a}
$$

$$
{}^{d}\!/_{dt}\,\underline{L}^{1}_{sr2} = -\omega_2 M_2 \begin{bmatrix}
Sin\,\theta_2 & Sin(\theta_2+\alpha) & Sin(\theta_2+2\alpha) & Sin(\theta_2+3\alpha) & Sin(\theta_2-3\alpha) & Sin(\theta_2-2\alpha) & Sin(\theta_2-\alpha) \\
Sin(\theta_2-2\alpha) & Sin(\theta_2-\alpha) & Sin\,\theta_2 & Sin(\theta_2+\alpha) & Sin(\theta_2+2\alpha) & Sin(\theta_2+3\alpha) & Sin(\theta_2-3\alpha) \\
Sin(\theta_2+3\alpha) & Sin(\theta_2-3\alpha) & Sin(\theta_2-2\alpha) & Sin(\theta_2-\alpha) & Sin\,\theta_2 & Sin(\theta_2+\alpha) & Sin(\theta_2+2\alpha) \\
Sin(\theta_2+\alpha) & Sin(\theta_2+2\alpha) & Sin(\theta_2+3\alpha) & Sin(\theta_2-2\alpha) & Sin(\theta_2-\alpha) & Sin(\theta_2-\alpha) & Sin\,\theta_2 \\
Sin(\theta_2-\alpha) & Sin\,\theta_2 & Sin(\theta_2+\alpha) & Sin(\theta_2+2\alpha) & Sin(\theta_2+3\alpha) & Sin(\theta_2-3\alpha) & Sin(\theta_2-\alpha) \\
Sin(\theta_2-3\alpha) & Sin(\theta_2-2\alpha) & Sin(\theta_2-\alpha) & Sin\,\theta_2 & Sin(\theta_2+\alpha) & Sin(\theta_2+2\alpha) & Sin(\theta_2+3\alpha) \\
Sin(\theta_2+2\alpha) & Sin(\theta_2+3\alpha) & Sin(\theta_2-3\alpha) & Sin(\theta_2-2\alpha) & Sin(\theta_2-\alpha) & Sin\,\theta_2 & Sin(\theta_2+\alpha)
\end{bmatrix} \tag{4.71b}
$$

$$
{}^{d}\!/_{dt}\,\underline{L}^{1}_{sr3} = -\omega_3 M_3 \begin{bmatrix}
Sin\,\theta_3 & Sin(\theta_3+\alpha) & Sin(\theta_3+2\alpha) & Sin(\theta_3+3\alpha) & Sin(\theta_3-3\alpha) & Sin(\theta_3-2\alpha) & Sin(\theta_3-\alpha) \\
Sin(\theta_3-3\alpha) & Sin(\theta_3-2\alpha) & Sin(\theta_3-\alpha) & Sin\,\theta_3 & Sin(\theta_3+\alpha) & Sin(\theta_3+2\alpha) & Sin(\theta_2+3\alpha) \\
Sin(\theta_3+\alpha) & Sin(\theta_3+3\alpha) & Sin(\theta_3+3\alpha) & Sin(\theta_3-2\alpha) & Sin(\theta_3-\alpha) & Sin(\theta_3-3\alpha) & Sin\,\theta_3 \\
Sin(\theta_3-2\alpha) & Sin(\theta_3-\alpha) & Sin\,\theta_3 & Sin(\theta_3+\alpha) & Sin(\theta_3+2\alpha) & Sin(\theta_3+3\alpha) & Sin(\theta_3-3\alpha) \\
Sin(\theta_3+2\alpha) & Sin(\theta_3+3\alpha) & Sin(\theta_3-3\alpha) & Sin(\theta_3-2\alpha) & Sin(\theta_2-\alpha) & Sin\,\theta_3 & Sin(\theta_3+\alpha) \\
Sin(\theta_3-\alpha) & Sin\,\theta_2 & Sin(\theta_3+\alpha) & Sin(\theta_3+2\alpha) & Sin(\theta_3+3\alpha) & Sin(\theta_3-3\alpha) & Sin(\theta_3-\alpha) \\
Sin(\theta_2+3\alpha) & Sin(\theta_3-3\alpha) & Sin(\theta_3-2\alpha) & Sin(\theta_3-\alpha) & Sin\,\theta_3 & Sin(\theta_3+\alpha) & Sin(\theta_3-3\alpha)
\end{bmatrix} \tag{4.71b}
$$

$$
\begin{aligned}
\frac{d}{dt}\underline{L}^{1}_{rs1} &= \frac{d}{dt}\underline{L}^{T1}{}_{sr1} \\
\frac{d}{dt}\underline{L}^{1}_{rs2} &= \frac{d}{dt}\underline{L}^{T1}{}_{sr2} \\
\frac{d}{dt}\underline{L}^{1}_{rs3} &= \frac{d}{dt}\underline{L}^{T1}{}_{sr3}
\end{aligned} \tag{4.72}
$$

Torque equations of the seven-phase induction machine in terms of source currents and their respective rotor currents and rotor positions are:

$$T_{e1} = -P_1 M_1 \begin{bmatrix} (i_A i_{ar1} + i_B i_{br1} + i_C i_{cr1} + i_D i_{dr1} + i_E i_{er1} + i_F i_{fr1} + i_G i_{gr1}) Sin\theta_1 + \\ (i_G i_{ar1} + i_A i_{br1} + i_B i_{cr1} + i_C i_{dr1} + i_D i_{er1} + i_E i_{fr1} + i_F i_{gr1}) \sin(\theta_1 + \alpha) + \\ (i_F i_{ar1} + i_G i_{br1} + i_A i_{cr1} + i_B i_{dr1} + i_C i_{er1} + i_D i_{fr1} + i_E i_{gr1}) Sin(\theta_1 + 2\alpha) + \\ (i_E i_{ar1} + i_F i_{br1} + i_G i_{cr1} + i_A i_{dr1} + i_B i_{er1} + i_C i_{fr1} + i_D i_{gr1}) Sin(\theta_1 + 3\alpha) + \\ (i_D i_{ar1} + i_E i_{br1} + i_F i_{cr1} + i_G i_{dr1} + i_A i_{er1} + i_B i_{fr1} + i_C i_{gr1}) Sin(\theta_1 - 3\alpha) + \\ (i_C i_{ar1} + i_D i_{br1} + i_E i_{cr1} + i_F i_{dr1} + i_G i_{er1} + i_A i_{fr1} + i_B i_{gr1}) Sin(\theta_1 - 2\alpha) + \\ (i_B i_{ar1} + i_C i_{br1} + i_D i_{cr1} + i_E i_{dr1} + i_F i_{er1} + i_G i_{fr1} + i_A i_{gr1}) Sin(\theta_1 - \alpha) \end{bmatrix} \tag{4.73}$$

$$T_{e2} = -P_2 M_2 \begin{bmatrix} (i_A i_{ar2} + i_B i_{br2} + i_C i_{cr2} + i_D i_{dr2} + i_E i_{er2} + i_F i_{fr2} + i_G i_{gr2}) Sin\theta_2 + \\ (i_G i_{ar2} + i_A i_{br2} + i_B i_{cr2} + i_C i_{dr2} + i_D i_{er2} + i_E i_{fr2} + i_F i_{gr2}) Sin(\theta_2 + \alpha) + \\ (i_F i_{ar2} + i_G i_{br2} + i_A i_{cr2} + i_B i_{dr2} + i_C i_{er2} + i_D i_{fr2} + i_E i_{gr2}) Sin(\theta_2 + 2\alpha) + \\ (i_E i_{ar2} + i_F i_{br2} + i_G i_{cr2} + i_A i_{dr2} + i_B i_{er2} + i_C i_{fr2} + i_D i_{gr2}) Sin(\theta_2 + 3\alpha) + \\ (i_D i_{ar2} + i_E i_{br2} + i_F i_{cr2} + i_G i_{dr2} + i_A i_{er2} + i_B i_{fr2} + i_C i_{gr2}) Sin(\theta_2 - 3\alpha) + \\ (i_C i_{ar2} + i_D i_{br2} + i_E i_{cr2} + i_F i_{dr2} + i_G i_{er2} + i_A i_{fr2} + i_B i_{gr2}) Sin(\theta_2 - 2\alpha) + \\ (i_B i_{ar2} + i_C i_{br2} + i_D i_{cr2} + i_E i_{dr2} + i_F i_{er2} + i_G i_{fr2} + i_A i_{gr2}) Sin(\theta_2 - \alpha) \end{bmatrix} \tag{4.74}$$

$$T_{e3} = -P_3 M_3 \begin{bmatrix} (i_A i_{ar3} + i_B i_{br3} + i_C i_{cr3} + i_D i_{dr3} + i_E i_{er3} + i_F i_{fr3} + i_G i_{gr3}) Sin\,\theta_3 + \\ (i_G i_{ar3} + i_A i_{br3} + i_B i_{cr3} + i_C i_{dr3} + i_D i_{er3} + i_E i_{fr3} + i_F i_{gr3}) Sin\,(\theta_3 + \alpha) + \\ (i_F i_{ar3} + i_G i_{br3} + i_A i_{cr3} + i_B i_{dr3} + i_C i_{er3} + i_D i_{fr3} + i_E i_{gr3}) Sin\,(\theta_3 + 2\alpha) + \\ (i_E i_{ar3} + i_F i_{br3} + i_G i_{cr3} + i_A i_{dr3} + i_B i_{er3} + i_C i_{fr3} + i_D i_{gr3}) Sin\,(\theta_3 + 3\alpha) + \\ (i_D i_{ar3} + i_E i_{br3} + i_F i_{cr3} + i_G i_{dr3} + i_A i_{er3} + i_B i_{fr3} + i_C i_{gr3}) Sin\,(\theta_3 - 3\alpha) + \\ (i_C i_{ar3} + i_D i_{br3} + i_E i_{cr3} + i_F i_{dr3} + i_G i_{er3} + i_A i_{fr3} + i_B i_{gr3}) Sin\,(\theta_3 - 2\alpha) + \\ (i_B i_{ar3} + i_C i_{br3} + i_D i_{cr3} + i_E i_{dr3} + i_F i_{er3} + i_G i_{fr3} + i_A i_{gr3}) Sin\,(\theta_3 - \alpha) \end{bmatrix} \tag{4.75}$$

Equation of motion:

$$\frac{d\omega_1}{dt} = \frac{p_1}{J_1}(T_{e1} - T_{L1})$$
$$\frac{d\omega_2}{dt} = \frac{p_2}{J_2}(T_{e2} - T_{L2}) \quad (4.76)$$
$$\frac{d\omega_3}{dt} = \frac{p_3}{J_3}(T_{e3} - T_{L3})$$

4.4b Model in the rotating reference frame

The decoupling transformation matrix to transfer from phase variable form to power invariant form of seven phase system can be written as:

$$\underline{C} = \sqrt{\frac{2}{7}} \begin{array}{c} \alpha \\ \beta \\ x_1 \\ y_1 \\ x_2 \\ y_2 \\ 0 \end{array} \begin{bmatrix} 1 & Cos\alpha & Cos2\alpha & Cos3\alpha & Cos4\alpha & Cos5\alpha & Cos6\alpha \\ 0 & Sin\alpha & Sin2\alpha & Sin3\alpha & Sin4\alpha & Sin5\alpha & Sin6\alpha \\ 1 & Cos2\alpha & Cos4\alpha & Cos6\alpha & Cos8\alpha & Cos10\alpha & Cos12\alpha \\ 0 & Sin2\alpha & Sin4\alpha & Sin6\alpha & Sin8\alpha & Sin10\alpha & Sin12\alpha \\ 1 & Cos3\alpha & Cos6\alpha & Cos9\alpha & Cos`12\alpha & Cos15\alpha & Cos18\alpha \\ 0 & Sin3\alpha & Sin6\alpha & Sin9\alpha & Sin12\alpha & Sin15\alpha & Sin18\alpha \\ 1/\sqrt{2} & 1/\sqrt{2} & 1/\sqrt{2} & 1/\sqrt{2} & 1/\sqrt{2} & 1/\sqrt{2} & 1/\sqrt{2} \end{bmatrix} \quad (4.77)$$

The first two rows of the decoupling matrix is defined all variables that will lead to fundamental flux and torque production (α, β components). The last row defined the zero sequence components and all x-y components are noted in middle.

The new variables are defined with transformation matrix:

$$\begin{aligned}
&\underline{V}_{\alpha\beta}^{MC} = \underline{C}\underline{v}^{MC}, \underline{V}_{\alpha\beta}^{r1} = \underline{C}\underline{v}^{r1} \\
&\underline{V}_{\alpha\beta}^{r2} = \underline{C}\underline{v}^{r2} \\
&\underline{V}_{\alpha\beta}^{r3} = \underline{C}\underline{v}^{r3} \\
&\underline{i}_{\alpha\beta}^{MC} = \underline{C}\underline{i}^{MC} \\
&\underline{i}_{\alpha\beta}^{r1} = \underline{C}\underline{i}^{r1} \\
&\underline{i}_{\alpha\beta}^{r2} = \underline{C}\underline{i}^{r2} \\
&\underline{i}_{\alpha\beta}^{r3} = \underline{C}\underline{i}^{r3} \\
&\underline{\psi}_{\alpha\beta}^{MC} = \underline{C}\underline{\psi}^{Inv}, \ \underline{\psi}_{\alpha\beta}^{r1} = \underline{C}\underline{\psi}^{r1}, \ \underline{\psi}_{\alpha\beta}^{r2} = \underline{C}\underline{\psi}^{r2}, \ \underline{\psi}_{\alpha\beta}^{r3} = \underline{C}\underline{\psi}^{r3}
\end{aligned} \quad (4.78)$$

The superscripts, *MC* stand for Matrix Converter quantities; r1, r2 and r3 refer to the rotor of machine-1, machine-2 and machine-3.

Application of the new variables in to voltage equation will yield following voltage equations:

$$\underline{V} = \begin{bmatrix} \underline{C}^{-1}\underline{V}_{\alpha\beta}^{MC} \\ 0 \\ 0 \\ 0 \end{bmatrix} = [\underline{R}] \begin{bmatrix} \underline{C}^{-1}\underline{i}_{\alpha\beta}^{MC} \\ \underline{C}^{-1}\underline{i}_{\alpha\beta}^{r1} \\ \underline{C}^{-1}\underline{i}_{\alpha\beta}^{r2} \\ \underline{C}^{-1}\underline{i}_{\alpha\beta}^{r3} \end{bmatrix} + [\underline{L}] \,{}^{d}\!/_{dt} \begin{bmatrix} \underline{C}^{-1}\underline{i}_{\alpha\beta}^{inv} \\ \underline{C}^{-1}\underline{i}_{\alpha\beta}^{r1} \\ \underline{C}^{-1}\underline{i}_{\alpha\beta}^{r2} \\ \underline{C}^{-1}\underline{i}_{\alpha\beta}^{r3} \end{bmatrix} \tag{4.79}$$

That is:

$$\begin{bmatrix} \underline{C}^{-1}\underline{V}_{\alpha\beta}^{MC} \\ 0 \\ 0 \\ 0 \end{bmatrix} = \begin{bmatrix} \underline{R}_{s1}+\underline{R}_{s2}+\underline{R}_{s3} & 0 & 0 & 0 \\ 0 & \underline{R}_{r1} & 0 & 0 \\ 0 & 0 & \underline{R}_{r2} & 0 \\ 0 & 0 & 0 & \underline{R}_{r3} \end{bmatrix} \begin{bmatrix} \underline{C}^{-1}\underline{i}_{\alpha\beta}^{MC} \\ \underline{C}^{-1}\underline{i}_{\alpha\beta}^{r1} \\ \underline{C}^{-1}\underline{i}_{\alpha\beta}^{r2} \\ \underline{C}^{-1}\underline{i}_{\alpha\beta}^{r3} \end{bmatrix} +$$

$$\begin{bmatrix} \underline{L}_{s1}+\underline{L}^{1}_{s2}+\underline{L}^{1}_{s3} & \underline{L}_{sr1} & \underline{L}^{1}_{sr2} & \underline{L}^{1}_{sr3} \\ \underline{L}_{rs1} & \underline{L}_{r1} & 0 & 0 \\ \underline{L}^{1}_{rs2} & 0 & \underline{L}_{r2} & 0 \\ \underline{L}^{1}_{rs3} & 0 & 0 & \underline{L}_{r3} \end{bmatrix} {}^{d}\!/_{dt} \begin{bmatrix} \underline{C}^{-1}\underline{i}_{\alpha\beta}^{MC} \\ \underline{C}^{-1}\underline{i}_{\alpha\beta}^{r1} \\ \underline{C}^{-1}\underline{i}_{\alpha\beta}^{r2} \\ \underline{C}^{-1}\underline{i}_{\alpha\beta}^{r3} \end{bmatrix} + \begin{bmatrix} 0 & \frac{d}{dt}\underline{L}_{sr1} & \frac{d}{dt}\underline{L}^{1}_{sr2} & \frac{d}{dt}\underline{L}^{1}_{sr3} \\ \frac{d}{dt}\underline{L}_{rs1} & 0 & 0 & 0 \\ \frac{d}{dt}\underline{L}^{1}_{rs2} & 0 & 0 & 0 \\ \frac{d}{dt}\underline{L}^{1}_{rs3} & 0 & 0 & 0 \end{bmatrix} \begin{bmatrix} \underline{C}^{-1}\underline{i}_{\alpha\beta}^{MC} \\ \underline{C}^{-1}\underline{i}_{\alpha\beta}^{r1} \\ \underline{C}^{-1}\underline{i}_{\alpha\beta}^{r2} \\ \underline{C}^{-1}\underline{i}_{\alpha\beta}^{r3} \end{bmatrix} \tag{4.80}$$

Multiply both sides with the decoupling transformation matrix$\underline{C}$ and separate terms of three machines will give:

$$\begin{bmatrix} \underline{V}_{\alpha\beta}^{MC} \\ 0 \\ 0 \\ 0 \end{bmatrix} = \begin{bmatrix} \underline{R}_{s1}+\underline{R}_{s2}+\underline{R}_{s3} & 0 & 0 & 0 \\ 0 & \underline{R}_{r1} & 0 & 0 \\ 0 & 0 & \underline{R}_{r2} & 0 \\ 0 & 0 & 0 & \underline{R}_{r3} \end{bmatrix} \begin{bmatrix} \underline{i}_{\alpha\beta}^{MC} \\ \underline{i}_{\alpha\beta}^{r1} \\ \underline{i}_{\alpha\beta}^{r2} \\ \underline{i}_{\alpha\beta}^{r3} \end{bmatrix} + \frac{d}{dt} \begin{bmatrix} \underline{C}\underline{L}_{s1}\underline{C}^{-1} & \underline{C}\underline{L}_{sr1}\underline{C}^{-1} & 0 & 0 \\ \underline{C}\underline{L}_{rs1}\underline{C}^{-1} & \underline{C}\underline{L}_{r1}\underline{C}^{-1} & 0 & 0 \\ 0 & 0 & 0 & 0 \\ 0 & 0 & 0 & 0 \end{bmatrix} \begin{bmatrix} \underline{i}_{\alpha\beta}^{MC} \\ \underline{i}_{\alpha\beta}^{r1} \\ \underline{i}_{\alpha\beta}^{r2} \\ \underline{i}_{\alpha\beta}^{r3} \end{bmatrix} +$$

$$\frac{d}{dt} \begin{bmatrix} \underline{C}\underline{L}_{s2}\underline{C}^{-1} & \underline{C}\underline{L}_{sr2}\underline{C}^{-1} & 0 & 0 \\ \underline{C}\underline{L}_{rs2}\underline{C}^{-1} & \underline{C}\underline{L}_{r2}\underline{C}^{-1} & 0 & 0 \\ 0 & 0 & 0 & 0 \\ 0 & 0 & 0 & 0 \end{bmatrix} \begin{bmatrix} \underline{i}_{\alpha\beta}^{MC} \\ \underline{i}_{\alpha\beta}^{r1} \\ \underline{i}_{\alpha\beta}^{r2} \\ \underline{i}_{\alpha\beta}^{r3} \end{bmatrix} + \frac{d}{dt} \begin{bmatrix} \underline{C}\underline{L}_{s3}\underline{C}^{-1} & \underline{C}\underline{L}_{sr3}\underline{C}^{-1} & 0 & 0 \\ \underline{C}\underline{L}_{rs3}\underline{C}^{-1} & \underline{C}\underline{L}_{r3}\underline{C}^{-1} & 0 & 0 \\ 0 & 0 & 0 & 0 \\ 0 & 0 & 0 & 0 \end{bmatrix} \begin{bmatrix} \underline{i}_{\alpha\beta}^{MC} \\ \underline{i}_{\alpha\beta}^{r1} \\ \underline{i}_{\alpha\beta}^{r2} \\ \underline{i}_{\alpha\beta}^{r3} \end{bmatrix} \tag{4.81}$$

This equation further written as:

$$\begin{bmatrix} \underline{V}_{\alpha\beta}^{MC} \\ 0 \\ 0 \\ 0 \end{bmatrix} = \begin{bmatrix} \underline{R}_{s1}+\underline{R}_{s2}+\underline{R}_{s3} & 0 & 0 & 0 \\ 0 & \underline{R}_{r1} & 0 & 0 \\ 0 & 0 & \underline{R}_{r2} & 0 \\ 0 & 0 & 0 & \underline{R}_{r3} \end{bmatrix} \begin{bmatrix} \underline{i}_{\alpha\beta}{}^{MC} \\ \underline{i}_{\alpha\beta}{}^{r1} \\ \underline{i}_{\alpha\beta}{}^{r2} \\ \underline{i}_{\alpha\beta}{}^{r3} \end{bmatrix} + \frac{d}{dt} \begin{bmatrix} \underline{L}_{\alpha\beta}^{s1} & \underline{L}_{\alpha\beta}^{sr1} & 0 & 0 \\ \underline{L}_{\alpha\beta}^{rs1} & \underline{L}_{\alpha\beta}^{r1} & 0 & 0 \\ 0 & 0 & 0 & 0 \\ 0 & 0 & 0 & 0 \end{bmatrix} \begin{bmatrix} \underline{i}_{\alpha\beta}{}^{MC} \\ \underline{i}_{\alpha\beta}{}^{r1} \\ \underline{i}_{\alpha\beta}{}^{r2} \\ \underline{i}_{\alpha\beta}{}^{r3} \end{bmatrix} +$$

$$\frac{d}{dt} \begin{bmatrix} \underline{L}_{\alpha\beta}^{s2^1} & 0 & \underline{L}_{\alpha\beta}^{sr2^1} & 0 \\ 0 & 0 & 0 & 0 \\ \underline{L}_{\alpha\beta}^{rs2^1} & 0 & \underline{L}_{\alpha\beta}^{r2^1} & 0 \\ 0 & 0 & 0 & 0 \end{bmatrix} \begin{bmatrix} \underline{i}_{\alpha\beta}{}^{MC} \\ \underline{i}_{\alpha\beta}{}^{r1} \\ \underline{i}_{\alpha\beta}{}^{r2} \\ \underline{i}_{\alpha\beta}{}^{r3} \end{bmatrix} + \frac{d}{dt} \begin{bmatrix} \underline{L}_{\alpha\beta}^{s3^1} & 0 & 0 & \underline{L}_{\alpha\beta}^{sr3^1} \\ 0 & 0 & 0 & 0 \\ 0 & 0 & 0 & 0 \\ \underline{L}_{\alpha\beta}^{rs3^1} & 0 & 0 & \underline{L}_{\alpha\beta}^{r3^1} \end{bmatrix} \begin{bmatrix} \underline{i}_{\alpha\beta}{}^{MC} \\ \underline{i}_{\alpha\beta}{}^{r1} \\ \underline{i}_{\alpha\beta}{}^{r2} \\ \underline{i}_{\alpha\beta}{}^{r3} \end{bmatrix} \tag{4.82a}$$

After taking individual matrices and solving, the top row belongs to the stator and the next three rows are that of three rotors.

$$\begin{bmatrix} \underline{V}_{\alpha\beta}^{MC} \\ 0 \\ 0 \\ 0 \end{bmatrix} = \begin{bmatrix} \underline{R}_{s1}+\underline{R}_{s2}+\underline{R}_{s3} & 0 & 0 & 0 \\ 0 & \underline{R}_{r1} & 0 & 0 \\ 0 & 0 & \underline{R}_{r2} & 0 \\ 0 & 0 & 0 & \underline{R}_{r3} \end{bmatrix} \begin{bmatrix} \underline{i}_{\alpha\beta}{}^{MC} \\ \underline{i}_{\alpha\beta}{}^{r1} \\ \underline{i}_{\alpha\beta}{}^{r2} \\ \underline{i}_{\alpha\beta}{}^{r3} \end{bmatrix} + \frac{d}{dt} \begin{bmatrix} \underline{L}_{\alpha\beta}^{s1} & \underline{L}_{\alpha\beta}^{sr1} & 0 & 0 \\ \underline{L}_{\alpha\beta}^{rs1} & \underline{L}_{\alpha\beta}^{r1} & 0 & 0 \\ 0 & 0 & 0 & 0 \\ 0 & 0 & 0 & 0 \end{bmatrix} \begin{bmatrix} \underline{i}_{\alpha\beta}{}^{MC} \\ \underline{i}_{\alpha\beta}{}^{r1} \\ \underline{i}_{\alpha\beta}{}^{r2} \\ \underline{i}_{\alpha\beta}{}^{r3} \end{bmatrix} +$$

$$\frac{d}{dt} \begin{bmatrix} \underline{L}_{\alpha\beta}^{s2^1} & 0 & \underline{L}_{\alpha\beta}^{sr2^1} & 0 \\ 0 & 0 & 0 & 0 \\ \underline{L}_{\alpha\beta}^{rs2^1} & 0 & \underline{L}_{\alpha\beta}^{r2^1} & 0 \\ 0 & 0 & 0 & 0 \end{bmatrix} \begin{bmatrix} \underline{i}_{\alpha\beta}{}^{MC} \\ \underline{i}_{\alpha\beta}{}^{r1} \\ \underline{i}_{\alpha\beta}{}^{r2} \\ \underline{i}_{\alpha\beta}{}^{r3} \end{bmatrix} + \frac{d}{dt} \begin{bmatrix} \underline{L}_{\alpha\beta}^{s3^1} & 0 & 0 & \underline{L}_{\alpha\beta}^{sr3^1} \\ 0 & 0 & 0 & 0 \\ 0 & 0 & 0 & 0 \\ \underline{L}_{\alpha\beta}^{rs3^1} & 0 & 0 & \underline{L}_{\alpha\beta}^{r3^1} \end{bmatrix} \begin{bmatrix} \underline{i}_{\alpha\beta}{}^{MC} \\ \underline{i}_{\alpha\beta}{}^{r1} \\ \underline{i}_{\alpha\beta}{}^{r2} \\ \underline{i}_{\alpha\beta}{}^{r3} \end{bmatrix} \tag{4.82b}$$

Individual sub matrices can be written as:

$$\underline{C}\underline{L}_{s1}\underline{C}^{-1} = \begin{bmatrix} L_{ls1}+2.5M_1 & 0 & 0 & 0 & 0 & 0 & 0 \\ 0 & L_{ls1}+2.5M_1 & 0 & 0 & 0 & 0 & 0 \\ 0 & 0 & L_{ls1} & 0 & 0 & 0 & 0 \\ 0 & 0 & 0 & L_{ls1} & 0 & 0 & 0 \\ 0 & 0 & 0 & 0 & L_{ls1} & 0 & 0 \\ 0 & 0 & 0 & 0 & 0 & L_{ls1} & 0 \\ 0 & 0 & 0 & 0 & 0 & 0 & L_{ls1} \end{bmatrix} \tag{4.83}$$

$$\underline{C}\underline{L}_{r1}\underline{C}^{-1} = \begin{bmatrix} L_{lr1}+2.5M_1 & 0 & 0 & 0 & 0 & 0 & 0 \\ 0 & L_{lr1}+2.5M_1 & 0 & 0 & 0 & 0 & 0 \\ 0 & 0 & L_{lr1} & 0 & 0 & 0 & 0 \\ 0 & 0 & 0 & L_{lr1} & 0 & 0 & 0 \\ 0 & 0 & 0 & 0 & L_{lr1} & 0 & 0 \\ 0 & 0 & 0 & 0 & 0 & L_{lr1} & 0 \\ 0 & 0 & 0 & 0 & 0 & 0 & L_{lr1} \end{bmatrix} \tag{4.84}$$

$$\underline{C}\underline{L}_{sr1}\underline{C}^{-1} = 2.5M_1 \begin{bmatrix} Cos(\theta_1) & -Sin(\theta_1) & 0 & 0 & 0 & 0 & 0 \\ Sin(\theta_1) & Cos(\theta_1) & 0 & 0 & 0 & 0 & 0 \\ 0 & 0 & 0 & 0 & 0 & 0 & 0 \\ 0 & 0 & 0 & 0 & 0 & 0 & 0 \\ 0 & 0 & 0 & 0 & 0 & 0 & 0 \\ 0 & 0 & 0 & 0 & 0 & 0 & 0 \\ 0 & 0 & 0 & 0 & 0 & 0 & 0 \end{bmatrix} \tag{4.85}$$

$$\underline{C}\underline{L}_{rs1}\underline{C}^{-1} = \left(\underline{C}\underline{L}_{sr1}\underline{C}^{-1}\right)^T \tag{4.86}$$

$$\underline{C}\underline{L}_{s2}\underline{C}^{-1} = \begin{bmatrix} L_{ls2} & 0 & 0 & 0 & 0 & 0 & 0 \\ 0 & L_{ls2} & 0 & 0 & 0 & 0 & 0 \\ 0 & 0 & L_{ls2}+2.5M_2 & 0 & 0 & 0 & 0 \\ 0 & 0 & 0 & L_{ls2}+2.5M_2 & 0 & 0 & 0 \\ 0 & 0 & 0 & 0 & L_{ls2} & 0 & 0 \\ 0 & 0 & 0 & 0 & 0 & L_{ls2} & 0 \\ 0 & 0 & 0 & 0 & 0 & 0 & L_{ls2} \end{bmatrix} \tag{4.87}$$

$$\underline{C}\underline{L}_{r2}\underline{C}^{-1} = \begin{bmatrix} L_{lr2} & 0 & 0 & 0 & 0 & 0 & 0 \\ 0 & L_{lr2} & 0 & 0 & 0 & 0 & 0 \\ 0 & 0 & L_{lr2}+2.5M_2 & 0 & 0 & 0 & 0 \\ 0 & 0 & 0 & L_{lr2}+2.5M_2 & 0 & 0 & 0 \\ 0 & 0 & 0 & 0 & L_{lr2} & 0 & 0 \\ 0 & 0 & 0 & 0 & 0 & L_{lr2} & 0 \\ 0 & 0 & 0 & 0 & 0 & 0 & L_{lr2} \end{bmatrix} \tag{4.88}$$

$$\underline{C}\,\underline{L}_{sr2}\,\underline{C}^{-1} = 2.5M_2 \begin{bmatrix} 0 & 0 & 0 & 0 & 0 & 0 & 0 \\ 0 & 0 & 0 & 0 & 0 & 0 & 0 \\ Cos(\theta_2) & -Sin(\theta_2) & 0 & 0 & 0 & 0 & 0 \\ Sin(\theta_2) & Cos(\theta_2) & 0 & 0 & 0 & 0 & 0 \\ 0 & 0 & 0 & 0 & 0 & 0 & 0 \\ 0 & 0 & 0 & 0 & 0 & 0 & 0 \\ 0 & 0 & 0 & 0 & 0 & 0 & 0 \end{bmatrix} \quad (4.89)$$

$$\underline{C}\,\underline{L}_{rs2}\,\underline{C}^{-1} = \left(CL_{sr2}C^{-1}\right)^T \quad (4.90)$$

$$\underline{C}\,\underline{L}_{s3}\,\underline{C}^{-1} = \begin{bmatrix} L_{ls3} & 0 & 0 & 0 & 0 & 0 & 0 \\ 0 & L_{ls3} & 0 & 0 & 0 & 0 & 0 \\ 0 & 0 & L_{ls_3} & 0 & 0 & 0 & 0 \\ 0 & 0 & 0 & L_{ls_3} & 0 & 0 & 0 \\ 0 & 0 & 0 & 0 & L_{ls3}+2.5M_3 & 0 & 0 \\ 0 & 0 & 0 & 0 & 0 & L_{ls3}+2.5M_3 & 0 \\ 0 & 0 & 0 & 0 & 0 & 0 & L_{ls3} \end{bmatrix} \quad (4.91)$$

$$\underline{C}\,\underline{L}_{r3}\,\underline{C}^{-1} = \begin{bmatrix} L_{lr3} & 0 & 0 & 0 & 0 & 0 & 0 \\ 0 & L_{lr3} & 0 & 0 & 0 & 0 & 0 \\ 0 & 0 & L_{lr3} & 0 & 0 & 0 & 0 \\ 0 & 0 & 0 & L_{lr3} & 0 & 0 & 0 \\ 0 & 0 & 0 & 0 & L_{lr3}+2.5M_3 & 0 & 0 \\ 0 & 0 & 0 & 0 & 0 & L_{lr3}+2.5M_3 & 0 \\ 0 & 0 & 0 & 0 & 0 & 0 & L_{lr3} \end{bmatrix} \quad (4.92)$$

$$\underline{C}\,\underline{L}_{sr3}\,\underline{C}^{-1} = 2.5M_3 \begin{bmatrix} 0 & 0 & 0 & 0 & 0 & 0 & 0 \\ 0 & 0 & 0 & 0 & 0 & 0 & 0 \\ 0 & 0 & 0 & 0 & 0 & 0 & 0 \\ 0 & 0 & 0 & 0 & 0 & 0 & 0 \\ Cos(\theta_3) & -Sin(\theta_3) & 0 & 0 & 0 & 0 & 0 \\ Sin(\theta_3) & Cos(\theta_3) & 0 & 0 & 0 & 0 & 0 \\ 0 & 0 & 0 & 0 & 0 & 0 & 0 \end{bmatrix} \quad (4.93)$$

$$\underline{C}\,\underline{L}_{rs3}\,\underline{C}^{-1} = \left(\underline{C}\,\underline{L}_{sr3}\,\underline{C}^{-1}\right)^T \quad (4.94)$$

On the basis of above equations, the developed form of stator and rotor voltage equation can be written as:

$$V_{\alpha}^{MC} = (R_{s1} + R_{s2} + R_{s3})i_{\alpha}^{MC} + \frac{d\psi_{\alpha}^{MC}}{dt} \tag{4.95}$$

$$V_{\alpha}^{MC} = (R_{s1} + R_{s2} + R_{s3})i_{\alpha}^{MC} + (L_{is1} + L_{is2} + L_{is3} + L_{m1})\frac{di_{\alpha}}{dt} + L_{m1}Cos\,\theta_1\frac{di_{\alpha r1}}{dt}$$
$$- L_{m1}Sin\,\theta_1\frac{di_{\beta r1}}{dt} - \omega_1 L_{m1}(Sin\,\theta_1 i_{\alpha r1} + Cos\,\theta_1 i_{\beta r1}) \tag{4.96}$$

$$V_{\beta}^{MC} = (R_{s1} + R_{s2} + R_{s3})i_{\beta}^{MC} + \frac{d\psi_{\beta}^{MC}}{dt} \tag{4.97}$$

$$V_{\beta}^{MC} = (R_{s1} + R_{s2} + R_{s3})i_{\beta}^{MC} + (L_{is1} + L_{is2} + L_{is3} + L_{m1})\frac{di_{\beta}^{MC}}{dt} + L_{m1}Sin\,\theta_1\frac{di_{\alpha r1}}{dt} +$$
$$L_{m1}Cos\,\theta_1\frac{di_{\beta r1}}{dt} + \omega_1 L_{m1}(Cos\,\theta_1 i_{\alpha r1} + Sin\,\theta_1 i_{\beta r1}) \tag{4.98}$$

$$V_{x1}^{MC} = (R_{s1} + R_{s2} + R_{s3})i_{x1}^{MC} + \frac{d\psi_{x1}^{MC}}{dt} \tag{4.99}$$

$$V_{x1}^{MC} = (R_{s1} + R_{s2} + R_{s3})i_{x1}^{MC} + (L_{is1} + L_{is2} + L_{is3} + L_{m2})\frac{di_{x1}^{MC}}{dt} + L_{m2}Cos\,\theta_2\frac{di_{x1r2}}{dt}$$
$$- L_{m2}Sin\,\theta_1\frac{di_{\beta r2}}{dt} - \omega_2 L_{m2}(Sin\,\theta_2 i_{\alpha r2} + Cos\,\theta_2 i_{\beta r2}) \tag{4.100}$$

$$V_{y1}^{MC} = (R_{s1} + R_{s2} + R_{s3})i_{y1}^{MC} + \frac{d\psi_{y1}^{MC}}{dt} \tag{4.101}$$

$$V_{y1}^{MC} = (R_{s1} + R_{s2} + R_{s3})i_{y1}^{MC} + (L_{is1} + L_{is2} + L_{is3} + L_{m2})\frac{di_{y1}^{MC}}{dt} + L_{m2}Sin\,\theta_2\frac{di_{y1r1}}{dt}$$
$$+ L_{m2}Cos\,\theta_2\frac{di_{\beta r2}}{dt} + \omega_2 L_{m2}(Cos\,\theta_2 i_{\alpha r2} + Sin\,\theta_2 i_{\beta r2}) \tag{4.102}$$

$$V_{x2}^{MC} = (R_{s1} + R_{s2} + R_{s3})i_{x2}^{inv} + \frac{d\psi_{x2}^{MC}}{dt} \tag{4.103}$$

$$V_{x2}^{MC} = (R_{s1} + R_{s2} + R_{s3})i_{x2}^{MC} + (L_{is1} + L_{is2} + L_{is3} + L_{m3})\frac{di_{x2}^{MC}}{dt} + L_{m3}Cos\ \theta_3 \frac{di_{x2r3}}{dt} -$$
$$L_{m3}Sin\ \theta_3 \frac{di_{\beta r3}}{dt} - \omega_3 L_{m3}(Sin\ \theta_3 i_{\alpha r3} + Cos\ \theta_3 i_{\beta r3})$$

(4.104)

$$V_{y2}^{MC} = (R_{s1} + R_{s2} + R_{s3})i_{y2}^{inv} + \frac{d\psi_{y2}^{MC}}{dt} \tag{4.105}$$

$$V_{y2}^{MC} = (R_{s1} + R_{s2} + R_{s3})i_{y2}^{MC} + (L_{is1} + L_{is2} + L_{is3} + L_{m3})\frac{di_{y2}^{MC}}{dt} + L_{m3}Sin\ \theta_3 \frac{di_{y2r1}}{dt} +$$
$$L_{m3}Cos\ \theta_3 \frac{di_{\beta r3}}{dt} + \omega_3 L_{m3}(Cos\ \theta_3 i_{\alpha r3} + Sin\ \theta_3 i_{\beta r3}$$

(4.106)

Rotor Equations of 1st machine

$$V_{\alpha r1} = 0 = R_{r1}i_{\alpha r1} + L_{m1}Cos\ \theta_1 \frac{di_{\alpha}^{MC}}{dt} - L_{m1}Sin\ \theta_1 \frac{di_{\beta}^{MC}}{dt} + (L_{r1} + L_{m1})\frac{di_{dr1}}{dt}$$
$$- \omega_1 L_{m1}(Sin\ \theta_1 i_{\alpha}^{MC} - Cos\ \theta_1 i_{\beta}^{MC})$$

(4.107)

$$V_{\beta r1} = 0 = R_{r1}i_{\beta r1} + L_{m1}Sin\ \theta_1 \frac{di_{\alpha}^{MC}}{dt} - L_{m1}Cos\ \theta_1 \frac{di_{\beta}^{MC}}{dt} + (L_{r1} + L_{m1})\frac{di_{\beta r1}}{dt} -$$
$$\omega_1 L_{m1}(Cos\ \theta_1 i_{\alpha}^{MC} + Sin\ \theta_1 i_{\beta}^{MC})$$

(4.108)

$$V_{x_1r_1} = 0 = R_{r1}i_{x_1r_1} + L_{ir_1}\frac{di_{x_1r_1}^{MC}}{dt} \tag{4.109}$$

$$V_{y_1r_1} = 0 = R_{r1}i_{y_1r_1} + L_{ir_1}\frac{di_{y_1r_1}^{MC}}{dt} \tag{4.110}$$

$$V_{x_2r_1} = 0 = R_{r1}i_{x_2r_1} + L_{ir_1}\frac{di_{x_2r_1}^{MC}}{dt} \tag{4.111}$$

$$V_{y_2r_1} = 0 = R_{r1}i_{y_2r_1} + L_{ir_1}\frac{di_{y_2r_1}^{MC}}{dt} \tag{4.112}$$

$$V_{0r_1} = 0 = R_{r1} i_{0r_1} + L_{ir_1} \frac{di_{0r_1}^{MC}}{dt} \tag{4.113}$$

Rotor Voltage Equations of machine 2:

$$\begin{aligned} V_{\alpha r2} &= 0 = R_{r2} i_{\alpha r1} + L_{m2} Cos(\theta_2) p i_{\alpha}^{MC} + L_{m2} Sin(\theta_2) p i_{\beta}^{MC} \\ &+ (Li_{r2} + L_{m2}) p i_{\alpha r2} - \omega_2 L_{m2} Sin(\theta_2) i_{\alpha}^{MC} - Cos(\theta_2) i_{\beta}^{MC} \end{aligned} \tag{4.114}$$

$$\begin{aligned} V_{\beta r2} &= 0 = R_{r2} i_{\beta r2} + L_{m2} Sin(\theta_2) p i_{\alpha}^{MC} + L_{m2} Cos(\theta_2) p i_{\beta}^{MC} \\ &+ (Li_{r2} + L_{m2}) p_{\beta r2} - \omega_2 L_{m2} Sin(\theta_2) i_{\alpha}^{MC} + Sin(\theta_2) i_{\beta}^{MC} \end{aligned} \tag{4.115}$$

$$V_{x_1 r_2} = 0 = R_{r2} i_{x_1 r2} + L_{ir2} p i_{x_1 r_2}^{MC} \tag{4.116}$$

$$V_{y_1 r2} = 0 = R_{r2} i_{y_1 r\ 2} + L_{ir2} p i_{y_1 r_2}^{MC} \tag{4.117}$$

$$V_{x_2 r2} = 0 = R_{r2} i_{x_2 r_2} + L_{ir_2} p i_{x_2 r_2}^{MC} \tag{4.118}$$

$$V_{y_2 r_2} = 0 = R_{r2} i_{y_2 r_2} + L_{ir_2} p i_{y_2 r 2}^{MC} \tag{4.119}$$

$$V_{0r2} = 0 = R_{r2} i_{0r_2} + L_{ir_2} p i_{0r_2}^{MC} \tag{4.120}$$

Rotor Voltage Equation of Machine 3:

$$\begin{aligned} V_{\alpha r3} &= 0 = R_{r3} i_{\alpha r3} + L_{m3} Cos(\theta_3) p i_{\alpha}^{MC} + L_{m3} Sin(\theta_3) p i_{\beta}^{MC} + (Li_{r3} + L_{m3}) p i_{\alpha r3} \\ &- \omega_3 L_{m3} Sin(\theta_3) i_{\alpha}^{MC} - Cos(\theta_3) i_{\beta}^{MC} \end{aligned} \tag{4.121}$$

$$\begin{aligned} V_{\beta r3} &= 0 = R_{r3} i_{\beta r3} + L_{m3} Sin(\theta_3) p i_{\alpha}^{MC} + L_{m3} Cos(\theta_3) p i_{\beta}^{MC} \\ &+ (Li_{r3} + L_{m3}) p i_{\beta r3} - \omega_3 L_{m3} Sin(\theta_3) i_{\alpha}^{MC} + Sin(\theta_3) i_{\beta}^{MC} \end{aligned} \tag{4.122}$$

$$V_{x_1 r3} = 0 = R_{r3} i_{x_1 r3} + L_{ir3} p i_{x_1 r3}^{MC} \tag{4.123}$$

$$V_{y_1 r3} = 0 = R_{r3} i_{y_1 r\ 3} + L_{ir3} p i_{y_1 r_3}^{MC} \tag{4.124}$$

$$V_{x_2 r3} = 0 = R_{r3} i_{x_2 r3} + L_{ir3} p i_{x_2 r3}^{inv} \tag{4.125}$$

$$V_{y_2 r3} = 0 = R_{r3} i_{y_2 r3} + L_{ir_3} p i_{y_2 r3}^{MC} \tag{4.126}$$

$$V_{0r3} = 0 = R_{r3} i_{0r_3} + L_{ir_3} p i_{0r3}^{MC} \tag{4.127}$$

The motor electromagnetic torque is entirely developed due to the interaction of *d-q* current components and is independent of *x-y* current components. Since rotor is short circuited, the *x-y* and zero sequence components of rotors are zero. Due to the star connection in stator make stator zero sequence components to zero. The motor torque equation can be written as:

$$\begin{aligned}
T_{e1} &= P_1 L_{m1} \left[Cos\ (\theta_1)(i_{\alpha r1} i_{\beta}^{MC} - i_{\beta r1} i_{\alpha}^{MC}) - Sin\ \theta_1 (i_{\alpha r1} i_{\alpha}^{MC} - i_{\beta r1} i_{\beta}^{MC}) \right] \\
T_{e2} &= P_2 L_{m2} \left[Cos\ (\theta_2)(i_{\alpha r2} i_{\beta}^{MC} - i_{\beta r2} i_{\alpha}^{MC}) - Sin\ \theta_2 (i_{\alpha r2} i_{\alpha}^{MC} - i_{\beta r2} i_{\beta}^{MC}) \right] \\
T_{e3} &= P_3 L_{m3} \left[Cos\ (\theta_3)(i_{\alpha r3} i_{\beta}^{MC} - i_{\beta r3} i_{\alpha}^{MC}) - Sin\ \theta_3 (i_{\alpha r3} i_{\alpha}^{MC} - i_{\beta r3} i_{\beta}^{MC}) \right]
\end{aligned} \tag{4.128}$$

4.4 c Transformation of model in to the stationary common reference frame

Stator and rotor transformation matrices are 7x7 matrices but, only *d-q* components need to transform to the stationary common reference frame as other *x-y* and zero sequence components are zero. The rotational transformation matrices are given as in equation (4.23);

$$\underline{D}1 = \begin{bmatrix} Cos\beta_1 & Sin\beta_1 & 0 & 0 & 0 & 0 & 0 \\ -Sin\beta_1 & Cos\beta_1 & 0 & 0 & 0 & 0 & 0 \\ 0 & 0 & 1 & 0 & 0 & 0 & 0 \\ 0 & 0 & 0 & 1 & 0 & 0 & 0 \\ 0 & 0 & 0 & 0 & 1 & 0 & 0 \\ 0 & 0 & 0 & 0 & 0 & 1 & 0 \\ 0 & 0 & 0 & 0 & 0 & 0 & 1 \end{bmatrix} \tag{4.129}$$

$$\underline{D}2 = \begin{bmatrix} Cos\beta_2 & Sin\beta_2 & 0 & 0 & 0 & 0 & 0 \\ -Sin\beta_2 & Cos\beta_2 & 0 & 0 & 0 & 0 & 0 \\ 0 & 0 & 1 & 0 & 0 & 0 & 0 \\ 0 & 0 & 0 & 1 & 0 & 0 & 0 \\ 0 & 0 & 0 & 0 & 1 & 0 & 0 \\ 0 & 0 & 0 & 0 & 0 & 1 & 0 \\ 0 & 0 & 0 & 0 & 0 & 0 & 1 \end{bmatrix} \tag{4.130}$$

$$\underline{D}3 = \begin{bmatrix} Cos\beta_3 & SIn\beta_3 & 0 & 0 & 0 & 0 & 0 \\ -Sin\beta_3 & Cos\beta_3 & 0 & 0 & 0 & 0 & 0 \\ 0 & 0 & 1 & 0 & 0 & 0 & 0 \\ 0 & 0 & 0 & 1 & 0 & 0 & 0 \\ 0 & 0 & 0 & 0 & 1 & 0 & 0 \\ 0 & 0 & 0 & 0 & 0 & 1 & 0 \\ 0 & 0 & 0 & 0 & 0 & 0 & 1 \end{bmatrix} \tag{4.131}$$

Here, Angle of transformation

$$\beta_1 = -\theta_1 = -\int \omega_1 dt \ , \ \beta_2 = -\theta_2 = -\int \omega_2 dt \ \text{ and } \beta_3 = -\theta_3 = -\int \omega_3 dt \tag{4.132}$$

So the new variables are defined as:

$$\underline{V}_{dq}^{r1} = \underline{D}_1 \underline{V}_{\alpha\beta}^{r1} \, , \ \underline{V}_{dq}^{r2} = \underline{D}_2 \underline{V}_{\alpha\beta}^{r2} \, , \underline{V}_{dq}^{r3} = \underline{D}_3 \underline{V}_{\alpha\beta}^{r3} \tag{4.133}$$

$$\underline{i}_{dq}^{r1} = \underline{D}_1 \underline{i}_{\alpha\beta}^{r1} \, , \ \underline{i}_{dq}^{r2} = \underline{D}_2 \underline{i}_{\alpha\beta}^{r2} \, , \ \underline{i}_{dq}^{r3} = \underline{D}_3 \underline{i}_{\alpha\beta}^{r3} \tag{4.134}$$

$$\underline{V} = \begin{bmatrix} \underline{V}_{\alpha\beta}^{MC} \\ \underline{D}_1^{-1} \underline{V}_{dq}^{r1} \\ \underline{D}_2^{-1} \underline{V}_{dq}^{r2} \\ \underline{D}_3^{-1} \underline{V}_{dq}^{r3} \end{bmatrix} = \left[R \right] \begin{bmatrix} \underline{i}_{\alpha\beta}^{MC} \\ \underline{D}_1^{-1} \underline{i}_{dq}^{r1} \\ \underline{D}_1^{-1} \underline{i}_{dq}^{r2} \\ \underline{D}_1^{-1} \underline{V}_{dq}^{r3} \end{bmatrix} + \frac{d}{dt} \left[L \right] \begin{bmatrix} \underline{i}_{\alpha\beta}^{MC} \\ \underline{D}_1^{-1} \underline{i}_{dq}^{r1} \\ \underline{D}_1^{-1} \underline{i}_{dq}^{r2} \\ \underline{D}_1^{-1} \underline{V}_{dq}^{r3} \end{bmatrix} \tag{4.135}$$

Here, Angles of transformation $\beta_1 = -\theta_1 = -\int \omega_1 dt$ and $\beta_2 = -\theta_2 = -\int \omega_2 dt$

So the new variables are defined as $\underline{V}_{dq}^{r1} = \underline{D}_1 \underline{V}_{\alpha\beta}^{r1} \, , \ \underline{V}_{dq}^{r2} = \underline{D}_2 \underline{V}_{\alpha\beta}^{r2} \, , \underline{V}_{dq}^{r3} = \underline{D}_3 \underline{V}_{\alpha\beta}^{r3}$ (4.136)

$$\underline{i}_{dq}^{r1} = \underline{D}_1 \underline{i}_{\alpha\beta}^{r1} \, , \ \underline{i}_{dq}^{r2} = \underline{D}_2 \underline{i}_{\alpha\beta}^{r2} \, , \ \underline{i}_{dq}^{r3} = \underline{D}_3 \underline{i}_{\alpha\beta}^{r3} \tag{4.137}$$

$$\underline{D} = \begin{bmatrix} \underline{I} & 0 & 0 & 0 \\ 0 & \underline{D}_1 & 0 & 0 \\ 0 & 0 & \underline{D}_2 & 0 \\ 0 & 0 & 0 & \underline{D}_3 \end{bmatrix} \tag{4.138}$$

Pre-multiplying both sides by ‘D’ one obtain:

$$\underline{V}_{dq} = \underline{R}\underline{i}_{dq} + \frac{d(\underline{L}_{dq}\underline{I}_{dq})}{dt} + \Omega \underline{G}\underline{i}_{dq} \tag{4.139}$$

where

$$\underline{V}_{dq} = \begin{bmatrix} \underline{V}_{\alpha\beta}^{MC} \\ 0 \\ 0 \\ 0 \end{bmatrix} \tag{4.140}$$

$$\underline{i}_{dq} = \begin{bmatrix} \underline{i}_{\alpha\beta}{}^{MC} \\ \underline{i}_{\alpha\beta}{}^{r1} \\ \underline{i}_{\alpha\beta}{}^{r2} \\ \underline{i}_{\alpha\beta}{}^{r3} \end{bmatrix} \tag{4.141}$$

$$\underline{R} = \begin{bmatrix} \underline{R}_{s1} + \underline{R}_{s2} + \underline{R}_{s3} & 0 & 0 & 0 \\ 0 & \underline{R}_{r1} & 0 & 0 \\ 0 & 0 & \underline{R}_{r2} & 0 \\ 0 & 0 & 0 & \underline{R}_{r3} \end{bmatrix} \tag{4.142}$$

Individual matrices are given as:

$$\underline{R}_{s1} = \begin{bmatrix} \underline{R}_{s1} & 0 & 0 & 0 & 0 & 0 & 0 \\ 0 & \underline{R}_{s1} & 0 & 0 & 0 & 0 & 0 \\ 0 & 0 & \underline{R}_{s1} & 0 & 0 & 0 & 0 \\ 0 & 0 & 0 & \underline{R}_{s1} & 0 & 0 & 0 \\ 0 & 0 & 0 & 0 & \underline{R}_{s1} & 0 & 0 \\ 0 & 0 & 0 & 0 & 0 & \underline{R}_{s1} & 0 \\ 0 & 0 & 0 & 0 & 0 & 0 & \underline{R}_{s1} \end{bmatrix} \tag{4.143}$$

$$\underline{L}_{dq} = \begin{bmatrix} \underline{L}_{dq}^{s1} + \underline{L}_{dq}^{s2} + \underline{L}_{dq}^{s3} & \underline{L}_{dq}^{sr1} & \underline{L}_{dq}^{sr2} & \underline{L}_{dq}^{sr3} \\ \underline{L}_{dq}^{rs1} & \underline{L}_{dq}^{r1} & 0 & 0 \\ \underline{L}_{dq}^{rs2} & 0 & \underline{L}_{dq}^{r2} & 0 \\ \underline{L}_{dq}^{rs3} & 0 & 0 & \underline{L}_{dq}^{r3} \end{bmatrix} \tag{4.144}$$

Torque Equations

Torque equation of the machine become

$$\begin{aligned} T_{e1} &= P_1 L_{m1}\left[(i_{dr1} i_{\beta}^{MC} - i_{qr1} i_{\alpha}^{MC})\right] \\ T_{e2} &= P_2 L_{m2}\left[(i_{dr2} i_{y1}^{MC} - i_{qr2} i_{x1}^{MC})\right] \\ T_{e3} &= P_2 L_{m2}\left[(i_{dr3} i_{y2}^{MC} - i_{qr3} i_{x2}^{MC})\right] \end{aligned} \tag{4.145}$$

By omitting zero sequence and x1-y1 and x2-y2 components from rotors and zero sequence from power source, the complete model in the stationary common reference frame for the three seven-phase series-connected induction machines is given as:

$$
\begin{aligned}
V_{\alpha}^{MC} &= R_{s1}i_{\alpha}^{MC} + (L_{ls1} + L_{m1})pi_{\alpha}^{MC} + L_{m1}pi_{dr1} + R_{s2}i_{\alpha}^{MC} + L_{ls2}pi_{\alpha}^{MC} + R_{s3}i_{\alpha}^{MC} + L_{ls3}pi_{\alpha}^{MC} \\
V_{\beta}^{MC} &= R_{s1}i_{\beta}^{MC} + (L_{ls1} + L_{m1})pi_{\beta}^{MC} + L_{m1}pi_{qr1} + R_{s2}i^{MC} + L_{ls2}pi_{\alpha}^{MC} + R_{s3}i_{\alpha}^{MC} + L_{ls3}pi_{\alpha}^{MC} \\
V_{x1}^{MC} &= R_{s1}i_{x1}^{MC} + L_{ls1}pi_{x1}^{MC} + R_{s2}i_{x1}^{MC} + (L_{ls2} + L_{m2})pi_{x1}^{MC} + L_{m2}pi_{dr2}^{MC} + R_{s3}i_{x1}^{MC} + (L_{ls3} + L_{m3})pi_{x1}^{MC} \\
V_{y1}^{MC} &= R_{s1}i_{y1}^{MC} + L_{ls1}pi_{y1}^{MC} + R_{s2}i_{y1}^{MC} + (L_{ls2} + L_{m2})pi_{y1}^{MC} + L_{m2}pi_{qr2}^{MC} + R_{s3}i_{y1}^{MC} + (L_{ls3} + L_{m3})pi_{y1}^{MC} \\
V_{x2}^{MC} &= R_{s1}i_{x2}^{MC} + L_{ls1}pi_{x2}^{MC} + R_{s2}i_{x2}^{MC} + (L_{ls2} + L_{m2})pi_{x2}^{MC} + L_{m2}pi_{dr3}^{MC} + R_{s3}i_{x2}^{MC} + (L_{ls3} + L_{m3})pi_{x2}^{MC} \\
V_{y2}^{MC} &= R_{s1}i_{y2}^{MC} + L_{ls1}pi_{y2}^{MC} + R_{s2}i_{y2}^{MC} + (L_{ls2} + L_{m2})pi_{y2}^{MC} + L_{m2}pi_{qr3}^{MC} + R_{s3}i_{y2}^{MC} + (L_{ls3} + L_{m3})pi_{y2}^{MC}
\end{aligned} \tag{4.146}
$$

Rotor Equations of machine 1 is obtained as:

$$
\begin{aligned}
0 = &R_{r1}i_{dr1} + L_{m1}pi_{\alpha}^{MC} + (L_{lr1} + L_{m1})pi_{dr1} \\
&+\omega_1(L_{m1}i_{\beta}^{MC} + (L_{lr1} + L_{m1})i_{qr1})
\end{aligned} \tag{4.147}
$$

$$
\begin{aligned}
0 = &R_{r1}i_{qr1} + L_{m1}pi_{\beta}^{MC} + (L_{r1} + L_{m1})pi_{qr1} \\
&+\omega_1(L_{m1}i_{\alpha}^{MC} + (L_{lr1} + L_{m1})i_{dr1}
\end{aligned} \tag{4.148}
$$

Rotor Equations of machine 2 is obtained as:

$$
\begin{aligned}
0 = &R_{r2}i_{dr2} + L_{m2}pi_{\alpha}^{MC} + (L_{r2} + L_{m2})pi_{dr2} \\
&+\omega_2(L_{m2}i_{\beta}^{MC} + (L_{lr2} + L_{m2})i_{qr2}
\end{aligned} \tag{4.149}
$$

$$
\begin{aligned}
0 = &R_{r1}i_{qr2} + L_{m2}pi_{\beta}^{MC} + (L_{r2} + L_{m2})pi_{qr2} \\
&+\omega_2(L_{m2}i_{\alpha}^{MC} + (L_{lr2} + L_{m2})i_{dr2}
\end{aligned} \tag{4.150}
$$

Rotor Equations of machine 3 is given as:

$$0 = R_{r3}i_{dr3} + L_{m3}pi_{\alpha}^{MC} + (L_{r3} + L_{m3})pi_{dr3}$$
$$+\omega_3(L_{m3}i_{\beta}^{MC} + (L_{lr3} + L_{m3})i_{qr3}) \quad (4.151)$$

$$0 = R_{r3}i_{qr3} + L_{m3}pi_{\beta}^{MC} + (L_{r3} + L_{m3})pi_{qr3}$$
$$+\omega_3(L_{m3}i_{\alpha}^{MC} + (L_{lr3} + L_{m3})i_{dr3}) \quad (4.152)$$

It is observed from the rotor equations of all three machines that the interaction of rotors and stator current is only in the α-β components. There is no interaction of *x1-y1* or *x2-y2* components of stator and rotor. The complete seven-phase three-motor drive system can thus be represented by equations (4.146) to (4.152). Hence, these voltage equations along with the torque equations of (4.153) and the following electromechanical equations can completely describe the system of Fig. 4.5

$$\begin{aligned} T_{e1} - T_{L1} &= \frac{J_1}{P_1}\frac{d\omega_1}{dt} \\ T_{e2} - T_{L2} &= \frac{J_2}{P_2}\frac{d\omega_2}{dt} \\ T_{e3} - T_{L3} &= \frac{J_3}{P_3}\frac{d\omega_3}{dt} \end{aligned} \quad (4.153)$$

4.4d Simulation Result

To validate the mathematical model developed in the previous section, equations (4.146) to (4.153) are simulated in MATLAB/SIMULINK. Since the aim is to validate the mathematical model, ideal seven-phase sinusoidal source is considered for simulation purpose. The source voltage is assumed as 220 V rms per phase, 50 Hz. The three machines are chosen identical with stator resistance of 10 Ω, rotor resistance of 6.3 Ω, leakage inductance of 40 mH, magnetizing inductance of 420 mH, inertia 0.01 and number of poles 4, and rated torque equal 11.662 Nm. Since the three machines are decoupled from each other, they can operate in different conditions. Three machines are simulated under v/f = constant control conditions. Machine-1 is allowed to run at rated speed (50 Hz) with applied voltage equal to rated value of 220 V rms. Machine-2 is allowed to run at half of the rated speed (25 Hz) with applied voltage of 110 V rms. Machine-3 is run at slightly less than quarter of the rated speed (12 Hz) and the applied voltage is accordingly reduced. The resulting waveforms are presented in Figs. 4.6a-c. The applied voltage of phase 'a' is presented in Fig.4.13 It comprises of three different frequencies voltages corresponding to the operating conditions of the three machines. The transformed source currents (assumed ideal sinusoidal currents) are depicted in Figs. 4.10-4.12, the three components are shown. It is seen from Figs. 4.10-4.12, that the frequencies and magnitude of each pair of currents are different and are matching the set operating conditions of the three machines. Fig. 4.6 shows the speed and torque responses of the three series connected machines. The response shows typical v/f = constant control behavior. The machine accelerates to the set speeds and the torque response is typical.

Fig. 4.13 illustrate the spectrum of the source side voltage of phase ‘a’ and its transformed components. The phase ‘a’ voltage shows three fundamental components at three different frequencies with different magnitudes. The frequency components match the commanded values. The transformed components show just one fundamental component. This clearly indicates the independence of control of three machines. The phase ‘a’ voltage components appear in three different planes that will control each machine individually. This validates the mathematical model developed in the previous section. The independent control of each machine is seen from the simulation results. The results also validate the model of derived in the previous section.

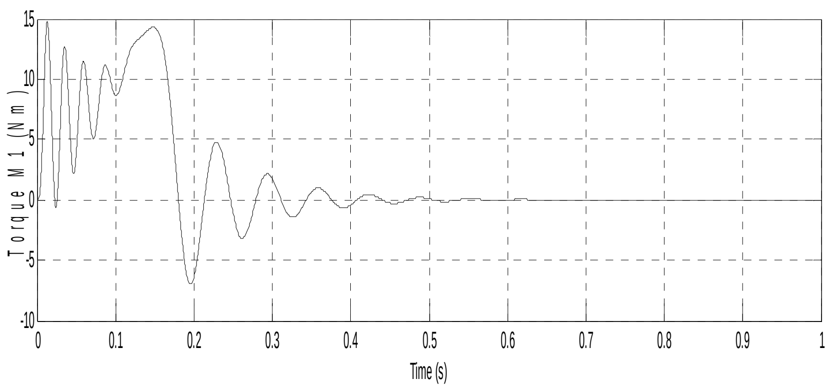

a.

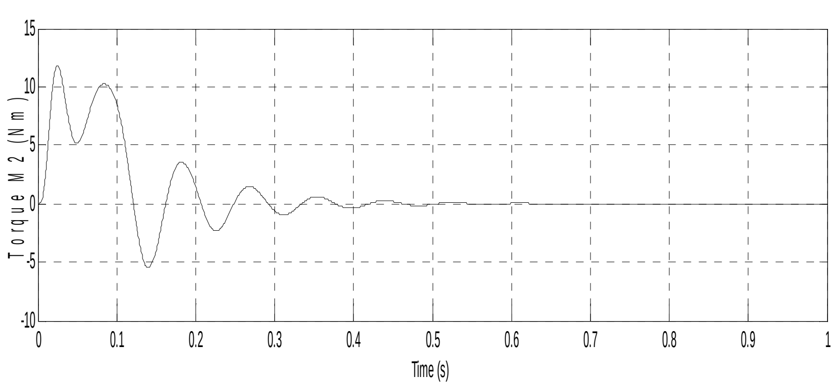

b.

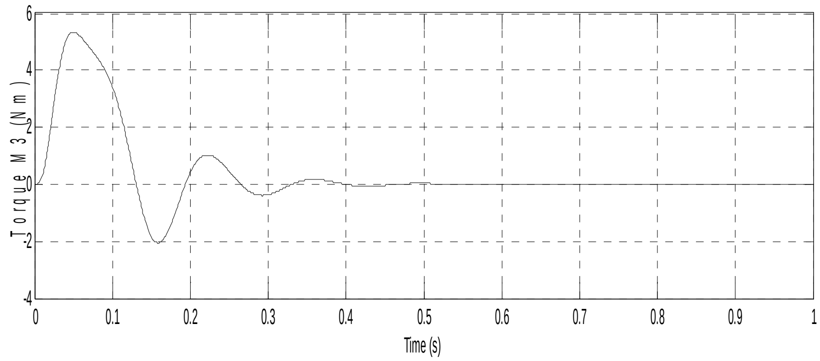

c.

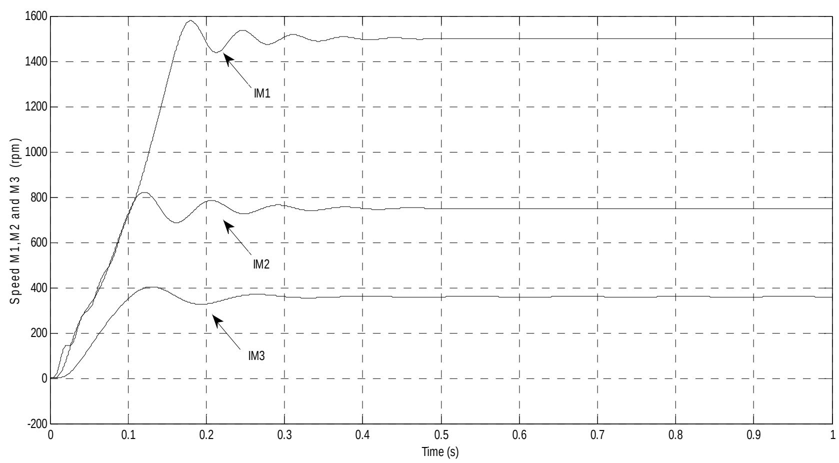

d.

Fig. 4.6. Response of Seven-phase Three-motor drive supplied by ideal voltage source**.**

he configuration of seven phase 3 motor system is verified by SIMULINK modeling. Result is verified with loading and reversing effect, shown in Fig (4.7)-(4.16).

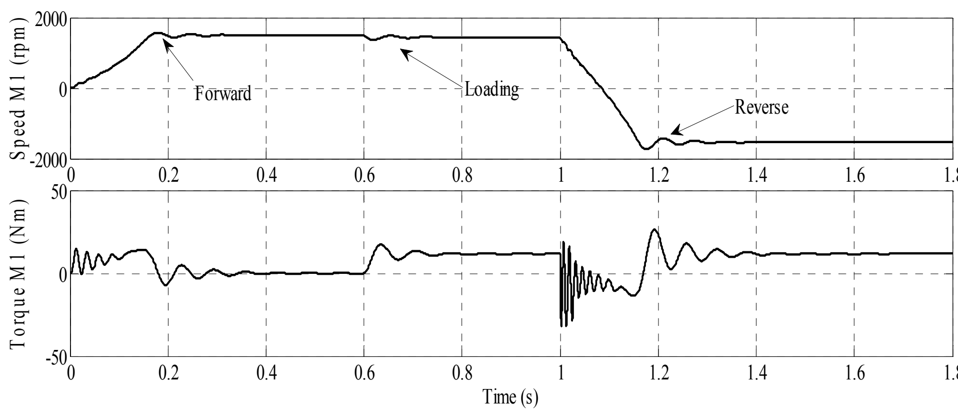

Fig. 4.7, Torque and speed characteristics of Machine 1.

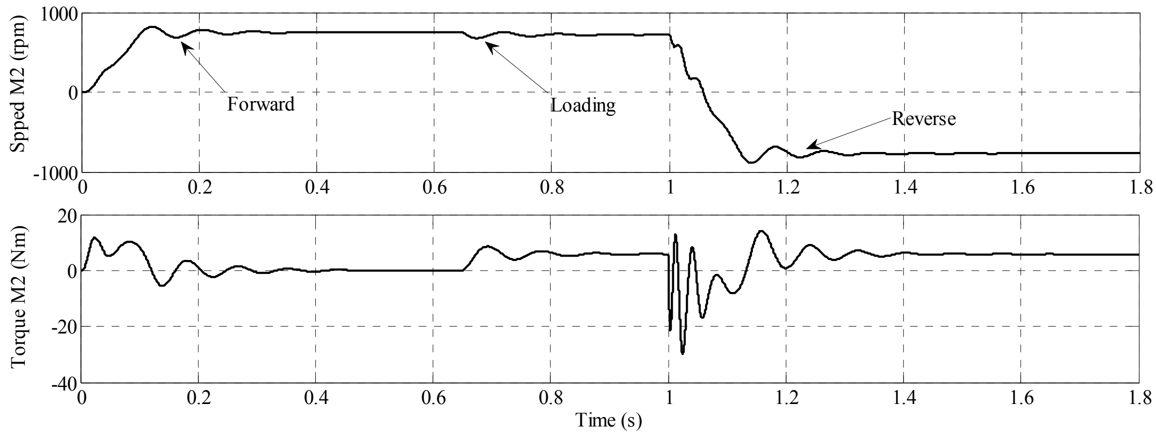

Fig. 4.8. Torque and Speed characteristics of Machine 2.

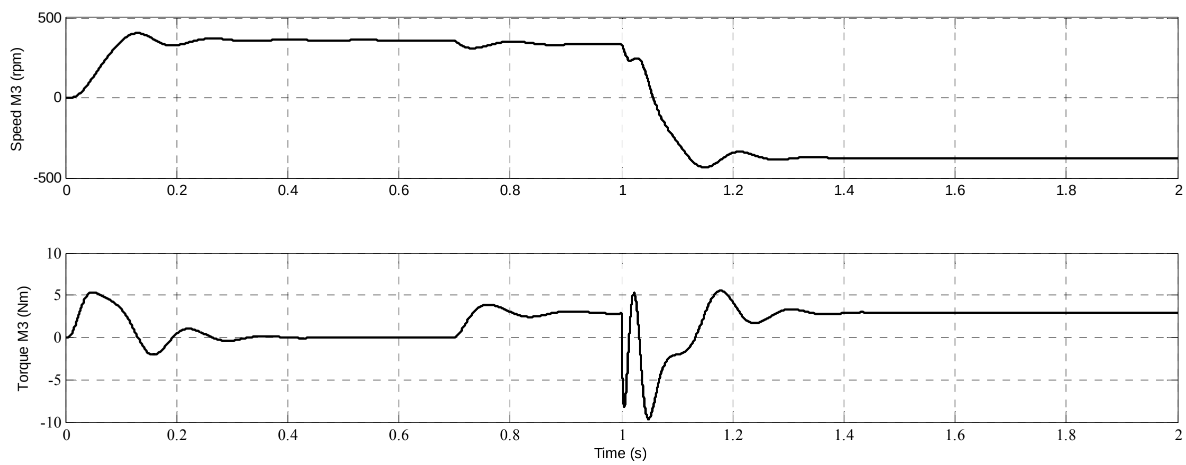

Fig. 4.9. Speed and Torque Characteristics of Machine 3.

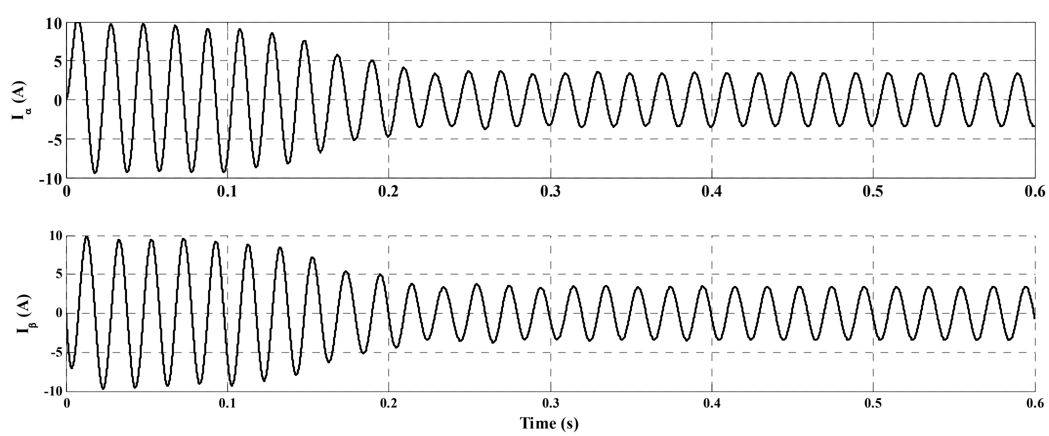

Fig. 4.10. Current 'I_α-I_β'.

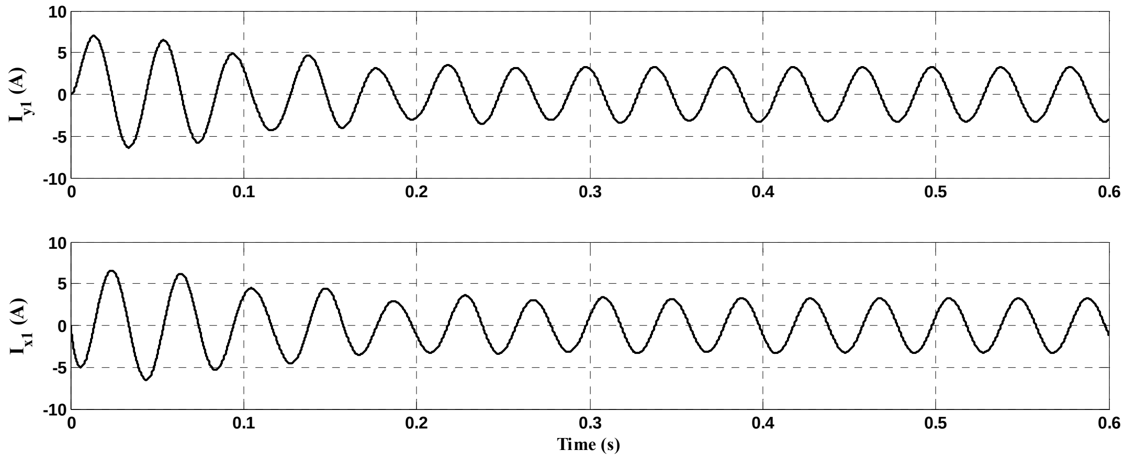

Fig. 4.11. Current ‘Ix_1-Iy_1’.

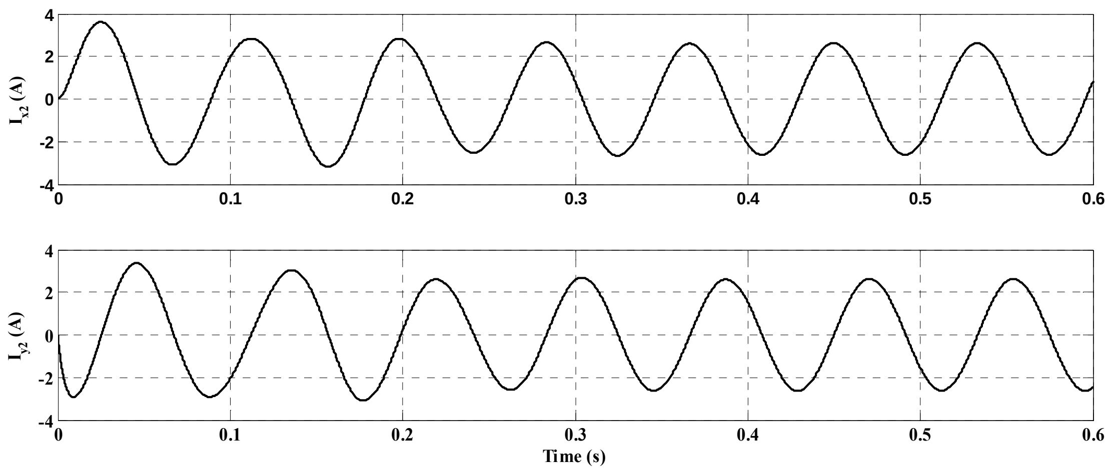

Fig. 4.12. Source current ‘Ix_2-Iy_2’.

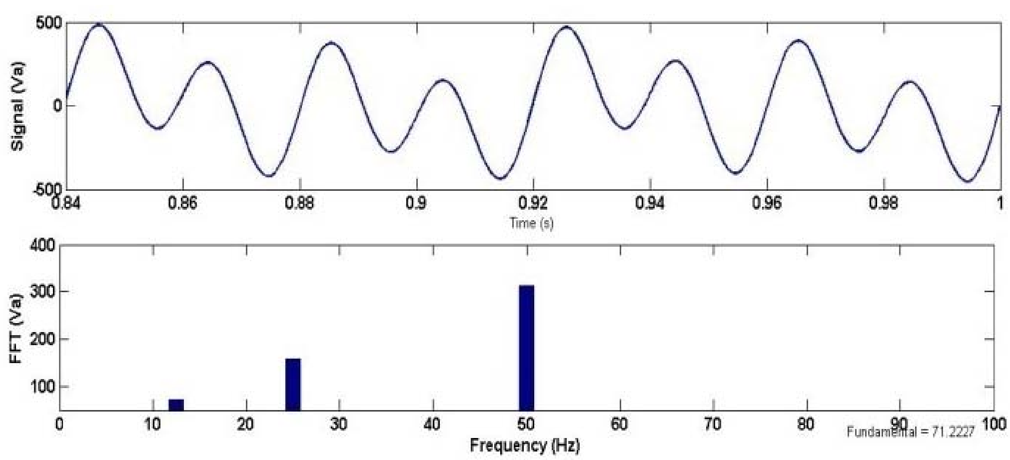

Fig. 4.13. Spectrum of source phase ‘a’ voltage.

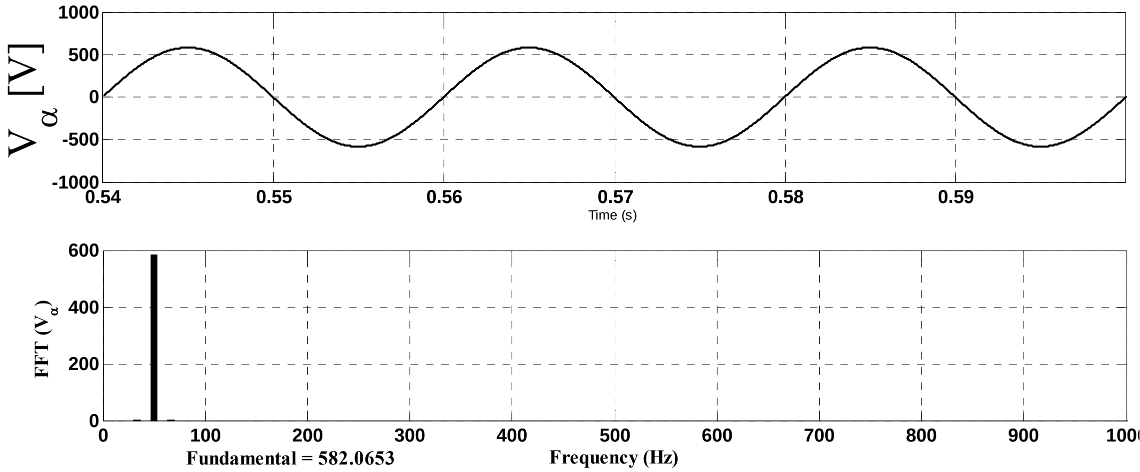

Fig. 4.14. Spectrum of source voltage Vα.

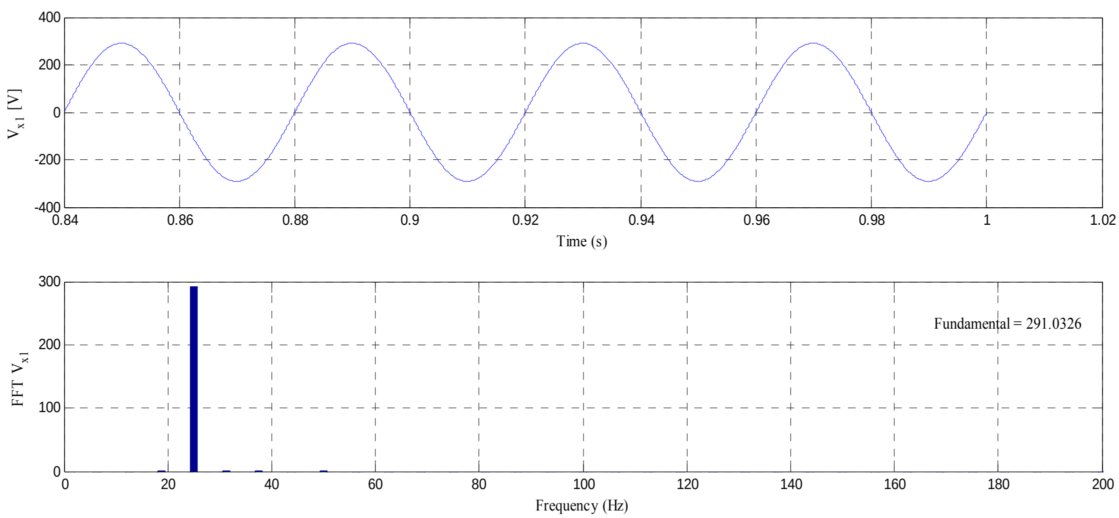

Fig. 4.15. Spectrum of source voltage V_{x1}.

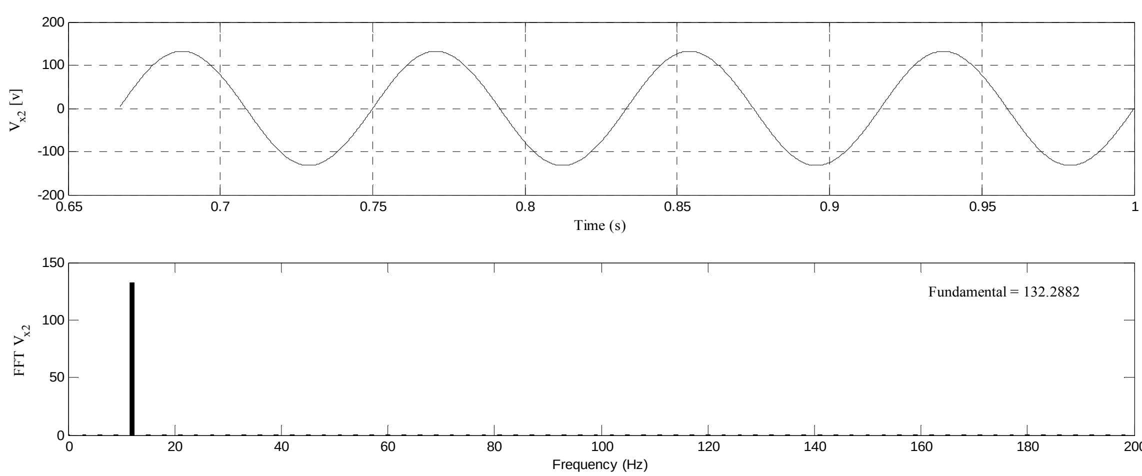

Fig. 4.16. Spectrum of source voltage V_{x2}.

It is seen from above figures that the phase voltage (Matrix Converter output voltage) has three different fundamental frequency components at 12 Hz, 25 Hz and 50 Hz corresponding to the operating speeds of the three series-connected induction machines. These fundamental components appear as d-q, x1-y1 and x2-y2 components and there is no interaction between them. This proves the correctness of the developed mathematical model and the concept of independence of control.

4.5 Summary

This chapter developed and reported complete mathematical models of multi-phase multi-motor drive system. Three different configurations are considered namely five-phase, six-phase and seven-phase systems. Phase variable models are developed and then transformed to appropriate number of axes. This is done in order to eliminate the position dependence of inductances. The developed mathematical models showed that the torque can be produced by using only two orthogonal components of currents. Hence in case of a five-phase and six-phase systems one pair of currents are free to use (since there are two sets of currents) in controlling the second machine. Thus stator windings of two-motors are connected in series or in parallel and are supplied by only one power converter and both motors are controlled independently. In similar fashion, a seven-phase system is seen to control three series or parallel connected machines. The developed mathematical models are verified using simulation approach.

References

[4.1] M. Jones, S.N. Vukosavic, E. Levi, A. Iqbal, "A six-phase series connected two-motor drive with decoupled dynamic control," IEEE Trans. Ind. Appl., vol. 41, no. 4, Jul./Aug. 2005a, pp. 1056–1066.

[4.2] M. Jones, E. Levi, "Series connected quasi six-phase two-motor drives with independent control", Math Comput. Simul. (Trans. IMACS), vol. 71, no. 4-6, June 2006, pp. 415-424.

[4.3] A. Iqbal, "Modeling and Control of Five-phase and six-phase series-connected two-motor drive system", *PhD Thesis,* Liverpool John Moores University, Liverpool, UK, 2006.

[4.4] E. Levi, M. Jones, S.N. Vukosavic, A. Iqbal, H.A. Toliyat, "Modelling Control and Experimental investigation of a five-phase series-connected two-motor drive with single inverter supply," IEEE Trans. On Industrial Electronics, vol. 54, no. 3, , pp. 1504-1516, June 2007.

[4.5] E. Levi, M. Jones, A. Iqbal, H.A. Toliyat, "An induction machine/syn-rel two-motor five-phase series-connected drive," IEEE Trans. On Energy Conversion, vol. 22, no. 2, June 2007, 281-289.

[4.6] M. Jones, "A novel concept of series connected multi-phase, multi-motor drive systems", *PhD. thesis,* School of Engineering, Liverpool John Moores University, Liverpool, UK in Jan 2005.

[4.7] J.W.Kelly, E.G.Strangas, J.M.Miller, "Multi-phase inverter analysis," Proc. IEEE Int. Electric Machines and Drives Conf. IEMDC, Cambridge, MA, 2001, pp. 147-155.

[4.8] O. Ojo, G. Dong, "Generalized discontinuous carrier-based PWM modulation scheme for multi-phase converter-machine systems," Proc. IEEE Ind. Appl. Soc. Annual Meeting IAS, Hong Kong, 2005, CD-ROM paper 38P3.

[4.9] A. Iqbal, E. Levi, M. Jones, S.N. Vukosavic, "Generalised sinusoidal PWM with harmonic injection for multi-phase VSIs," Proc. IEEE Power Elec. Spec. Conf. PESC, Jeju, Korea, 2006, pp. 2871-2877.

[4.10] M.J. Duran, E. Levi, "Multi-dimensional approach to multi-phase space vector pulse width modulation," Proc. IEEE Ind. Elec. Soc. Annual Meeting IECON, Paris, France, 2006, pp. 2103-2108.

[4.11] A. Iqbal, E. Levi, "Space vector PWM techniques for sinusoidal output voltage generation with a five-phase voltage source inverter," Electric Power Components and Systems, vol. 34, no. 2, 2006, pp. 119-140.

[4.12] J.W. Kelly, E.G. Strangas, J.M. Miller, "Multi-phase space vector pulse width modulation," IEEE Trans. on Energy Conversion, vol. 18, no. 2, 2003, pp. 259-264.

[4.13] H.M. Ryu, J.H. Kim, S.K. Sul, "Analysis of multi-phase space vector pulse-width modulation based on multiple d-q spaces concept," IEEE Trans. on Power Electronics, vol. 20, no. 6, 2005, pp. 1364-1371.

[4.14] D. Casadei, G. Serra, A. Tani, L. Zarri, "Multi-phase inverter modulation strategies based on duty-cycle space vector approach," Proc. Ship Propulsion and Railway Traction Systems Conf. SPRTS, Bologna, Italy, 2005, pp. 222-229.

[4.15] P.S.N. De Silva, J.E. Fletcher, B.W. Williams, "Development of space vector modulation strategies for five-phase voltage source inverters," Proc. IEE Power Electronics, Machines and Drives Conf. PEMD, Edinburgh, UK, 2004, pp. 650-655.

[4.16] A. Iqbal, E. Levi, "Space vector modulation schemes for a five-phase voltage source inverter," Proc. European Power Electronics and Applications Conf. EPE, Dresden, Germany, 2005, CD-ROM paper 0006.

[4.17] X. Kestelyn, E. Semail, J.P. Hautier, "Multi-phase system supplied by SVM VSI: A new fast algorithm to compute duty cycles," EPE Journal, vol. 14, no. 3, 2004, pp. 25-31.

[4.18] P. Delarue, A. Bouscayrol, E. Semail, "Generic control method of multi-leg voltage-source converters for fast practical implementation," IEEE Trans. on Power Electronics, vol. 18, no. 2, 2003, pp. 517-526.

[4.19] S. Xue, X. Wen, Z. Feng, "A novel multi-dimensional SVPWM strategy of multi-phase motor drives," Proc. Power Electronics and Motion Control Conf. EPE-PEMC, Portoroz, Slovenia, 2006, pp. 931-935.

[4.20] O. Ojo, G. Dong, Z. Wu, "Pulse-width modulation for five-phase converters based on device turn-on times," Proc. IEEE Ind. Appl. Soc. Annual Meeting IAS, Tampa, FL, 2006, CD-ROM paper IAS15p7.

[4.21] S. Xue, X. Wen, “Simulation analysis of two novel multi-phase SVPWM strategies,” Proc. IEEE Int. Conf. on Industrial Technology ICIT, Hong Kong, 2005, pp. 1401-1406.

[4.22] D. Casadei, D.Dujić, E.Levi, G.Serra, A.Tani, L.Zarri, “General modulation strategy for seven-phase inverters with independent control of multiple voltage space vectors," IEEE Trans. on Industrial Electronics, vol. 55, no. 5, 2008, pp. 1921-1932.

[4.23] D. Dujic, G. Grandi, M. Jones, E. Levi; “A space vector PWM scheme for multi-frequency output voltage generation with multi-phase voltage source inverters,” IEEE Trans. on Industrial Electronics, vol. 55, no. 5, 2008, pp. 1943-1955.

[4.24] M. Duran, S. Toral, F. Barrero, E. Levi, “Real-time implementation of multi-dimensional five-phase space vector pulse-width modulation,” Electronics Letters, vol. 43, no. 17, 16th August 2007, pp. 949-950.

[4.25] E. Levi, D. Dujic, M. Jones, G. Grandi, “Analytical determination of DC-bus utilization limits in multi-phase VSI supplied AC drives,” IEEE Trans. on Energy Conversion, vol. 23, no. 2, 2008, pp. 433-443.

[4.26] M. Jones, S.N. Vukosavic, E. Levi, “Parallel-connected multi-phase multi-drive systems with single inverter supply,” IEEE Transactions on Industrial Electronics, vol. 56, no. 6, June 2009, pp. 2047-2057.

[4.27] M. Jones, E. Levi, S.N. Vukosavic, H. A. Toliyat, **“**Independent vector control of a seven-phase three-motor drive system supplied from a single voltage source inverter,” 34th Annual IEEE Power Electronics Specialists Conference. ,vol. 4, Jun 2003, pp. 1865-1870.

[4.28] S. Moinuddin, A. Iqbal, M.R. Khan, “Space vector approach to model a seven-phase voltage source inverter,” Proceedings of IEEE International Conference on Recent Advancements and Applications of Computer in Electrical Engineering (RACE 2007) Bikaner, India , 2007, CD-ROM. Paper F-398.

[4.29] S. Moinuddin, A. Iqbal, "Modelling and Simulation of a Seven-Phase Voltage Source Inverter Using Space Vector Theory,” I-manager's Journal on Electrical Engineering, vol. 1, No. 1, July – September 2007, pp 30 – 41.

[4.30] D. Casadei, D. Dujic E. Levi G. Serra, A. Tani, L. Zarri, “general modulation strategy for seven phase inverters with independent control of multiple voltage space vectors”, IEEE Trans. Ind. Elect., vol. 55, no. 5, May 2008, pp. 1921-1932.

Chapter 5
Space Vector Modelling of Multi-phase Matrix Converter

Introduction

This chapter discusses the modelling procedures for a Matrix Converter with three-phase input and five-phase, six-phase and seven-phase outputs. The model is developed in space vector form. At first the topology of three-phase input and five-phase output is considered. The switching combinations are identified. The total number of possible switching combinations is obtained as 2^n where n is the number of power semiconductor switching devices being used. However, all these switching states are not permitted due to the fact that the input source should not be short-circuited and the output phases should not be open-circuited. The load is considered to be inductive and hence this safety condition is imposed. With such constraints, the number of permitted switching states reduces. Further, the space voltage vectors that arise due to these switching combinations are analyzed on the basis of their amplitude and frequency. They are grouped according to the number of output and input phase connections. It is observed that amplitude and frequency are variable in several cases. It is concluded that the space voltage vectors whose amplitude and frequency are constant, are only viable for space vector PWM implementation. The other two topologies analyzed are three-phase input and six-phase output, and three-phase input and seven-phase output.

5.2 Space Vector Model of a Three-phase to Five-phase Matrix Converter

The space vector model of a multi-phase Matrix Converter (three-phase input and five-phase output) is developed on the basis of representation of the three-phase input current and five-phase output line voltages on the space vector plane. The input current is three-phase and hence the traditional space vector model is sufficient to describe the input side. The output is five-phase and hence five-phase output voltage is to be modelled in five dimensional space. During Matrix Converter operation all output phases are connected to each input phases depending on the state of the switches. For a three-phase input and five-phase output Matrix Converter, total numbers of bi-directional power semiconductor switches (IGBTs) are fifteen (three switches per leg). One input line is connected to five bi-directional switches and hence three input line is connected to fifteen switches in all. A small LC filter is connected at the source side (three-phase side) to remove the switching ripples from the source current waveforms, thus making it sinusoidal. A general switching circuit is shown in Fig. 5.1. The filter is not shown in the Fig. 5.1. Each switch is shown with two sided arrows in order to show its bi-directional nature. There are several methods to realize the bi-directional power switches as discussed in reference [5.1] - [5.3].

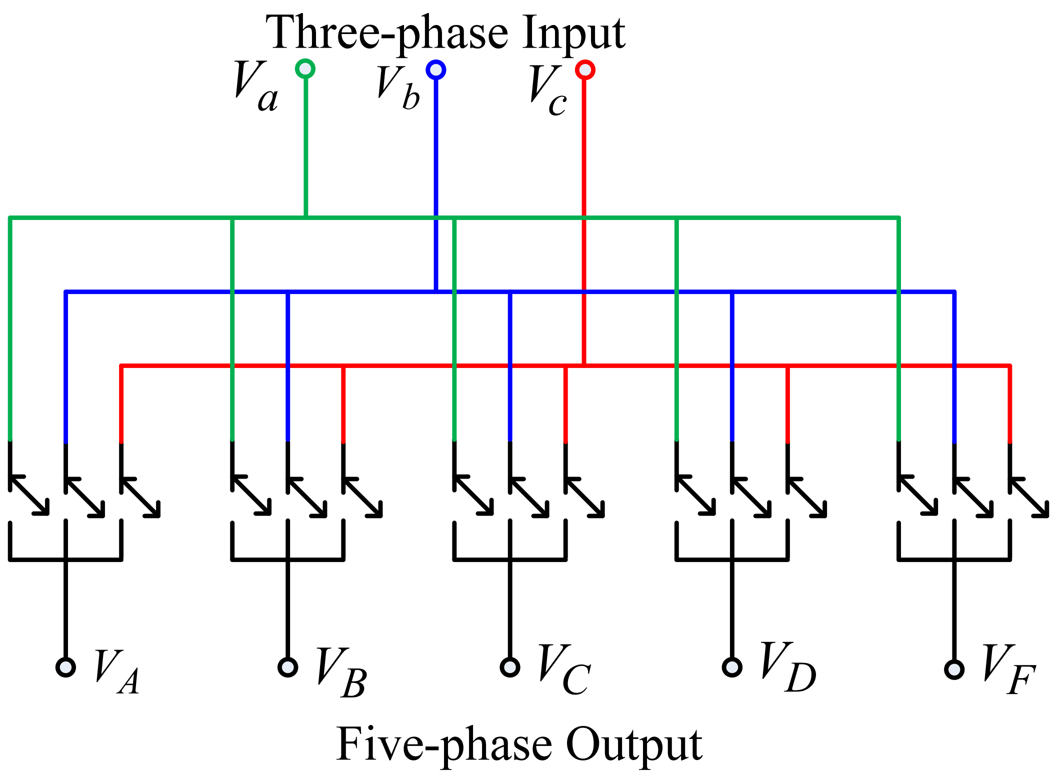

Fig. 5.1. Basic topology of a three-phase to five-phase Matrix Converter.

With this number of switches a total combination of switching can be made in the range of $2^{15} = 32768$. However, out of these many possible switching states, not all are permissible. To obtain the permissible switching states, one has to consider the safety of the source side as well as load side. It is well known that the switching states that cause a short circuit at the source side are not allowed. Similarly, opening of the load side is also not permitted, since the loads are mostly inductive and sudden opening of inductive circuit causes high voltage spikes that may damage the switching devices. . Hence, for the safe operation of Matrix Converter protecting the source and load, the following conditions must be considered at any switching time:

- Input phases (three-phase side) should never be short circuited,
- Output phases (five-phase side) should never be open circuited.

Considering the above two major constraints, there are 3^5 = 243, different switching combinations for connecting output phases to input phases. It is important to note here that the number of switching combinations is same as that of a three-level five-phase inverters as given in reference [5.4]. Therefore, one can say that the operation of a Matrix Converter is similar to the operation of a three-level back-to-back converter. These switching combinations can be put in five different groups or in other words, all these vectors are divided into five different groups. The space vector group nomenclature is defined as [x,y,z], where x represent the number of output phase connected to input phase ‘a’, y represent the number of output phase connected to input phase ‘b’ and z shows the number of output phases being connected to input phase ‘c’.

1. [5, 0, 0]: All the five output phases are connected to the same input phase. Since there are three phases at the input side, so three possible situation are possible, i.e. all five phases are connected to phase ‘a’ of input, or phase ‘b’ of input or finally to phase ‘c’ of input. Hence, this group consists of three different switching combinations. These vectors have zero magnitude and zero frequency, therefore they are termed as zero vectors.
2. [4, 1, 0]: Four of the output phases are connected to the same input phase and the fifth output phase is connected to any of the other two remaining input phases, e.g. if ABCD is connected to phase ‘a’ then ‘e’ can either connect with phase ‘b’ or phase ‘c’. This group consists of total 30 switching combinations. The space vectors produced due to these switching combinations have variable amplitude at a constant frequency in space. It means amplitude of the output voltages depend on the selected input line voltages. In this case the phase angle of the output voltage space vector does not depend on the phase angle of the input voltage space vector. The 30 combinations in this group determine 10 pre-fixed positions of the output voltage space vectors which are not dependent on α_i (input voltage vector position as shown in Fig.5.5). Similar condition is also valid for current vectors. The 30 combinations in this group determine 6 prefixed positions of the input current space vectors which are not dependent on β_o (output current vector position). The input side space vectors are not shown.
3. [3, 2, 0]: Three of the output phases are connected to the same input phase and the two other output phases are connected to any one of the other two input phases. This group consists of 60 switching combinations. These vectors have also variable

amplitude at a constant frequency in space. It means amplitude of the output voltages depend on the selected input line voltages. Also in this case the phase angle of the output voltage space vector does not depend on the phase angle of the input voltage space vector. The 60 combinations in this group determine 10 prefixed positions of the output voltage space vectors which are not dependent on α_i. Similar condition is also valid for current vectors. The 60 combinations in this group determine 6 prefixed positions of the input current space vectors which are not dependent on β_o.

4. [3, 1, 1]: Three of the output phases are connected to the same input phase and the two other output phases are connected to the other two input phases respectively. This group consists of total 60 switching combinations. These vectors have variable amplitude variable frequency in space. It means amplitude of the output voltages depend on the selected input line voltages. In this case the phase angle of the output voltage space vector depends on the phase angle of the input voltage space vector. The 60 combinations in this group do not determine any prefixed positions of the output voltage space vector. The locus of the output voltage space vectors form ellipses in different orientations in space as α_i is varied. Similar condition is also valid for current vectors. For the space vector modulation technique these switching states are not used in the Matrix Converter since the phase angle of both input and output vectors cannot be controlled independently. This control condition is important in Matrix Converter operation.
5. [2, 2, 1]: Two of the output phases are connected to the same input phase and the two other output phases are connected to another input phase and the fifth output phase is connected the remaining third input phase. This group consists of altogether 90 switching combinations. The space vectors generated due to these switching combinations produces also variable amplitude variable frequency in space. That is the amplitude of the output voltages depend on the selected input line voltages. In this case the phase angle of the output voltage space vector depends on the phase angle of the input voltage space vector. The 90 combinations in this group do not determine any prefixed positions of the output voltage space vector. The locus of the output voltage space vectors form ellipses in different orientations in space as α_i is varied i.e. with the rotation of the input space vector. Similar condition is also valid for current vectors. For the space vector modulation technique these switching states are

also not used in the Matrix Converter since the phase angle of both input and output vectors cannot be controlled independently.

The active switching states that produce constant amplitude voltage and constant frequency that can be further used for space vector pulse width modulation schemes are:

Group 1 :[5, 0, 0] consists of 3 space voltage vectors,-Zero vectors

Group 2 :[4, 1, 0] consists of 30 space voltage vectors,-Active vectors

Group 3 :[3, 2, 0] consists of 60 space voltage vectors,-Active vectors.

As such total 93 space voltage vector combinations can be used to realize the space vector modulation technique.

The switching circuit condition conditions corresponding to Group 1 ([5,0,0]), is illustrated in Fig. 5.2. The bold circle indicates the connection of the input and output phases.

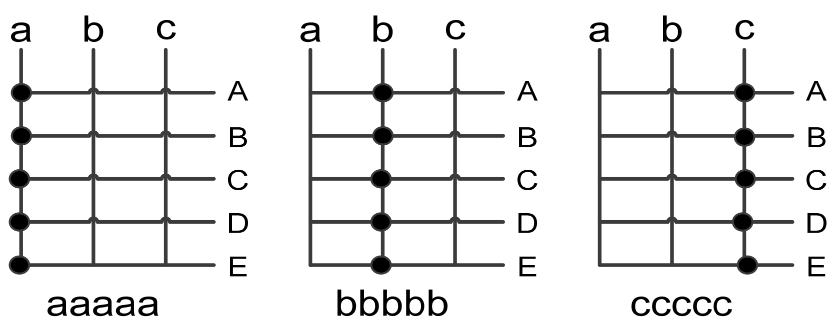

Fig. 5.2. Switching states of Group-1.

The switching circuit condition conditions corresponding to Group 2 ([4,1,0]), is illustrated in Fig. 5.3. The bold circle indicates the connection of the input and output phases.

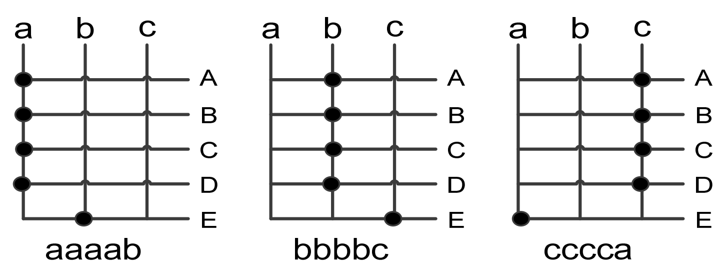

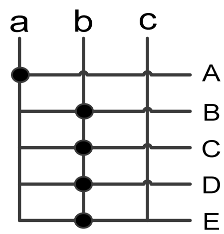

abbbb

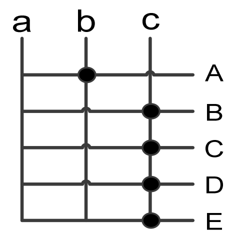

bcccc

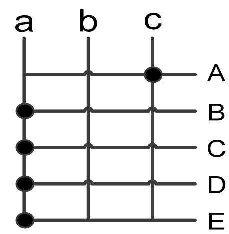

caaaa

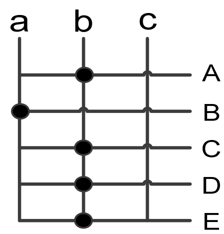

babbb

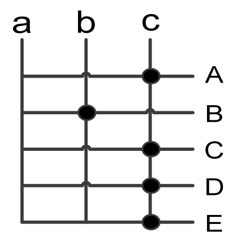

cbccc

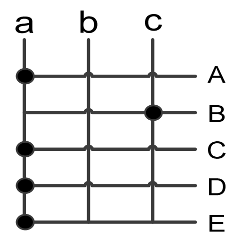

acaaa

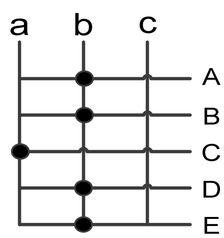

bbabb

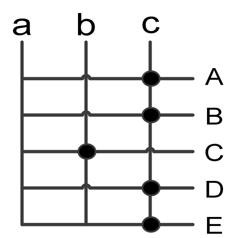

ccbcc

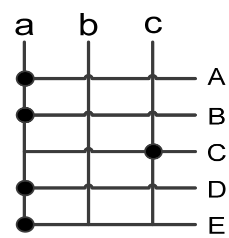

aacaa

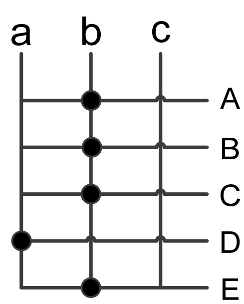

bbbab

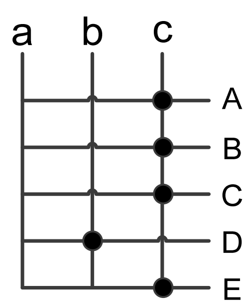

cccbc

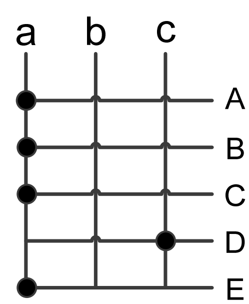

aaaca

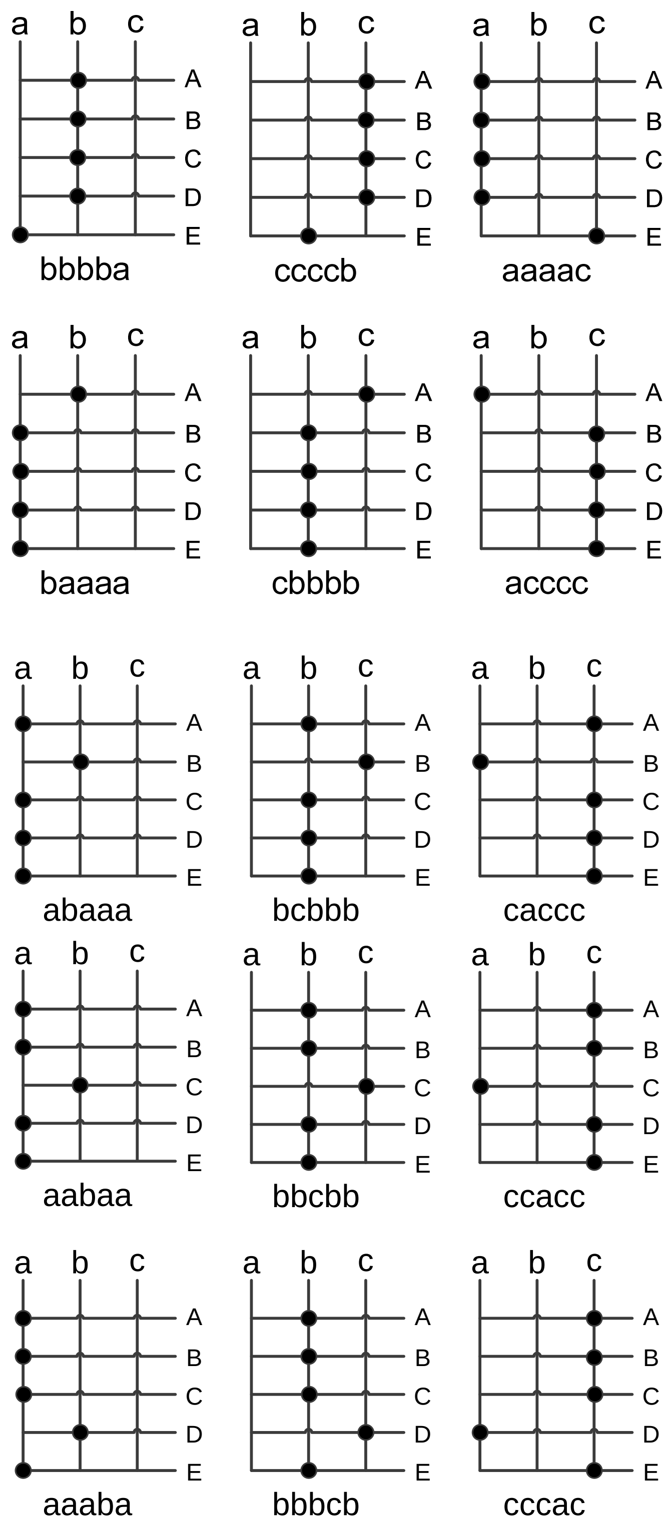

Fig. 5.3. Switching states of Group-2 [4,1,0].

The switching circuit condition conditions corresponding to Group 3 ([3,2,0]), is illustrated in Fig. 5.4. The bold circle indicates the connection of the input and output phases.

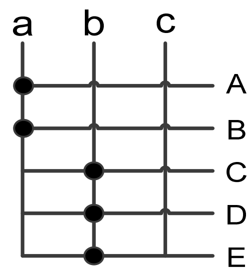

aabbb

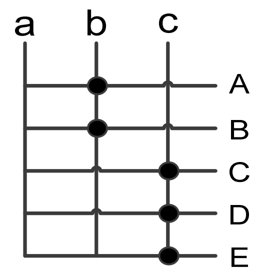

bbccc

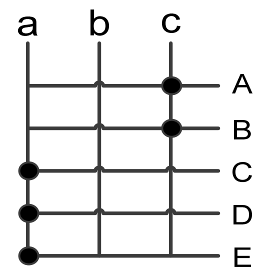

ccaaa

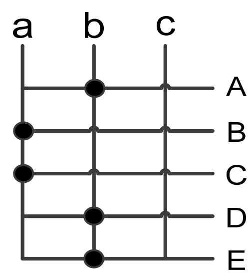

baabb

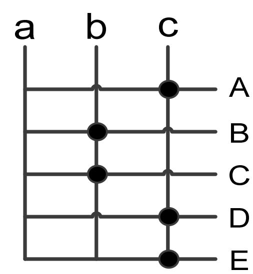

cbbcc

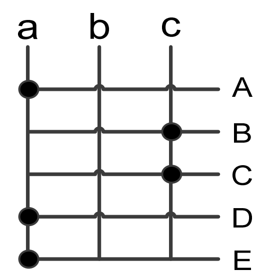

accaa

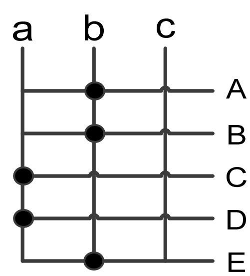

bbaab

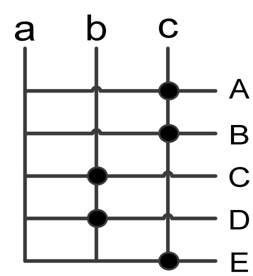

ccbbc

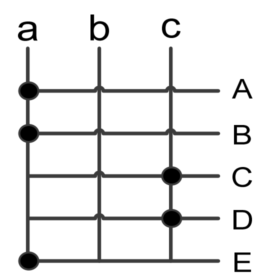

aacca

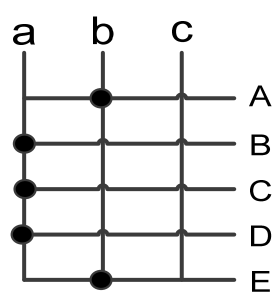

baaab

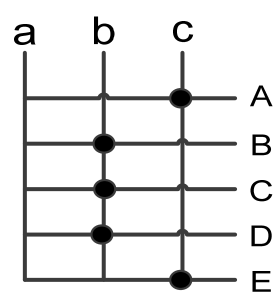

cbbbc

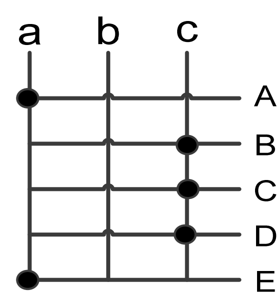

accca

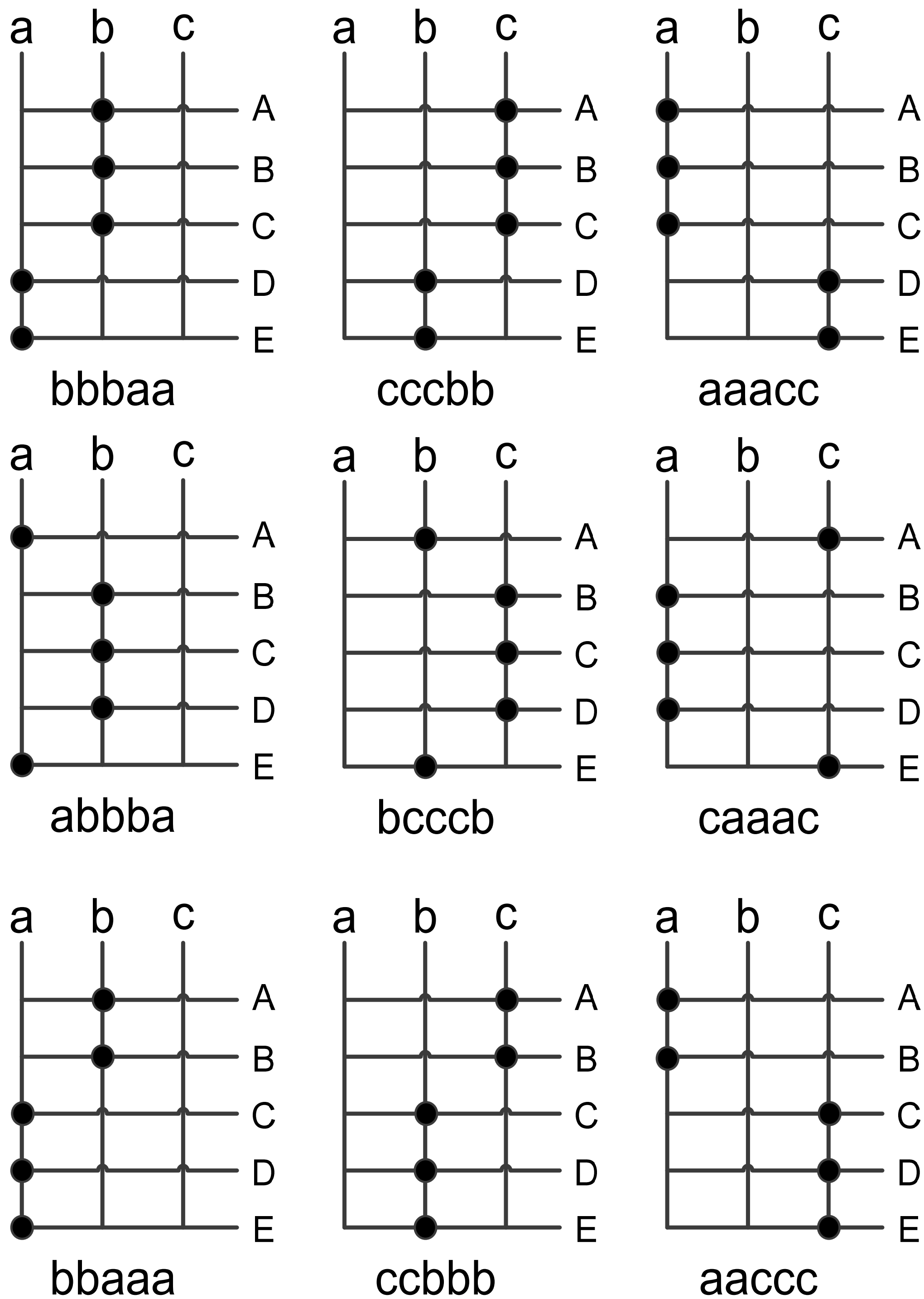

a b c
A B C D E
bbbaa
cccbb
aaacc
abbba
bcccb
caaac
bbaaa
ccbbb
aaccc

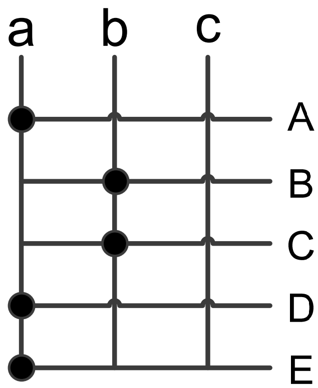

abbaa

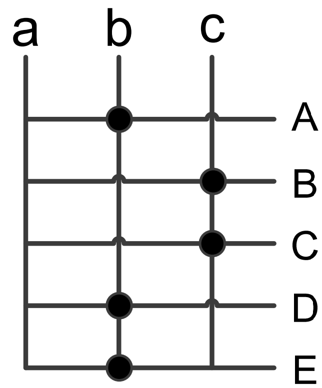

bccbb

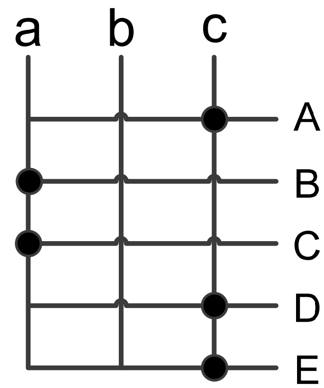

caacc

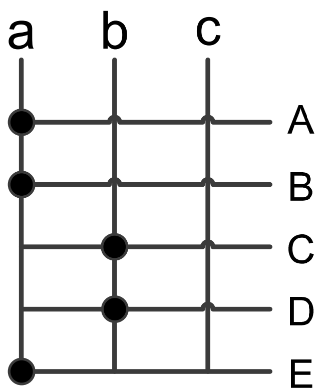

aabba

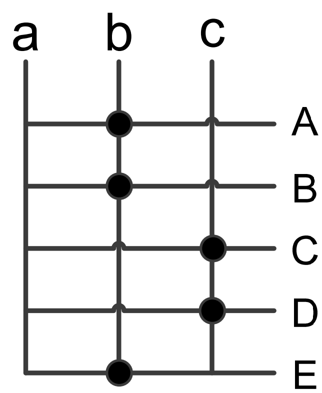

bbccb

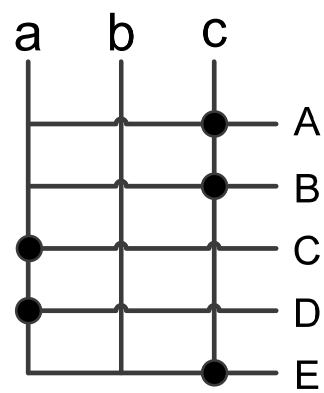

ccaac

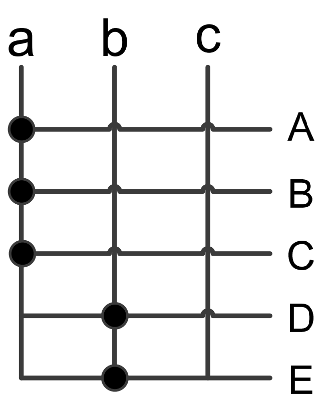

aaabb

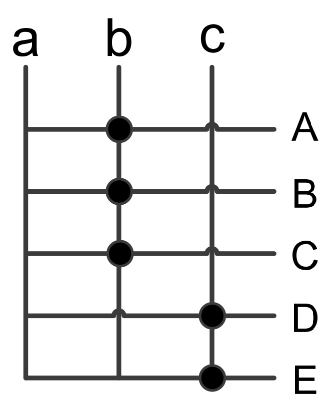

bbbcc

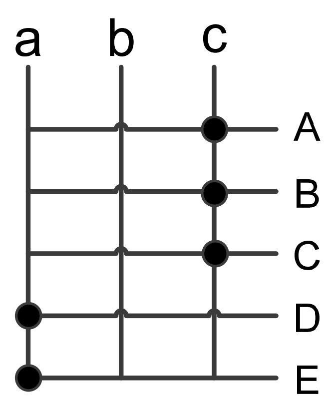

cccaa

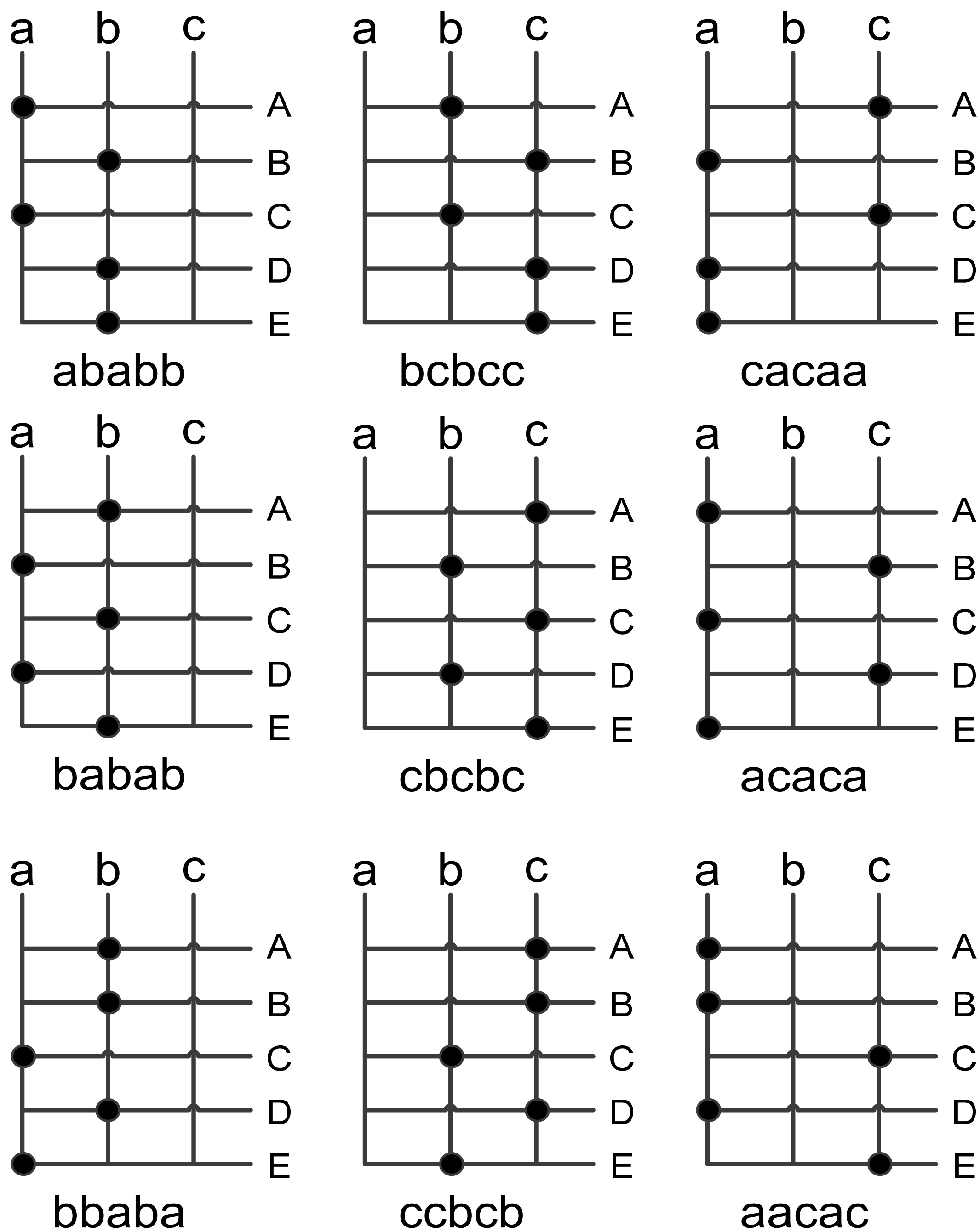
a b c
A
B
C
D
E
ababb
bcbcc
cacaa
babab
cbcbc
acaca
bbaba
ccbcb
aacac

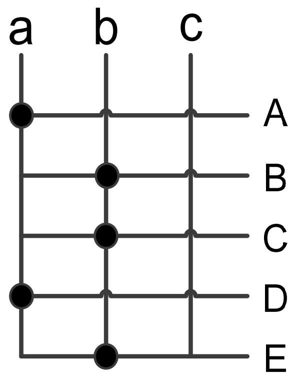

abbab

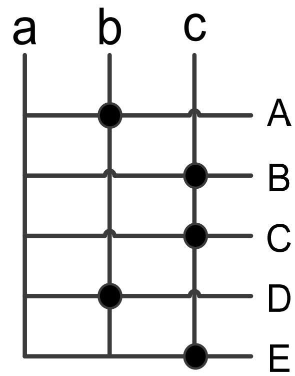

bccbc

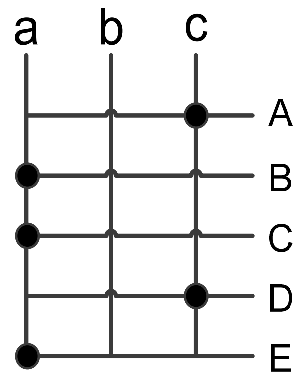

caaca

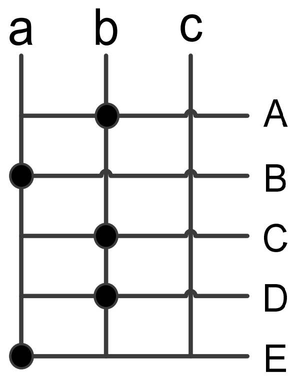

babba

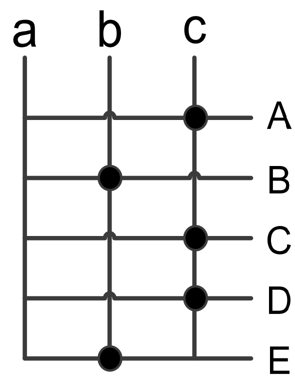

cbccb

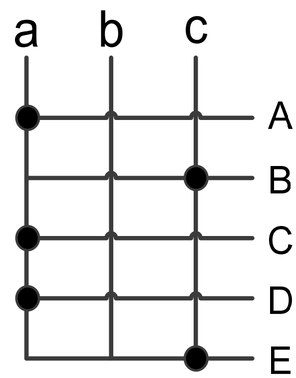

acaac

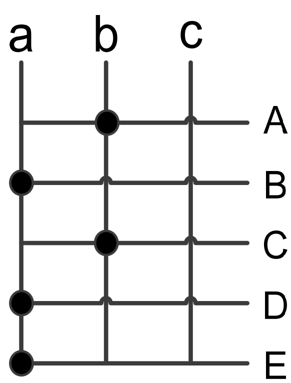

babaa

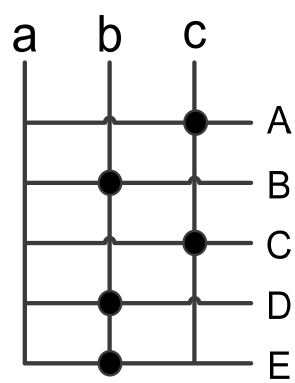

cbcbb

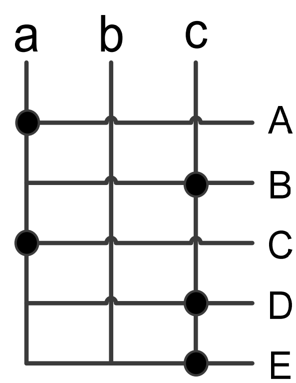

acacc

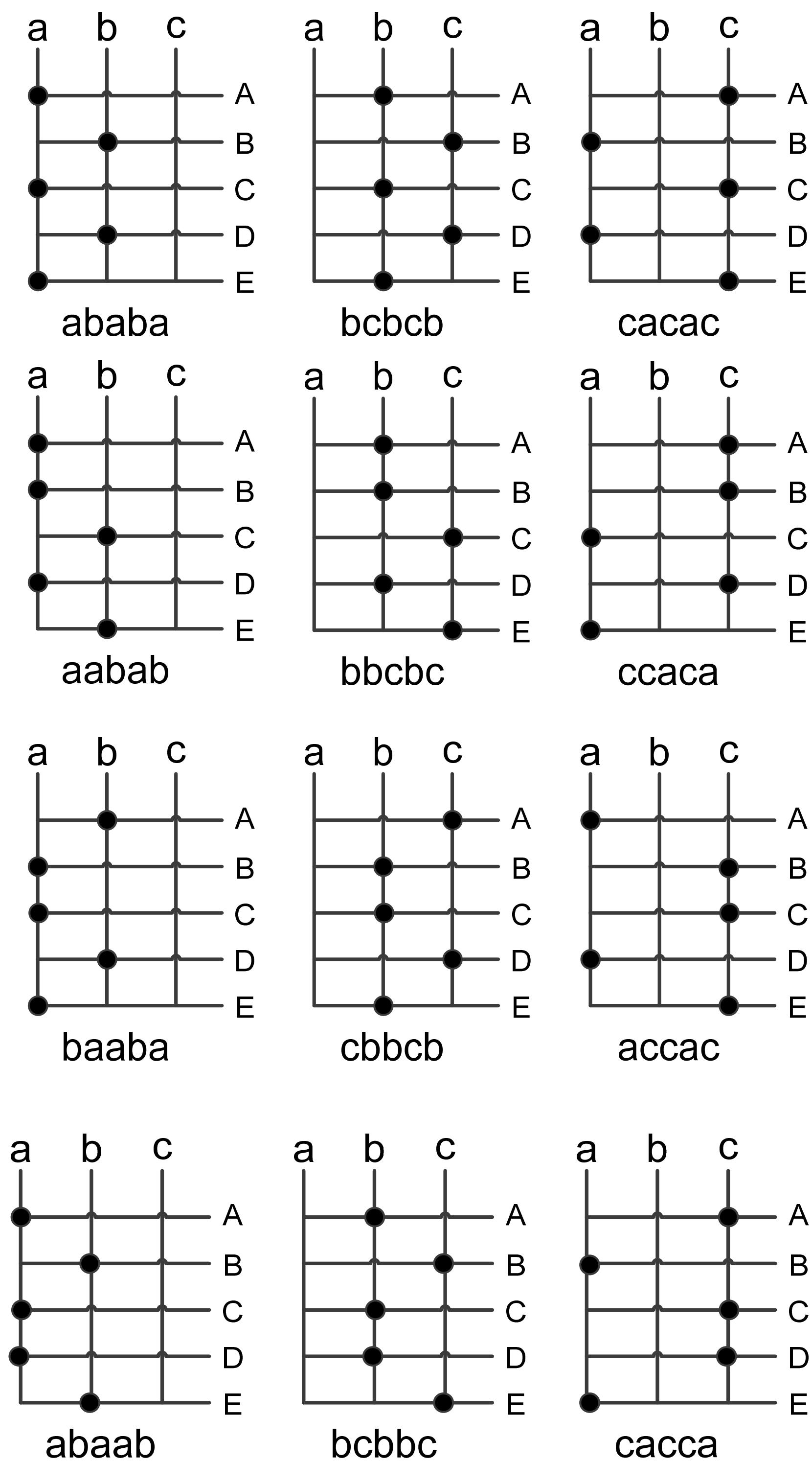

Fig. 5.4. Switching states for Group-4 [3,2,0].

The permitted voltage space vectors are then transformed into two set of orthogonal planes namely α-β and x-y in the stationary common reference frame. The transformation matrix used as given in reference [5.4]:

$$\underline{A}_s = \frac{2}{5}\begin{bmatrix} 1 & \cos(\alpha) & \cos(2\alpha) & \cos(2\alpha) & \cos(\alpha) \\ 0 & \sin(\alpha) & \sin(2\alpha) & -\sin(2\alpha) & -\sin(\alpha) \\ 1 & \cos(2\alpha) & \cos(4\alpha) & \cos(4\alpha) & \cos(2\alpha) \\ 0 & \sin(2\alpha) & \sin(4\alpha) & -\sin(4\alpha) & -\sin(2\alpha) \\ \frac{1}{2} & \frac{1}{2} & \frac{1}{2} & \frac{1}{2} & \frac{1}{2} \end{bmatrix} \tag{5.1}$$

The 93 space voltage vectors that are finally used to implement space vector pulse width modulation scheme are given in Fig. 5.5 in the orthogonal planes.

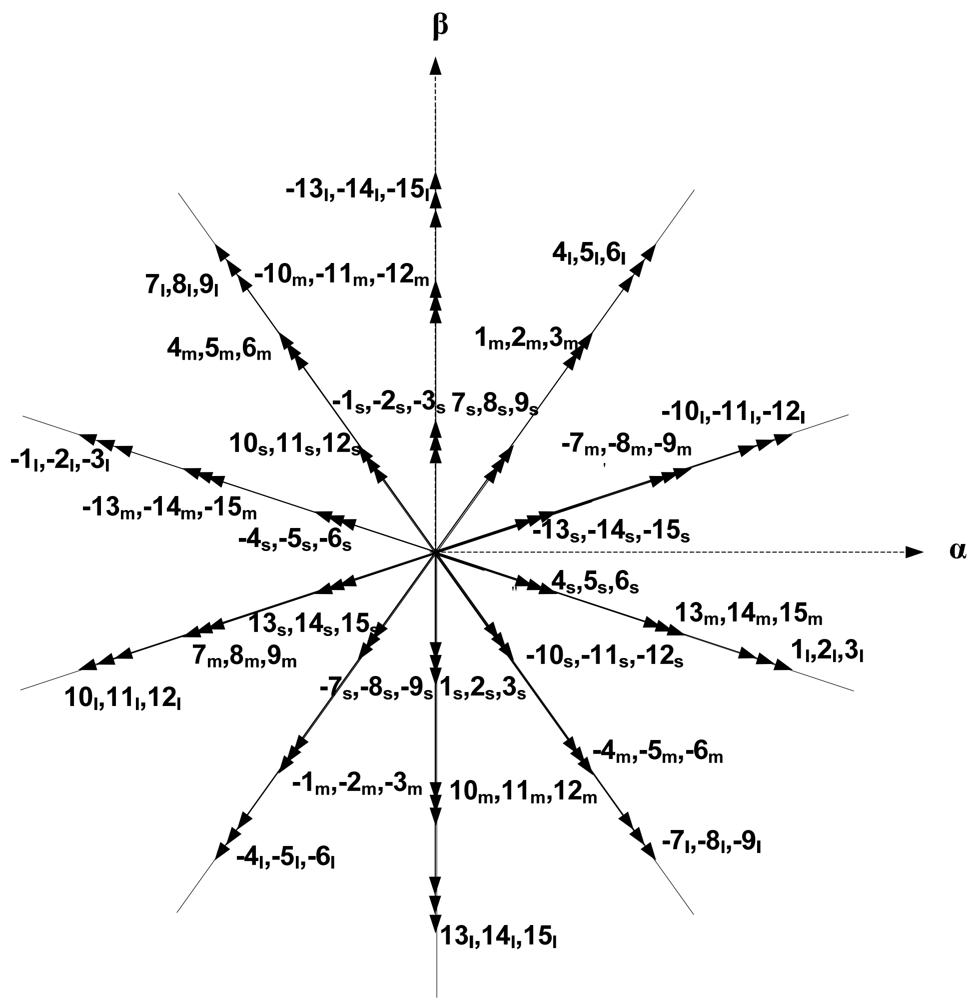

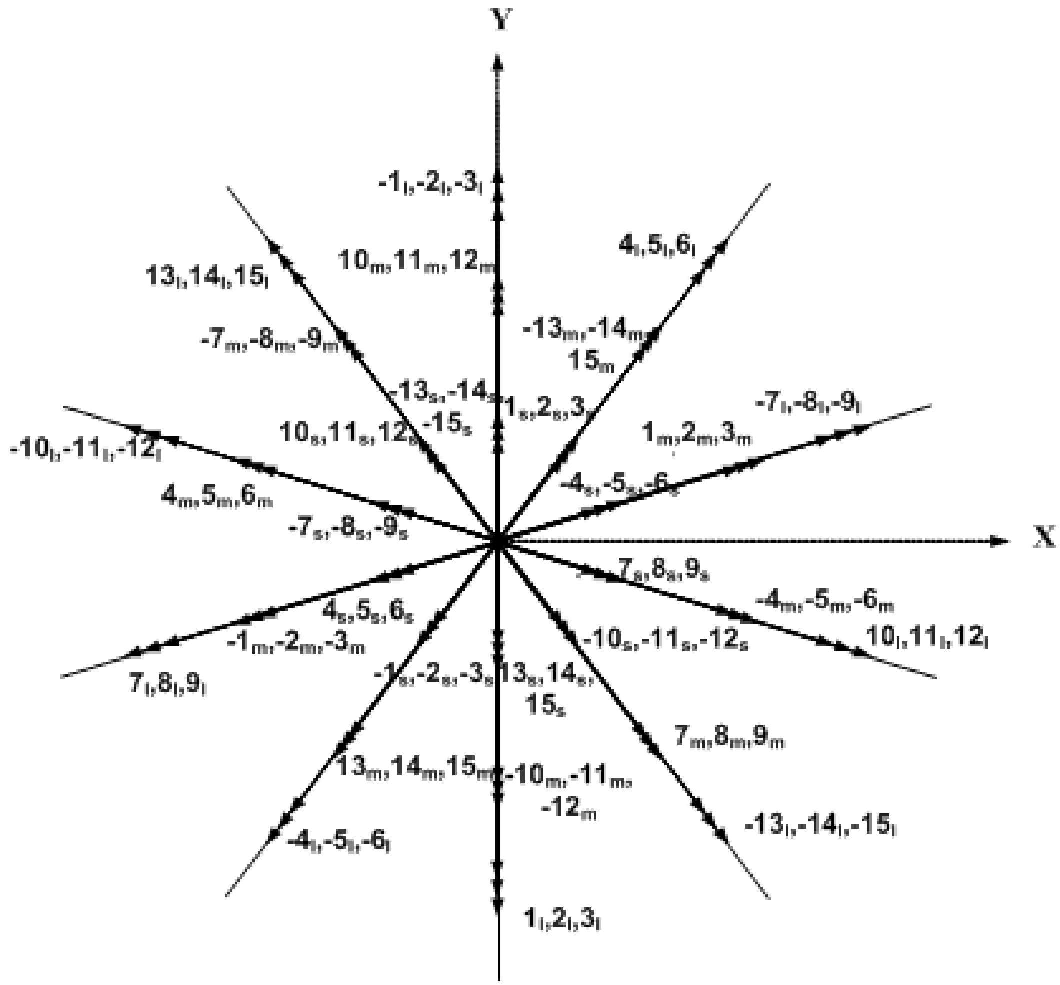

Fig. 5.5. Output voltage space vectors corresponding to the permitted switching combinations.

The large length space voltage vectors are shown in Fig. 5.6.

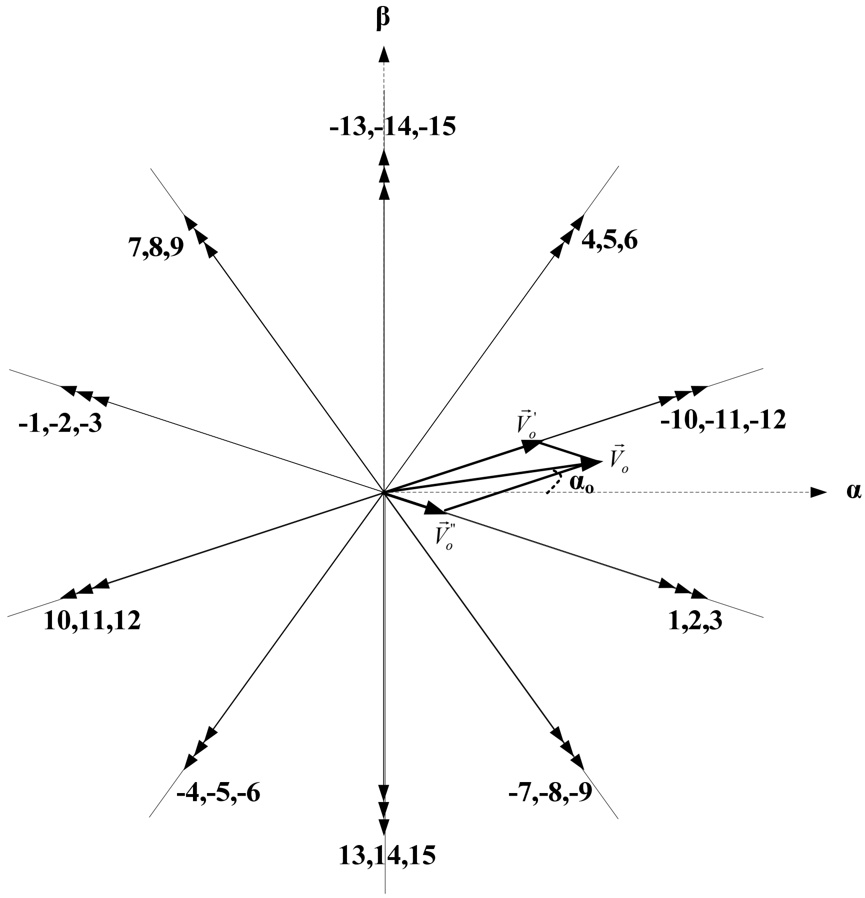

Fig. 5.6. Output large length voltage space vectors.

The large length space voltage vectors detail are tabulated in Table 5.1. The table shows the output phases connected to the input phase, the relation between the output line voltage and input line voltage, the relation between the output line current and input line current, the output voltage and the position. e.g. column 3, row 1, the input phase 'a' is connected to the output phase 'A'. The output line voltage, V_{AB} is same as input line voltage V_{ab}, the input current Ia is same as output line current I_A. The output voltage vector Vo is equal to 0.7608Vab (input line voltage), the position of vector is -18°, and the input current vector is $1.156*i_A$ and its position is -30°. It is to be noted that 'l' in Table 5.1 is equal to

$$\frac{2}{5}\left[\frac{\sqrt{2\left(5+\sqrt{5}\right)}}{2}\right] = 0.7608$$

Table 5.1. Large length vectors.

Group	Name	A	B	C	D	E	V_{AB}	V_{BC}	V_{CD}	V_{DE}	V_{EA}	i_a	i_b	i_c	V_o	α_o	I_i	β_i
Large A	+1	a	b	b	a	a	V_{ab}	0	$-V_{ab}$	0	0	i_A	$-i_A$	0	$1V_{ab}$	$-\frac{\pi}{10}$	$\frac{2}{\sqrt{3}}i_A$	$-\frac{\pi}{6}$
	-1	b	a	a	b	b	$-V_{ab}$	0	V_{ab}	0	0	$-i_A$	i_A	0	$-1V_{ab}$	$-\frac{\pi}{10}$	$-\frac{2}{\sqrt{3}}i_A$	$-\frac{\pi}{6}$
	+2	b	c	c	b	b	V_{bc}	0	$-V_{bc}$	0	0	0	i_A	$-i_A$	$1V_{bc}$	$-\frac{\pi}{10}$	$\frac{2}{\sqrt{3}}i_A$	$\frac{\pi}{2}$
	-2	c	b	b	c	c	$-V_{bc}$	0	V_{bc}	0	0	0	$-i_A$	i_A	$-1V_{bc}$	$-\frac{\pi}{10}$	$-\frac{2}{\sqrt{3}}i_A$	$\frac{\pi}{2}$
	+3	c	a	a	c	c	V_{ca}	0	$-V_{ca}$	0	0	$-i_A$	0	i_A	$1V_{ca}$	$-\frac{\pi}{10}$	$\frac{2}{\sqrt{3}}i_A$	$\frac{7\pi}{6}$
	-3	a	c	c	a	a	$-V_{ca}$	0	V_{ca}	0	0	i_A	0	$-i_A$	$-1V_{ca}$	$-\frac{\pi}{10}$	$-\frac{2}{\sqrt{3}}i_A$	$\frac{7\pi}{6}$

Group	Name	A	B	C	D	E	V_{AB}	V_{BC}	V_{CD}	V_{DE}	V_{EA}	i_a	i_b	i_c	V_o	α_o	I_i	β_i
Large B	+4	a	a	b	b	a	0	V_{ab}	0	$-V_{ab}$	0	i_B	$-i_B$	0	$1V_{ab}$	$\frac{3\pi}{10}$	$\frac{2}{\sqrt{3}}i_B$	$-\frac{\pi}{6}$
	-4	b	b	a	a	b	0	$-V_{ab}$	0	V_{ab}	0	$-i_B$	i_B	0	$-1V_{ab}$	$\frac{3\pi}{10}$	$-\frac{2}{\sqrt{3}}i_B$	$-\frac{\pi}{6}$
	+5	b	b	c	c	b	0	V_{bc}	0	$-V_{bc}$	0	0	i_B	$-i_B$	$1V_{bc}$	$\frac{3\pi}{10}$	$\frac{2}{\sqrt{3}}i_B$	$\frac{\pi}{2}$
	-5	c	c	b	b	c	0	$-V_{bc}$	0	V_{bc}	0	0	$-i_B$	i_B	$-1V_{bc}$	$\frac{3\pi}{10}$	$-\frac{2}{\sqrt{3}}i_B$	$\frac{\pi}{2}$
	+6	c	c	a	a	c	0	V_{ca}	0	$-V_{ca}$	0	$-i_B$	0	i_B	$1V_{ca}$	$\frac{3\pi}{10}$	$\frac{2}{\sqrt{3}}i_B$	$\frac{7\pi}{6}$
	-6	a	a	c	c	a	0	$-V_{ca}$	0	V_{ca}	0	i_B	0	$-i_B$	$-1V_{ca}$	$\frac{3\pi}{10}$	$-\frac{2}{\sqrt{3}}i_B$	$\frac{7\pi}{6}$

Group	Name	A	B	C	D	E	V_{AB}	V_{BC}	V_{CD}	V_{DE}	V_{EA}	i_a	i_b	i_c	V_o	α_o	I_i	β_i
Large C	+7	a	a	a	b	b	0	0	V_{ab}	0	$-V_{ab}$	i_C	$-i_C$	0	$1V_{ab}$	$\frac{7\pi}{10}$	$\frac{2}{\sqrt{3}}i_C$	$-\frac{\pi}{6}$
	-7	b	b	b	a	a	0	0	$-V_{ab}$	0	V_{ab}	$-i_C$	i_C	0	$-1V_{ab}$	$\frac{7\pi}{10}$	$-\frac{2}{\sqrt{3}}i_C$	$-\frac{\pi}{6}$
	+8	b	b	b	c	c	0	0	V_{bc}	0	$-V_{bc}$	0	i_C	$-i_C$	$1V_{bc}$	$\frac{7\pi}{10}$	$\frac{2}{\sqrt{3}}i_C$	$\frac{\pi}{2}$
	-8	c	c	c	b	b	0	0	$-V_{bc}$	0	V_{bc}	0	$-i_C$	i_C	$-1V_{bc}$	$\frac{7\pi}{10}$	$-\frac{2}{\sqrt{3}}i_C$	$\frac{\pi}{2}$
	+9	c	c	c	a	a	0	0	V_{ca}	0	$-V_{ca}$	$-i_C$	0	i_C	$1V_{ca}$	$\frac{7\pi}{10}$	$\frac{2}{\sqrt{3}}i_C$	$\frac{7\pi}{6}$
	-9	a	a	a	c	c	0	0	$-V_{ca}$	0	V_{ca}	i_C	0	$-i_C$	$-1V_{ca}$	$\frac{7\pi}{10}$	$-\frac{2}{\sqrt{3}}i_C$	$\frac{7\pi}{6}$

Group	Name	A	B	C	D	E	V_{AB}	V_{BC}	V_{CD}	V_{DE}	V_{EA}	i_a	i_b	i_c	V_o	α_o	I_i	β_i
Large D	+10	b	a	a	a	b	$-V_{ab}$	0	0	V_{ab}	0	i_D	$-i_D$	0	$1V_{ab}$	$\frac{11\pi}{2}$	$\frac{2}{\sqrt{3}}i_D$	$-\frac{\pi}{6}$
	-10	a	b	b	b	a	V_{ab}	0	0	$-V_{ab}$	0	$-i_D$	i_D	0	$-1V_{ab}$	$\frac{11\pi}{2}$	$-\frac{2}{\sqrt{3}}i_D$	$-\frac{\pi}{6}$
	+11	c	b	b	b	c	$-V_{bc}$	0	0	V_{bc}	0	0	i_D	$-i_D$	$1V_{bc}$	$\frac{11\pi}{2}$	$\frac{2}{\sqrt{3}}i_D$	$\frac{\pi}{2}$
	-11	b	c	c	c	b	V_{bc}	0	0	$-V_{bc}$	0	0	$-i_D$	i_D	$-1V_{bc}$	$\frac{11\pi}{2}$	$-\frac{2}{\sqrt{3}}i_D$	$\frac{\pi}{2}$
	+12	a	c	c	c	a	$-V_{ca}$	0	0	V_{ca}	0	$-i_D$	0	i_D	$1V_{ca}$	$\frac{11\pi}{2}$	$\frac{2}{\sqrt{3}}i_D$	$\frac{7\pi}{6}$
	-12	c	a	a	a	c	V_{ca}	0	0	$-V_{ca}$	0	i_D	0	$-i_D$	$-1V_{ca}$	$\frac{11\pi}{2}$	$-\frac{2}{\sqrt{3}}i_D$	$\frac{7\pi}{6}$

Group	Name	A	B	C	D	E	V_{AB}	V_{BC}	V_{CD}	V_{DE}	V_{EA}	i_a	i_b	i_c	V_o	α_o	I_i	β_i
Large E	+13	b	b	a	a	a	0	$-V_{ab}$	0	0	V_{ab}	i_E	$-i_E$	0	$1V_{ab}$	$-\frac{\pi}{2}$	$\frac{2}{\sqrt{3}}i_E$	$-\frac{\pi}{6}$
	-13	a	a	b	b	b	0	V_{ab}	0	0	$-V_{ab}$	$-i_E$	i_E	0	$-1V_{ab}$	$-\frac{\pi}{2}$	$-\frac{2}{\sqrt{3}}i_E$	$-\frac{\pi}{6}$
	+14	c	c	b	b	b	0	$-V_{bc}$	0	0	V_{bc}	0	i_E	$-i_E$	$1V_{bc}$	$-\frac{\pi}{2}$	$\frac{2}{\sqrt{3}}i_E$	$\frac{\pi}{2}$
	-14	b	b	c	c	c	0	V_{bc}	0	0	$-V_{bc}$	0	$-i_E$	i_E	$-1V_{bc}$	$-\frac{\pi}{2}$	$-\frac{2}{\sqrt{3}}i_E$	$\frac{\pi}{2}$
	+15	a	a	c	c	c	0	$-V_{ca}$	0	0	V_{ca}	$-i_E$	0	i_E	$1V_{ca}$	$-\frac{\pi}{2}$	$\frac{2}{\sqrt{3}}i_E$	$\frac{7\pi}{6}$
	-15	c	c	a	a	a	0	V_{ca}	0	0	$-V_{ca}$	i_E	0	$-i_E$	$-1V_{ca}$	$-\frac{\pi}{2}$	$-\frac{2}{\sqrt{3}}i_E$	$\frac{7\pi}{6}$

The medium length space vectors are also analysed and the set is shown in Fig. 5.7

The medium length space voltage vectors details are tabulated in Table 5.2. The table shows the output phases connected to the input phase, the relation between the output line voltages and output line voltages, the relation between the output line current and input line current, the output voltage and the position. e.g. column 3, row 1, the input phase 'a' is connected to the output phase 'A'. The output line voltage, V_{AB} is same as input line voltage V_{ab}, the input current Ia is same as output line current I_A. The output voltage vector Vo is 0.4706xVab (input line voltage), the position of vector is 54°, and the input current vector is 1.156*i_A and its position is -30°. Note that $m = \frac{2}{5}\left[\frac{\sqrt{2\left(5-\sqrt{5}\right)}}{2}\right] = 0.4702$.

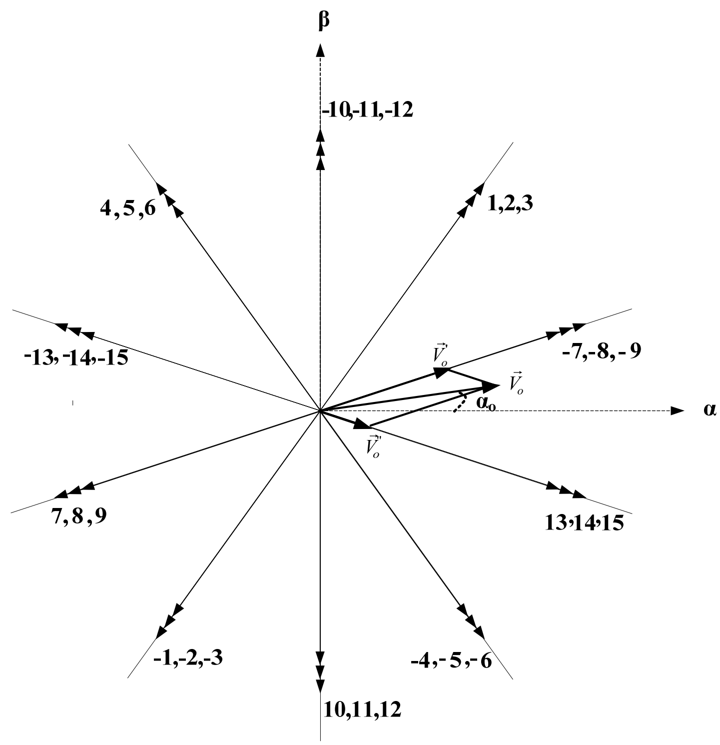

Fig. 5.7. Output medium length voltage space vectors.

Table 5.2. Medium length vectors

Group	Name	A	B	C	D	E	V_{AB}	V_{BC}	V_{CD}	V_{DE}	V_{EA}	i_a	i_b	i_c	V_o	α_o	I_i	β_i
Medium A	+1	a	b	b	b	b	V_{ab}	0	0	0	$-V_{ab}$	i_A	$-i_A$	0	mV_{ab}	$\frac{3\pi}{10}$	$\frac{2}{\sqrt{3}}i_A$	$-\frac{\pi}{6}$
	-1	b	a	a	a	a	$-V_{ab}$	0	0	0	V_{ab}	$-i_A$	i_A	0	$-mV_{ab}$	$\frac{3\pi}{10}$	$-\frac{2}{\sqrt{3}}i_A$	$-\frac{\pi}{6}$
	+2	b	c	c	c	c	V_{bc}	0	0	0	$-V_{bc}$	0	i_A	$-i_A$	mV_{bc}	$\frac{3\pi}{10}$	$\frac{2}{\sqrt{3}}i_A$	$\frac{\pi}{2}$
	-2	c	b	b	b	b	$-V_{bc}$	0	0	0	V_{bc}	0	$-i_A$	i_A	$-mV_{bc}$	$\frac{3\pi}{10}$	$-\frac{2}{\sqrt{3}}i_A$	$\frac{\pi}{2}$
	+3	c	a	a	a	a	V_{ca}	0	0	0	$-V_{ca}$	$-i_A$	0	i_A	mV_{ca}	$\frac{3\pi}{10}$	$\frac{2}{\sqrt{3}}i_A$	$\frac{7\pi}{6}$
	-3	a	c	c	c	c	$-V_{ca}$	0	0	0	V_{ca}	i_A	0	$-i_A$	$-mV_{ca}$	$\frac{3\pi}{10}$	$-\frac{2}{\sqrt{3}}i_A$	$\frac{7\pi}{6}$

Group	Name	A	B	C	D	E	V_{AB}	V_{BC}	V_{CD}	V_{DE}	V_{EA}	i_a	i_b	i_c	V_o	α_o	I_i	β_i
Medium B	+4	b	a	b	b	b	$-V_{ab}$	V_{ab}	0	0	0	i_B	$-i_B$	0	mV_{ab}	$\frac{7\pi}{10}$	$\frac{2}{\sqrt{3}}i_B$	$-\frac{\pi}{6}$
	-4	a	b	a	a	a	V_{ab}	$-V_{ab}$	0	0	0	$-i_B$	i_B	0	$-mV_{ab}$	$\frac{7\pi}{10}$	$-\frac{2}{\sqrt{3}}i_B$	$-\frac{\pi}{6}$
	+5	c	b	c	c	c	$-V_{bc}$	V_{bc}	0	0	0	0	i_B	$-i_B$	mV_{bc}	$\frac{7\pi}{10}$	$\frac{2}{\sqrt{3}}i_B$	$\frac{\pi}{2}$
	-5	b	c	b	b	b	V_{bc}	$-V_{bc}$	0	0	0	0	$-i_B$	i_B	$-mV_{bc}$	$\frac{7\pi}{10}$	$-\frac{2}{\sqrt{3}}i_B$	$\frac{\pi}{2}$
	+6	a	c	a	a	a	$-V_{ca}$	V_{ca}	0	0	0	$-i_B$	0	i_B	mV_{ca}	$\frac{7\pi}{10}$	$\frac{2}{\sqrt{3}}i_B$	$\frac{7\pi}{6}$
	-6	c	a	c	c	c	V_{ca}	$-V_{ca}$	0	0	0	i_B	0	$-i_B$	$-mV_{ca}$	$\frac{7\pi}{10}$	$-\frac{2}{\sqrt{3}}i_B$	$\frac{7\pi}{6}$

Group	Name	A	B	C	D	E	V_{AB}	V_{BC}	V_{CD}	V_{DE}	V_{EA}	i_a	i_b	i_c	V_o	α_o	I_i	β_i
Medium C	+7	b	b	a	b	b	0	$-V_{ab}$	V_{ab}	0	0	i_C	$-i_C$	0	mV_{ab}	$\frac{11\pi}{10}$	$\frac{2}{\sqrt{3}}i_C$	$-\frac{\pi}{6}$
	-7	a	a	b	a	a	0	V_{ab}	$-V_{ab}$	0	0	$-i_C$	i_C	0	$-mV_{ab}$	$\frac{11\pi}{10}$	$-\frac{2}{\sqrt{3}}i_C$	$-\frac{\pi}{6}$
	+8	c	c	b	c	c	0	$-V_{bc}$	V_{bc}	0	0	0	i_C	$-i_C$	mV_{bc}	$\frac{11\pi}{10}$	$\frac{2}{\sqrt{3}}i_C$	$\frac{\pi}{2}$
	-8	b	b	c	b	b	0	V_{bc}	$-V_{bc}$	0	0	0	$-i_C$	i_C	$-mV_{bc}$	$\frac{11\pi}{10}$	$-\frac{2}{\sqrt{3}}i_C$	$\frac{\pi}{2}$
	+9	a	a	c	a	a	0	$-V_{ca}$	V_{ca}	0	0	$-i_C$	0	i_C	mV_{ca}	$\frac{11\pi}{10}$	$\frac{2}{\sqrt{3}}i_C$	$\frac{7\pi}{6}$
	-9	c	c	a	c	c	0	V_{ca}	$-V_{ca}$	0	0	i_C	0	$-i_C$	$-mV_{ca}$	$\frac{11\pi}{10}$	$-\frac{2}{\sqrt{3}}i_C$	$\frac{7\pi}{6}$

Group	Name	A	B	C	D	E	V_{AB}	V_{BC}	V_{CD}	V_{DE}	V_{EA}	i_a	i_b	i_c	V_o	α_o	I_i	β_i
Medium D	+10	b	b	b	a	b	0	0	$-V_{ab}$	V_{ab}	0	i_D	$-i_D$	0	mV_{ab}	$-\frac{\pi}{2}$	$\frac{2}{\sqrt{3}}i_D$	$-\frac{\pi}{6}$
	-10	a	a	a	b	a	0	0	V_{ab}	$-V_{ab}$	0	$-i_D$	i_D	0	$-mV_{ab}$	$-\frac{\pi}{2}$	$-\frac{2}{\sqrt{3}}i_D$	$-\frac{\pi}{6}$
	+11	c	c	c	b	c	0	0	$-V_{bc}$	V_{bc}	0	0	i_D	$-i_D$	mV_{bc}	$-\frac{\pi}{2}$	$\frac{2}{\sqrt{3}}i_D$	$\frac{\pi}{2}$
	-11	b	b	b	c	b	0	0	V_{bc}	$-V_{bc}$	0	0	$-i_D$	i_D	$-mV_{bc}$	$-\frac{\pi}{2}$	$-\frac{2}{\sqrt{3}}i_D$	$\frac{\pi}{2}$
	+12	a	a	a	c	a	0	0	$-V_{ca}$	V_{ca}	0	$-i_D$	0	i_D	mV_{ca}	$-\frac{\pi}{2}$	$\frac{2}{\sqrt{3}}i_D$	$\frac{7\pi}{6}$
	-12	c	c	c	a	c	0	0	V_{ca}	$-V_{ca}$	0	i_D	0	$-i_D$	$-mV_{ca}$	$-\frac{\pi}{2}$	$-\frac{2}{\sqrt{3}}i_D$	$\frac{7\pi}{6}$

Group	Name	A	B	C	D	E	V_{AB}	V_{BC}	V_{CD}	V_{DE}	V_{EA}	i_a	i_b	i_c	V_o	α_o	I_i	β_i
Medium E	+13	b	b	b	b	a	0	0	0	$-V_{ab}$	V_{ab}	i_E	$-i_E$	0	mV_{ab}	$-\frac{\pi}{10}$	$\frac{2}{\sqrt{3}}i_E$	$-\frac{\pi}{6}$
	-13	a	a	a	a	b	0	0	0	V_{ab}	$-V_{ab}$	$-i_E$	i_E	0	$-mV_{ab}$	$-\frac{\pi}{10}$	$-\frac{2}{\sqrt{3}}i_E$	$-\frac{\pi}{6}$
	+14	c	c	c	c	b	0	0	0	$-V_{bc}$	V_{bc}	0	i_E	$-i_E$	mV_{bc}	$-\frac{\pi}{10}$	$\frac{2}{\sqrt{3}}i_E$	$\frac{\pi}{2}$
	-14	b	b	b	b	c	0	0	0	V_{bc}	$-V_{bc}$	0	$-i_E$	i_E	$-mV_{bc}$	$-\frac{\pi}{10}$	$-\frac{2}{\sqrt{3}}i_E$	$\frac{\pi}{2}$
	+15	a	a	a	a	c	0	0	0	$-V_{ca}$	V_{ca}	$-i_E$	0	i_E	mV_{ca}	$-\frac{\pi}{10}$	$\frac{2}{\sqrt{3}}i_E$	$\frac{7\pi}{6}$
	-15	c	c	c	c	a	0	0	0	V_{ca}	$-V_{ca}$	i_E	0	$-i_E$	$-mV_{ca}$	$-\frac{\pi}{10}$	$-\frac{2}{\sqrt{3}}i_E$	$\frac{7\pi}{6}$

The small vectors are also analysed and are shown in Fig. 5.8.

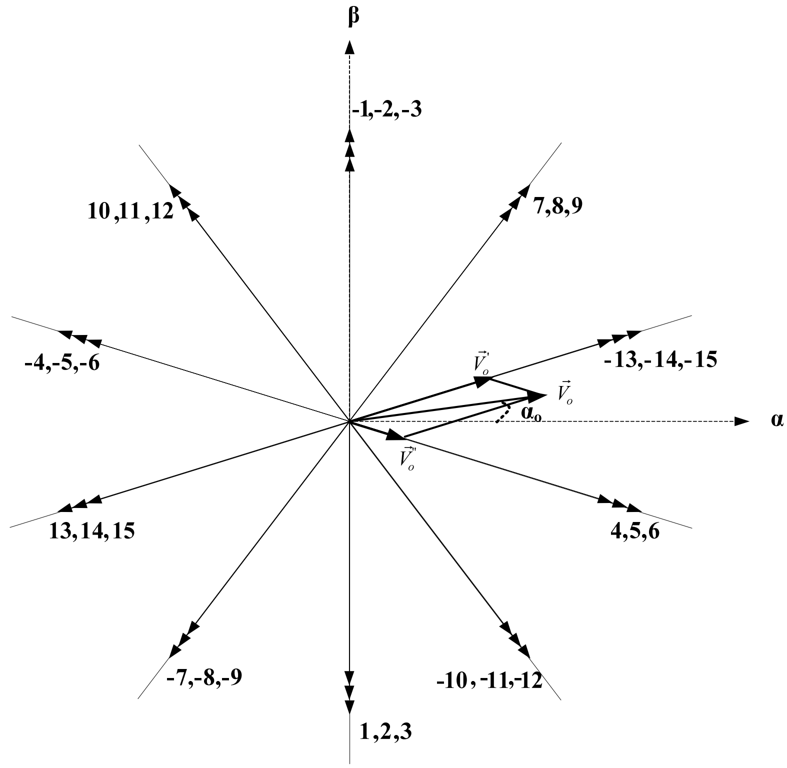

Fig. 5.8. Output small length voltage space vectors.

The small length space voltage vectors details are tabulated in Table 5.3. The table shows the output phases connected to the input phase, the relation between the output line voltages and output line voltages, the relation between the output line current and input line current, the output voltage and the position. e.g. column 3, row 1, the input phase 'a' is connected to the output phase 'A'. The output line voltage, V_{AB} is same as input line voltage V_{ab} but in opposite phase, the input current Ia is same as output line current I_A. The output voltage vector Vo is 0.2906 x Vab (input line voltage), the position of vector is -90̊, and the input current vector is 1.156*i_A and its position is -30̊. Note that

where $s = \frac{2}{5}\left[2\mathrm{Cos}54^0.2\mathrm{Cos}72^0\right] = 0.2906$.

Table 5.3. Small space voltage vectors.

Group	Name	A	B	C	D	E	V_{AB}	V_{BC}	V_{CD}	V_{DE}	V_{EA}	i_a	i_b	i_c	V_o	α_o	I_i	β_i
Small A	+1	b	b	a	b	a	0	$-V_{ab}$	V_{ab}	$-V_{ab}$	V_{ab}	i_A	$-i_A$	0	sV_{ab}	$-\frac{\pi}{2}$	$\frac{2}{\sqrt{3}}i_A$	$-\frac{\pi}{6}$
	-1	a	a	b	a	b	0	V_{ab}	$-V_{ab}$	V_{ab}	$-V_{ab}$	$-i_A$	i_A	0	$-sV_{ab}$	$-\frac{\pi}{2}$	$-\frac{2}{\sqrt{3}}i_A$	$-\frac{\pi}{6}$
	+2	c	c	b	c	b	0	$-V_{bc}$	V_{bc}	$-V_{bc}$	V_{bc}	0	i_A	$-i_A$	sV_{bc}	$-\frac{\pi}{2}$	$\frac{2}{\sqrt{3}}i_A$	$\frac{\pi}{2}$
	-2	b	b	c	b	c	0	V_{bc}	$-V_{bc}$	V_{bc}	$-V_{bc}$	0	$-i_A$	i_A	$-sV_{bc}$	$-\frac{\pi}{2}$	$-\frac{2}{\sqrt{3}}i_A$	$\frac{\pi}{2}$
	+3	a	a	c	a	c	0	$-V_{ca}$	V_{ca}	$-V_{ca}$	V_{ca}	$-i_A$	0	i_A	sV_{ca}	$-\frac{\pi}{2}$	$\frac{2}{\sqrt{3}}i_A$	$\frac{7\pi}{6}$
	-3	c	c	a	c	a	0	V_{ca}	$-V_{ca}$	V_{ca}	$-V_{ca}$	i_A	0	$-i_A$	$-sV_{ca}$	$-\frac{\pi}{2}$	$-\frac{2}{\sqrt{3}}i_A$	$\frac{7\pi}{6}$

Group	Name	A	B	C	D	E	V_{AB}	V_{BC}	V_{CD}	V_{DE}	V_{EA}	i_a	i_b	i_c	V_o	α_o	I_i	β_i
Small B	+4	a	b	b	a	b	V_{ab}	0	$-V_{ab}$	V_{ab}	$-V_{ab}$	i_B	$-i_B$	0	sV_{ab}	$-\frac{\pi}{10}$	$\frac{2}{\sqrt{3}}i_B$	$-\frac{\pi}{6}$
	-4	b	a	a	b	a	$-V_{ab}$	0	V_{ab}	$-V_{ab}$	V_{ab}	$-i_B$	i_B	0	$-sV_{ab}$	$-\frac{\pi}{10}$	$-\frac{2}{\sqrt{3}}i_B$	$-\frac{\pi}{6}$
	+5	b	c	c	b	c	V_{bc}	0	$-V_{bc}$	V_{bc}	$-V_{bc}$	0	i_B	$-i_B$	sV_{bc}	$-\frac{\pi}{10}$	$\frac{2}{\sqrt{3}}i_B$	$\frac{\pi}{2}$
	-5	c	b	b	c	b	$-V_{bc}$	0	V_{bc}	$-V_{bc}$	V_{bc}	0	$-i_B$	i_B	$-sV_{bc}$	$-\frac{\pi}{10}$	$-\frac{2}{\sqrt{3}}i_B$	$\frac{\pi}{2}$
	+6	c	a	a	c	a	V_{ca}	0	$-V_{ca}$	V_{ca}	$-V_{ca}$	$-i_B$	0	i_B	sV_{ca}	$-\frac{\pi}{10}$	$\frac{2}{\sqrt{3}}i_B$	$\frac{7\pi}{6}$
	-6	a	c	c	a	c	$-V_{ca}$	0	V_{ca}	$-V_{ca}$	V_{ca}	i_B	0	$-i_B$	$-sV_{ca}$	$-\frac{\pi}{10}$	$-\frac{2}{\sqrt{3}}i_B$	$\frac{7\pi}{6}$

Group	Name	A	B	C	D	E	V_{AB}	V_{BC}	V_{CD}	V_{DE}	V_{EA}	i_a	i_b	i_c	V_o	α_o	I_i	β_i
Small C	+7	b	a	b	b	a	$-V_{ab}$	V_{ab}	0	$-V_{ab}$	V_{ab}	i_C	$-i_C$	0	sV_{ab}	$\frac{3\pi}{10}$	$\frac{2}{\sqrt{3}}i_C$	$-\frac{\pi}{6}$
	-7	a	b	a	a	b	V_{ab}	$-V_{ab}$	0	V_{ab}	$-V_{ab}$	$-i_C$	i_C	0	$-sV_{ab}$	$\frac{3\pi}{10}$	$-\frac{2}{\sqrt{3}}i_C$	$-\frac{\pi}{6}$
	+8	c	b	c	c	b	$-V_{bc}$	V_{bc}	0	$-V_{bc}$	V_{bc}	0	i_C	$-i_C$	sV_{bc}	$\frac{3\pi}{10}$	$\frac{2}{\sqrt{3}}i_C$	$\frac{\pi}{2}$
	-8	b	c	b	b	c	V_{bc}	$-V_{bc}$	0	V_{bc}	$-V_{bc}$	0	$-i_C$	i_C	$-sV_{bc}$	$\frac{3\pi}{10}$	$-\frac{2}{\sqrt{3}}i_C$	$\frac{\pi}{2}$
	+9	a	c	a	a	c	$-V_{ca}$	V_{ca}	0	$-V_{ca}$	V_{ca}	$-i_C$	0	i_C	sV_{ca}	$\frac{3\pi}{10}$	$\frac{2}{\sqrt{3}}i_C$	$\frac{7\pi}{6}$
	-9	c	a	c	c	a	V_{ca}	$-V_{ca}$	0	V_{ca}	$-V_{ca}$	i_C	0	$-i_C$	$-sV_{ca}$	$\frac{3\pi}{10}$	$-\frac{2}{\sqrt{3}}i_C$	$\frac{7\pi}{6}$

Group	Name	A	B	C	D	E	V_{AB}	V_{BC}	V_{CD}	V_{DE}	V_{EA}	i_a	i_b	i_c	V_o	α_o	I_i	β_i
Small D	+10	a	b	a	b	b	V_{ab}	$-V_{ab}$	V_{ab}	0	$-V_{ab}$	i_D	$-i_D$	0	sV_{ab}	$\frac{7\pi}{10}$	$\frac{2}{\sqrt{3}}i_D$	$-\frac{\pi}{6}$
	-10	b	a	b	a	a	$-V_{ab}$	V_{ab}	$-V_{ab}$	0	V_{ab}	$-i_D$	i_D	0	$-sV_{ab}$	$\frac{7\pi}{10}$	$-\frac{2}{\sqrt{3}}i_D$	$-\frac{\pi}{6}$
	+11	b	c	b	c	c	V_{bc}	$-V_{bc}$	V_{bc}	0	$-V_{bc}$	0	i_D	$-i_D$	sV_{bc}	$\frac{7\pi}{10}$	$\frac{2}{\sqrt{3}}i_D$	$\frac{\pi}{2}$
	-11	c	b	c	b	b	$-V_{bc}$	V_{bc}	$-V_{bc}$	0	V_{bc}	0	$-i_D$	i_D	$-sV_{bc}$	$\frac{7\pi}{10}$	$-\frac{2}{\sqrt{3}}i_D$	$\frac{\pi}{2}$
	+12	c	a	c	a	a	V_{ca}	$-V_{ca}$	V_{ca}	0	$-V_{ca}$	$-i_D$	0	i_D	sV_{ca}	$\frac{7\pi}{10}$	$\frac{2}{\sqrt{3}}i_D$	$\frac{7\pi}{6}$
	-12	a	c	a	c	c	$-V_{ca}$	V_{ca}	$-V_{ca}$	0	V_{ca}	i_D	0	$-i_D$	$-sV_{ca}$	$\frac{7\pi}{10}$	$-\frac{2}{\sqrt{3}}i_D$	$\frac{7\pi}{6}$

Group	Name	A	B	C	D	E	V_{AB}	V_{BC}	V_{CD}	V_{DE}	V_{EA}	i_a	i_b	i_c	V_o	α_o	I_i	β_i
Small E	+13	b	a	b	a	b	$-V_{ab}$	V_{ab}	$-V_{ab}$	V_{ab}	0	i_E	$-i_E$	0	sV_{ab}	$\frac{11\pi}{10}$	$\frac{2}{\sqrt{3}}i_E$	$-\frac{\pi}{6}$
	-13	a	b	a	b	a	V_{ab}	$-V_{ab}$	V_{ab}	$-V_{ab}$	0	$-i_E$	i_E	0	$-sV_{ab}$	$\frac{11\pi}{10}$	$-\frac{2}{\sqrt{3}}i_E$	$-\frac{\pi}{6}$
	+14	c	b	c	b	c	$-V_{bc}$	V_{bc}	$-V_{bc}$	V_{bc}	0	0	i_E	$-i_E$	sV_{bc}	$\frac{11\pi}{10}$	$\frac{2}{\sqrt{3}}i_E$	$\frac{\pi}{2}$
	-14	b	c	b	c	b	V_{bc}	$-V_{bc}$	V_{bc}	$-V_{bc}$	0	0	$-i_E$	i_E	$-sV_{bc}$	$\frac{11\pi}{10}$	$-\frac{2}{\sqrt{3}}i_E$	$\frac{\pi}{2}$
	+15	a	c	a	c	a	$-V_{ca}$	V_{ca}	$-V_{ca}$	V_{ca}	0	$-i_E$	0	i_E	sV_{ca}	$\frac{11\pi}{10}$	$\frac{2}{\sqrt{3}}i_E$	$\frac{7\pi}{6}$
	-15	c	a	c	a	c	V_{ca}	$-V_{ca}$	V_{ca}	$-V_{ca}$	0	i_E	0	$-i_E$	$-sV_{ca}$	$\frac{11\pi}{10}$	$-\frac{2}{\sqrt{3}}i_E$	$\frac{7\pi}{6}$

For each combination, the input and output line voltages can be expressed in terms of space vectors as;

$$\overrightarrow{V_{i\alpha\beta}} = \frac{2}{3}\left(V_{ab} + V_{bc}.e^{j\frac{2\pi}{3}} + V_{ca}.e^{j\frac{4\pi}{3}} \right) = V_{i}.e^{j\alpha_i} \tag{5.2}$$

$$\overrightarrow{V_{o\alpha\beta}} = \frac{2}{5}\left(V_{AB} + V_{BC}.e^{j\frac{2\pi}{5}} + V_{CD}.e^{j\frac{4\pi}{5}} + V_{DE}.e^{j\frac{6\pi}{5}} + V_{EA}.e^{j\frac{8\pi}{5}} \right) = V_{O}e^{j\alpha_O} \tag{5.3a}$$

$$\overrightarrow{V_{oxy}} = \frac{2}{5}\left(V_{AB} + V_{BC}.e^{j\frac{4\pi}{5}} + V_{CD}.e^{j\frac{8\pi}{5}} + V_{DE}.e^{j\frac{12\pi}{5}} + V_{EA}.e^{j\frac{16\pi}{5}} \right) = V_{O}e^{j\alpha_O} \tag{5.3b}$$

In the same way, the input and output line currents result is as follows:

$$\overrightarrow{I_i} = \frac{2}{3}\left(I_a + I_b.e^{j\frac{2\pi}{3}} + I_c.e^{j\frac{4\pi}{3}} \right) = I_{i}.e^{j\beta_i} \tag{5.4}$$

$$\overrightarrow{I_o} = \frac{2}{5}\left(I_A + I_B.e^{j\frac{2\pi}{5}} + I_C.e^{j\frac{4\pi}{5}} + I_D.e^{j\frac{6\pi}{5}} + I_E.e^{j\frac{8\pi}{5}} \right) = I_{O}.e^{j\beta_O} \tag{5.5}$$

5.3 Space Vector Model of Three-phase to Six-phase Direct Matrix Converter

The space vector algorithm is based on the representation of the three phase input current and five-phase output line voltages on the space vector plane. In Matrix Converters output phase is connected to each input phase depending on the state of the switches. For a three to six-phase Matrix Converter, total numbers of switches are eighteen. The circuit topology is shown in Fig. 5.9.

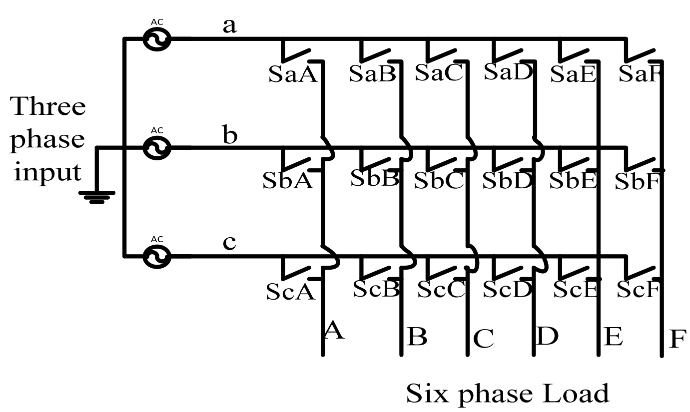

Fig. 5.9. Three-six phase direct Matrix Converter.

With this number of switches a total combination of switching can be made in the range of 2^{12}= 4096. For the safe switching in the Matrix Converter:

- Input phases should never be short circuited,
- Output phases should never be open circuited, at any switching time.

Considering the above two rules, there are 3^6 i.e. 729 different switching combinations for connecting output phases to input phases. These switching combinations can be analysed in five groups.

The switching combinations are represented as: There are six switches and each switch is free to connect any of the three phases of input. In this way there are 3*6=18 possible connections. Every switch can have two states on (1) or off (0). In this way there are 2^{18} switching combinations. Considering the constraints "that any two input cannot be shorted and output phase cannot be opened throughout the operation" switching combination reduces to 3^6=729 only.

These 729 switching combinations are analysed in seven groups that shows how many output phases are connected from input phase a, b, c. It is represented as [x, y, z] where x, y and z are no of output phases connected to input phase a, b and c.

Group-1: [6,0,0]:- In this group all the output phases are connected to the same input phase. Following it there are three possible combinations that are either all are connected to input phase a or b or c. [6,0,0], [0,6,0],[0,0,6] there are 3 possible switching.

Group-2: [5,0,1]:- In this group 5 output phases are connected to the same input phase and remaining phase is connected to any of the remaining input phases. Thus there are ${}^6C_5$ (5 out of 6 output phases are connected to same input) and ${}^1C_1$ (remaining one output from any one input) (6!/5!*1!)=6 combinations. In this way [5,0,1], [5, 1,0], [0,5,1], [1,5, 0], [0,1,5], [1,0,5]. (6!/5!*1!)=6 combinations for every state combining all total 6*6=36 switching combinations

Group-3: In this group four of the output phases are connected to one of the three input phase simultaneously. Two remaining output phases are connected to one input phase and one input phase not connected. All the possible sub groups are [4,0,2],[4,2,0],[0,4,2],[2,4, 0],[0,2,4] and [2,0,4]. Hence the following combinational logic can be used to obtain the possible number of switching and hence number of space voltage vectors:

${}^{6}C_4 *{}^{2}C_2$ =(6!/4!*2!) * (2!/2!*0!) =15*6=90.

Group-4: In this group three of the output phases are connected to one of the three input phase simultaneously. Three remaining output phases are connected to one input phase and one input phase is not connected. All the possible sub groups are [3,3,0], [3,0,3] and [0,3,3]. Hence the following combinational logic can be used to obtain the possible number of switching and hence number of space voltage vectors:
${}^{6}C_3 *{}^{3}C_3$ =(6!/3!*3!) * (3!/1!*3!)=20*3=60.

Group-5: In this group four of the output phases are connected to one of the three input phase simultaneously. One output phase are connected to one input phase and the last remaining input phase is connected to one output phase. All the possible sub groups are [4,1,1], [1,4,1] and [1,1,4]. Hence the following combinational logic can be used to obtain the possible number of switching and hence number of space voltage vectors:
${}^{6}C_4 *{}^{2}C_1 *{}^{1}C_1$ =(6!/4!*2!) * (2!/1!*1!)=15*2*3=90

Group-6. In this group three of the output phases are connected to one of the three input phase simultaneously. Two of the remaining output phases are connected to one input phase and one input phase is connected to one output phase. All the possible sub groups are [3,1,2], [3,2,1], [1,3,2], [1,3,2], [2,1,3], and [1,2,3]. Hence, the following combinational logic can be used to obtain the possible number of switching and hence number of space voltage vectors:
${}^{6}C_3 *{}^{3}C_2 *{}^{1}C_1$ =(6!/3!*3!) * (3!/2!*1!) =30*3 *6=360

Group-7: In this group two of the output phases are connected to one of the three input phase simultaneously. Two of the output phases are connected to one input phase and one input phase is connected to the remaining two output phase. The group can be mentioned as [2,2,2]. Hence the following combinational logic can be used to obtain the possible number of switching and hence number of space voltage vectors:
${}^{6}C_2 *{}^{4}C_2 *{}^{2}C_2$ =(6!/2!*4!) * (4!/2!*2!) =15*6*1 =90.

Thus total switching vectors are given as:

Group 1 :{ 6, 0, 0} consists of 3 vectors,
Group 2 :{ 5, 1, 0} consists of 36 vectors,

Group 3 :{ 4, 2, 0} consists of 90 vectors.
Group 4 :{ 3,3, 0} consists of 60 vectors.
Group 5 :{ 4, 1, 1} consists of 90 vectors,
Group 6 :{ 3, 2, 1} consists of 360 vectors.
Group 7 :{ 2, 2, 2} consists of 90 vectors.

In this way there are total= 3+36+90+60+90+360+90=729 switching combinations in which the space voltage vectors produced from switching of Groups-1,2, and 3 are having varying amplitude and fixed frequency. Such switching combinations are 3+36+90+60=189 which is used as active switching. Remaining are having varying amplitude and frequency both so they are not helpful to find out the output voltage. These 189 switching states to find out voltage is given in table 5.4. The Table 5.4 shows the output line voltage of the Matrix Converter having lowest phase difference from reference one that is $V_{AB.}$

The obtained output line voltages from switching combinations can be used to find out voltages and currents in *d-q* and *x-y* planes by using decoupling transformation matrix as given the equations (5.6) to (5.9:

$$V_{dq} = \frac{2}{6}(V_{AB} + aV_{BC} + a^2V_{CD} + a^3V_{DE} + a^4V_{EF} + a^5V_{FA}) \tag{5.6}$$

$$V_{x1y1} = \frac{2}{6}(V_{AB} + a^2V_{BC} + a^4V_{CD} + a^6V_{DE} + a^8V_{EF} + a^{10}V_{FA}) \tag{5.7}$$

$$V_{0+0-} = \frac{2}{6}(V_{AB} + a^3V_{BC} + a^6V_{CD} + a^9V_{DE} + a^{12}V_{EF} + a^{15}V_{FA}) \tag{5.8}$$

$$a = e^{j2pi/6} \tag{5.9}$$

Table 5.4. Three to Six phase output voltage and input current.

Vec	A	B	C	D	E	F	V_{AB}	V_{BC}	V_{CD}	V_{DE}	V_{EF}	V_{FA}	V_{dq}	α	Vxy	B	Ii	$α_i$
0	a	a	a	a	a	a	0	0	0	0	0	0	0	0	0	0	0	0
0	b	b	b	b	b	b	0	0	0	0	0	0	0	0	0	0	0	0
0	c	c	c	c	c	c	0	0	0	0	0	0	0	0	0	0	0	0
1	a	b	a	a	b	a	1	-1	0	1	-1	0	0 V_{ab}	0	1.1546	-30	0	0
2	a	a	b	a	a	b	0	1	-1	0	1	-1	0V_{ab}	180	1.1546	90	0	0
3	c	c	b	c	c	b	0	-1	1	0	-1	1	0 V_{bc}	0	1.1546	-90	0	90
4	c	b	c	c	b	c	-1	1	0	-1	1	0	0 V_{bc}	-180	1.1546	150	0	90
5	c	a	c	c	a	c	1	-1	0	1	-1	0	0 V_{ca}	0	1.1546	-30	0	30
6	c	c	a	c	c	a	0	1	-1	0	1	-1	0 V_{ca}	180	1.1546	90	0	30
7	b	b	a	b	b	a	0	-1	1	0	-1	1	0 V_{ab}	0	1.1546	-90	0	-30
8	b	a	b	b	a	b	-1	1	0	-1	1	0	0 V_{ab}	-180	1.1546	150	0	-30
9	c	b	b	c	b	b	-1	0	1	-1	0	1	0 V_{bc}	0	1.1546	-150	0	-90
10	b	c	c	b	c	c	1	0	-1	1	0	-1	0 V_{bc}	180	1.1546	30	0	90
11	a	a	c	a	a	c	0	-1	1	0	-1	1	0 V_{ca}	0	1.1546	-90	0	-150
12	c	a	a	c	a	a	1	0	-1	1	0	-1	0 V_{ca}	180	1.1546	30	0	-150
13	b	a	a	b	a	a	-1	0	1	-1	0	1	0 V_{ab}	0	1.1546	-150	0	150
14	a	b	b	a	b	b	1	0	-1	1	0	-1	0V_{ab}	180	1.1546	30	0	-30
15	b	c	b	b	c	b	1	-1	0	1	-1	0	0 V_{bc}	0	1.1546	-30	0	-90

16	**b**	**b**	**c**	**b**	**b**	**c**	**0**	**1**	**-1**	**0**	**1**	**-1**	0 V_{bc}	180	1.1546	90	0	-90
17	**a**	**c**	**c**	**a**	**c**	**c**	**-1**	**0**	**1**	**-1**	**0**	**1**	0 V_{ca}	0	1.1546	-150	0	30
18	**a**	**c**	**a**	**a**	**c**	**a**	**-1**	**1**	**0**	**-1**	**1**	**0**	0 V_{ca}	-180	1.1546	150	0	-150
19	**b**	**a**	**b**	**a**	**b**	**a**	**-1**	**1**	**-1**	**1**	**-1**	**1**	0 V_{ab}	-11.3	0	-86.4	0	150
20	**a**	**b**	**a**	**b**	**a**	**b**	**1**	**-1**	**1**	**-1**	**1**	**-1**	0V_{ab}	168.7	0	93.58	0	-30
21	**c**	**b**	**c**	**b**	**c**	**b**	**-1**	**1**	**-1**	**1**	**-1**	**1**	0 V_{bc}	-11.3	0	-86.4	0	-90
22	**b**	**c**	**b**	**c**	**b**	**c**	**1**	**-1**	**1**	**-1**	**1**	**-1**	0 V_{bc}	168.7	0	93.58	0	90
23	**a**	**c**	**a**	**c**	**a**	**c**	**-1**	**1**	**-1**	**1**	**-1**	**1**	0 V_{ca}	-11.3	0	-86.4	0	30
24	**c**	**a**	**c**	**a**	**c**	**a**	**1**	**-1**	**1**	**-1**	**1**	**-1**	0 V_{ca}	168.7	0	93.58	0	-150
25	**a**	**a**	**b**	**a**	**a**	**a**	**0**	**1**	**-1**	**0**	**0**	**0**	0.33V_{ab}	0	0.5773	90	1.155	150
26	**a**	**b**	**a**	**b**	**a**	**a**	**1**	**-1**	**1**	**-1**	**0**	**0**	0.33V_{ab}	0	0.5773	-90	1.155	150
27	**a**	**b**	**b**	**a**	**b**	**a**	**1**	**0**	**-1**	**1**	**-1**	**0**	0.33V_{ab}	0	0.9999	0	1.155	-30
28	**a**	**b**	**b**	**b**	**a**	**b**	**1**	**0**	**0**	**-1**	**1**	**-1**	0.33V_{ab}	0	0.5773	90	1.155	-30
29	**a**	**a**	**a**	**b**	**a**	**A**	**0**	**0**	**1**	**-1**	**0**	**0**	0.33 V_{ab}	60	0.5773	-150	1.155	150
30	**a**	**a**	**b**	**a**	**b**	**a**	**0**	**1**	**-1**	**1**	**-1**	**0**	0.33 V_{ab}	60	0.5773	30	1.155	150
31	**a**	**b**	**a**	**b**	**b**	**a**	**1**	**-1**	**1**	**0**	**-1**	**0**	0.33 V_{ab}	60	0.9999	-60	1.155	-30
32	**a**	**a**	**b**	**b**	**a**	**b**	**0**	**1**	**0**	**-1**	**1**	**-1**	0.33V_{ab}	60	0.9999	120	1.155	-30
33	**a**	**b**	**b**	**b**	**b**	**b**	**1**	**0**	**0**	**0**	**0**	**-1**	0.33V_{ab}	60	0.5773	30	1.155	-30
34	**a**	**a**	**a**	**a**	**b**	**A**	**0**	**0**	**0**	**1**	**-1**	**0**	0.33V_{ab}	120	0.5773	-30	1.155	150
35	**a**	**a**	**b**	**a**	**b**	**b**	**0**	**1**	**-1**	**1**	**0**	**-1**	0.33V_{ab}	120	0.9999	60	1.155	-30
36	**a**	**b**	**a**	**b**	**b**	**b**	**1**	**-1**	**1**	**0**	**0**	**-1**	0.33V_{ab}	120	0.5773	-30	1.155	-30
37	**a**	**a**	**a**	**b**	**a**	**b**	**0**	**0**	**1**	**-1**	**1**	**-1**	0.33V_{ab}	120	0.5773	150	1.155	150
38	**a**	**a**	**a**	**a**	**a**	**B**	**0**	**0**	**0**	**0**	**1**	**-1**	0.33V_{ab}	180	0.5773	90	1.155	150
39	**a**	**b**	**a**	**a**	**b**	**b**	**1**	**-1**	**0**	**1**	**0**	**-1**	0.33V_{ab}	180	0.9999	0	1.155	-30
40	**a**	**b**	**a**	**a**	**a**	**b**	**1**	**-1**	**0**	**0**	**1**	**-1**	0.33V_{ab}	-120	0.5773	30	1.155	150
41	**a**	**b**	**a**	**a**	**a**	**a**	**1**	**-1**	**0**	**0**	**0**	**0**	0.33V_{ab}	-60	0.5773	-30	1.155	150
42	**a**	**b**	**b**	**a**	**a**	**b**	**1**	**0**	**-1**	**0**	**1**	**-1**	0.33V_{ab}	-60	0.9999	60	1.155	-30
43	**a**	**a**	**a**	**a**	**a**	**c**	**0**	**0**	**0**	**0**	**-1**	**1**	0.33V_{ca}	0	0.5773	-90	1.155	-150
44	**a**	**a**	**a**	**a**	**c**	**a**	**0**	**0**	**0**	**-1**	**1**	**0**	0.33V_{ca}	-60	0.5773	150	1.155	-150
45	**a**	**a**	**a**	**c**	**a**	**a**	**0**	**0**	**-1**	**1**	**0**	**0**	0.33V_{ca}	-120	0.5773	30	1.155	-150
46	**a**	**a**	**c**	**a**	**a**	**a**	**0**	**-1**	**1**	**0**	**0**	**0**	0.33V_{ca}	-180	0.5773	-90	1.155	-150
47	**a**	**c**	**a**	**a**	**a**	**a**	**-1**	**1**	**0**	**0**	**0**	**0**	0.33V_{ca}	120	0.5773	150	1.155	-150
48	**a**	**a**	**a**	**c**	**a**	**c**	**0**	**0**	**-1**	**1**	**-1**	**1**	0.33V_{ca}	-60	0.5773	-30	1.155	-150
49	**a**	**c**	**a**	**a**	**a**	**c**	**-1**	**1**	**0**	**0**	**-1**	**1**	0.33V_{ca}	60	0.5773	-150	1.155	-150
50	**a**	**a**	**c**	**a**	**c**	**a**	**0**	**-1**	**1**	**-1**	**1**	**0**	0.33V_{ca}	-120	0.5773	-150	1.155	-150
51	**a**	**c**	**a**	**c**	**a**	**a**	**-1**	**1**	**-1**	**1**	**0**	**0**	0.33V_{ca}	-180	0.5773	90	1.155	-150
52	**a**	**a**	**c**	**a**	**c**	**c**	**0**	**-1**	**1**	**-1**	**0**	**1**	0.33V_{ca}	-60	0.9999	-120	1.155	30
53	**a**	**c**	**a**	**a**	**c**	**c**	**-1**	**1**	**0**	**-1**	**0**	**1**	0.33V_{ca}	0	0.9999	-180	1.155	30
54	**a**	**c**	**a**	**c**	**c**	**a**	**-1**	**1**	**-1**	**0**	**1**	**0**	0.33V_{ca}	-120	0.9999	120	1.155	30
55	**a**	**a**	**c**	**c**	**a**	**c**	**0**	**-1**	**0**	**1**	**-1**	**1**	0.33V_{ca}	-120	0.9999	-60	1.155	30
56	**a**	**c**	**c**	**a**	**a**	**c**	**-1**	**0**	**1**	**0**	**-1**	**1**	0.33V_{ca}	120	0.9999	-120	1.155	30
57	**a**	**c**	**c**	**a**	**c**	**a**	**-1**	**0**	**1**	**-1**	**1**	**0**	0.33V_{ca}	-180	0.9999	-180	1.155	30
58	**a**	**c**	**a**	**c**	**c**	**c**	**-1**	**1**	**-1**	**0**	**0**	**1**	0.33V_{ca}	-60	0.5773	150	1.155	30
59	**a**	**c**	**c**	**c**	**a**	**c**	**-1**	**0**	**0**	**1**	**-1**	**1**	0.33V_{ca}	-180	0.5773	-90	1.155	30
60	**a**	**c**	**c**	**c**	**c**	**c**	**-1**	**0**	**0**	**0**	**0**	**1**	0.33V_{ca}	-120	0.5773	-150	1.155	30
61	**b**	**b**	**b**	**b**	**b**	**c**	**0**	**0**	**0**	**0**	**1**	**-1**	0.33V_{bc}	180	0.5773	90	1.155	-90
62	**b**	**b**	**b**	**b**	**c**	**b**	**0**	**0**	**0**	**1**	**-1**	**0**	0.33V_{bc}	120	0.5773	-30	1.155	-90
63	**b**	**b**	**b**	**c**	**b**	**b**	**0**	**0**	**1**	**-1**	**0**	**0**	0.33V_{bc}	60	0.5773	-150	1.155	-90
64	**b**	**b**	**c**	**b**	**b**	**b**	**0**	**1**	**-1**	**0**	**0**	**0**	0.33V_{bc}	0	0.5773	90	1.155	-90
65	**b**	**c**	**b**	**b**	**b**	**b**	**1**	**-1**	**0**	**0**	**0**	**0**	0.33V_{bc}	-60	0.5773	-30	1.155	-90
66	**b**	**b**	**b**	**c**	**b**	**c**	**0**	**0**	**1**	**-1**	**1**	**-1**	0.33V_{bc}	120	0.5773	150	1.155	-90
67	**b**	**c**	**b**	**b**	**b**	**c**	**1**	**-1**	**0**	**0**	**1**	**-1**	0.33V_{bc}	-120	0.5773	30	1.155	-90
68	**b**	**b**	**c**	**b**	**c**	**b**	**0**	**1**	**-1**	**1**	**-1**	**0**	0.33V_{bc}	60	0.5773	30	1.155	-90
69	**b**	**c**	**b**	**c**	**b**	**b**	**1**	**-1**	**1**	**-1**	**0**	**0**	0.33V_{bc}	0	0.5773	-90	1.155	-90
70	**b**	**b**	**c**	**b**	**c**	**c**	**0**	**1**	**-1**	**1**	**0**	**-1**	0.33V_{bc}	120	0.9999	60	1.155	90
71	**b**	**c**	**b**	**b**	**c**	**c**	**1**	**-1**	**0**	**1**	**0**	**-1**	0.33V_{bc}	180	0.9999	0	1.155	90
72	**b**	**c**	**b**	**c**	**c**	**b**	**1**	**-1**	**1**	**0**	**-1**	**0**	0.33V_{bc}	60	0.9999	-60	1.155	90
73	**b**	**b**	**c**	**c**	**b**	**c**	**0**	**1**	**0**	**-1**	**1**	**-1**	0.33V_{bc}	60	0.9999	120	1.155	90

74	**b**	**c**	**c**	**b**	**b**	**c**	**1**	**0**	**-1**	**0**	**1**	**-1**	0.33V_{bc}	-60	0.9999	60	1.155	90
75	**b**	**c**	**c**	**b**	**c**	**b**	**1**	**0**	**-1**	**1**	**-1**	**0**	0.33V_{bc}	0	0.9999	0	1.155	90
76	**b**	**c**	**b**	**c**	**c**	**c**	**1**	**-1**	**1**	**0**	**0**	**-1**	0.33V_{bc}	120	0.5773	-30	1.155	90
77	**b**	**c**	**c**	**c**	**b**	**c**	**1**	**0**	**0**	**-1**	**1**	**-1**	0.33V_{bc}	0	0.5773	90	1.155	90
78	**b**	**c**	**c**	**c**	**c**	**c**	**1**	**0**	**0**	**0**	**0**	**-1**	0.33V_{bc}	60	0.5773	30	1.155	90
79	**b**	**b**	**b**	**b**	**b**	**a**	**0**	**0**	**0**	**0**	**-1**	**1**	0.33V_{ab}	0	0.5773	-90	1.155	-30
80	**b**	**b**	**b**	**b**	**a**	**b**	**0**	**0**	**0**	**-1**	**1**	**0**	0.33 V_{ab}	-60	0.5773	150	1.155	-30
81	**b**	**b**	**b**	**a**	**b**	**b**	**0**	**0**	**-1**	**1**	**0**	**0**	0.33 V_{ab}	-120	0.5773	30	1.155	-30
82	**b**	**b**	**a**	**b**	**b**	**b**	**0**	**-1**	**1**	**0**	**0**	**0**	0.33 V_{ab}	-180	0.5773	-90	1.155	-30
83	**b**	**a**	**b**	**b**	**b**	**b**	**-1**	**1**	**0**	**0**	**0**	**0**	0.33V_{ab}	120	0.5773	150	1.155	-30
84	**b**	**b**	**b**	**a**	**b**	**a**	**0**	**0**	**-1**	**1**	**-1**	**1**	0.33V_{ab}	-60	0.5773	-30	1.155	-30
85	**b**	**a**	**b**	**b**	**b**	**a**	**-1**	**1**	**0**	**0**	**-1**	**1**	0.33V_{ab}	60	0.5773	-150	1.155	-30
86	**b**	**b**	**a**	**b**	**a**	**b**	**0**	**-1**	**1**	**-1**	**1**	**0**	0.33V_{ab}	-120	0.5773	-150	1.155	-30
87	**b**	**a**	**b**	**a**	**b**	**b**	**-1**	**1**	**-1**	**1**	**0**	**0**	0.33V_{ab}	-180	0.5773	90	1.155	-30
88	**b**	**b**	**a**	**b**	**a**	**a**	**0**	**-1**	**1**	**-1**	**0**	**1**	0.33V_{ab}	-60	0.9999	-120	1.155	150
89	**b**	**a**	**b**	**b**	**a**	**a**	**-1**	**1**	**0**	**-1**	**0**	**1**	0.33V_{ab}	0	0.9999	-180	1.155	150
90	**b**	**a**	**b**	**a**	**a**	**b**	**-1**	**1**	**-1**	**0**	**1**	**0**	0.33V_{ab}	-120	0.9999	120	1.155	150
91	**b**	**b**	**a**	**a**	**b**	**a**	**0**	**-1**	**0**	**1**	**-1**	**1**	0.33 V_{ab}	-120	0.9999	-60	1.155	150
92	**b**	**a**	**a**	**b**	**b**	**a**	**-1**	**0**	**1**	**0**	**-1**	**1**	0.33V_{ab}	120	0.9999	-120	1.155	150
93	**b**	**a**	**a**	**b**	**a**	**b**	**-1**	**0**	**1**	**-1**	**1**	**0**	0.33V_{ab}	-180	0.9999	-180	1.155	150
94	**b**	**a**	**b**	**a**	**a**	**a**	**-1**	**1**	**-1**	**0**	**0**	**1**	0.33V_{ab}	-60	0.5773	150	1.155	150
95	**b**	**a**	**a**	**a**	**b**	**a**	**-1**	**0**	**0**	**1**	**-1**	**1**	0.33V_{ab}	-180	0.5773	-90	1.155	150
96	**b**	**a**	**a**	**a**	**a**	**a**	**-1**	**0**	**0**	**0**	**0**	**1**	0.33V_{ab}	-120	0.5773	-150	1.155	150
97	**c**	**c**	**c**	**c**	**c**	**a**	**0**	**0**	**0**	**0**	**1**	**-1**	0.33V_{ca}	180	0.5773	90	1.155	30
98	**c**	**c**	**c**	**c**	**a**	**c**	**0**	**0**	**0**	**1**	**-1**	**0**	0.33V_{ca}	120	0.5773	-30	1.155	30
99	**c**	**c**	**c**	**a**	**c**	**c**	**0**	**0**	**1**	**-1**	**0**	**0**	0.33V_{ca}	60	0.5773	-150	1.155	30
100	**c**	**c**	**a**	**c**	**c**	**c**	**0**	**1**	**-1**	**0**	**0**	**0**	0.33V_{ca}	0	0.5773	90	1.155	30
101	**c**	**a**	**c**	**c**	**c**	**c**	**1**	**-1**	**0**	**0**	**0**	**0**	0.33V_{ca}	-60	0.5773	-30	1.155	30
102	**c**	**c**	**c**	**a**	**c**	**a**	**0**	**0**	**1**	**-1**	**1**	**-1**	0.33V_{ca}	120	0.5773	150	1.155	30
103	**c**	**a**	**c**	**c**	**c**	**a**	**1**	**-1**	**0**	**0**	**1**	**-1**	0.33V_{ca}	-120	0.5773	30	1.155	30
104	**c**	**c**	**a**	**c**	**a**	**c**	**0**	**1**	**-1**	**1**	**-1**	**0**	0.33V_{ca}	60	0.5773	30	1.155	30
105	**c**	**a**	**c**	**a**	**c**	**c**	**1**	**-1**	**1**	**-1**	**0**	**0**	0.33V_{ca}	0	0.5773	-90	1.155	30
106	**c**	**c**	**a**	**c**	**a**	**a**	**0**	**1**	**-1**	**1**	**0**	**-1**	0.33V_{ca}	120	0.9999	60	1.155	-150
107	**c**	**a**	**c**	**c**	**a**	**a**	**1**	**-1**	**0**	**1**	**0**	**-1**	0.33V_{ca}	180	0.9999	0	1.155	-150
108	**c**	**a**	**c**	**a**	**a**	**c**	**1**	**-1**	**1**	**0**	**-1**	**0**	0.33V_{ca}	60	0.9999	-60	1.155	-150
109	**c**	**c**	**a**	**a**	**c**	**a**	**0**	**1**	**0**	**-1**	**1**	**-1**	0.33V_{ca}	60	0.9999	120	1.155	-150
110	**c**	**a**	**a**	**c**	**c**	**a**	**1**	**0**	**-1**	**0**	**1**	**-1**	0.33V_{ca}	-60	0.9999	60	1.155	-150
111	**c**	**a**	**a**	**c**	**a**	**c**	**1**	**0**	**-1**	**1**	**-1**	**0**	0.33V_{ca}	0	0.9999	0	1.155	-150
112	**c**	**a**	**c**	**a**	**a**	**a**	**1**	**-1**	**1**	**0**	**0**	**-1**	0.33V_{ca}	120	0.5773	-30	1.155	-150
113	**c**	**a**	**a**	**a**	**c**	**a**	**1**	**0**	**0**	**-1**	**1**	**-1**	0.33V_{ca}	0	0.5773	90	1.155	-150
114	**c**	**a**	**a**	**a**	**a**	**a**	**1**	**0**	**0**	**0**	**0**	**-1**	0.33V_{ca}	60	0.5773	30	1.155	-150
115	**c**	**c**	**c**	**c**	**c**	**b**	**0**	**0**	**0**	**0**	**-1**	**1**	0.33V_{bc}	0	0.5773	-90	1.155	90
116	**c**	**c**	**c**	**c**	**b**	**c**	**0**	**0**	**0**	**-1**	**1**	**0**	0.33V_{bc}	-60	0.5773	150	1.155	90
117	**c**	**c**	**c**	**b**	**c**	**c**	**0**	**0**	**-1**	**1**	**0**	**0**	0.33V_{bc}	-120	0.5773	30	1.155	90
118	**c**	**c**	**b**	**c**	**c**	**c**	**0**	**-1**	**1**	**0**	**0**	**0**	0.33V_{bc}	-180	0.5773	-90	1.155	90
119	**c**	**b**	**c**	**c**	**c**	**c**	**-1**	**1**	**0**	**0**	**0**	**0**	0.33V_{bc}	120	0.5773	150	1.155	90
120	**c**	**c**	**c**	**b**	**c**	**b**	**0**	**0**	**-1**	**1**	**-1**	**1**	0.33V_{bc}	-60	0.5773	-30	1.155	90
121	**c**	**b**	**c**	**c**	**c**	**b**	**-1**	**1**	**0**	**0**	**-1**	**1**	0.33V_{bc}	60	0.5773	-150	1.155	90
122	**c**	**c**	**b**	**c**	**b**	**c**	**0**	**-1**	**1**	**-1**	**1**	**0**	0.33V_{bc}	-120	0.5773	-150	1.155	90
123	**c**	**b**	**c**	**b**	**c**	**c**	**-1**	**1**	**-1**	**1**	**0**	**0**	0.33V_{bc}	-180	0.5773	90	1.155	90
124	**c**	**c**	**b**	**c**	**b**	**b**	**0**	**-1**	**1**	**-1**	**0**	**1**	0.33V_{bc}	-60	0.9999	-120	1.155	-90
125	**c**	**b**	**c**	**c**	**b**	**b**	**-1**	**1**	**0**	**-1**	**0**	**1**	0.33V_{bc}	0	0.9999	-180	1.155	-90
126	**c**	**b**	**c**	**b**	**b**	**c**	**-1**	**1**	**-1**	**0**	**1**	**0**	0.33V_{bc}	-120	0.9999	120	1.155	-90
127	**c**	**c**	**b**	**b**	**c**	**b**	**0**	**-1**	**0**	**1**	**-1**	**1**	0.33V_{bc}	-120	0.9999	-60	1.155	-90
128	**c**	**b**	**b**	**c**	**c**	**b**	**-1**	**0**	**1**	**0**	**-1**	**1**	0.33V_{bc}	120	0.9999	-120	1.155	-90
129	**c**	**b**	**b**	**c**	**b**	**c**	**-1**	**0**	**1**	**-1**	**1**	**0**	0.33V_{bc}	-180	0.9999	-180	1.155	-90
130	**c**	**b**	**c**	**b**	**b**	**b**	**-1**	**1**	**-1**	**0**	**0**	**1**	0.33V_{bc}	-60	0.5773	150	1.155	-90
131	**c**	**b**	**b**	**b**	**c**	**b**	**-1**	**0**	**0**	**1**	**-1**	**1**	0.33V_{bc}	-180	0.5773	-90	1.155	-90
132	**c**	**b**	**b**	**b**	**b**	**b**	**-1**	**0**	**0**	**0**	**0**	**1**	0.33V_{bc}	-120	0.5773	-150	1.155	-90

133	**c**	**c**	**c**	**c**	**b**	**b**	**0**	**0**	**0**	**-1**	**0**	**1**	0.5773 V_{bc}	-30	0.5773	-150	2	90
134	**c**	**c**	**c**	**b**	**b**	**c**	**0**	**0**	**-1**	**0**	**1**	**0**	0.5773 V_{bc}	-90	0.5773	90	2	90
135	**c**	**c**	**b**	**b**	**c**	**c**	**0**	**-1**	**0**	**1**	**0**	**0**	0.5773 V_{bc}	-150	0.5773	-30	2	90
136	**c**	**b**	**b**	**c**	**c**	**c**	**-1**	**0**	**1**	**0**	**0**	**0**	0.5773 V_{bc}	150	0.5773	-150	2	90
137	**c**	**c**	**b**	**b**	**b**	**b**	**0**	**-1**	**0**	**0**	**0**	**1**	0.5773 V_{bc}	-90	0.5773	-90	2	-90
138	**c**	**b**	**b**	**b**	**b**	**c**	**-1**	**0**	**0**	**0**	**1**	**0**	0.5773 V_{bc}	-150	0.5773	150	2	-90
139	**b**	**b**	**a**	**a**	**a**	**a**	**0**	**-1**	**0**	**0**	**0**	**1**	0.5773 V_{ab}	-90	0.5773	-90	2	150
140	**b**	**a**	**a**	**a**	**a**	**b**	**-1**	**0**	**0**	**0**	**1**	**0**	0.5773 V_{ab}	-150	0.5773	150	2	150
141	**c**	**c**	**c**	**c**	**a**	**a**	**0**	**0**	**0**	**1**	**0**	**-1**	0.5773 V_{ca}	150	0.5773	30	2	30
142	**c**	**c**	**c**	**a**	**a**	**c**	**0**	**0**	**1**	**0**	**-1**	**0**	0.5773 V_{ca}	90	0.5773	-90	2	30
143	**c**	**c**	**a**	**a**	**c**	**c**	**0**	**1**	**0**	**-1**	**0**	**0**	0.5773 V_{ca}	30	0.5773	150	2	30
144	**c**	**a**	**a**	**c**	**c**	**c**	**1**	**0**	**-1**	**0**	**0**	**0**	0.5773 V_{ca}	-30	0.5773	30	2	30
145	**c**	**c**	**a**	**a**	**a**	**a**	**0**	**1**	**0**	**0**	**0**	**-1**	0.5773 V_{ca}	90	0.5773	90	2	-150
146	**c**	**a**	**a**	**a**	**a**	**c**	**1**	**0**	**0**	**0**	**-1**	**0**	0.5773 V_{ca}	30	0.5773	-30	2	-150
147	**b**	**b**	**b**	**b**	**a**	**a**	**0**	**0**	**0**	**-1**	**0**	**1**	0.5773 V_{ab}	-30	0.5773	-150	2	-30
148	**b**	**b**	**b**	**a**	**a**	**b**	**0**	**0**	**-1**	**0**	**1**	**0**	0.5773 V_{ab}	-90	0.5773	90	2	-30
149	**b**	**b**	**a**	**a**	**b**	**b**	**0**	**-1**	**0**	**1**	**0**	**0**	0.5773 V_{ab}	-150	0.5773	-30	2	-30
150	**b**	**a**	**a**	**b**	**b**	**b**	**-1**	**0**	**1**	**0**	**0**	**0**	0.5773 V_{ab}	150	0.5773	-150	2	-30
151	**b**	**b**	**c**	**c**	**c**	**c**	**0**	**1**	**0**	**0**	**0**	**-1**	0.5773 V_{bc}	90	0.5773	90	2	90
152	**b**	**c**	**c**	**c**	**c**	**b**	**1**	**0**	**0**	**0**	**-1**	**0**	0.5773 V_{bc}	30	0.5773	-30	2	90
153	**a**	**a**	**c**	**c**	**c**	**c**	**0**	**-1**	**0**	**0**	**0**	**1**	0.5773 V_{ca}	-90	0.5773	-90	2	30
154	**a**	**c**	**c**	**c**	**c**	**a**	**-1**	**0**	**0**	**0**	**1**	**0**	0.5773 V_{ca}	-150	0.5773	150	2	30
155	**b**	**b**	**b**	**b**	**c**	**c**	**0**	**0**	**0**	**1**	**0**	**-1**	0.5773 V_{bc}	150	0.5773	30	2	-90
156	**b**	**b**	**b**	**c**	**c**	**b**	**0**	**0**	**1**	**0**	**-1**	**0**	0.5773 V_{bc}	90	0.5773	-90	2	-90
157	**b**	**b**	**c**	**c**	**b**	**b**	**0**	**1**	**0**	**-1**	**0**	**0**	0.5773 V_{bc}	30	0.5773	150	2	-90
158	**b**	**c**	**c**	**b**	**b**	**b**	**1**	**0**	**-1**	**0**	**0**	**0**	0.5773 V_{bc}	-30	0.5773	30	2	-90
159	**a**	**a**	**a**	**a**	**c**	**c**	**0**	**0**	**0**	**-1**	**0**	**1**	0.5773 V_{ca}	-30	0.5773	-150	2	-150
160	**a**	**a**	**a**	**a**	**b**	**b**	**0**	**0**	**0**	**1**	**0**	**-1**	0.5773 V_{ab}	150	0.5773	30	2	150
161	**a**	**a**	**a**	**b**	**b**	**a**	**0**	**0**	**1**	**0**	**-1**	**0**	0.5773 V_{ab}	90	0.5773	-90	2	150
162	**a**	**a**	**b**	**b**	**a**	**a**	**0**	**1**	**0**	**-1**	**0**	**0**	0.5773 V_{ab}	30	0.5773	150	2	150
163	**a**	**b**	**b**	**a**	**a**	**a**	**1**	**0**	**-1**	**0**	**0**	**0**	0.5773 V_{ab}	-30	0.5773	30	2	150
164	**a**	**a**	**b**	**b**	**b**	**b**	**0**	**1**	**0**	**0**	**0**	**-1**	0.5773 V_{ab}	90	0.5773	90	2	-30
165	**a**	**b**	**b**	**b**	**b**	**a**	**1**	**0**	**0**	**0**	**-1**	**0**	0.5773 V_{ab}	30	0.5773	-30	2	-30
166	**a**	**a**	**a**	**c**	**c**	**a**	**0**	**0**	**-1**	**0**	**1**	**0**	0.5773 V_{ca}	-90	0.5773	90	2	-150
167	**a**	**a**	**c**	**c**	**a**	**a**	**0**	**-1**	**0**	**1**	**0**	**0**	0.5773 V_{ca}	-150	0.5773	-30	2	-150
168	**a**	**c**	**c**	**a**	**a**	**a**	**-1**	**0**	**1**	**0**	**0**	**0**	0.5773 V_{ca}	150	0.5773	-150	2	-150
169	**a**	**a**	**a**	**b**	**b**	**b**	**0**	**0**	**1**	**0**	**0**	**-1**	0.6666V_{ab}	120	0	160.0	2.31	-30
170	**a**	**a**	**b**	**b**	**b**	**a**	**0**	**1**	**0**	**0**	**-1**	**0**	0.6666V_{ab}	60	0	-141.3	2.31	-30
171	**a**	**b**	**b**	**b**	**a**	**a**	**1**	**0**	**0**	**-1**	**0**	**0**	0.6666V_{ab}	0	0	90	2.31	-30
172	**a**	**a**	**c**	**c**	**c**	**a**	**0**	**-1**	**0**	**0**	**1**	**0**	0.6666 V_{ca}	-120	0	38.66	2.31	30
173	**a**	**a**	**a**	**c**	**c**	**c**	**0**	**0**	**-1**	**0**	**0**	**1**	0.6666 V_{ca}	-60	0	-19.98	2.31	30
174	**a**	**c**	**c**	**c**	**a**	**a**	**-1**	**0**	**0**	**1**	**0**	**0**	0.6666 V_{ca}	-180	0	-90	2.31	30
175	**b**	**b**	**b**	**c**	**c**	**c**	**0**	**0**	**1**	**0**	**0**	**-1**	0.6666 V_{bc}	120	0	160.0	2.31	90
176	**b**	**b**	**c**	**c**	**c**	**b**	**0**	**1**	**0**	**0**	**-1**	**0**	0.6666 V_{bc}	60	0	-141.3	2.31	90
177	**b**	**c**	**c**	**c**	**b**	**b**	**1**	**0**	**0**	**-1**	**0**	**0**	0.6666 V_{bc}	0	0	90	2.31	90
178	**b**	**b**	**b**	**a**	**a**	**a**	**0**	**0**	**-1**	**0**	**0**	**1**	0.6666V_{ab}	-60	0	-19.98	2.31	150
179	**b**	**b**	**a**	**a**	**a**	**b**	**0**	**-1**	**0**	**0**	**1**	**0**	0.6666V_{ab}	-120	0	38.66	2.31	150
180	**b**	**a**	**a**	**a**	**b**	**b**	**-1**	**0**	**0**	**1**	**0**	**0**	0.6666V_{ab}	-180	0	-90	2.31	150
181	**c**	**c**	**c**	**a**	**a**	**a**	**0**	**0**	**1**	**0**	**0**	**-1**	0.6666 V_{ca}	120	0	160.0	2.31	-150
182	**c**	**c**	**a**	**a**	**a**	**c**	**0**	**1**	**0**	**0**	**-1**	**0**	0.6666 V_{ca}	60	0	-141.3	2.31	-150
183	**c**	**a**	**a**	**a**	**c**	**c**	**1**	**0**	**0**	**-1**	**0**	**0**	0.6666 V_{ca}	0	0	90	2.31	-150
184	**c**	**c**	**c**	**b**	**b**	**b**	**0**	**0**	**-1**	**0**	**0**	**1**	0.6666 V_{bc}	-60	0	-19.98	2.31	-90
185	**c**	**c**	**b**	**b**	**b**	**c**	**0**	**-1**	**0**	**0**	**1**	**0**	0.6666 V_{bc}	-120	0	38.66	2.31	-90
186	**c**	**b**	**b**	**b**	**c**	**c**	**-1**	**0**	**0**	**1**	**0**	**0**	0.6666 V_{bc}	-180	0	-90	2.31	-90

All the 189 space voltage vectors can be summarized in Table 5.5.

Table 5.5. The 189 vectors of table.5.4 are distributed as:

Space vectors	No of vectors	Magnitude of Vdq	Magnitude of Vxy	Magnitude of V0+0-	Input current Corresponding to output voltage
1-24	18	0	1.1546	0	0
	6	0	0	1.9998	0
25-132	72	0.3333	0.5773	0.6666	1.155
	36	0.3333	0.9999	1.13332	1.155
132-168	36	0.5773	0.5773	0.000	2
169-186	18	0.6666	0.000	0.6666	2.31
186-189	3	0	0	0	0

The space voltage vectors are shown in Fig. 5.10. There are several redundant voltage vectors. Hence at each location several vectors are located.

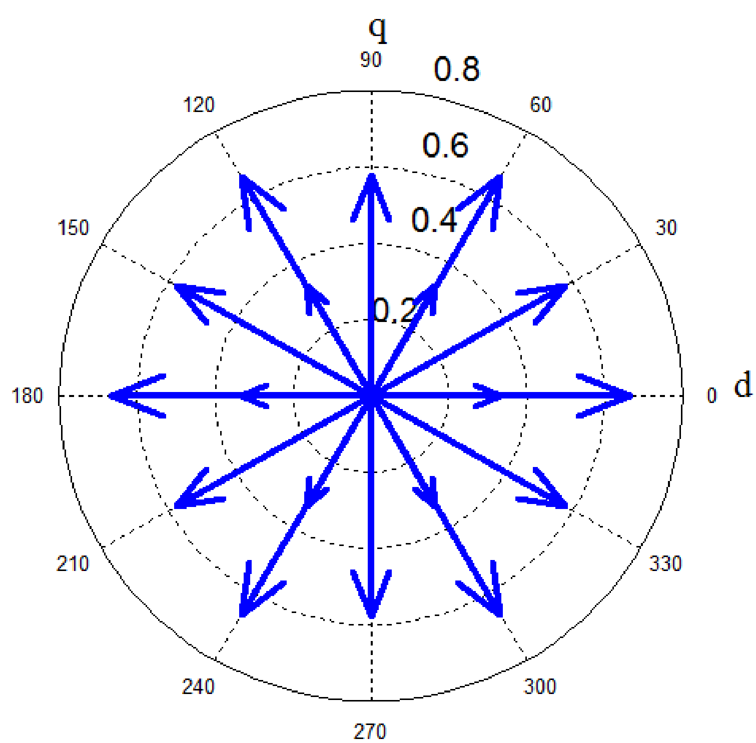

Fig. 5.10. Three-phase to six-phase DMC output voltage (Vdq).

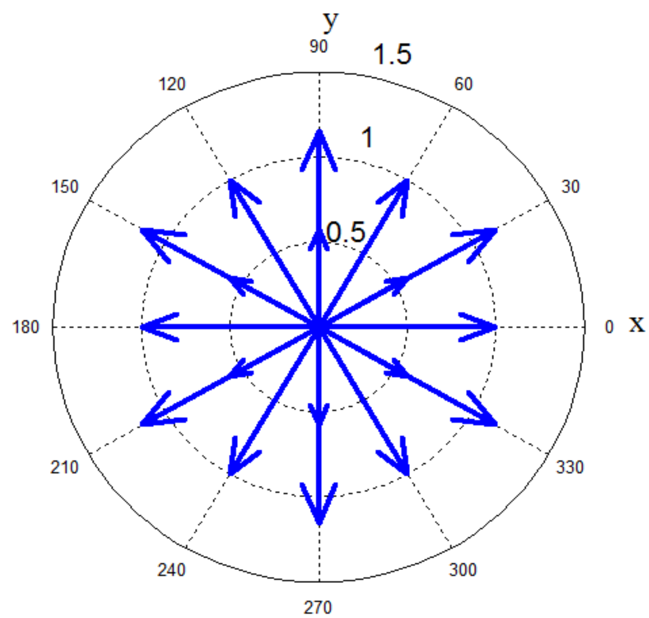

Fig. 5.10a. Three-phase to six-phase DMC output voltage (V_{xy}).

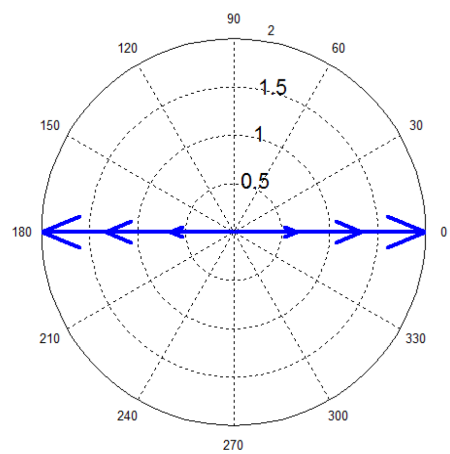

Fig. 5.10b. Three-phase to six-phase DMC output voltage ($V_{o+,o-}$).

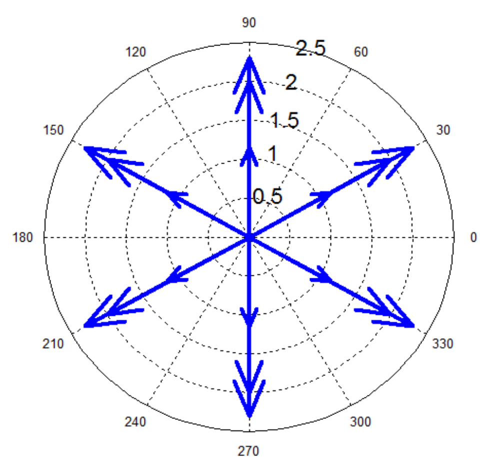

Fig. 5.10c. Three-phase to six-phase DMC input current.

5.4 Space Vector Model of Three-phase to Seven-phase Direct Matrix Converter

The topology of the Matrix Converter elaborated in this thesis is fed using a standard three-phase supply and outputs seven-phase. Each leg has three bi-directional power semi-conductor switches and as such twenty one switches are used. A three-to-seven phase Matrix Converter can be represented in two ways: direct and indirect. The direct Matrix Converter considers the whole circuit as one entity and on the other hand indirect Matrix Converter is assumed as a combination of a rectifier and an inverter fictitious DC link. A general topology of a three-phase to seven-phase DMC is shown in Fig 5.11.

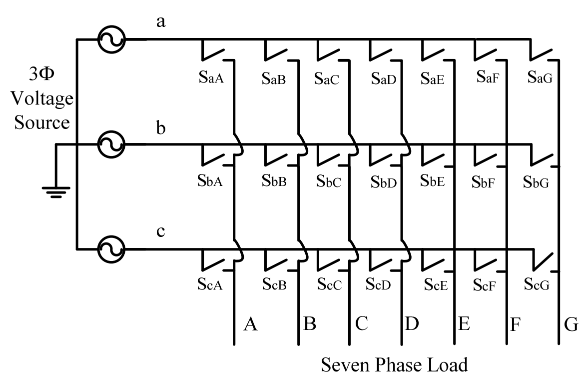

Fig. 5.11. Three-phase to seven-phase direct Matrix Converter.

For a balanced seven phase sinusoidal system the instantaneous voltages maybe expressed as;

$$\begin{bmatrix} V_A \\ V_B \\ V_C \\ V_D \\ V_E \\ V_F \\ V_G \end{bmatrix} = V_0 \begin{bmatrix} \cos\omega_o t \\ \cos(\omega_o t - 2\pi/7) \\ \cos(\omega_o t - 4\pi/7) \\ \cos(\omega_o t - 6\pi/7) \\ \cos(\omega_o t - 8\pi/7) \\ \cos(\omega_o t - 10\pi/7) \\ co(\omega_o t - 12\pi/7) \end{bmatrix} \tag{5.10}$$

In terms of space vector representation it can be expressed as:

$$V_0 = \frac{2}{7}(V_A + aV_B + a^2V_C + a^3V_D + a^4V_E + a^5V_F + a^6V_g) \tag{5.11}$$

$a = e^{-j2\pi/7}$ (Seventh root of unity) and 2/7 is a scaling factor equal to the ratio between the magnitude of the output line-to-line voltage and that of output voltage vector. The angular velocity of the vector is ω_o and its magnitude V_0.

Similarly, the space vector representation of the three-phase input voltage is given by;

$$V_i = \frac{2}{3}(V_a + aV_b + a^2V_c) \tag{5.12}$$

$a = e^{-j2\pi/3}$ (cube root of unity) and 2/3 is a scaling factor equal to the ratio between the magnitude of the input line-to-line voltage and that of input voltage vector.

If a balanced seven-phase load is connected to the output terminals of the direct Matrix Converter, the space vector forms of the seven phase output currents and input currents are given by:

$$I_0 = \frac{2}{7}(I_A + aI_B + a^2 I_C + a^3 I_D + a^4 I_E + a^5 I_F + a^6 I_G)$$
$$= I_o e^{j(\omega_o t - \varphi_o)} \tag{5.13}$$
$$I_i = \frac{2}{3}(I_a(t) + aI_b(t) + a^2 I_c(t)) \tag{5.14}$$
$$= I_i e^{j(\omega_o t - \varphi_i)}$$

where, φ_O is the phase shift angle of the output current to the output voltage and φ_i is that of the input current to the input voltage. There are twenty one power semiconductor switches and each switch is free to connect any of the three phases of input (Fig 5.11). In this way there are 3*7=21 possible equivalent switch. Every switch can have two states 'on' (1)or 'off' (0). In this way there are 2^{21} switching combinations. Considering the constraints "that any two input cannot be shorted and output phase cannot be opened throughout the operation" switching combination reduces to 3^7 = 2187 only. These 2187 switching combinations are analyzed in eight groups that shows how many output phases are connected from input phase (a, b, c). It is represented as {x,y,z} where x, y and z are no of output phases connected to input phase a, b and c, respectively. These groups are elaborated below:

Group-1, [7,0,0]:- This group encompasses those switching vectors that are produced when all seven output phases are connected with the input phase 'a'. Hence, as such there exist two more situations, where all the output phases are connected to phase 'b' and all output phases are connected to phase 'c' and they are denoted as {7,0,0}, {0,7,0},{0,0,7}. Here {7,0,0}, means all seven output phases are connected to phase 'a' of input. Hence, three possible switching states are available.

Group-2, [6,0,1]:- In this group 6 output phases are connected to the same input phase and remaining phase is connected to any of the remaining input phases. Thus there are $^7C_6$ (6 out of 7 output phases are connected to same input) and $^1C_1$ (remaining one output from any one input).

(7!/6!*1!) = 7 combinations , In this way the possible switching combination sub-groups are;

{6,0,1},{6,1,0},{0,6,1},{1,6,0},{0,1,6},{1,0,6}. One sub group can have (7!/6!*1!) = 7 combinations. As such there are 6 sub-groups and thus the total possible combination will be 7*6 = 42 switching combinations.

Group-3, [5,0,2]:-This group encompasses those switching combination where 5 output phases are connected to one input phase and the rest two outputs are connected to any other remaining input phases. The nomenclature {5,0,2} indicates that five output phases are connected to input phase ‘a’, no output phase are connected to input phase ‘b’ and two output phases are connected to input phase ‘c’. The other possible combinations are: ,{5,2,0},{0,5,2},{2,5,0},{0,2,5},{2,0,5}. Thus this group yield:

${}^{7}C_5 * {}^{2}C_2$ =(7!/5!*2!) * (2!/2!*0!) =21*6 = 126 possible switching states and hence 126 space vectors.

Group-4,[5,1,1]:- This group present those switching states where five output phases are connected to one input phase and the rest two output phases are connected to two inputs. As such three possible situation can occur {5,1,1},{1,5,1},{1,1,5}. The total number of possible switching states and hence space vectors are:

${}^{7}C_5 * {}^{2}C_1 * {}^{1}C_1$ =(7!/5!*2!) * (2!/1!*1!) =21*2*3 = 126.

Group-5, [4,0,3]:- This group is comprised of those states that are produced when four output phases are connected to one input phase and the remaining three output phases are connected to any of the two available input phases. Hence the possible situations are {4,0,3, {4,3,0}, {0,4,3}, {3,4,0}, {0,3,4}, {3,0,4}. The total number of space vectors yield are:

${}^{7}C_4 * {}^{3}C_3$ = (7!/4!*3!) * (3!/3!*0!) =35*6 = 210.

Group-6, [4,2,1]:-This group yield largest number of switching combinations. The possible cases are such that four output phases are connected with one input phase, two output phases are connected to another input phase and one output is connected with one input. Hence the complete sets are {4,2,1}, {4,1,2},{1,4,2},{2,4,1},{1,2,4},{2,1,4}. The possible number of switching combination and hence space vectors are obtained by the following combinational rule:

${}^{7}C_4 * {}^{3}C_2 * {}^{1}C_1$ =(7!/4!*3!) * (3!/3!*0!) =35*3*6 = 630.

Group-7, [3,2,2]:- This group also encompasses largest number of possible space vectors. The set comprised of situation where three output phases are connected to one input, the remaining two outputs each are connected to the remaining one input each. Thus the possible sets are {3,2,2},{2,3,2},{2,2,3}. The total number of possible space vectors are:
$^7C_3 * ^4C_2 * ^2C_2$ =(7!/4!*3!) * (4!/2!*2!) =35*6*3 = 630.

Group-8,[3,1,3]:- This group is second largest. The possible sets are when three output phases each are connected to one input phase each and the remaining one output phase is connected to one remaining input phase. The possible group subsets are {3, 13}, {3, 3, 1}, {1,3,3}. The possible switching states and hence space vector are:

$^7C_3 * ^4C_3 * ^1C_1$ =(7!/4!*3!) * (4!/3!*1!) =35*4*3 = 420.

There are in total = 3 + 42 + 126 + 126 + 210 + 630 + 420 + 630 = 2187 switching combinations in which group [1], [2], [3] and [5] are having varying amplitude and fixed frequency. Such switching combinations are 3 + 42 + 126 + 210 = 381. Remaining are having varying amplitude and frequency both so they are not helpful to realize space vector modulation. These 381 switching states that are realizable using space vector PWM is given in Table.5.5. The total 381 vectors are then classified or sub-grouped of 42 vectors each according to their position and magnitude. This table shows the output line voltage of the Matrix Converter having lowest phase difference between phase voltages i.e. adjacent line voltages, V_{AB}, V_{BC}, V_{CD}, V_{DE}, V_{EF}, V_{FG}, V_{GA}. The other sets of line voltages are possible in a seven-phase system that are called non-adjacent-1 and non-adjacent-2 but they are not considered in this discussion. The voltages can be transformed into three sets of orthogonal planes in a seven dimensional space namely V_{dq}, V_{x1y1} and V_{x2y2} and are obtained by using the following transformation equations (5.15) given in reference [5.5],

$$V_{dq} = \frac{2}{7}(V_{AB} + aV_{BC} + a^2V_{CD} + a^3V_{DE} + a^4V_{EF} + a^5V_{FG} + a^6V_{GA})$$
$$V_{x1y1} = \frac{2}{7}(V_{AB} + a^2V_{BC} + a^4V_{CD} + a^6V_{DE} + a^8V_{EF} + a^{10}V_{FG} + a^{12}V_{GA})$$
$$V_{x2y2} = \frac{2}{7}(V_{AB} + a^3V_{BC} + a^6V_{CD} + a^9V_{DE} + a^{12}V_{EF} + a^{15}V_{FG} + a^{18}V_{GA}) \tag{5.15}$$

Where $a = e^{j2\pi/7}$, the space vectors of x_1-y_1 planes represent the third harmonic of d-q and x_2-y_2 represent fifth harmonics. The space vectors obtained are illustrated in Figs. 5.12-5.14.

The zero sequence vectors are not considered as the load assumed is with isolated neutral point.

The space vectors are generated in pairs such that they have equal magnitude but opposite polarity (180° phase shift), hence they are denoted by + and – signs. Further they appear in terms of Vab, Vbc and Vca (input line voltages).

Table.5.5. Output voltage space vectors in d-q plane.

Groups	*number of vectors*	*vectors*	*Magnitude*
[G1]	3	1 to 3	$0\,V_{ab,bc,ca} * e^{j(2k-1)\frac{\pi}{14}}$
[G2]	21	+1 to +21	$0.11\,V_{ab,bc,ca} * e^{j(2k-1)\frac{\pi}{14}}$
[G3]	21	+1 to +21	$0.14\,V_{ab,bc,ca} * e^{j(2k-1)\frac{\pi}{14}}$
[G4]	21	+1 to +21	$0.20\,V_{ab,bc,ca} * e^{j(2k-1)\frac{\pi}{14}}$
[G5]	21	+1 to +21	$0.25\,V_{ab,bc,ca} * e^{j(2k-1)\frac{\pi}{14}}$
[G6]	21	+1 to +21	$0.31\,V_{ab,bc,ca} * e^{j(2k-1)\frac{\pi}{14}}$
[G8]	21 (Medium)	+1 to +21	$0.45\,V_{ab,bc,ca} * e^{j(2k-1)\frac{\pi}{14}}$
[G9]	21 (Large)	+1 to +21	$0.56\,V_{ab,bc,ca} * e^{j(2k-1)\frac{\pi}{14}}$

These 383 active vectors are named on the basis of magnitude and position from ±1 to ±21. Hence there are But in the Table (5.5) only +1 to +21 are shown with their magnitude and direction, remaining -1 to -21 is not shown as those are completely same but 180^o phase opposition of +1to +21. Group seven is not shown in the Table. It has 84 vectors these are unequally spaced but of same magnitude and these vectors are not considered for voltage and current analysis. The group vectors G[8] and G[9] are further utilized in implementing space vector PWM since they have higher magnitude.

The space vector diagram has 3 space vectors at each locations and hence there are only 127 (383/3) location as shown in the Figs. 5.12 - 5.15. It is to be noted that the total space vectors are encompassed within a circle with sub division of 14 major sectors (considering only large length vectors). However, within the larger sectors there are two distinct positions of space vectors. On the large length there are seven vectors lying on the same line but with different switching combinations.

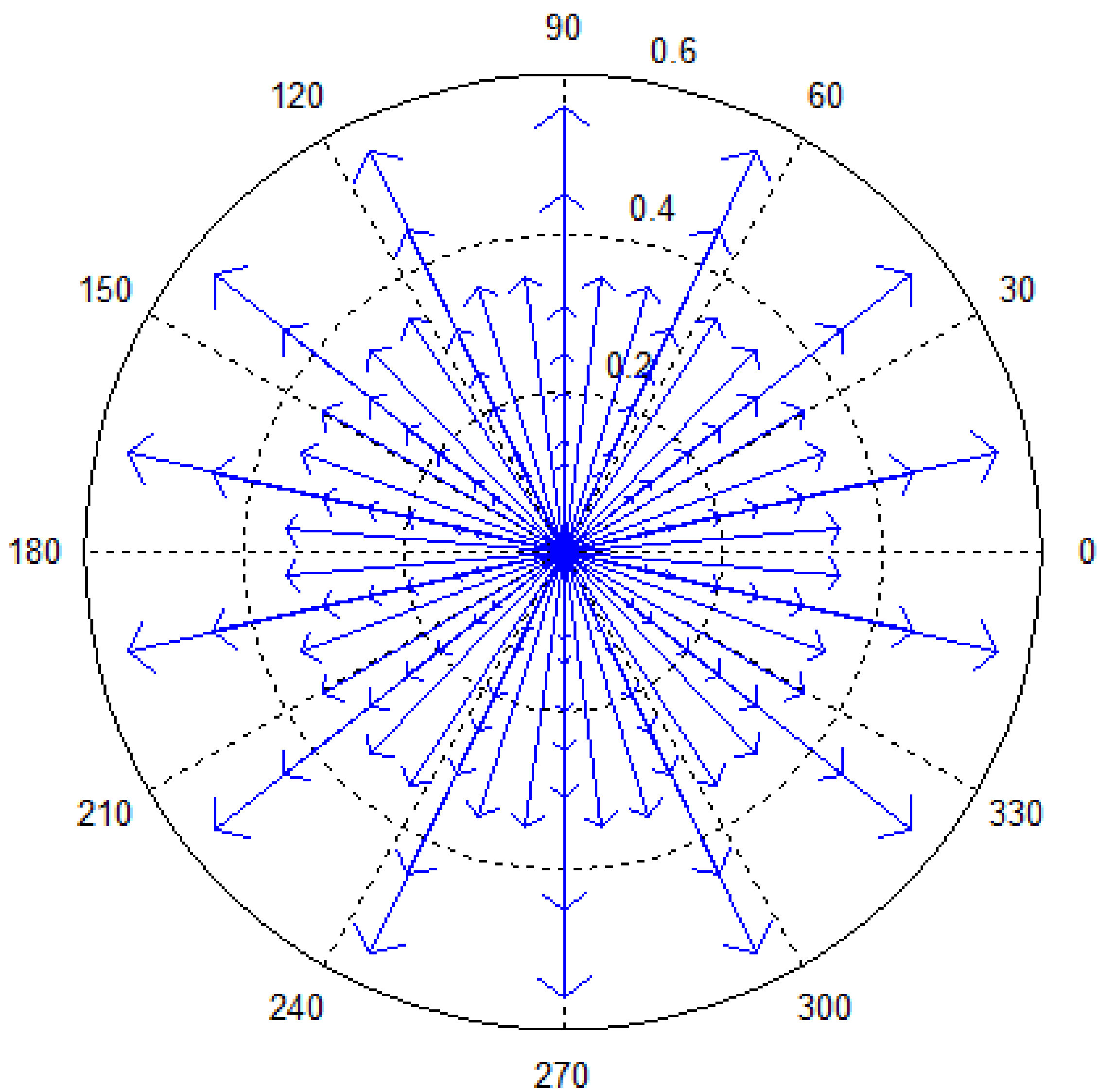

Fig. 5.12. Adjacent line space vectors in d-q plane.

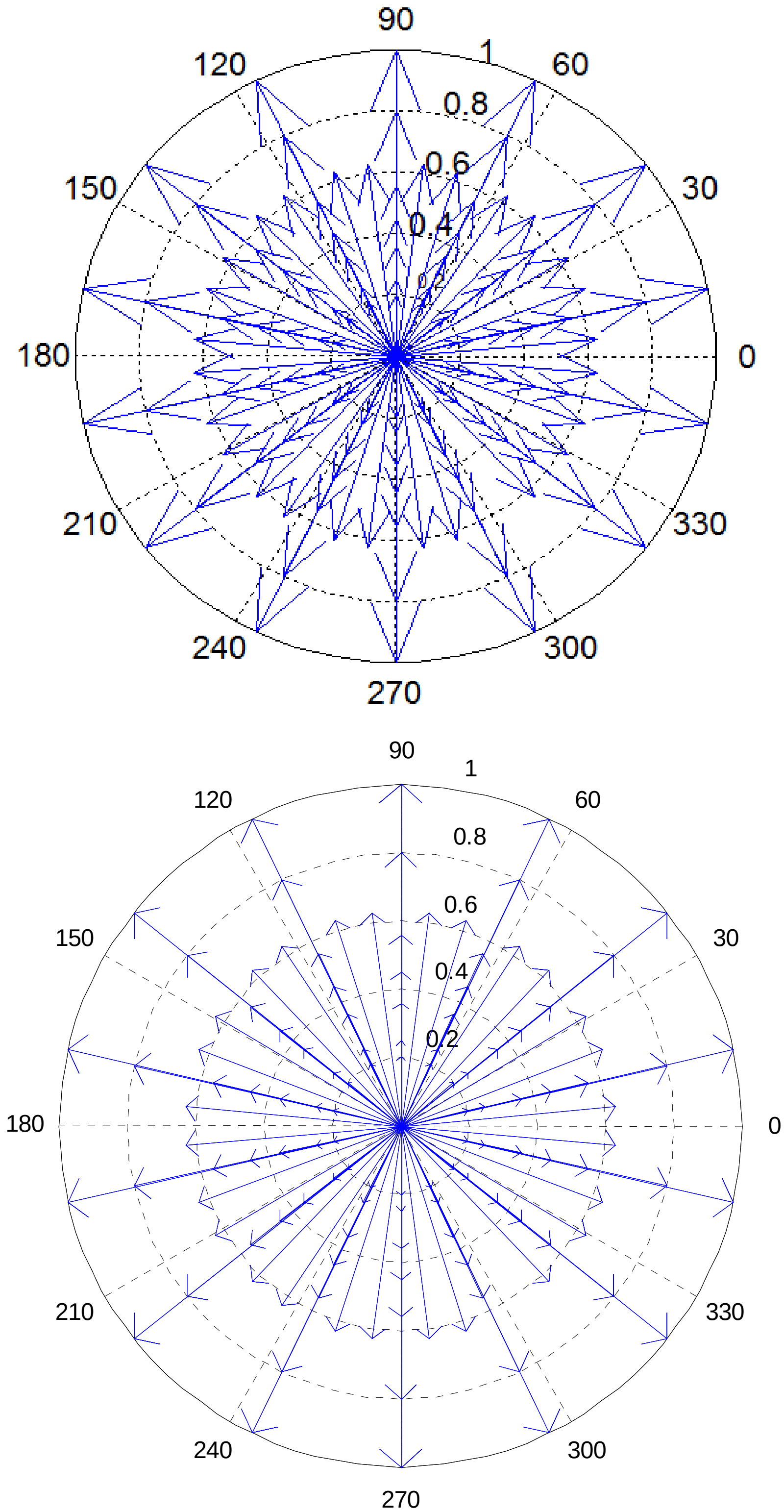

Fig. 5.13. Adjacent Line voltage space vectors in x1-y1 plane.

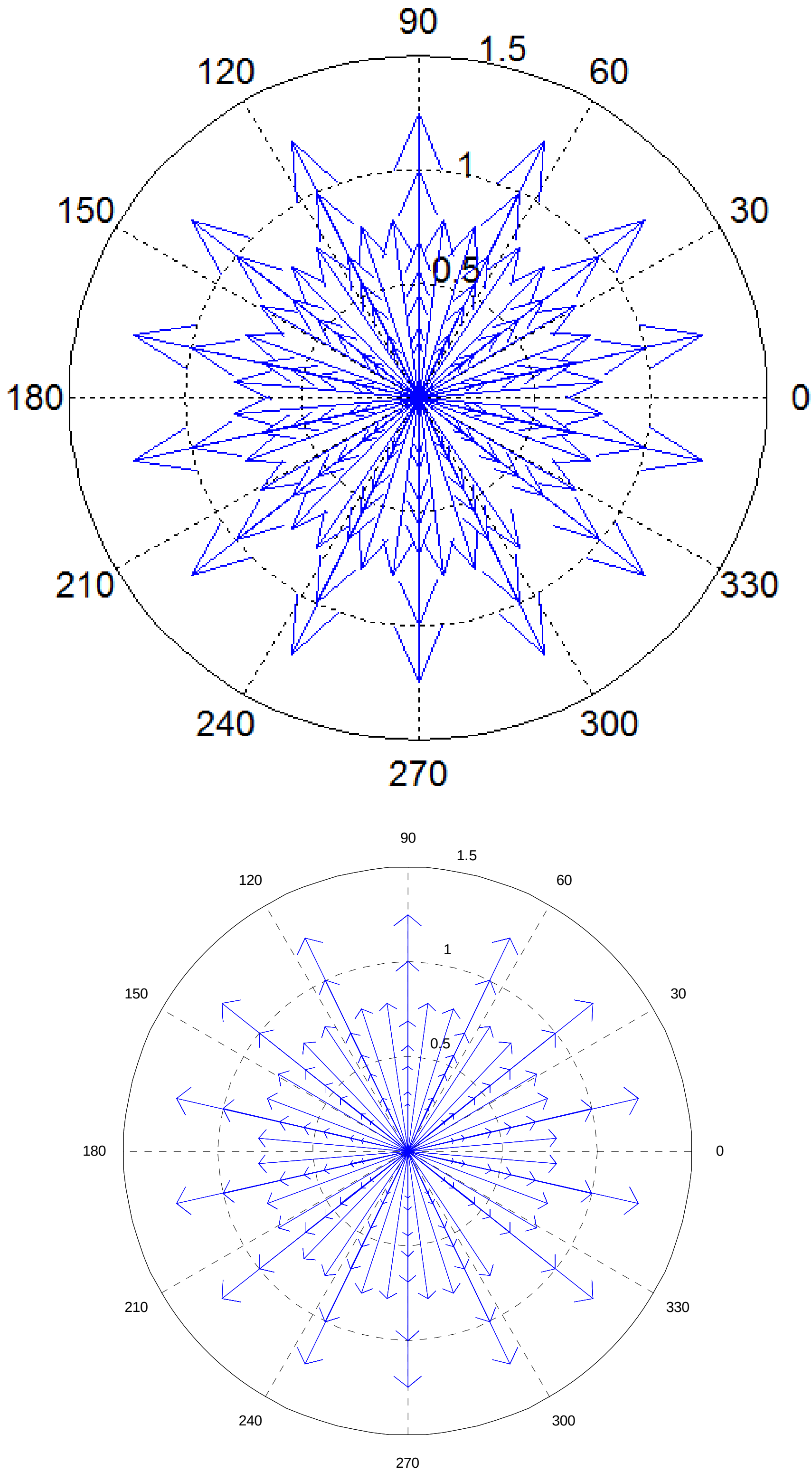

Fig. 5.14. Adjacent Line voltage space vectors in x2-y2 plane.

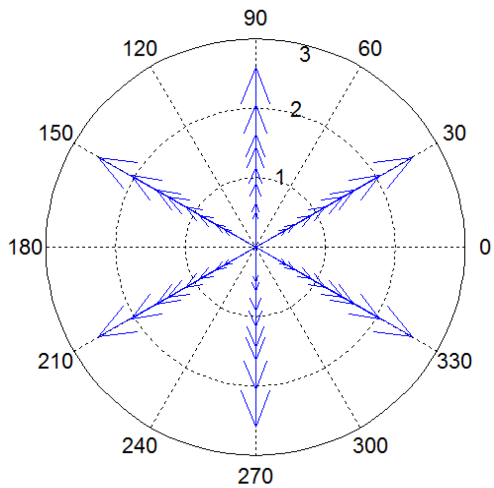

Fig. 5.15. Three phase source current for 3-7 phase MC.

5.5 Summary

This chapter developed complete space vector model of three configurations of Matrix Converter:

- Three-phase input Five-phase output
- Three-phase input Six-phase output
- Three-phase input Seven-phase output.

In case of five-phase output the number switching combinations are2^{15}= 32768. Out of these many switching combinations not all of them are useful. When choosing practically possible switching combination, the safe operation of Matrix Converter is to be considered. The input side should not be short circuited an the output side should not be open circuited. When considering these constraints the possible number of switching combination reduces to 3^5 = 243. It is seen that the number of switching combinations is same as that of a three-level five-phase inverters. Therefore, one can say that the operation of a Matrix Converter is similar to the operation of a three-level back-to-back converter. These switching combinations produce space vectors that are grouped appropriately.

In case of three-phase input and six-phase output the total possible numbers of switching combinations are 2^{18}=262144. Once again the switching combinations are reduced by considering the safety of operation. The actual number of permissible switching combinations are3^6 = 729. They produced the same number of space vectors that can be grouped according to their magnitude.

In case of three-phase input and seven-phase output the total possible numbers of switching combinations are 2^{21} =262144. Once again the switching combinations are reduced by considering the safety of operation. The actual number of permissible switching combinations are3^6 = 729. They produced the same number of space vectors that can be grouped according to their magnitude.

In case of three-phase input and seven-phase output there are 2^{21} = 2097152 possible switching combinations. Considering the constraints "that any two input cannot be shorted and output phase cannot be opened throughout the operation" switching combination reduces to 3^7 = 2187 only. These produce 2187 switching combinations. The sorting and grouping of vectors are reported.

References:

[5.1]. SK. M. Ahmed, A. Iqbal, H. Abu-Rub, M. Saleh, A. Kalam. "Vector Control of a Five-phase induction motor supplied by a Non-square 3X5 phase Matrix Converter," Australian Journal of Electrical Engineering, vol. 10, no. 1, March 2013, pp. 55-63.

[5.2]. SK. M. Ahmed, H. Abu-Rub, A. Iqbal, M.A. S. Payami, "A three-to-five-phase Matrix Converter based five-phase induction motor drive system," Int. Journal of Recent Trend in Engg. & Tech., vol. 8, no. 2, Jan 2013, pp. 82-86. DOI: 01.IJRTET.8.2.94_503.

[5.3]. A. Iqbal, SK. M. Ahmed, H. Abu-Rub, "Space vector PWM technique for a three to five-phase Matrix Converter," IEEE Tran. On Ind. Appl. Vol. 48, No. 2, March/April 2012, pp. 697-707.

[5.4]. H. Abu-Rub, A. Iqbal, J. Guzisnki, "*High Performance control of AC Drives With MATLAB/SIMULINKModels",* Wiley UK, 2012.

[5.5]. E. Levi, "Multi-phase Machines for Variable speed applications" IEEE Trans. Ind. Elect., vol. 55, no. 5, pp. 1893-1909, May 2008.

Chapter 6
Carrier Based PWM Schemes for Feeding Multi-Motor Drive System

6.1 Introduction

This chapter aims to investigate control algorithm of a Matrix Converter. Multi-phase Matrix Converters are discussed in detail with the help of MATLAB simulation. The presentation in this thesis started from three to three-phase Matrix Converter through the control of three to five, three to six and three to seven phase configurations.

An AC to AC power converter is widely used in high-performance drive systems due to its bi-directional power flow and unity input power factor operation capabilities. It allows a wide range of output voltage. A conventional AC-AC converter consists of pulse width modulation (PWM) buck converter and a PWM inverter with DC voltage link. As an energy storage component, it requires a large capacitor in the DC link and a bulky inductor at the input terminal. The DC-link capacitor can be a critical component, especially in high-power or high-voltage applications, since it is large and expensive, and it has a limited lifetime. The source-side inductors are also a burden to the system. An AC/AC converter with bi-directional switches and no reactive components are implemented to overcome all listed disadvantage of conventional AC/AC converters.

Controlled bi-directional power flow using direct AC-AC conversion using semi-conductor switches arranged in the form of matrix array, popularly known as Matrix Converter. Matrix Converter fed motor drive is superior to voltage source inverter because of its bi-directional power switching characteristic and compact design without bulky capacitors. Even though, Matrix Converter is used less in industries due to its complex switching design and modulation techniques. Modulation methods of Matrix Converters are complex and are generally classified in two different groups, called direct and indirect. The direct PWM method developed by Alesina and Venturini in reference [1.18] limits the output to half the input voltage. This limit was subsequently raised to 0.866 by taking advantage of third harmonic injection and it was realized that this is maximum output that can be obtained from a three-to-three phase Matrix Converter in the linear modulation region. Indirect method assumes a Matrix Converter as a cascaded virtual three-phase rectifier and a virtual voltage source inverter with imaginary DC link. With this representation, space vector PWM method of VSI is extended to a Matrix Converter. Although the space vector PWM method is suited to three-phase system but the complexity of implementation increases with the increase in the number of switches/phases. Motivated from the simple implementation, carrier-based PWM scheme has been introduced recently for three to three phase Matrix Converter. The same is extended in this thesis for multi-phase Matrix Converter. The investigated topologies are for single-motor drive and two-motor drive.

6.2 Generalized Carrier-based PWM Techniques for three-to N-phase

In this section generalised 3xN-phase Matrix Converter is discussed and developed scheme is modular in nature and is thus applicable to the generalised circuit topology of Fig 6.1 which shows a Matrix Converter that produces 'N' phase output with three sinusoidal input and 'Nx3' array of switching circuit.

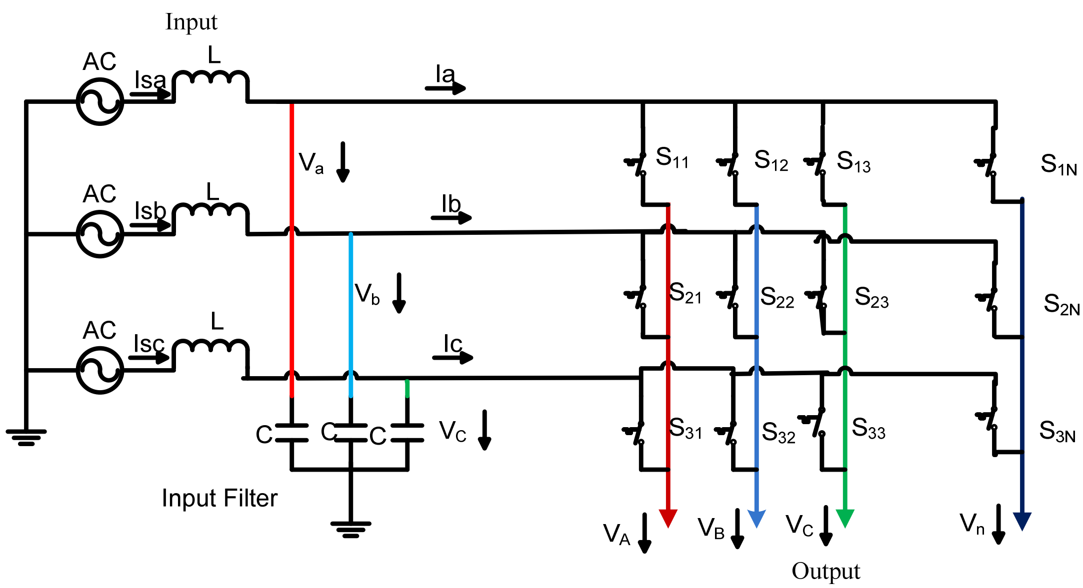

Fig. 6.1. Power circuit topology of 3xN-phase Matrix Converter.

The load to the Matrix Converter is assumed as star-connected N-phase AC machine. Switching function is defined as:

S_{jk}= {1 for closed switch, 0 for open switch}, j = {a,b,c} (input), k= {A,B,C,D,E} (output). The switching constraint is:

$$S_{ak} + S_{bk} + S_{ck} = 1 \tag{6.1}$$

The modulation technique is developed by assuming input side as three-phase controlled rectifier and the output is N -phase voltage source inverter with a fictitious DC link.

Let '$\delta_{KJ}(t)$' as duty ratio

and We can define as $\delta_{KJ}(t) = \frac{\tau_{on}}{\tau_{on} + \tau_{off}}$ (6.2)

where $0 \leq \delta_{KJ}(t) \leq 1$

The low frequency components of output phase voltage

$$V_0(t) = D(t).V_i(t) \tag{6.3}$$

where, V_i is the instantaneous input voltage vector. D(t) is the low frequency transfer Matrix Converter and can be defined as;

$$D(t) = \begin{bmatrix} \delta_{aA}(t) & \delta_{bA}(t) & \delta_{cA}(t) \\ \delta_{aB}(t) & \delta_{bB}(t) & \delta_{cB}(t) \\ \delta_{aC}(t) & \delta_{bC}(t) & \delta_{cC}(t) \\ \vdots & \vdots & \vdots \\ \vdots & \vdots & \vdots \\ \vdots & \vdots & \vdots \\ \delta_{aN}(t) & \delta_{bN}(t) & \delta_{cN}(t) \end{bmatrix} \tag{6.4}$$

In a 3xN Matrix Converter the input three levels are V_a, V_b, V_c. The output levels are $V_A, V_B, V_C \ldots V_N$ Output waveforms of the matrix converter are generated by a small portion of the input waveform with respect to the control signal. Equation (6.5) shows a switching matrix formed by duty ratio of the 3xN Matrix Converter.

$$\begin{bmatrix} V_A \\ V_B \\ V_C \\ \vdots \\ V_N \end{bmatrix} = \begin{bmatrix} \delta_{aA} & \delta_{bA} & \delta_{cA} \\ \delta_{aB} & \delta_{bB} & \delta_{cB} \\ \delta_{aC} & \delta_{bC} & \delta_{cC} \\ \vdots & \vdots & \vdots \\ \delta_{aN} & \delta_{bN} & \delta_{cN} \end{bmatrix} \begin{bmatrix} V_a \\ V_b \\ V_c \end{bmatrix} \tag{6.5}$$

And input current:

$$\begin{bmatrix} I_a \\ I_b \\ I_c \end{bmatrix} = \begin{bmatrix} \delta_{aA} & \delta_{bA} & \delta_{cA} \\ \delta_{aB} & \delta_{bB} & \delta_{cB} \\ \delta_{aC} & \delta_{bC} & \delta_{cC} \\ \vdots & \vdots & \vdots \\ \delta_{aN} & \delta_{bN} & \delta_{cN} \end{bmatrix} \begin{bmatrix} I_A \\ I_B \\ I_C \\ \vdots \\ I_N \end{bmatrix} \tag{6.6}$$

In this chapter a balanced three-phase system is considered in the input side. The input voltages are given as:

$$\begin{aligned} v_a &= \vec{V}\sin(\omega t), \\ v_b &= \vec{V}\sin(\omega t - 2\pi/3), \\ v_c &= \vec{V}\sin(\omega t - 4\pi/3) \end{aligned} \tag{6.7}$$

The output voltage duty ratios should be calculated in such a way that output voltages remains independent of input frequency. In a different way, the output voltages can be considered in synchronous reference frame and the three-phase input voltages can be considered to be in stationary reference frame, so that the input frequency term will be absent in output voltages. Considering the above points in mind duty ratios of M^{th} output phase are chosen as given in references [6.1-6.2]:

$$\begin{aligned} d_{aM} &= k_M \cos(\omega t - \rho), \\ d_{bM} &= k_M \cos(\omega t - 2\pi/3 - \rho), \\ d_{cM} &= k_M \cos(\omega t - 4\pi/3 - \rho) \end{aligned} \tag{6.8}$$

Therefore the M^{th} phase output voltage can be obtained by using the above duty ratios as

$$\begin{aligned} v_A = k_M \vec{V}[&\cos(\omega t)\bullet\cos(\omega t - \rho) + \cos(\omega t - 2\pi/3)\bullet\cos(\omega t - 2\pi/3 - \rho) \\ &+ \cos(\omega t - 4\pi/3)\bullet\cos(\omega t - 4\pi/3 - \rho)] \end{aligned} \tag{6.9}$$

Equation (6.9) can be also written as:

$$v_A = \frac{3}{2} k_M \vec{V} \cos(\rho) \tag{6.10}$$

In equation (6.10), $\cos(\rho)$ term indicates that the output voltage is affected by ρ. Thus, the output voltage v_M is independent of the input frequency and only depends on the amplitude $\vec{V}$ of the input voltage and k_M is a reference output voltage time-varying modulating signal for the M^{th} output phase with the desired output frequency ω_o. The N-phase reference output voltages can be represented as:

$$k_A = k\cos(\omega_o t),$$
$$k_B = k\cos(\omega_o t - 2\pi/n),$$
$$k_n = k\cos(\omega_o t - \{2(n-1)\pi\}/n) \tag{6.11}$$

Therefore, from equation (6.10), the output voltage in phase-*M* is:

$$v_A = \left[\frac{3}{2}k_M \vec{V}\cos(\rho)\right]\cos(\omega_o t) \tag{6.12}$$

6.2a Application of offset duty ratios

While considering any of the phase output the duty ratio will become negative. To overcome this 'n' offset duty ratios are added to the all phases equally which lies between zero and one in all instances. These offset voltages will appear as a common mode voltage in output and nullify in output phases.

Thus offset duty ratio will be added to final duty ratio of any phase output as shown in equation (6.13).

$$d_{aN} = \delta_{aN} + D_a(t) \tag{6.13}$$

The sum of input duty ratio is zero at any instant. Thus additional offset duty ratio can be calculates as

$$(1 - \{D_a(t) + D_b(t) + D_c(t)\}) \tag{6.14}$$

To make unity output, this duty ratio is added to any of the duty ratio such as $D_a(t), D_b(t) and D_c(t)$ . . When added to three duty ratio the offset duty ratio will become:

$$(1 - \{D_a(t) + D_b(t) + D_c(t)\})/3 \tag{6.15}$$

The maximum value of K is 0.5. So total new duty ratio after adding offset will become:

$$\delta_{aA} = \delta_{aA} + |0.5Cos(\omega t - \rho)| + |K_A(t)Cos(\omega t - \rho)|$$
$$\delta_{bA} = \delta_{bA} + |0.5Cos(\omega t - 2\pi/3 - \rho)| + |K_A(t)Cos(\omega t - 2\pi/3 - \rho)|$$
$$\delta_{cA} = \delta_{cA} + |0.5Cos(\omega t - 4\pi/3 - \rho)| + |K_A(t)Cos(\omega t - 4\pi/3 - \rho)| \tag{6.16}$$

Here, in any of the cycle the output phase should not be open circuited. Thus the system maintains output voltage and input current is unaffected. To utilise the maximum input voltage capability an additional components is also used and it enhances the value of $K_{a,}$ $K_{b,}$ K_c from 0.5 to 0.57.

$$\text{i.e. } \{Max(K_{A,}K_{B,}K_C) + Min(K_{A,}K_{B,}K_C)\}/2] \tag{6.17}$$

Thus the final duty ratio of output phase 'a' is:

$$\begin{aligned}
\delta_{aA} &= D_a(t) + (1 - \{D_a(t) + D_b(t) + D_c(t)\})/3 + K_{A,} - \{Max(K_{A,}K_{B,}K_C) + Min(K_{A,}K_{B,}K_C)\}/2]K_A Cos(\omega t - \rho) \\
\delta_{bA} &= D_b(t) + (1 - \{D_a(t) + D_b(t) + D_c(t)\})/3 + K_{A,} - \{Max(K_{A,}K_{B,}K_C) + Min(K_{A,}K_{B,}K_C)\}/2]K_A Cos(\omega t - \rho) \\
\delta_{cA} &= D_c(t) + (1 - \{D_a(t) + D_b(t) + D_c(t)\})/3 + K_{A,} - \{Max(K_{A,}K_{B,}K_C) + Min(K_{A,}K_{B,}K_C)\}/2]K_A Cos(\omega t - \rho
\end{aligned} \tag{6.18}$$

The input current is represented as the sum of time weighting current and duty ratio. The input current of phase 'a' can be represented as:

$$I_a = \delta_{aA} i_A + \delta_{aB} i_B + \delta_{aC} i_C \tag{6.19}$$

In the balanced three phase supply, the offset duty ratio present in final duty ratio will not affect the input current. So

$$I_a = (K_A i_A + K_B i_B + K_C i_C) Cos(\omega t - \rho) \tag{6.20}$$

We can simplify the above equation (6.20) can be simplified as k equal to amplitude of the modulation and I_0 as the amplitude of the output current and ϕ_0 as the output power factor angle.

$$\text{i.e. } \begin{aligned} I_a &= \frac{3}{2} k I_0 Cos\phi_0 \\ KI_0 &= K_A i_A + K_B i_B + K_C i_C \end{aligned} \tag{6.21}$$

The switching signals are generated after comparing the input with a triangular waveform.

$$\begin{aligned}
d_{aM} &= D_a(t) + k_M \cos(\omega t - \rho), \\
d_{bM} &= D_b(t) + k_M \cos(\omega t - 2\pi/3 - \rho), \\
d_{cM} &= D_c(t) + k_M \cos(\omega t - 4\pi/3 - \rho)
\end{aligned} \tag{6.22}$$

In any switching cycle the output phase has to be connected to any of the input phases. The summation of the duty ratios must be equal to unity. But the summation $D_a(t) + D_b(t) + D_c(t)$ is less than or equal to unity. Hence, another offset duty-ratio $[1 - \{D_a(t) + D_b(t) + D_c(t)\}]/3$ is added to $D_a(t), D_b(t)$ *and* $D_c(t)$. The addition of this offset duty-ratio in all switches will maintain the output voltages and input currents unaffected. Similarly, the duty-ratios are calculated for the other output phases.

If $k_A, k_B.........k_n$ are chosen to be n-phase sinusoidal references as given in Equation. (6.17), the input voltage capability is not fully utilized for output voltage generation. To overcome this, an additional common mode term equal to

$$\{\max(k_A, k_B,........, k_n) + \min(k_A, k_B,........, k_n)\}/2] \quad (6.23)$$

is added as in the carrier-based space-vector PWM principle as implemented in two-level inverters. Thus the amplitude of $k_A, k_B.........k_n$ can be enhanced from 0.5 with respect to the number of output phases.

6.2b Without Common Mode Voltage Addition

The duty ratio for Mth output phase can be written as:

$$\begin{aligned}
d_{aM} &= D_a(t) + (1 - \{D_a(t) + D_b(t) + D_c(t)\})/3 + k_M \times \cos(\omega t - \rho) \\
d_{bM} &= D_a(t) + (1 - \{D_a(t) + D_b(t) + D_c(t)\})/3 + k_M \times \cos(\omega t - 2\pi/3 - \rho) \\
d_{cM} &= D_a(t) + (1 - \{D_a(t) + D_b(t) + D_c(t)\})/3 + k_M \times \cos(\omega t - 4\pi/3 - \rho)
\end{aligned} \quad (6.24)$$

6.2.c With Common Mode Voltage Addition

The duty ratio for Mth output phase can be written as:

$$\begin{aligned}
d_{aM} &= D_a(t) + (1 - \{D_a(t) + D_b(t) + D_c(t)\})/3 \\
&+ [k_M - \{\max(k_A,......., k_M) + \min(k_A,......k_M)\}/2] \times \cos(\omega t - \rho) \\
d_{bM} &= D_a(t) + (1 - \{D_a(t) + D_b(t) + D_c(t)\})/3 \\
&+ [k_M - \{\max(k_A,......., k_M) + \min(k_A,......k_M)\}/2] \times \cos(\omega t - 2\pi/3 - \rho) \\
d_{cM} &= D_a(t) + (1 - \{D_a(t) + D_b(t) + D_c(t)\})/3 \\
&+ [k_M - \{\max(k_A,......., k_M) + \min(k_A,......k_M)\}/2] \times \cos(\omega t - 4\pi/3 - \rho)
\end{aligned} \quad (6.25)$$

where

$$\begin{aligned}
D_a(t) &= |0.5\cos(\omega t - \rho)| \\
D_b(t) &= |0.5\cos(\omega t - 2\pi/3 - \rho)| \\
D_c(t) &= |0.5\cos(\omega t - 4\pi/3 - \rho)|
\end{aligned}$$

(6.26)

6.2d Output Side over Modulation

Any increase from the maximum amplitude of the reference signal, reduces the fundamental gain of the modulator. Six-step square wave operating mode gives the maximum fundamental output voltage. The maximum possible magnitude of the factious DC voltage depends on the peak input voltage amplitude and input power factor:

$$V_{\max\_Fictious} = \frac{3}{2} v_{in} \cos(\rho) \tag{6.27}$$

Maximum fundamental output voltage can be calculated as:

$$v_o = \frac{2v_{\max - Fict}}{\pi} = \frac{3}{\pi} V_{in} \tag{6.28}$$

Equation (6.27) shows that over modulation in output side increases the input voltage transfer ratio from 0.866 to 0.95. This increase in input voltage transfer ratio increases the low frequency harmonics in the output voltage and input current.

6.2e Modulator Gain

The output side over modulation can be divided into two operating mode when using space-vector modulation. The fundamental gain of the modulator as a function of peak amplitude modulation can be expressed as shown in reference [6.3]

(6.28)

$$\frac{K_{A\_fund}}{K_A} = -\frac{3}{\pi} \sin^{-1}\left[\frac{1}{3K_A}\right] + \frac{1}{2}\sqrt{1 - \left[\frac{1}{3K_A}\right]^2} \tag{6.29}$$

$$V_{a\_fund} = K_A * V_{dc\_fict} \tag{6.30}$$

Where, K_{A_fund} is the fundamental component of the output modulating signal in the over-modulation region and is equal to k_A when operating in the linear modulation range.

6.3.1 Carrier Based PWM Technique for a Three-to-Five Phase Matrix Converter

In this section, a carrier based PWM strategy is presented based on the comparison of the modulating signals (five-phase target output voltages) with the high frequency triangular carrier wave. The output voltage is limited to 0.75 of the input voltage magnitude. Another scheme is suggested in this result utilising the injection of common mode voltage in the output five-phase target voltage. This results in enhanced output voltage equal to 0.7886 of the input magnitude. Theoretically, this is the maximum output magnitude that can be obtained in this Matrix Converter configuration in the linear modulation region. Analytical approach is used to develop and analyse the proposed modulation techniques and are further supported by simulation and experimental results.

6.3a Three-To-Five Phase Matrix Converter

The power circuit topology of a three-phase to five-phase Matrix Converter is illustrated in Fig. (6-2). There are five legs with each leg having three bi-directional power switches connected in series. Each power switch is bi-directional in nature with anti-parallel connected IGBTs and diodes. The input is similar to a three-phase to three-phase Matrix Converter having LC filters and the output is five-phases with 72˚ phase displacement between each phases. Diode clamped circuit is also used in the hardware to protect the power devices while commutating. The input side uses three diodes while the output side uses five diodes for clamping circuit.

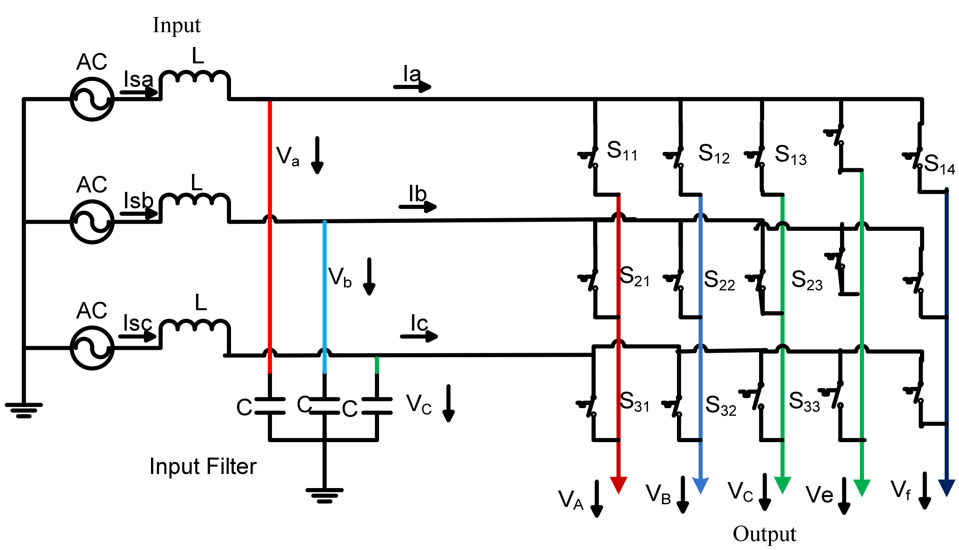

Fig. 6.2. Power Circuit topology of three-phase to five-phase Matrix Converter.

The load to the Matrix Converter is assumed as star-connected five-phase AC machine. The modulation technique is developed by assuming input side as three-phase controlled rectifier and the output is a five-phase voltage source inverter with a fictitious DC link. In a 3x5 Matrix Converter the input three levels are V_a, V_b, V_c. The output five levels are

V_A, V_B, V_C, V_D, V_E . Output waveforms of the Matrix Converter are generated by a small portion of the input waveform with respect to the control signal. Equation (6.31) shows a switching matrix formed by duty ratio of the 3x5 Matrix Converter as shown in reference [6.4].

$$\begin{bmatrix} V_A \\ V_B \\ V_C \\ V_D \\ V_E \end{bmatrix} = \begin{bmatrix} \delta_{aA} & \delta_{bA} & \delta_{cA} \\ \delta_{aB} & \delta_{bB} & \delta_{cB} \\ \delta_{aC} & \delta_{bC} & \delta_{cC} \\ \delta_{aD} & \delta_{bD} & \delta_{aD} \\ \delta_{aE} & \delta_{bE} & \delta_{cE} \end{bmatrix} \begin{bmatrix} V_a \\ V_b \\ V_c \end{bmatrix} \tag{6.31}$$

The input current

$$\begin{bmatrix} I_A \\ I_B \\ I_C \\ I_D \\ I_E \end{bmatrix} = \begin{bmatrix} \delta_{aA} & \delta_{bA} & \delta_{cA} \\ \delta_{aB} & \delta_{bB} & \delta_{cB} \\ \delta_{aC} & \delta_{bC} & \delta_{cC} \\ \delta_{aD} & \delta_{bD} & \delta_{aD} \\ \delta_{aE} & \delta_{bE} & \delta_{cE} \end{bmatrix} \begin{bmatrix} I_a \\ I_b \\ I_c \end{bmatrix} \tag{6.32}$$

The balanced three system is considered as input; so the input voltage is:

$$\begin{aligned} v_a &= \vec{V}\sin(\omega t), \\ v_b &= \vec{V}\sin(\omega t - 2\pi/3), \\ v_c &= \vec{V}\sin(\omega t - 4\pi/3) \end{aligned} \tag{6.33}$$

The output voltage duty ratios should be calculated such as output frequency should be independent of input frequency. So that input frequency term will be absent in output voltages. Hence, the duty ratios of output phase are chosen as:

$$\begin{aligned} d_{aA} &= k_A\cos(\omega t - \rho), \\ d_{bA} &= k_A\cos(\omega t - 2\pi/3 - \rho), \\ d_{cA} &= k_A\cos(\omega t - 4\pi/3 - \rho) \end{aligned} \tag{6.34}$$

Therefore the output voltage of phase 'A' can be written as:

$$v_A = \frac{3}{2}k_A\vec{V}\cos(\rho) \tag{6.35}$$

The five-phase reference output voltages can be written as:

$$\begin{aligned} k_A &= m\cos(\omega_o t) \\ k_B &= m\cos(\omega_o t - 2\pi/5) \\ k_C &= m\cos(\omega_o t - 4\pi/5) \\ k_D &= m\cos(\omega_o t - 6\pi/5) \\ k_E &= m\cos(\omega_o t - 8\pi/5) \end{aligned} \tag{6.36}$$

where ω is input frequency and ω_o is the output frequency, m is the modulation index. For unity power factor ρ has to be chosen as zero.

The output voltage can be computed as:

$$\begin{aligned}
V_A &= \left[\frac{3}{2}k_A|V|\cos(\rho)\right]\cos(\omega_o t) \\
V_B &= \left[\frac{3}{2}k_B|V|\cos(\rho)\right]\cos(\omega_o t - 2\frac{\pi}{5}) \\
V_C &= \left[\frac{3}{2}k_C|V|\cos(\rho)\right]\cos(\omega_o t - 4\frac{\pi}{5}) \\
V_D &= \left[\frac{3}{2}k_D|V|\cos(\rho)\right]\cos(\omega_o t - 6\frac{\pi}{5}) \\
V_E &= \left[\frac{3}{2}k_E|V|\cos(\rho)\right]\cos(\omega_o t - 8\frac{\pi}{5})
\end{aligned} \tag{6.37}$$

6.3b Simulation Results

Simulation results are shown in Figs. 6.3 and 6.4 for the modulation without common mode voltage addition in the output target voltage. The results with common mode voltage addition will remain the same except with the enhanced output magnitude. For simulation purpose, switching frequency is kept at 6 kHz and fundamental frequency is chose as 50 Hz. The input voltages are kept at 100 V peak. The spectrum of source current shows only fundamental component, that indicates sinusoidal source current. The source signal contains switching ripple that is filtered out using small LC filter at the input side.

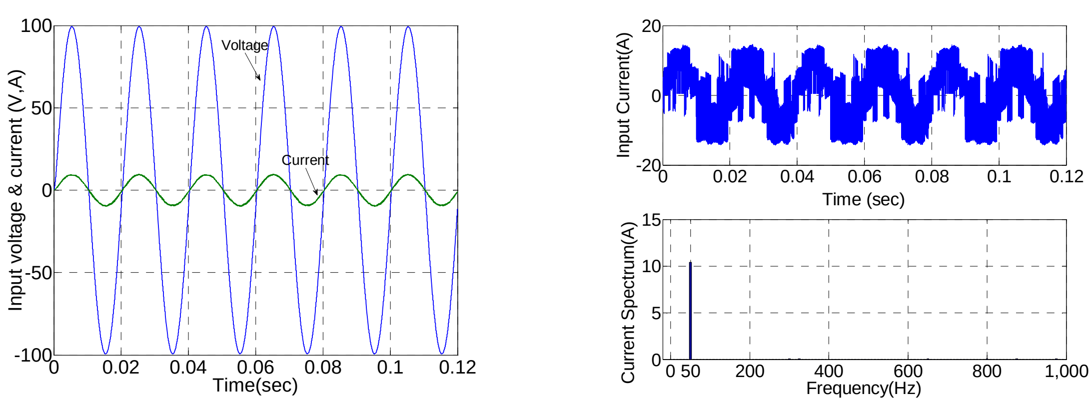

a. b.

Fig. 6.3. Input side waveforms of 3 to 5-phase Matrix Converter: (a) Input voltage and current (b) Spectrum Input current.

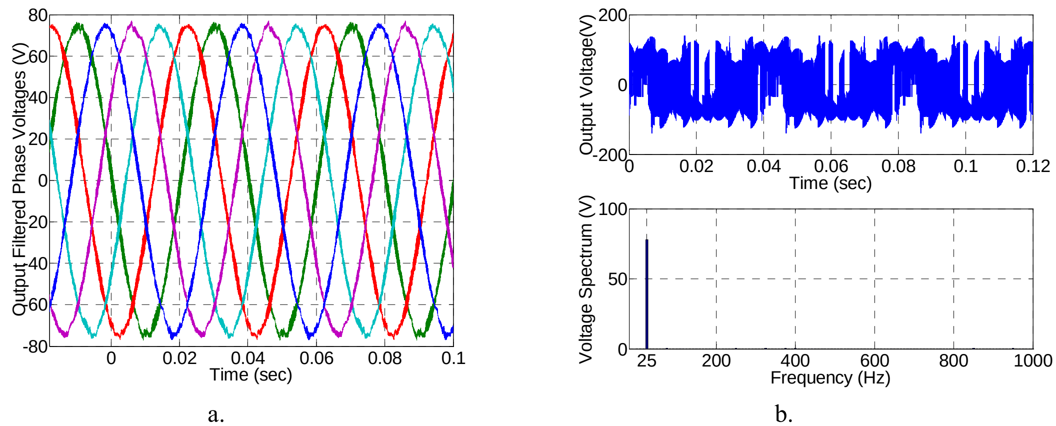

Fig. 6.4. Output side waveforms of 3 to 5-phase Matrix Converter: (a) Five-phase filtered output phase voltages (b) Spectrum output voltage.

6.3.2 Career Based PWM Technique for a Three-to-Five Phase Matrix Converter for Supplying Five-phase Two-motor Drives

This section focuses on the development of a topology of Matrix Converter which is a single stage power converter to produce more than three phases supplying five-phase two-motor drive system. Here, a carrier based PWM strategy is presented based on the comparison of the modulating signals (five-phase two-frequency target output voltages) with the high frequency triangular carrier wave for a three to five-phase Matrix Converter. The output voltage is limited to 0.75 of the input voltage magnitude if common-mode voltage is not injected. Another scheme is utilising the injection of common mode voltage in the output five-phase target voltage. This results in enhanced output voltage which is equal to 0.7886 of the input magnitude. Theoretically, this is the maximum output magnitude that can be obtained in this Matrix Converter configuration in the linear modulation region. Analytical approach is used to develop and analyse the proposed modulation techniques and are further supported by simulation results. The major aim of the thesis is to produce two fundamental frequency output from the Matrix Converter that can be used to control two series/parallel connected five-phase machines independently.

6.4a Five-Phase Two-Motor Drive System

For the sake of completeness of the discussion, a brief description is presented for five-phase two-motor drive. As mentioned in Chapter 4, in five-phase system two set of orthogonal voltage/current components are produced namely d-q and x-y. In single-motor drive system, only d-q components are utilised and the x-y components are free to flow creating losses. Thus concept of two-motor five-phase drive system is developed where both these components are utilised, d-q by one machine and x-y by other machine. The extra set of current components (*x-y*) available in a five-phase system is effectively utilised independently, controlling an additional five-phase machine when the stator windings of two five-phase machines are connected in series (Fig. 6.5)/parallel (Fig. 6.6) and are supplied from a single five-phase VSI. In Fig. 6.5, reference currents generated by two independent vector controllers, are summed up as per the transposition rules and are supplied to the series-connected five-phase machines. As such the two five-phase machines are supplied from one five-phase inverter, but are controlled independently. More detail on this configuration of the drive system is available in references [6.5]. The voltage and current relationship of this drive topology is shown in equation (6.38).

$$\begin{aligned}
v_A^s &= v_{a1} + v_{a2} & \qquad i_A^s &= i_{a1} = i_{a2} \\
v_B^s &= v_{b1} + v_{c2} & \qquad i_B^s &= i_{b1} = i_{c2} \\
v_C^s &= v_{c1} + v_{e2} & \qquad i_C^s &= i_{c1} = i_{e2} \\
v_D^s &= v_{d1} + v_{b2} & \qquad i_D^s &= i_{d1} = i_{b2} \\
v_E^s &= v_{e1} + v_{d2} & \qquad i_E^s &= i_{e1} = i_{d2}
\end{aligned} \tag{6.38}$$

Here 's' stands for source quantity, capital letters denote source and small letters represents motor side quantities.

Another analogue stator winding connection of five-phase two-motor drive is parallel-connected drive (Fig.6.6) which is directly derived from the analogy of series and parallel circuits. The source (three to five-phase Matrix Converters) supplies both the machines and these machines are connected in parallel with appropriate phase transposition. The control decoupling is possible due to decoupling of the α-β and *x-y* components. The d-q components of one machine become the *x-y* to the other and vice-versa. Here, the vector controller produces voltage references in contrary to series-connected drive where current references are generated from the vector controller. Once again independent control is achieved of the two five-phase motors. The voltage and current relations for this drive topology are given as shown in equation (6.39);

$$\begin{aligned}
v_A^s &= v_{a1} = v_{a2} & \qquad i_A^s &= i_{a1} + i_{a2} \\
v_B^s &= v_{b1} = v_{c2} & \qquad i_B^s &= i_{b1} + i_{c2} \\
v_C^s &= v_{c1} = v_{e2} & \qquad i_C^s &= i_{c1} + i_{e2} \\
v_D^s &= v_{d1} = v_{b2} & \qquad i_D^s &= i_{d1} + i_{b2} \\
v_E^s &= v_{e1} = v_{d2} & \qquad i_E^s &= i_{e1} + i_{d2}
\end{aligned} \tag{6.39}$$

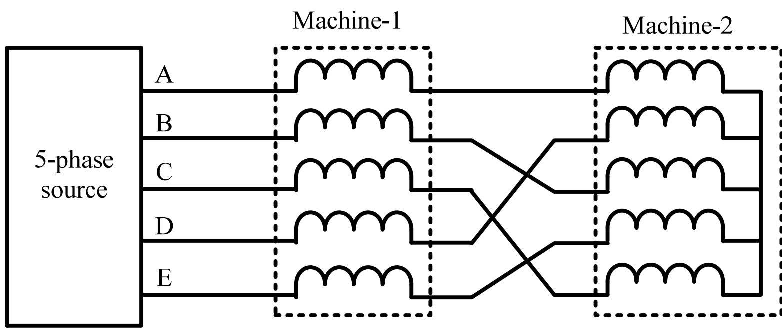

Fig. 6.5. Five-phase series-connected two-motor drive structure.

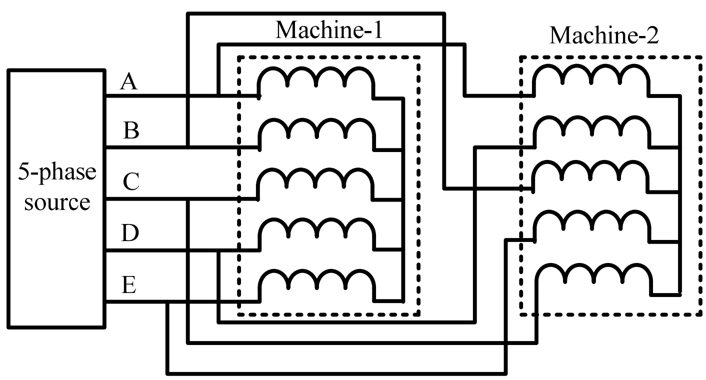

Fig. 6.6. Five-phase parallel-connected two-motor drive structure.

If current control in the rotating reference frame is to be utilized for vector control operation, appropriate PWM scheme for five-phase supply source needs to be developed to generate voltage references instead of current references for both series and parallel connected drives. This proposes alternative solution of supplying the two-motor drive system using a three-phase to five-phase Matrix Converter. The PWM technique develops and produces two-frequency voltage reference outputs to control independently the two series/parallel connected machines.

6.4b Carrier Based PWM Technique for a two motor system

Carrier-based PWM scheme developed in this section follows the similar concept presented in section 6.1. Since the input side is three-phase, the analytical treatment remains the same as that of single-motor drive system. However, the output is now increased to five and hence the analysis will be modified to suit the requisite output phase number. A balanced three-phase system is assumed at the input side.

$$\begin{aligned} v_a &= |V|\cos(\omega t) \\ v_b &= |V|\cos(\omega t - 2\pi/3) \\ v_b &= |V|\cos(\omega t - 4\pi/3) \end{aligned} \tag{6.40}$$

From equation (6.35) we can find that the generalised equation for output voltage of phase a as:

$$V_A = \frac{3}{2} k_A |V| \cos(\rho) \tag{6.41}$$

In equation (6.41), cos (ρ) term indicates that the output voltage is affected by ρ . Thus, the output voltage V_A is independent of the input frequency and only depends on the amplitude V of the input voltage and k_A is a reference output voltage time-varying modulating signal for the output phase A with the desired output frequency ω_{01} is the operating frequency of machine-1 or the first fundamental output frequency and ω_{02} is the operating frequency of machine-2 or the second fundamental output frequency. The fundamental output voltage magnitude corresponding to ω_{01} is given as *m1* and corresponding to ω_{02} is given as *m2.* The five-phase reference output voltages can then be represented as:

$$\begin{aligned} k_{A1} &= m_1 \cos(\omega_{01} t), \\ k_{B1} &= m_1 \cos(\omega_{01} t - 2\pi/5), \\ k_{C1} &= m_1 \cos(\omega_{01} t - 4\pi/5), \\ k_{D1} &= m_1 \cos(\omega_{01}\ t - 6\pi/5), \\ k_{E1} &= m_1 \cos(\omega_{01} t - 8\pi/3), \end{aligned} \tag{6.42}$$

$$\begin{aligned} K_A &= K_{A1} + K_{A2} \\ K_B &= K_{B1} + K_{B2} \\ K_C &= K_{C1} + K_{C2} \\ K_D &= K_{D1} + K_{D2} \\ K_E &= K_{E1} + K_{E2} \end{aligned} \tag{6.43}$$

Therefore the output voltages are obtained as:

$$
\begin{aligned}
V_{A} &= \left[\frac{3}{2}k_{A1}\left|V\right|\cos(\rho)\right]\cos(\omega_{01}t)+\left[\frac{3}{2}k_{A2}\left|V\right|\cos(\rho)\right]\cos(\omega_{02}t) \\
V_{B} &= \left[\frac{3}{2}k_{B1}\left|V\right|\cos(\rho)\right]\cos(\omega_{01}t-2\frac{\pi}{5})+\left[\frac{3}{2}k_{B2}\left|V\right|\cos(\rho)\right]\cos(\omega_{02}t-\frac{4\pi}{5}) \\
V_{C} &= \left[\frac{3}{2}k_{C1}\left|V\right|\cos(\rho)\right]\cos(\omega_{01}t-4\frac{\pi}{3})+\left[\frac{3}{2}k_{C2}\left|V\right|\cos(\rho)\right]\cos(\omega_{02}t-8\frac{\pi}{5}) \\
V_{D} &= \left[\frac{3}{2}k_{D1}\left|V\right|\cos(\rho)\right]\cos(\omega_{01}t-6\frac{\pi}{5})+\left[\frac{3}{2}k_{D2}\left|V\right|\cos(\rho)\right]\cos(\omega_{02}t-2\frac{\pi}{5}) \\
V_{E} &= \left[\frac{3}{2}k_{E1}\left|V\right|\cos(\rho)\right]\cos(\omega_{01}t-8\frac{\pi}{5})+\left[\frac{3}{2}k_{E2}\left|V\right|\cos(\rho)\right]\cos(\omega_{02}t-6\frac{\pi}{5})
\end{aligned}
\tag{6.44}
$$

The five phase reference output voltage can be written as:

$$
\begin{aligned}
k_A &= m_1\cos(\omega_{01}t)+m_2\cos(\omega_{02}t), \\
k_{B1} &= m_1\cos(\omega_{01}t-2\pi/5)+m_2\cos(\omega_{02}t-4\pi/5) \\
k_{C1} &= m_1\cos(\omega_{01}t-4\pi/5)+m_2\cos(\omega_{02}t-8\pi/5) \\
k_{D1} &= m_1\cos(\omega_{01}\ t-6\pi/5)+m_2\cos(\omega_{02}t-6\pi/5) \\
k_{E1} &= m_1\cos(\omega_{01}t-8\pi/3)+m_2\cos(\omega_{02}t-2\pi/5)
\end{aligned}
\tag{6.45}
$$

where ω is input frequency and ω_{o1} and ω_{o2} are the output frequencies of machine-1 and machine-2 respectively, *m1* and *m2*are the modulation indices for machine-1 and machine 2, respectively. For the unity power factor ρ has to be chosen as zero. The modulating signals are shown in Fig. 6.7, after adding the output common mode voltages. These duty ratios is given in equation (6.34) are then compared with the high frequency triangular carrier signals to generate the gating signals as illustrated in Fig. 6.7, for phase A. Similarly fifteen more duty ratios will be compared with the triangular carrier to generate overall gating signals.

A complete block schematic of the PWM signal generation is presented in Fig. 6.8. The reference voltages for two machines with the desired speeds and appropriate voltage magnitudes are generated. These references are then summed according to the phase transposition rule. The overall modulating signal thus generated is given to the PWM block. This PWM block then generate appropriate gate signals for the Matrix Converter. The Matrix Converter then produces appropriate voltages which drive the two series/ parallel connected machines.

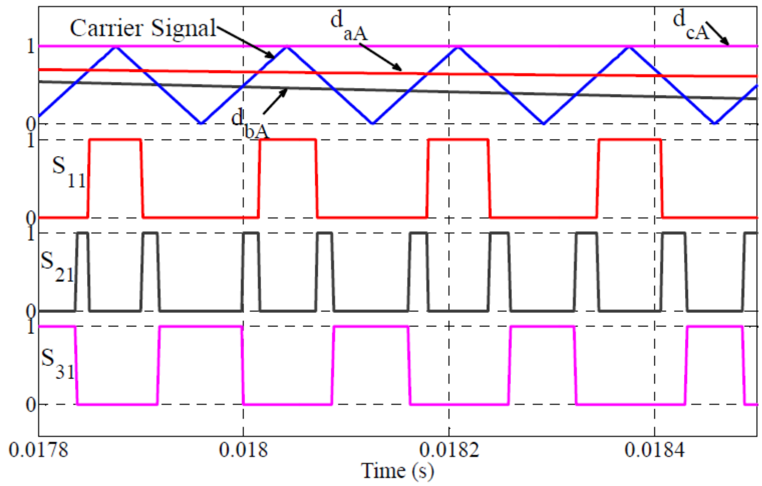

Fig. 6.7. Gate signal generation for output phase A.

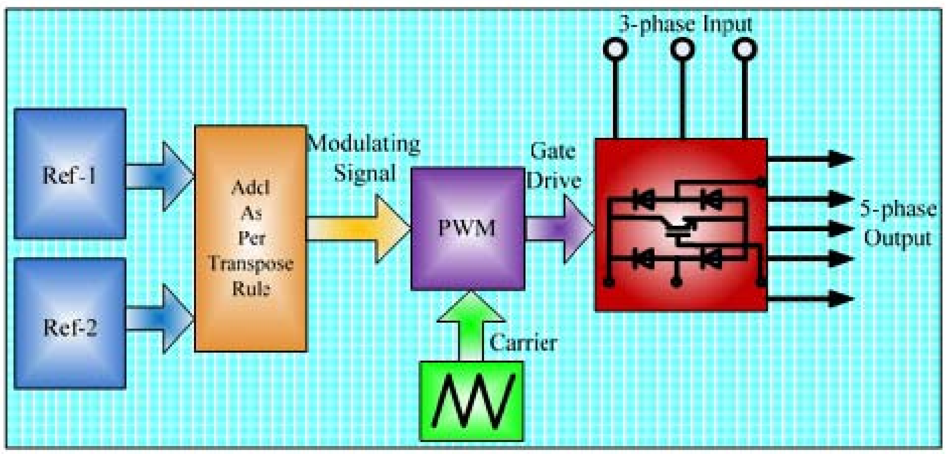

Fig. 6.8. Block diagram of Carrier-based PWM for two frequency output.

6.4c Simulation Results for RL Load

MATLAB/SIMULINK model is developed for the proposed Matrix Converter control. The input voltage is fixed at 100 V to show the exact gain at the output side. The switching frequency of the devices is kept at 6 kHz. The purpose here is to show two fundamental components of current produced by the Matrix Converter. These voltage components are independent from each other and thus can independently control the two machines. The results shown here is only limited to the production of the appropriate voltage components. The motor behaviour is not discussed in this section. It is assumed that one voltage component has frequency of 30 Hz and second voltage component has 60 Hz. To respect the v/f=constant control the voltage magnitude of the lower frequency component is half compared to the higher frequency component. For the simulation purpose, a R-L load is connected with R = 10 Ω and L = 10 mH. Simulation results are shown for the modulation with common mode voltage addition in the output target voltage. Thus the maximum output of the Matrix Converter is limited to 78.8 V as the input is 100 V. The results without common mode voltage addition will remain the same except with the lower output magnitude. The resulting waveforms are presented in Figs. 6.9 - 6.10. The input source side and converter side waveforms are presented in Fig. 6.9. The results clearly shows unity power factor at the input side. The converter side current shows PWM signal and the spectrum is clearly sinusoidal with no lower order harmonics.

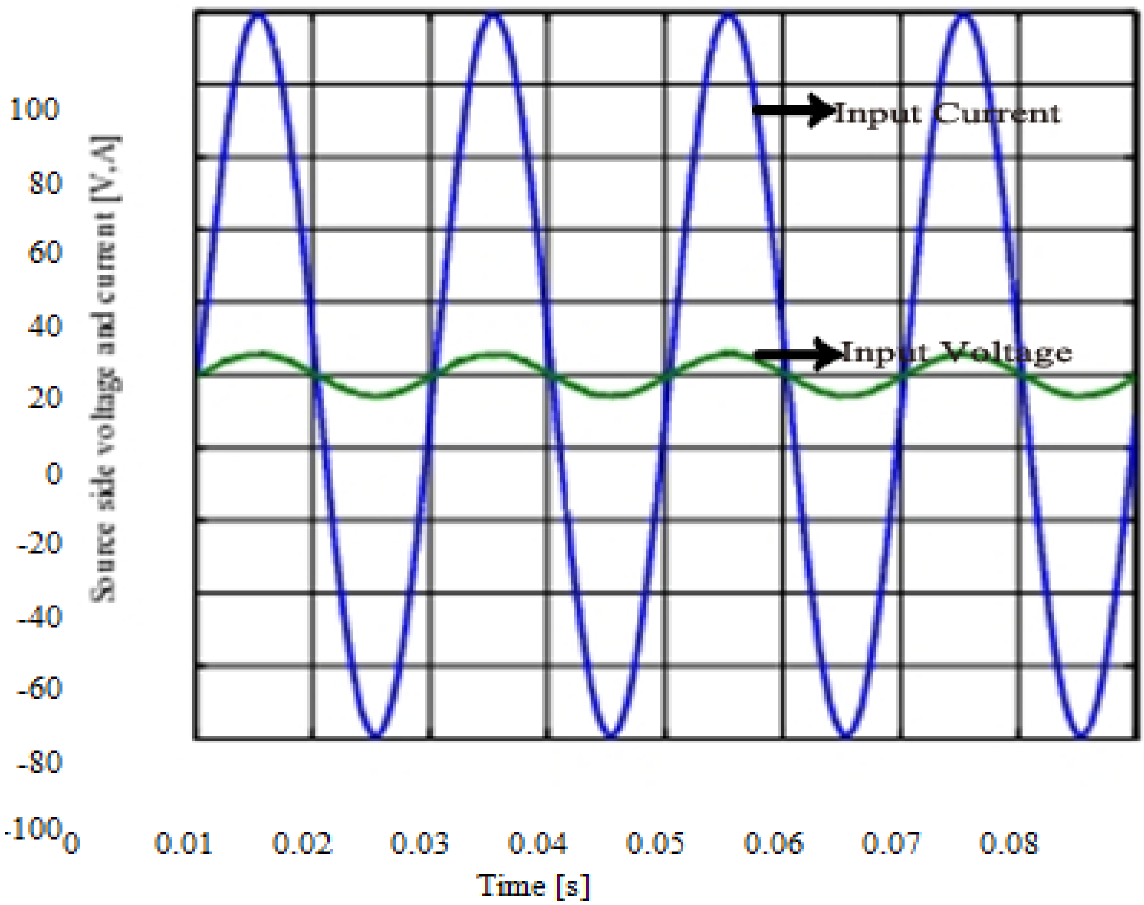

Fig. 6.9. Input side waveforms of 3 to 5-phase Matrix Converter: upper trace.

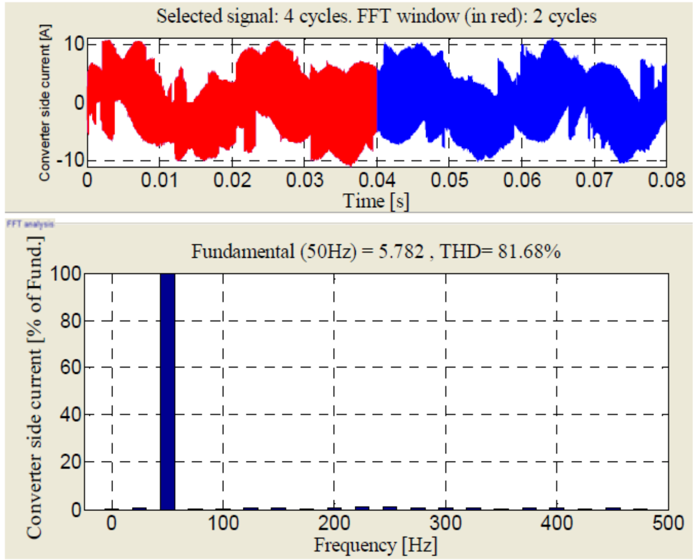

Fig. 6.10. Input voltage and current, bottom trace, Spectrum Input current.

The output side filtered voltages are given in Fig. 6.11 and the spectrum of the output PWM signal voltages are presented in Figs.6.11 - 6.13. The output filtered phase voltages shows superimposed fundamental and second harmonic components. The spectrum of phase 'A' voltage and the transformed voltages are given in Fig.6.14. The phase voltage is transformed into the two orthogonal planes and the voltage of α-axis and x-axis and their spectrum is presented in Fig. 6.13 and Fig. 6.14, respectively. It is clearly evident that the phase 'A' voltage contains two fundamental components at 30 Hz and 60 Hz. These voltages are then decoupled and appear in α-β plane (60 Hz) and x-y plane (30 Hz). Thus the aim of control is achieved. Also the magnitude of the two voltages follows *v/f*=constant rule.

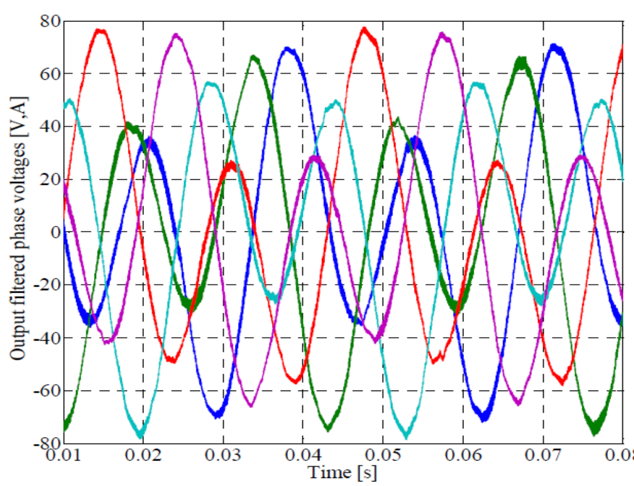

Fig. 6.11. Output filtered five-phase voltages.

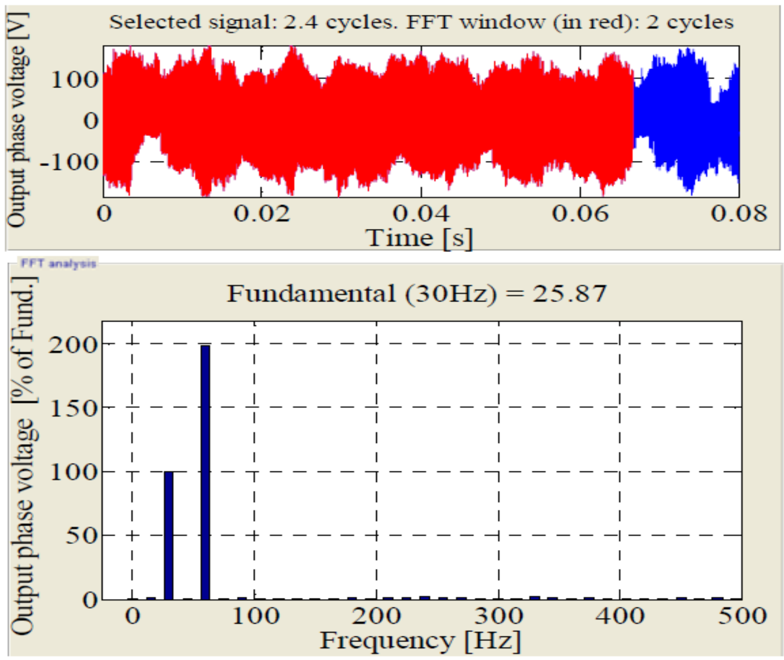

Fig. 6.12. Spectrum of output voltages; phase 'A'.

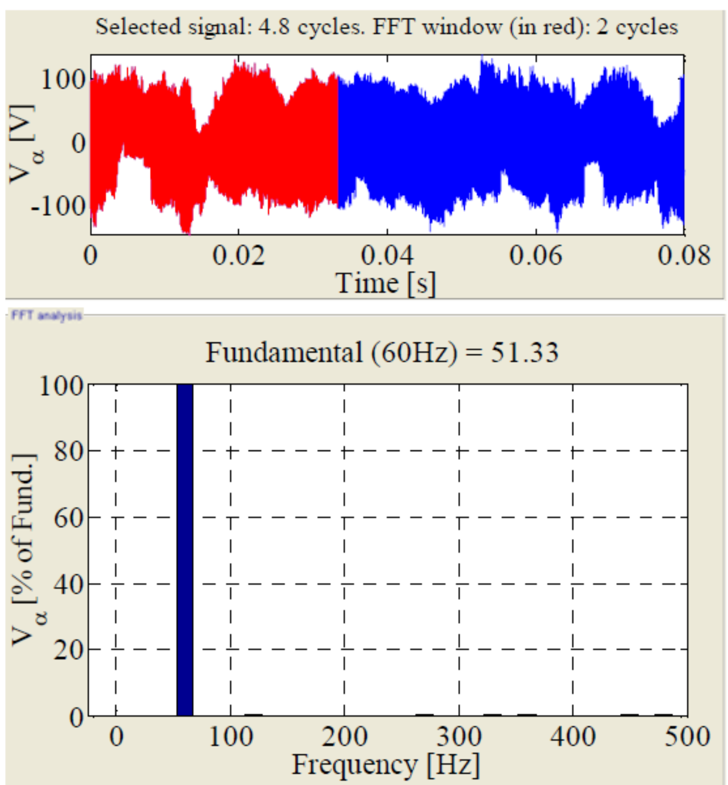

Fig. 6.13. Spectrum of output voltages; α-axis voltage.

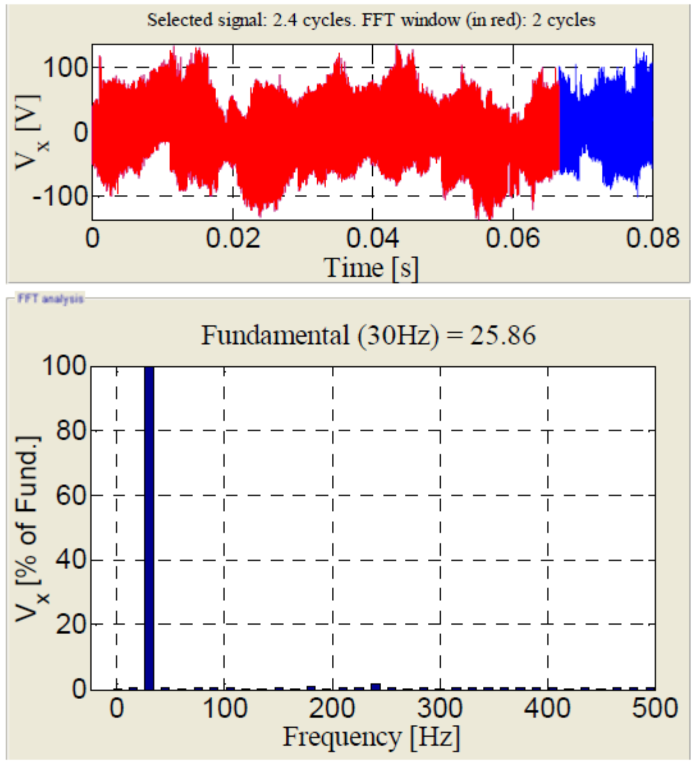

Fig. 6.14. Spectrum of output voltages; x-axis voltage.

6.4d Simulation Results for Motor Load

The simulation model is developed in MATLAB/SIMULINK for the whole drive system. Three-phase grid supply is assumed as 50 Hz, 440 V rms phase voltage (double voltage is assumed since two-motor drive is considered). Five-phase reference voltage is chosen for the first motor and another set of five-phase reference is assumed for the second motor. The five-phase modulating signal is formulated by adding the two five-phase references according to the transposition rule (Fig. 6.5). The parameter of the simulation is given in Table 6.1.

The simulation condition is taken as:

Motor-1 operating at rated speed of 1500 rpm (reference frequency of 50 Hz)

Motor-2 operating at half rated speed of 750 rpm (reference frequency of 5 Hz)

Load (half rated) applied to motor-1 at t = 1.2 sec

Load (one quarter of rated value) applied to motor-2 at t = 1.1

Switching frequency of the Matrix Converter is kept at 6 kHz.

The resulting waveforms for motor side and Matrix Converter sides are shown in Figs. 6.15 and 6.16, respectively.

Table 6.1: Simulation Parameters.

Parameters Name	Parameters Values
Source side resistance Rs	0.05 Ω
Source side inductance Ls	8 mH
DC link capacitor	2000 μF
Stator resistance	10 Ω
Rotor Resistance	6.5 Ω
Stator leakage inductance	40 mH
Mutual inductance	420 mH
Inertia J	0.03 kg sq m
Number of Poles	4
Rated Torque	8.33 Nm
Rated Voltage	440 V

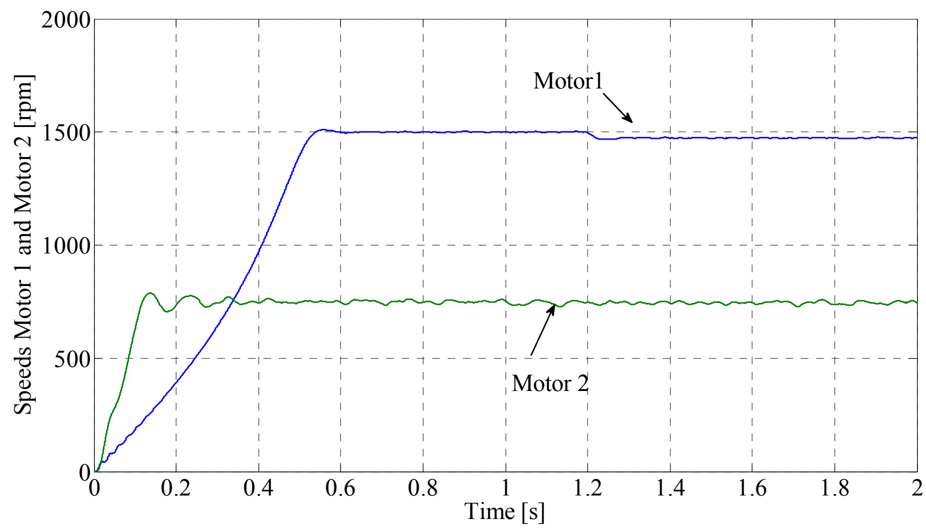

a.

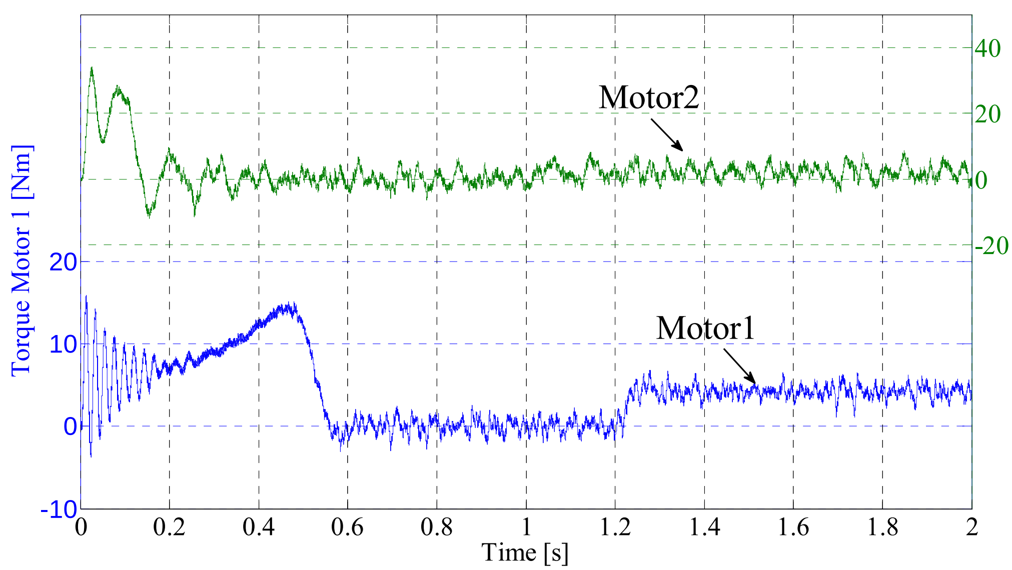

b.

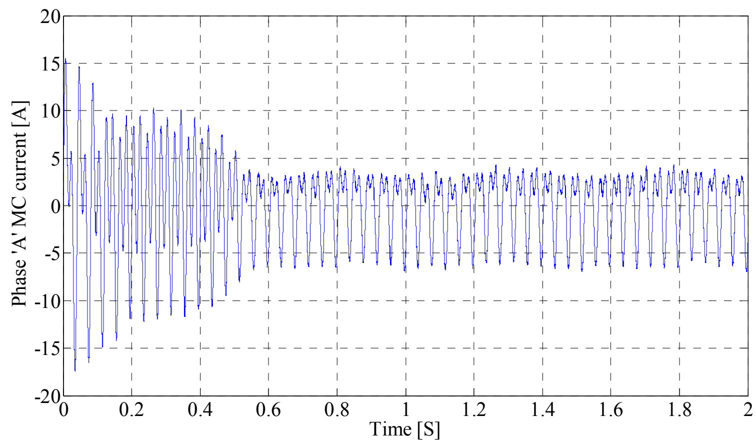

c.

Fig. 6.15. Response of two-motor drive, a. Speeds, b. torques, c. phase ‘a’ current from Matrix Converter.

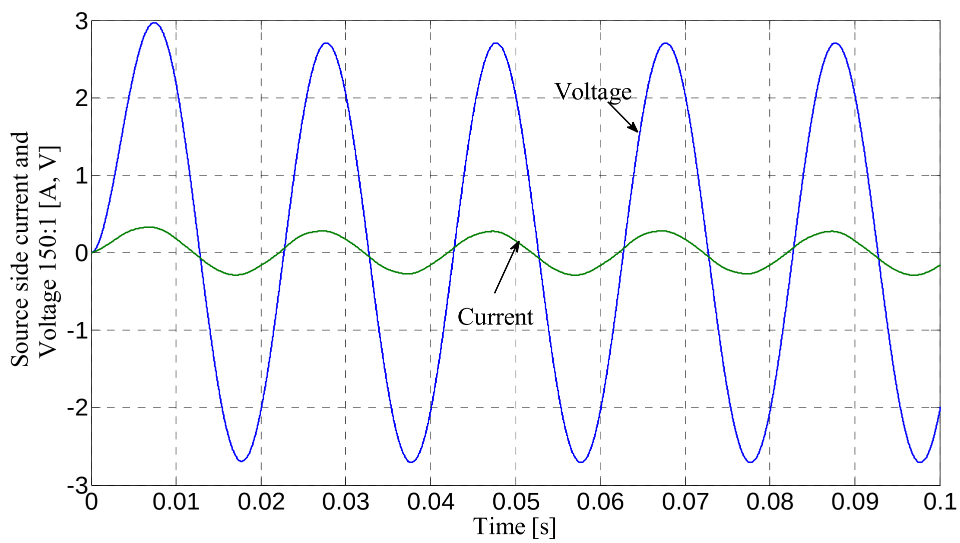

Fig. 6.16. Source side voltage and current, voltage is reduced to 150 times.

The spectrum for the output side current and voltage is shown in Figs. 6.17i and 6.17ii and that of source side current filtered is shown in Fig. 6.17ii .

The output voltage and current waveform shows two frequency components at the two operating frequencies of the two motors. The two machines show acceleration at the initial response. When load is applied the speeds drops and the motor settles at the same speed. The speed is not corrected as no closed-loop controller is employed in this analysis. The motor torque is typical of a five-phase induction machine.

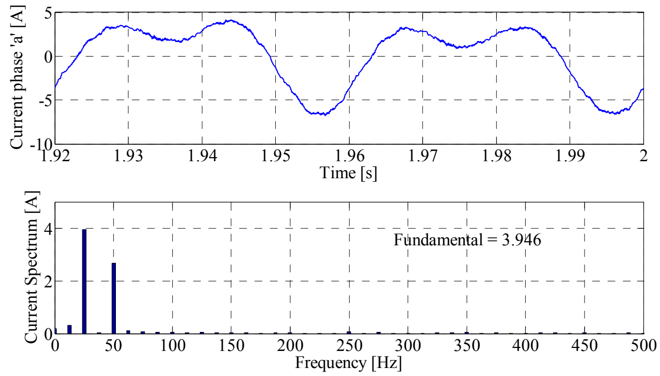

a.

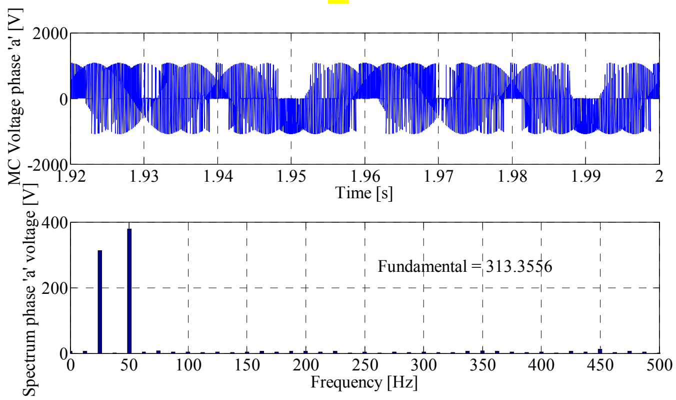

b.

Fig. 6.17i. Matrix Converter output current and voltage time domain and frequency domain waveform.

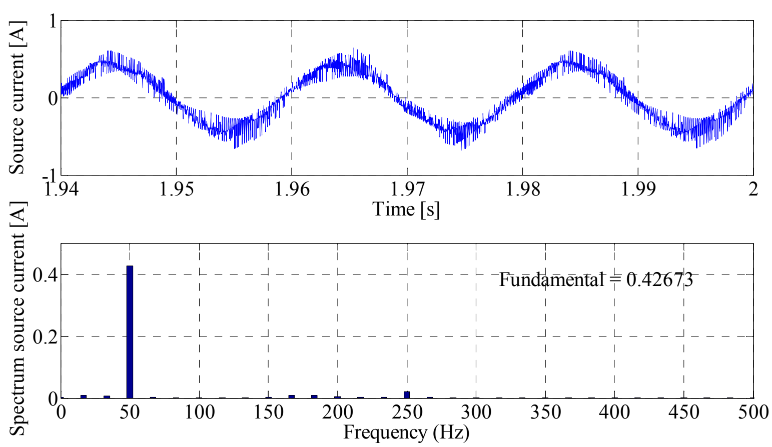

Fig. 6.17ii. Filtered source side current spectrum.

The source side current is sinusoidal and working at unity power factor. This is the distinct feature of the Matrix Converter based drives. The total harmonic distortion (THD) is computed for the voltage and current as follows:

$$\text{THD} = \sqrt{\sum_{n=3,5,7..}^{\infty} \left(\frac{v_n}{v_1}\right)^2} \tag{6.46}$$

where v_n is the nth harmonic component and v_1 is the fundamental component magnitude. For the computation of THD, upto 10^{th} lower order harmonic components are taken.

The THD for the source side current is calculated as 1.66%, the output side current THD is 4.55% while the output voltage THD is 4.48%. These values are well within the specified limit.

6.5 Carrier Based PWM Technique for a Three-to-Six Phase Matrix Converter

Three to six-phase Matrix Converters consists of six legs with three bi-directional power semi-conductor switches in series, which is capable to block voltage in both direction and switch at high speed. Such system can be used to feed a quasi double-star six-phase drives. Fig 6.18 illustrated the design of two step commutation scheme with a total number of 18 IGBTs. LC filter is used in input side to reduce the harmonics and output having two sets of three phase outputs having 30^o phase differences. Its inputs are the phase voltages V_a, V_b, V_C and output voltages are V_A ,V_B, V_C, V_D, V_E, V_F. Eighteen bi-directional switches are represented as S_{11} to S_{36}.

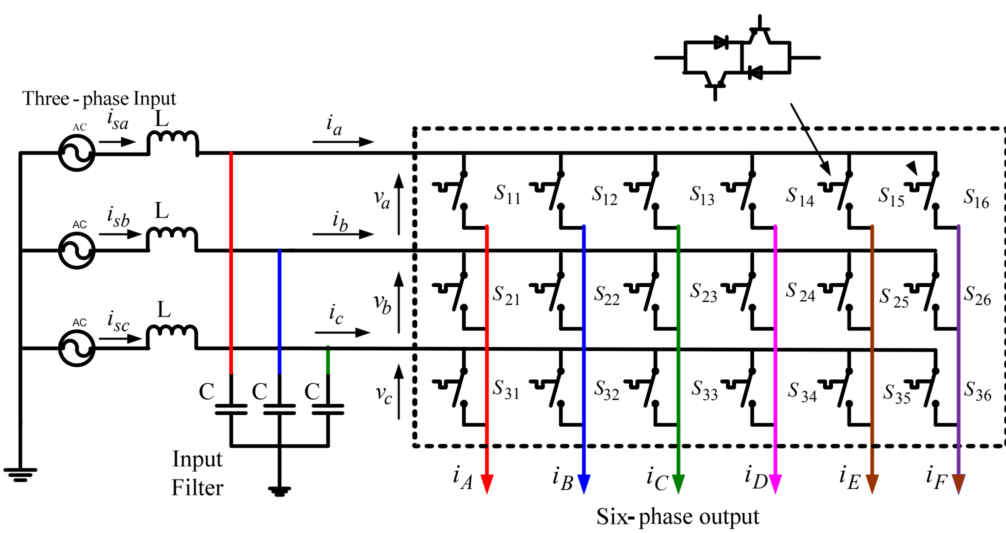

Fig. 6.18. Power Circuit topology of Three-phase to quasi six-phase Matrix Converter.

The load to the Matrix Converter is assumed as double star-connected six-phase ac machine as shown in Fig.6-19.

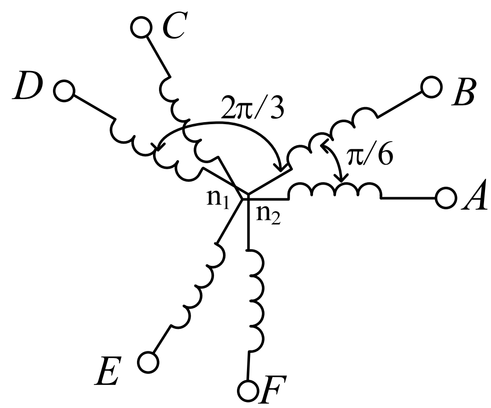

Fig. 6.19. Stator winding displacement of a quasi or double star six-phase ac machine.

6.5a Three-to-Six Phase Matrix Converter system

The balanced three-phase system is assumed at the input

$$\begin{aligned} v_a &= |V|\cos(\omega t) \\ v_b &= |V|\cos(\omega t - 2\pi/3) \\ v_b &= |V|\cos(\omega t - 4\pi/3) \end{aligned} \tag{6.47}$$

Since the Matrix Converter output voltages with frequency decoupled from the input voltages, the duty ratios of the switches are to be calculated accordingly. The six-phase output voltage duty ratios should be calculated in such a way that output voltages remains independent of input frequency. In other words, the six-phase output voltages can be considered in synchronous reference frame and the three-phase input voltages can be considered to be in stationary reference frame, so that the input frequency term will be absent in output voltages. Considering the above, duty ratios of output phase k is chosen as:

$$\begin{aligned} \delta_{ak} &= k_k \cos(\omega t - \rho), \\ \delta_{bk} &= k_k \cos(\omega t - 2\pi/3 - \rho), \\ \delta_{ck} &= k_k \cos(\omega t - 4\pi/3 - \rho) \end{aligned} \tag{6.48}$$

where ρ is the input displacement angle. Therefore the phase A output voltage can be obtained by using the above duty ratios as

$$V_A = k_A |V| [\cos(\omega t) \bullet \cos(\omega t - \rho) + \cos(\omega t - 2\pi/3) \bullet \cos(\omega t - 2\pi/3 - \rho) + \cos(\omega t - 4\pi/3) \bullet \cos(\omega t - 4\pi/3 - \rho)] \tag{6.49}$$

The quasi-6-phase reference output voltages can be represented as:

$$
\begin{aligned}
k_A &= m\cos(\omega_o t), \\
k_B &= m\cos(\omega_o t - \pi/6), \\
k_C &= m\cos(\omega_o t - 2\pi/3), \\
k_D &= m\cos(\omega_o t - 5\pi/6), \\
k_E &= m\cos(\omega_o t - 4\pi/3), \\
k_F &= m\cos(\omega_o t - 3\pi/2),
\end{aligned}
\tag{6.50}
$$

Therefore, from equation (6.41), the output voltages are obtained as:

$$
\begin{aligned}
V_A &= \left[\frac{3}{2}k_A|V|\cos(\rho)\right]\cos(\omega_o t) \\
V_B &= \left[\frac{3}{2}k_B|V|\cos(\rho)\right]\cos(\omega_o t - 2\frac{\pi}{6}) \\
V_C &= \left[\frac{3}{2}k_C|V|\cos(\rho)\right]\cos(\omega_o t - 2\frac{\pi}{3}) \\
V_D &= \left[\frac{3}{2}k_D|V|\cos(\rho)\right]\cos(\omega_o t - 5\frac{\pi}{6}) \\
V_E &= \left[\frac{3}{2}k_E|V|\cos(\rho)\right]\cos(\omega_o t - 4\frac{\pi}{3}) \\
V_F &= \left[\frac{3}{2}k_F|V|\cos(\rho)\right]\cos(\omega_o t - 3\frac{\pi}{2})
\end{aligned}
\tag{6.51}
$$

6.5b Application of Offset Duty Ratio

The final modified duty ratios are shown in Fig. 6.20. If $k_A, k_B, k_C, k_D, k_E, k_F$ are chosen to be 6-phase sinusoidal references as given in equation (9), the input voltage capability is not fully utilized for output voltage generation and the output magnitude remains only 50% of the input magnitude. To overcome this, an additional common mode term equal to $\{\max(k_A, k_B, k_C, k_D, k_E, k_F) + \min(k_A, k_B, k_C, k_D, k_E, k_F)\}/2]$ is added as in the carrier-based PWM principle as implemented in two-level inverters. Thus the amplitude of $(k_A, k_B, k_C, k_D, k_E, k_F)$ can be enhanced from 0.5 to 0.5176.

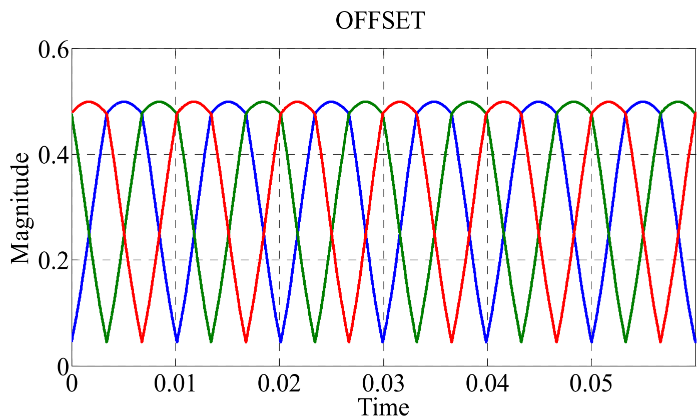

Fig. 6.20. Modified offset duty ratios for all input phases.

6.5c With Harmonic Injection

The duty ratios can further be modified by harmonic injection of the output voltage references to improve the output voltage magnitude. The output voltage magnitude increases and reaches its limiting value of 88.6% of the input magnitude. The amount of harmonic injection that is added to obtain new duty ratios are:

$$V_{cm} = \frac{1}{6} \times m \times \cos(6\omega_0 t) \tag{6.52}$$

The duty ratio for output phase p can be written as:

$$\begin{aligned}
d_{ap} &= D_a(t) + (1 - \{D_a(t) + D_b(t) + D_c(t)\})/3 + [k_p + V_{cm}] \times \cos(\omega t - \rho) \\
d_{bp} &= D_b(t) + (1 - \{D_a(t) + D_b(t) + D_c(t)\})/3 + [k_p + V_{cm}] \times \cos(\omega t - 2\pi/3 - \rho) \\
d_{cp} &= D_c(t) + (1 - \{D_a(t) + D_b(t) + D_c(t)\})/3 + [k_p + V_{cm}] \times \cos(\omega t - 4\pi/3 - \rho)
\end{aligned} \tag{6.53}$$

where $p \in A, B, C, D, E, F$

The quasi six-phase output voltages can be written as:

$$\begin{aligned}
k_A &= m\cos(\omega_o t), \\
k_B &= m\cos(\omega_o t - \pi/6), \\
k_C &= m\cos(\omega_o t - 2\pi/3), \\
k_D &= m\cos(\omega_o t - 5\pi/6), \\
k_E &= m\cos(\omega_o t - 4\pi/3), \\
k_F &= m\cos(\omega_o t - 3\pi/2),
\end{aligned} \tag{6.54}$$

where ω is input frequency and ω_o is the output frequency, m is the modulation index. For unity power factor ρ has to be chosen as zero. The modulating signals are shown in Fig. 6.21, after adding the output common mode voltages. The duty ratios obtained using equation

(6.53) for phase A is depicted in Fig. 6.22. These duty ratios are then compared with the high frequency triangular carrier signals to generate the gating signals as illustrated in Fig. 6.23, for phase A. Similarly fifteen more duty ratios are compared with the triangular carrier to generate overall gating signals.

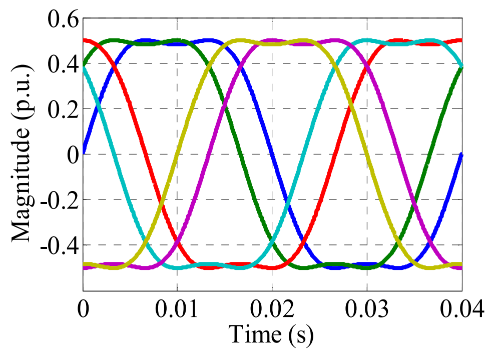

Fig. 6.21. Common mode added reference for output phases.

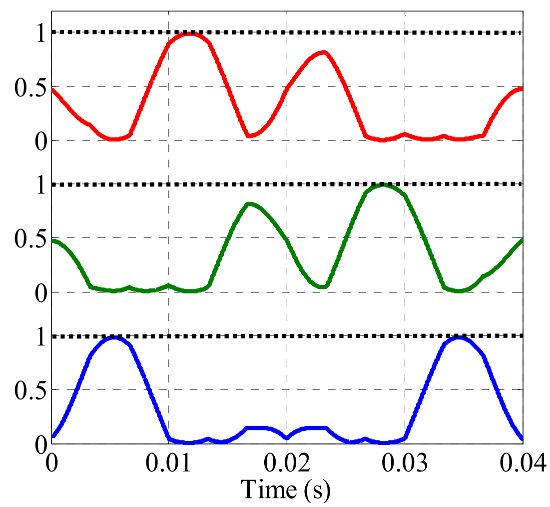

Fig. 6.22. Duty ratio for output phase A.

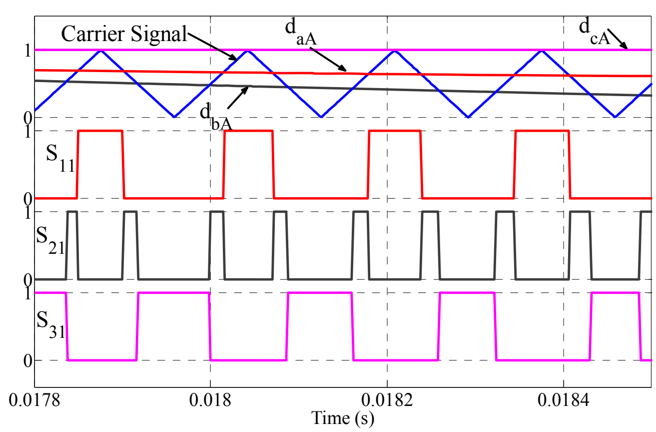

Fig. 6.23.. Gate signal generation for output phase A.

6.5d Output Voltage Magnitude

In a conventional three-phase to three-phase Matrix Converter, the output voltage magnitude reaches 50% of the input voltage using the conventional modulation method or simple carrier based PWM. This limit improves to 75% when the offset corresponding to the input signals are added. It is important to note that this limit of 75% is irrespective of the output number of phases of the Matrix Converter. Hence, this is the realizable output in Matrix Converter topology with three phase input and n phase output. The output voltages are further enhanced to 86.6% in three to three-phase Matrix Converter by adding common mode signal corresponding to the output voltages. This increase in the output voltage magnitude is (86.6-75)/75 = 15.47%, this is interesting value as the same increase is achieved in a two level three-phase voltage source inverter when modulating signals are modified by adding common mode voltages. Following the same principle the increase in the output voltage magnitude in a multi-phase two-level inverter is obtained as $1/\cos(\pi/2n)$, where n is the number of phases of inverter given in reference [6.6]. This study of quasi six-phase Matrix Converter also follows the same principle and an increase of (77.64-75)/75 = 3.52% in recorded. It is important to mention here that the gain in the output voltage reduces with the increase in the number of output phases of the Matrix Converter.

6.5e Simulation Results

MATLAB/SIMULINK model is developed for the proposed Matrix Converter control. The input voltage is fixed at 100 V to show the exact gain at the output side. The switching frequency of the devices is kept at 6 kHz. The output fundamental frequency is chosen as 25 Hz. Simulation results are shown for the modulation without common mode voltage addition in the output target voltage. The load chosen is a quasi six-phase R-L with two separate neutrals with R = 10 Ω and L = 10 mH. The results with common mode voltage addition will remain the same except with the enhanced output magnitude. The resulting waveforms are depicted in Figs. 6.24 and Fig. 6.25, for input side and output side, respectively. The results of Fig. 6.25, clearly shows unity power factor at the input side and completely sinusoidal source current. The input converter side current is seen as PWM signals due to switching and current modulation. The spectrum of the input converter side current is also shown in the lower trace. It is evident that the current is completely sinusoidal and does not contain any low order harmonic. The total harmonic distortion in the input converter side current is very low and is 0.84%. The output filtered voltages are seen as sinusoidal and the spectrum of the output phase A voltage also shows the same results. The total harmonic distortion in the output phase is observed as 0.95%. The load current is also completely sinusoidal. This indicates the viability of the proposed modulation technique.

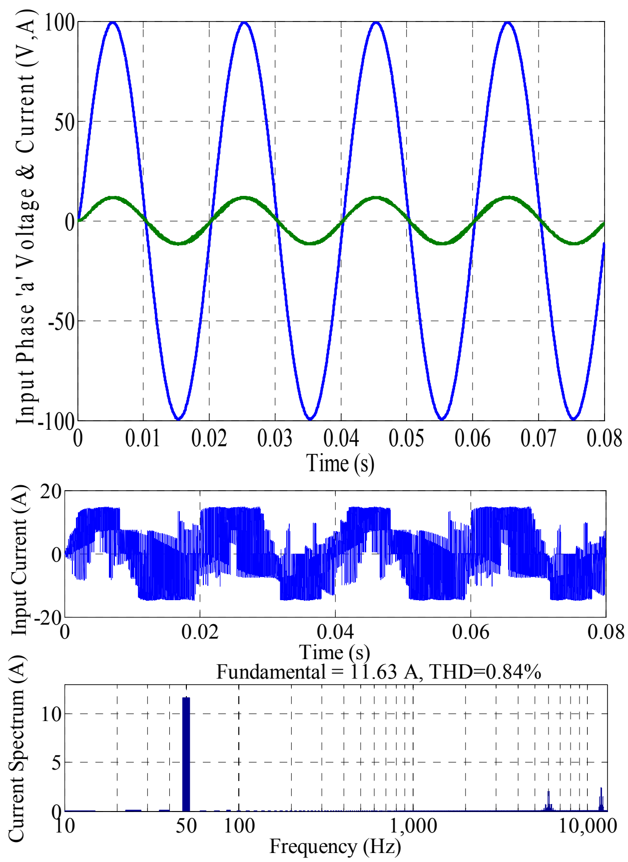

Fig. 6.24. Input side waveforms of 3 to quasi 6-phase Matrix Converter: upper trace, Input voltage and filtered current, bottom trace, Spectrum Input current.

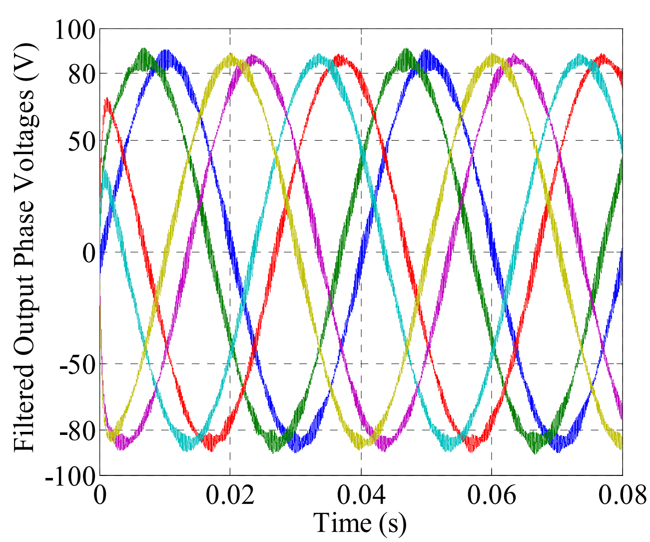

(a)

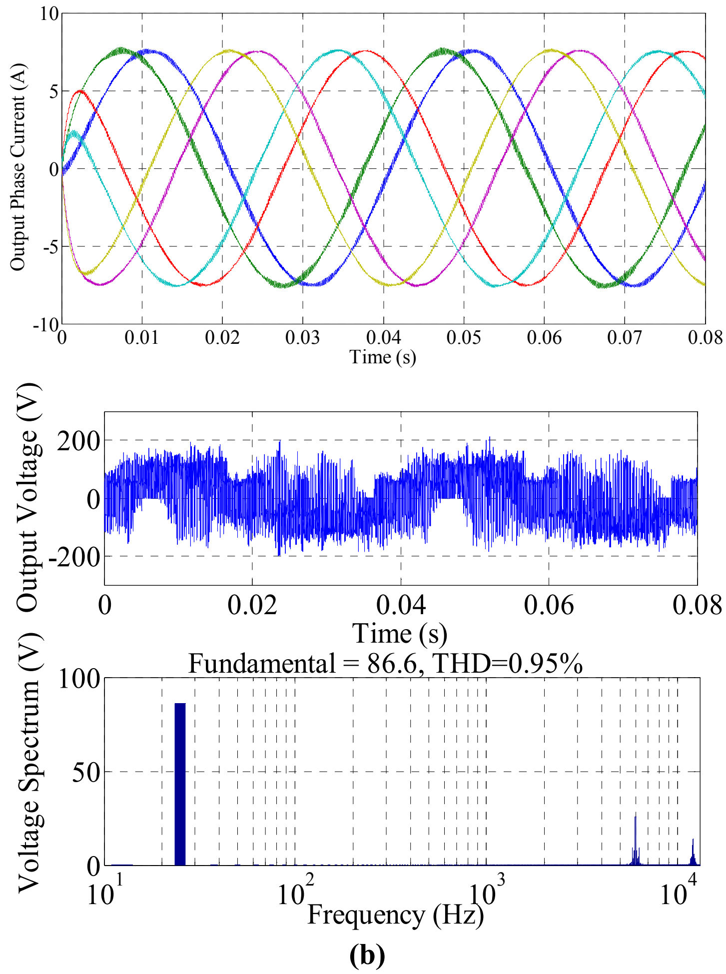

Fig. 6.25. Output side waveforms of 3 to quasi 6-phase Matrix Converter:, a) quasi 6-phase filtered output phase voltages, , b) Spectrum output voltage and output current.

6.6 Carrier Based PWM Technique for a Three-to-Six Phase Matrix Converter for Supplying Six-phase Two-motor Drives

As discussed in Chapter 4, vector control of any multi-phase machine requires only two stator current components; the additional stator current components are used to control other machines. It has been shown that, by connecting multi-phase stator windings in series and in parallel with an appropriate phase transposition, it is possible to control independently all the machines with supply coming from a single multi-phase voltage source inverter. Another specific drive system, covered by this general concept, is the six-phase series-connected two-motor drive, consisting of one symmetrical six-phase and a three-phase machine and supplied from a single six-phase voltage source inverter. The multi-motor drive system discussed uses multi-phase voltage source inverter as their supply. In contrast this section proposes a multi-phase Matrix Converter to supply such drive topology.

In this section, a carrier based PWM strategy is presented based on the comparison of the modulating signals (six-phase target voltages) with the high frequency triangular carrier wave for a three to six-phase Matrix Converter. The output voltage is limited to 0.75 of the input voltage magnitude. Theoretically this is the maximum output magnitude that can be obtained in this Matrix Converter configuration in the linear modulation region. Analytical approach is used to develop and analyse the proposed modulation techniques and are further supported by simulation results. The major aim of this section is to produce two fundamental frequency output from the Matrix Converter that can be used to control two series-connected six-phase and three-phase machines.

6.6a Six-Phase Series-Connected Two-Motor Drive Configuration

The two-motor drive, used in this thesis, is shown in Figure 6.26. It consists of a six-phase source (capital letters A, B,…F), a six-phase and a three-phase ac machine. Stator windings of the two machines are connected in series with appropriate phase transposition. The six-phase machine has the spatial displacement between any two consecutive stator phases of 60° (i.e. $\alpha = 2\pi/6$). The type of the ac machine is irrelevant as long as the mmf distribution in the air-gap is sinusoidal. Both machines are considered here as induction motors. Spatial displacement between any two consecutive phases of the three-phase machine is $2\alpha = 120°$.

The control of the two motors is decoupled although they are supplied from a single six-phase source. The control decoupling is obtained by using indirect rotor field oriented control. Flux and torque of the six-phase machine are controllable by source *d-q* axis current components, while flux and torque of the three-phase machine can be controlled using source *x-y* current components. The detailed modeling and experimental results of this configuration are reported in reference [6.7], using current control in stationary reference frame. However, current control in rotating reference frame requires an appropriate PWM for six-phase source. This thesis presents as simple carrier-based PWM method for the three to six-phase Matrix Converters which has not reported so far.

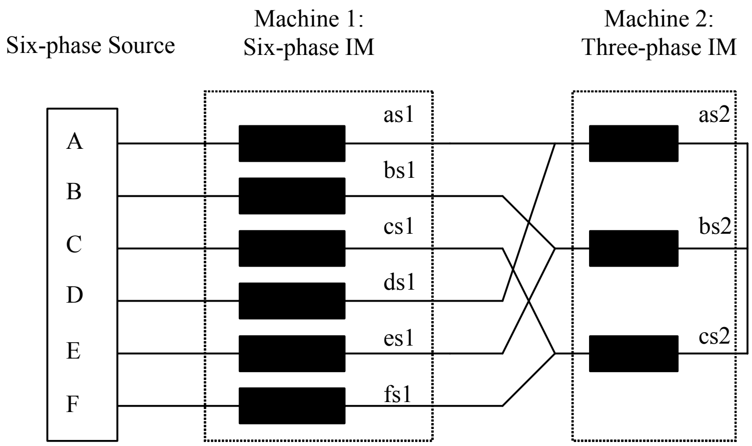

Fig. 6.26. Six-phase series-connected two-motor drive system.

6.6b Carrier-Based PWM Technique For Six-Phase Two-Motor Drive

The input and output voltages are related as:

$$\begin{bmatrix} V_A \\ V_B \\ V_C \\ V_D \\ V_E \\ V_F \end{bmatrix} = \begin{bmatrix} \delta_{aA} & \delta_{bA} & \delta_{cA} \\ \delta_{aB} & \delta_{bB} & \delta_{cB} \\ \delta_{aC} & \delta_{bC} & \delta_{cC} \\ \delta_{aD} & \delta_{bD} & \delta_{cD} \\ \delta_{aE} & \delta_{bE} & \delta_{cE} \\ \delta_{aF} & \delta_{bF} & \delta_{cF} \end{bmatrix} \begin{bmatrix} V_a \\ V_b \\ V_c \end{bmatrix} \tag{6.56}$$

Therefore, the phase A output voltage can be obtained by using the duty ratio matrix

$$\begin{aligned} V_A = k_A |V| [&\cos(\omega t) \bullet \cos(\omega t - \rho) + \cos(\omega t - 2\pi/3) \bullet \\ &\cos(\omega t - 2\pi/3 - \rho) + \cos(\omega t - 4\pi/3) \bullet \cos(\omega t - 4\pi/3 - \rho)] \end{aligned} \tag{6.57}$$

In equation (6.41), $\cos(\rho)$ term indicates that the output voltage is affected by ρ. The term k_A is defined in equation (6.59). Thus, the output voltage V_A is independent of the input frequency and only depends on the amplitude $|V|$ of the input voltage and k_A is a reference output voltage time-varying modulating signal for the output phase A with the desired output frequency $\omega_{o1} + \omega_{o2}$, ω_{o1} is the operating frequency of machine-1 or the first fundamental output frequency and ω_{o2} is the operating frequency of machine-2 or the second fundamental output frequency. The fundamental output voltage magnitude corresponding to ω_{o1} is given as m_1 and corresponding to ω_{o2} is given as m_2.The six-phase reference output voltages can then be represented as:

$$
\begin{aligned}
k_{A1} &= m_1 \cos(\omega_{o1} t), \\
k_{B1} &= m_1 \cos(\omega_{o1} t - 2\pi/6) \\
k_{C1} &= m_1 \cos(\omega_{o1} t - 4\pi/6) \\
k_{D1} &= m_1 \cos(\omega_{o1} t - 6\pi/6) \\
k_{E1} &= m_1 \cos(\omega_{o1} t - 8\pi/6) \\
k_{F1} &= m_1 \cos\left(\omega_{o1} t - 10\pi/6\right)
\end{aligned} \tag{6.58}
$$

$$
\begin{aligned}
k_{A2} &= m_2 \cos(\omega_{o2} t) \\
k_{B2} &= m_2 \cos(\omega_{o2} t - 2\pi/3) \\
k_{C2} &= m_2 \cos(\omega_{o2} t - 4\pi/3)
\end{aligned} \tag{6.59}
$$

6.6c Application of Offset Duty Ratio

For the switches connected to output phase-A, at any instant, the condition $0 \le \mathrm{d_{aA}}, \mathrm{d_{bA}}, \mathrm{d_{cA}} \le 1$ should be valid. Therefore, offset duty ratios should to be added to the existing duty-ratios, so that the net resultant duty-ratios of individual switches are always positive. Furthermore, the offset duty-ratios should be added equally to all the output phases to ensure that the effect of resultant output voltage vector produced by the offset duty-ratios is null in the load. That is, the offset duty-ratios can only add the common-mode voltages in the output. Considering the case of output phase-A:

$$
\begin{aligned}
k_A &= k_{A1} + \frac{1}{2} k_{A2} \\
k_B &= k_{B1} + \frac{1}{2} k_{B2} \\
k_C &= k_{C1} + \frac{1}{2} k_{C2} \\
k_D &= k_{D1} + \frac{1}{2} k_{A2} \\
k_E &= k_{E1} + \frac{1}{2} k_{B2} \\
k_F &= k_{F1} + \frac{1}{2} k_{C2}
\end{aligned} \tag{6.60}
$$

Therefore, from equation (6.60), the output voltages are obtained as:

$$
\begin{aligned}
V_A &= \left[\frac{3}{2} k_A |V| \cos(\rho)\right] \\
V_B &= \left[\frac{3}{2} k_B |V| \cos(\rho)\right] \\
V_C &= \left[\frac{3}{2} k_C |V| \cos(\rho)\right] \\
V_D &= \left[\frac{3}{2} k_D |V| \cos(\rho)\right] \\
V_E &= \left[\frac{3}{2} k_E |V| \cos(\rho)\right] \\
V_F &= \left[\frac{3}{2} k_F |V| \cos(\rho)\right]
\end{aligned} \tag{6.61}
$$

$$
\delta_{aA} + \delta_{bA} + \delta_{cA} = k_A \cos(\omega t - \rho) + k_A \cos(\omega t - 2\pi/3 - \rho) + k_A \cos(\omega t - 4\pi/3 - \rho) = 0 \tag{6.62}
$$

Absolute values of the duty-ratios are added to cancel the negative components from individual duty ratios. Thus the minimum individual offset duty ratios should be:

$$
\begin{aligned}
&D_a(t) = |\delta_{aA}| = |k_A \cos(\omega t - \rho)| \\
&D_b(t) = |\delta_{bA}| = |k_A \cos(\omega t - 2\pi/3 - \rho)| \\
&\textit{and} \\
&D_c(t) = |\delta_{cA}| = |k_A \cos(\omega t - 4\pi/3 - \rho)|
\end{aligned} \tag{6.63}
$$

The effective duty ratios are:

$$
\begin{aligned}
\delta'_{aA} &= \delta_{aA} + D_a(t), \\
\delta'_{bA} &= \delta_{bA} + D_b(t), \\
\delta'_{cA} &= \delta_{cA} + D_c(t)
\end{aligned} \tag{6.64}
$$

Other output phases can be written in the similar fashion. The net duty ratio $0 \le \delta'_{ak} \le 1$ should be within the range of 0 to 1.

For the worst case:

$$
0 \le 2.|k_A| \le 1 \tag{6.65}
$$

The maximum value of k_A is equal to 0.5. The duty-ratios are calculated for the other five output phases. In the section (6.6b), two offsets are added to the original duty ratios to form the following effective duty ratio for output phase p:

$$
\begin{aligned}
\Delta_{ap} &= D_a(t) + (1 - \{D_a(t) + D_b(t) + D_c(t)\})/3 + k_p \times \cos(\omega t - \rho) \\
\Delta_{bp} &= D_b(t) + (1 - \{D_a(t) + D_b(t) + D_c(t)\})/3 + k_p \times \cos(\omega t - 2\pi/3 - \rho) \\
\Delta_{cp} &= D_c(t) + (1 - \{D_a(t) + D_b(t) + D_c(t)\})/3 + k_p \times \cos(\omega t - 4\pi/3 - \rho)
\end{aligned} \tag{6.66}
$$

where $p \in A, B, C, D, E, F$

These duty ratios (equation 6.66) can be compared to the triangular carrier wave to generate the gating signals for the bi-directional power switches as shown in fig.6.27. The output phase voltage magnitude will reach 75% of the input voltage magnitude with this method.

A complete block schematic of the PWM signal generation is presented in Fig. 6.28. The reference voltages for two machines with the desired speeds and appropriate voltage magnitudes are generated. These references are then summed according to the phase transposition rule. The overall modulating signal thus generated is given to the PWM block. This PWM block then generate appropriate gate signals for the Matrix Converter. The Matrix Converter then produces appropriate voltages which drive the two series/parallel connected machines.

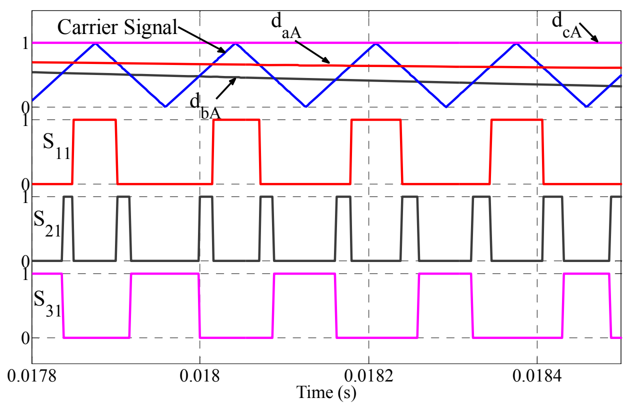

Fig. 6.27. Gate signal generation for output phase A.

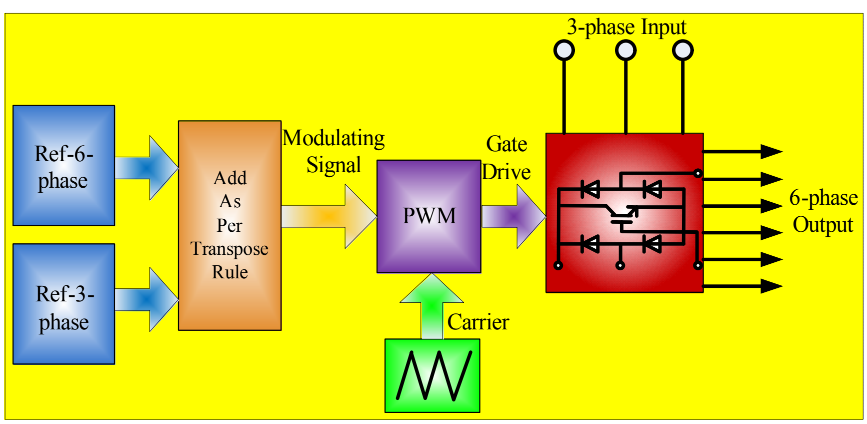

Fig. 6.28. Block diagram of Carrier-based PWM for two frequency output.

6.6d Simulation Results

MATLAB/SIMULINK model is developed for the proposed Matrix Converter control. The input voltage is fixed at 100 V to show the exact gain at the output side. The switching frequency of the devices is kept at 6 kHz. The purpose here is to show two fundamental components of current produced by the Matrix Converter. These voltage components are independent from each other and thus can independently control the two machines.

The results shown in this thesis is only limited to the production of the appropriate voltage components. The motor behaviour is not discussed in this thesis and will be reported separately. It is assumed that one voltage component has frequency of 25 Hz and second voltage component has 50 Hz. To respect the *v/f*=constant control the voltage magnitude of the lower frequency component is half compared to the higher frequency component. For the simulation purpose a R-L load is connected with R = 10 Ω and L = 10 mH. Simulation results are shown for the modulation with common mode voltage addition in the output target voltage. Thus the maximum output of the Matrix Converter is limited to 75 V as the input is 100 V.

The resulting waveforms are presented in Figs. 6.29 to 6.31. The input source side and converter side waveforms are presented in Fig. 6.29. The results clearly shows unity power factor at the input side. The converter side current shows PWM signal and the spectrum is clearly sinusoidal with no lower order harmonics. The output side filtered voltages are given in Fig. 6.30 and one phase filtered voltage and current is illustrated in Fig. 6.30. The spectrum of the output PWM signal voltages are presented in Fig. 6.31. The output filtered phase voltages shows superimposed fundamental and second harmonic components. The spectrum of phase 'A' voltage and the transformed voltage are given in Fig. 6.31. It is clearly evident that the phase 'A' voltage contains two fundamental components at 25 Hz and 50 Hz. These voltages are then decoupled and appear in α-β plane (50 Hz) and *x-y* plane (25 Hz). Thus is aim of the control is achieved. Also the magnitude of the two voltages follows *v/f*=constant rule.

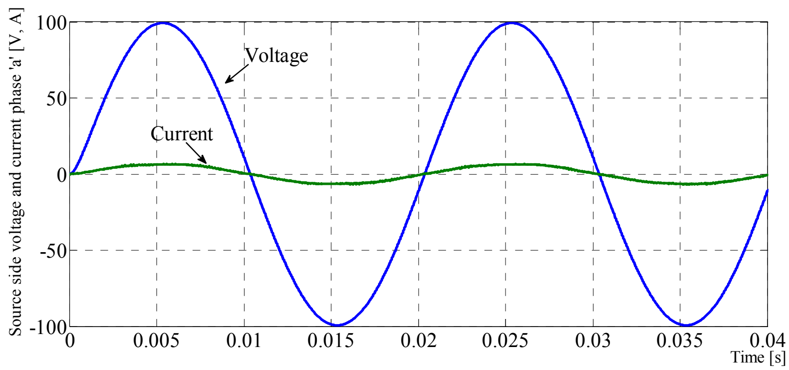

a.

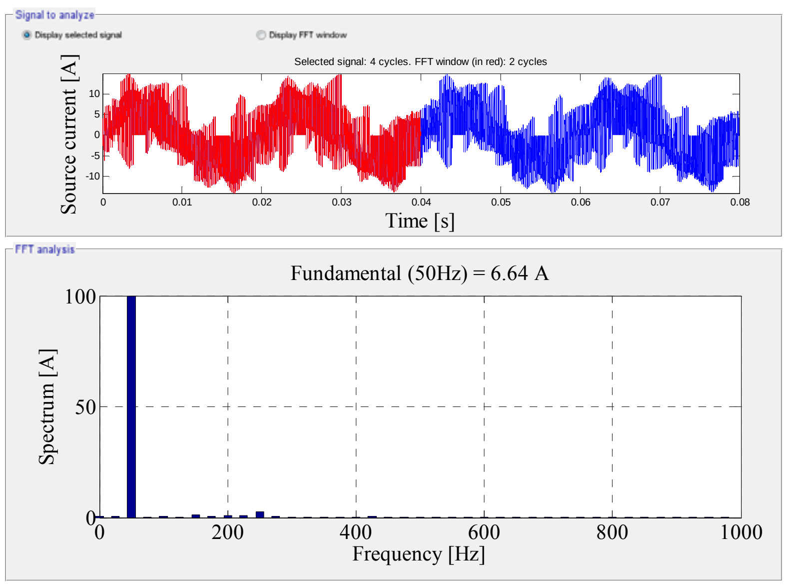

b.

Fig. 6.29 Input side waveforms of 3 to 5-phase Matrix Converter: (a) Input voltage and current, (b) Spectrum Input current.

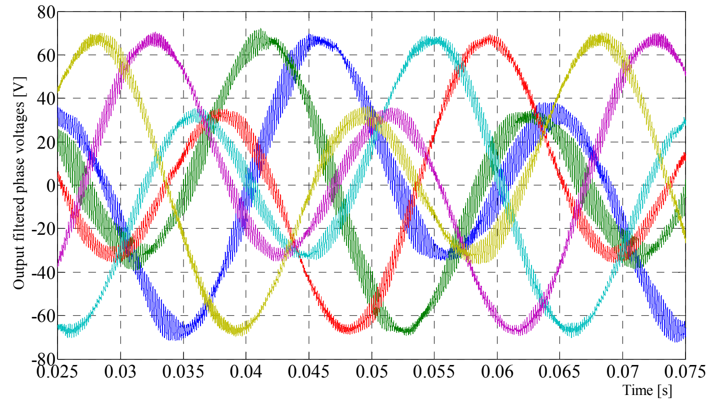

a.

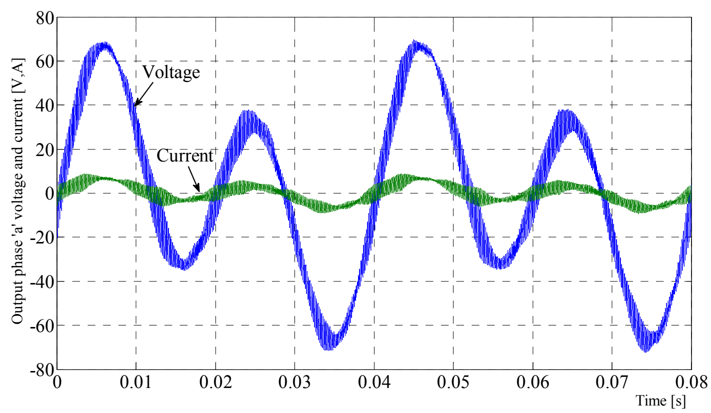

b.

Fig. 6.30. Output waveforms, a. filtered voltages, b. phase ‘a’ output filtered voltage and current.

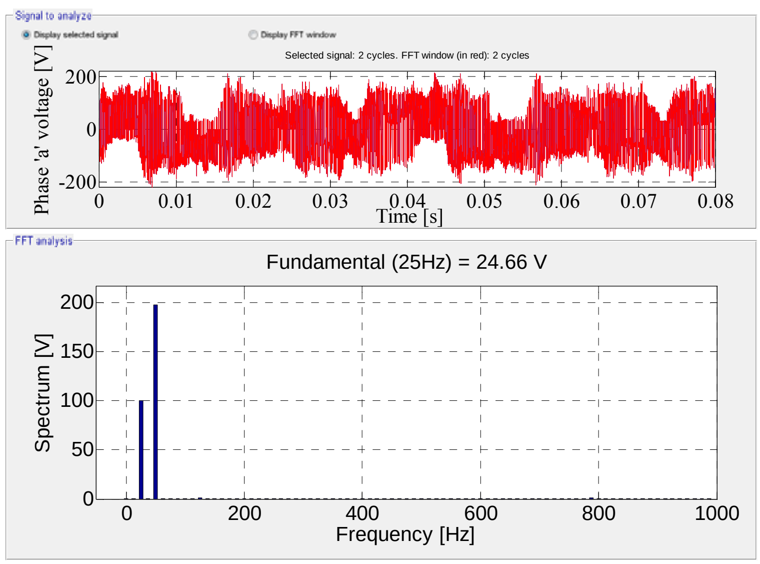

a.

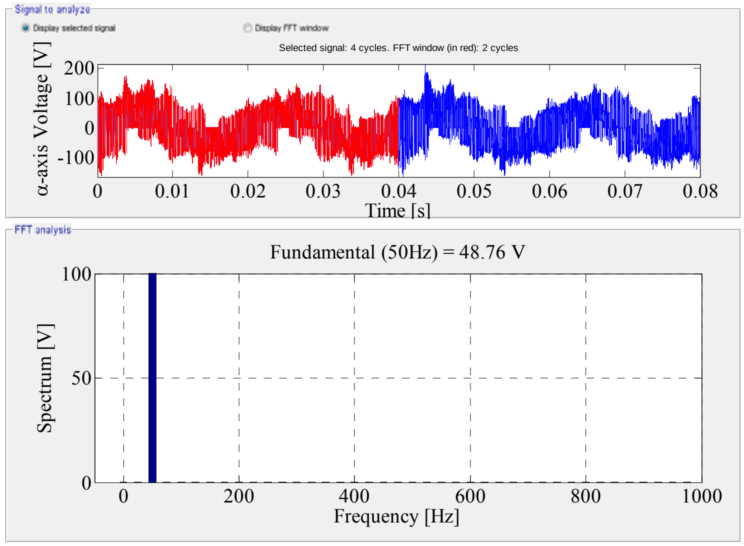

b.

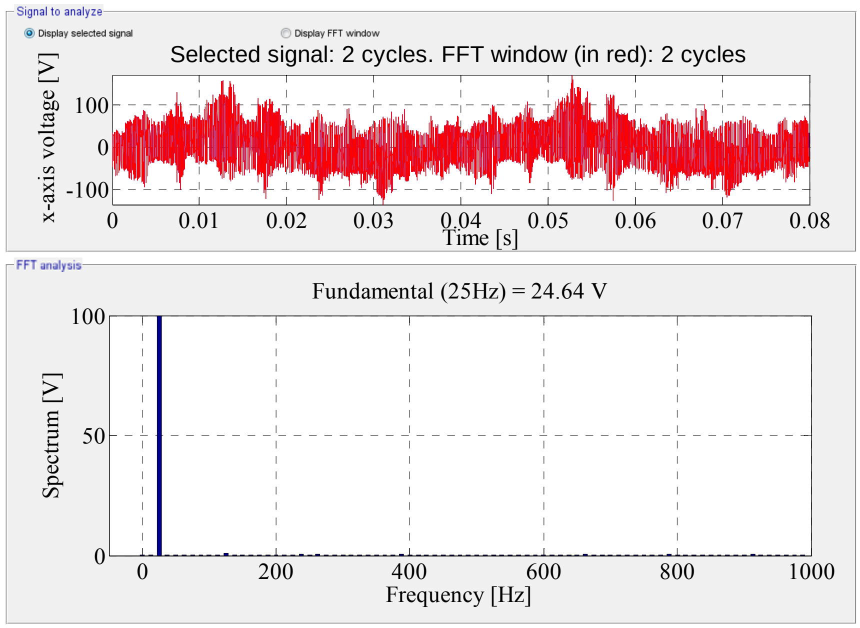

c.

Fig. 6.23. Spectrum of output voltages; a. phase 'A', b. α-axis voltage and c. x-axis voltage.

6.7 Carrier Based PWM Technique Strategies for a Three-to-Seven Phase Matrix Converter

The power circuit topology of a three-phase to seven-phase Matrix Converter is illustrated in Fig. 6.32. There are seven legs with each leg having three bi-directional power switches connected in series. Each power switch is bi-directional in nature with anti-parallel connected

IGBTs and diodes. The input is similar to a three-phase to three-phase Matrix Converter having LC filters and the output is seven phases with 51.4 degree phase displacement between each phases.

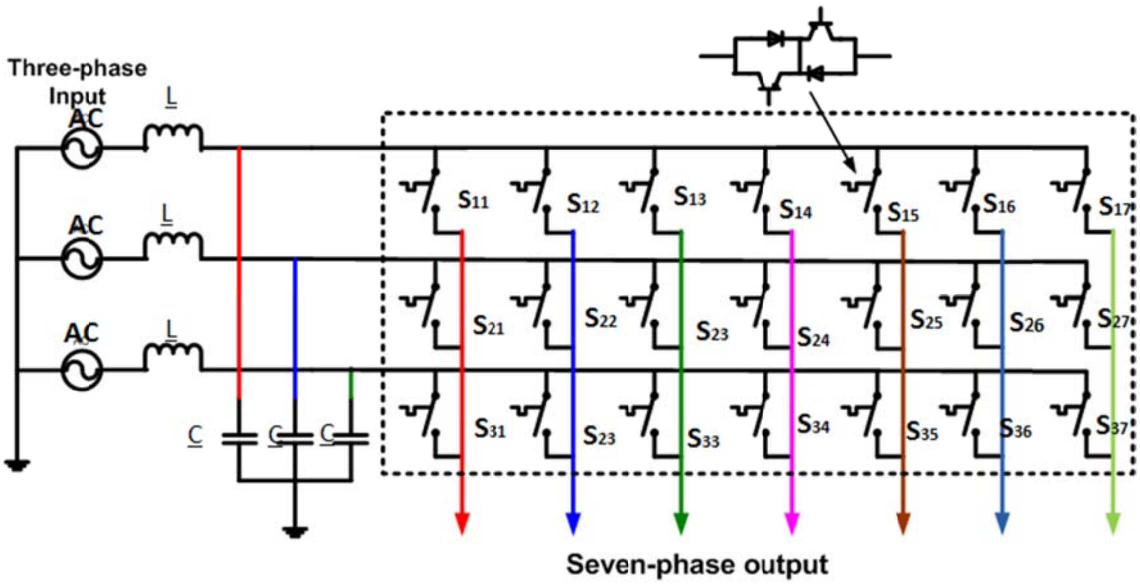

Fig. 6.32. Power Circuit topology of Three-phase to seven-phase Matrix Converter.

The 7-phase reference output voltages can be represented as:

$$\begin{aligned}
k_A &= m\cos(\omega_o t), \\
k_B &= m\cos(\omega_o t - 2\pi/7), \\
k_C &= m\cos(\omega_o t - 4\pi/7), \\
k_D &= m\cos(\omega_o t - 6\pi/7), \\
k_E &= m\cos(\omega_o t - 8\pi/7), \\
k_F &= m\cos(\omega_o t - 10\pi/7), \\
k_G &= m\cos(\omega_o t - 12\pi/7),
\end{aligned} \tag{6.67}$$

6.7a Application of Offset Duty Ratio

In the equation (6.67), duty-ratios become negative which are not practically realizable. For the switches connected to output phase-A, at any instant, the condition $0 \le d_{aA}, d_{bA}, d_{cA} \le 1$ should be valid. Therefore, offset duty ratios should to be added to the existing duty-ratios, so that the net resultant duty-ratios of individual switches are always positive. Furthermore, the offset duty-ratios should be added equally to all the output phases to ensure that the effect of resultant output voltage vector produced by the offset duty-ratios is null in the load. That is, the offset duty-ratios can only add the common-mode voltages in the output. Considering the case of output phase-A:

$$d_{aA}+d_{bA}+d_{cA}= k_A\cos(\omega t-\rho)+ \\ k_A\cos(\omega t-2\pi/3-\rho) \\ +k_A\cos(\omega t-4\pi/3-\rho)=0 \tag{6.69}$$

Absolute values of the duty-ratios are added to cancel the negative components from individual duty ratios. Thus the minimum individual offset duty ratios should be:

$$D_a(t)=\left|K_A cos(wt-\rho)\right| \\ D_b(t)=\left|K_A cos(wt-\frac{2\pi}{3}-\rho)\right| \\ D_b(t)=\left|K_A cos(wt-\frac{4\pi}{3}-\rho)\right| \tag{6.70}$$

The effective duty ratios are $d_{aA}+D_a(t), d_{bA}+D_b(t), d_{cA}+D_c(t)$. Other output phases can be written similarly. The net duty ratio $d_{aA}+D_a(t)$ should be accommodated within a range of 0 to 1. Therefore,

$0\le d_{aA}+D_a(t)\le 1$ can be written as:

$$0\le k_A\cos(\omega t-\rho)+\left|k_A\cos(\omega t-\rho)\right|\le 1 \tag{6.71}$$

For the worst case

$$0\le 2.\left|k_A\right|\le 2 \tag{6.72}$$

The maximum value of k_A or in other words k in equation (6.73) is equal to 0.5 or *sin(π/6)*. Hence the offset duty-ratios corresponding to the three input phases are chosen as:

$$D_a(t)=\left|0.5\cos(\omega t-\rho)\right|, \\ D_b(t)=\left|0.5\cos(\omega t-2\pi/3-\rho)\right| \\ and\ldots D_c(t)=\left|0.5\cos(\omega t-4\pi/3-\rho)\right| \tag{6.73}$$

The modified duty ratios for output phase A are:

$$d_{aA}= D_a(t)+k_A\cos(\omega t-\rho), \\ d_{bA}= D_b(t)+k_A\cos(\omega t-2\pi/3-\rho), \\ d_{cA}= D_c(t)+k_A\cos(\omega t-4\pi/3-\rho) \tag{6.74}$$

In any switching cycle the output phase should not be open circuited. Thus the sum of the duty ratios in equation (6.74) must equal to unity. But the summation $D_a(t)+D_b(t)+D_c(t)$ is less than or equal to unity. Hence another offset duty-ratio $\left[1-\{D_a(t)+D_b(t)+D_c(t)\}\right]/3$ is added to $D_a(t), D_b(t), D_c(t)$. The addition of this offset duty-ratio in all switches will maintain the output voltages and input currents are unaffected. The equation (6.74) derives the maximum modulation index for three phase input with seven phase output from equation (6.68) as $\frac{3}{2}k_A = \frac{3}{2}\times\sin(\frac{\pi}{6}) = 0.75 \text{ or } 75\%$.

If $k_A, k_B, k_C, k_D, k_E, k_F, k_G$ are chosen to be 7-phase sinusoidal references, the input voltage capability is not fully utilized for output voltage generation. To overcome this, an additional common mode term equal to $\{\max(k_A, k_B, k_C, k_D, k_E, k_F, k_G) + \min(k_A, k_B, k_C, k_D, k_E, k_F, k_G)\}/2]$ is added as in the carrier-based space-vector PWM principle as implemented in two-level inverters. Thus the amplitude of $(k_A, k_B, k_C, k_D, k_E, k_F, k_G)$ can be enhanced from 0.5 with 0.5129.This is shown in fig.6.33. for an output phase. Therefore the maximum modulation index that can be achieved in the linear modulation range with common mode addition is $\frac{3}{2}k_A = \frac{3}{2}\times 0.5129 = 0.7694 \text{ or } 76.94\%$.

In the section (6.7b) the analytical expressions are given for the case of a three to seven phase Matrix Converter.

6.7b Without Common-mode voltage addition

The duty ratio for output phase A can be written as:

$$\begin{aligned}
&d_{aA} = D_a(t) + (1 - \{D_a(t) + D_b(t) + D_c(t)\})/3 + \\
&k_A \times cos(\omega t - \rho) \\
&d_{bA} = D_a(t) + (1 - \{D_a(t) + D_b(t) + D_c(t)\})/3 + \\
&k_A \times cos(\omega t - 2\pi/3 - \rho) \\
&d_{cA} = D_a(t) + (1 - \{D_a(t) + D_b(t) + D_c(t)\})/3 + \\
&k_A \times cos(\omega t - 4\pi/3 - \rho)
\end{aligned} \tag{6.75}$$

6.7b With Common mode voltage Addition

The duty ratio for output phase A can be written as:

$$
\begin{aligned}
d_{aA} &= D_a(t) + (1 - \{D_a(t) + D_b(t) + D_c(t)\})/3 \\
&+ [k_A - \{\max(k_A, k_B, k_C, k_D, k_E, k_F, k_G) + \\
&\min(k_A, k_B, k_C, k_D, k_E, k_F, k_G)\}/2] \times \cos(\omega t - \rho) \\
d_{bA} &= D_a(t) + (1 - \{D_a(t) + D_b(t) + D_c(t)\})/3 \\
&+ [k_A - \{\max(k_A, k_B, k_C, k_D, k_E, k_F, k_G) + \\
&\min(k_A, k_B, k_C, k_D, k_E, k_F, k_G)\}/2] \times \cos(\omega t - 2\pi/3 - \rho) \\
d_{cA} &= D_a(t) + (1 - \{D_a(t) + D_b(t) + D_c(t)\})/3 \\
&+ [k_A - \{\max(k_A, k_B, k_C, k_D, k_E, k_F, k_G) + \\
&\min(k_A, k_B, k_C, k_D, k_E, k_F, k_G)\}/2] \times \cos(\omega t - 4\pi/3 - \rho)
\end{aligned}
\tag{6.76}
$$

where

$$
\begin{aligned}
D_a(t) &= |0.5\cos(\omega t - \rho)| \\
D_b(t) &= |0.5\cos(\omega t - 2\pi/3 - \rho)| \\
D_b(t) &= |0.5\cos(\omega t - 4\pi/3 - \rho)|
\end{aligned}
\qquad (6.77
$$

The seven-phase output voltages can be written as:

$$
\begin{aligned}
k_A &= m\cos(\omega_o t) \\
k_B &= m\cos(\omega_o t - 2\pi/7) \\
k_C &= m\cos(\omega_o t - 4\pi/7) \\
k_D &= m\cos(\omega_o t - 6\pi/7) \\
k_E &= m\cos(\omega_o t - 8\pi/7) \\
k_F &= m\cos(\omega_o t - 10\pi/7) \\
k_G &= m\cos(\omega_o t - 12\pi/7)
\end{aligned}
\tag{6.78}
$$

where ω is input frequency and ω_o is the output frequency, m is the modulation index. For unity power factor ρ has to be chosen zero.

6.7c Simulation Results

MATLAB/SIMULINK model is developed for the proposed three to seven-phase Matrix Converter control. The input voltage is fixed at 100 V to show the exact gain at the output side. The switching frequency of the devices is kept at 6 kHz. The fundamental frequency of the output is chosen as 25 Hz. Simulation results are shown for the modulation with common mode voltage addition in the output target voltage. The resulting waveforms are presented in Figs. 6.33 - 6.34. The results of source voltage and source current clearly shows unity power factor at the source side, Fig. 6.33. The filtered output seven-phase voltages are shown in Fig. 6.33 and are seen to be as sinusoidal. The magnitude of the fundamental component proves the enhanced output without any lower-order harmonics. This indicates the viability of the proposed modulation technique. Both simulation as well as experimental results are taken using sample time of 50 microsecond.

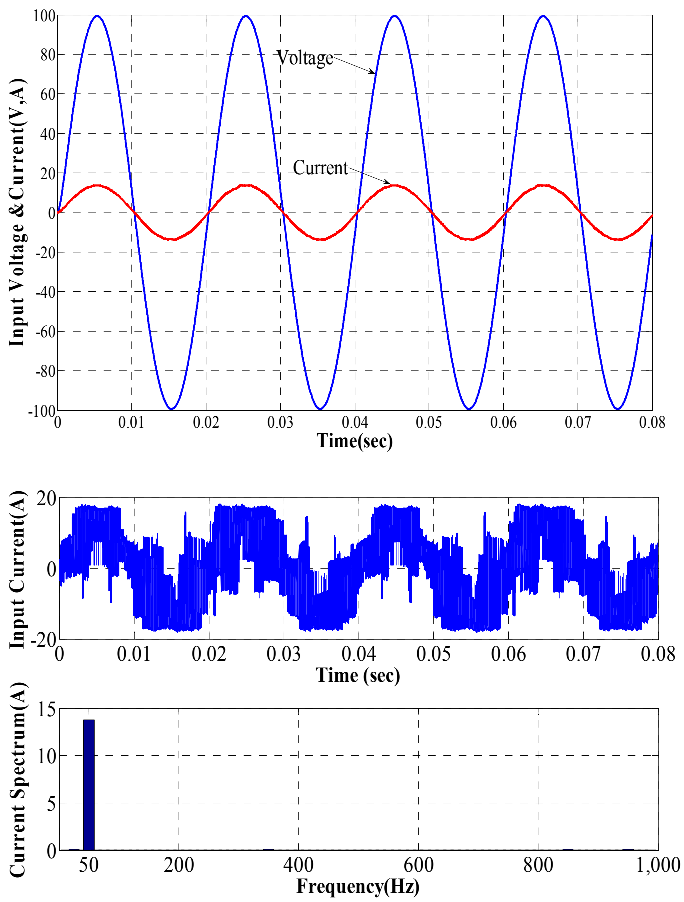

Fig. 6.33. Input side waveforms of 3 to 7-phase Matrix Converter.

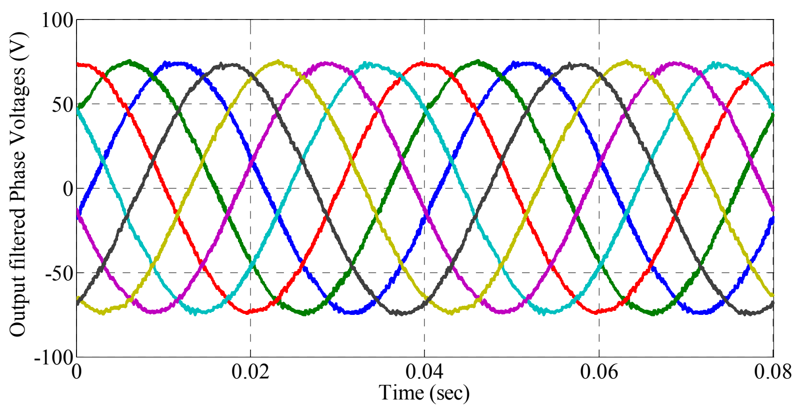

Fig. 6.34. Output side waveforms of 3 to 7-phase Matrix Converter, seven-phase filtered output phase voltages.

The results with input side over modulation are presented in Fig. 6.35 and 6.36. The distortion in the source side current is clearly visible in Fig. 6.35. Additionally the distortion in the load current is also evident from Fig. 6.35. The distortion in the voltage can be seen form Fig. 6.36.

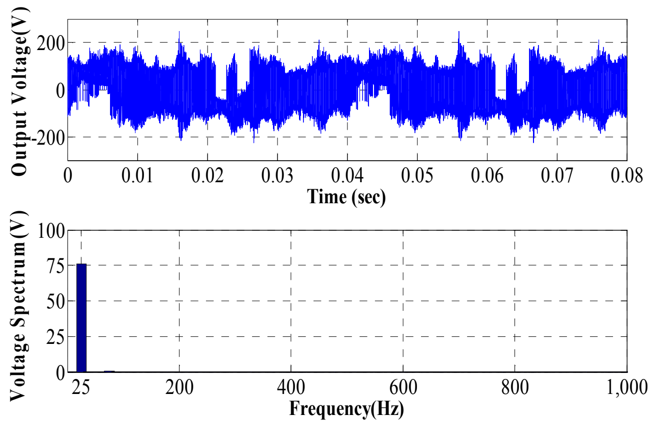

Fig. 6.35 Spectrum output voltage.

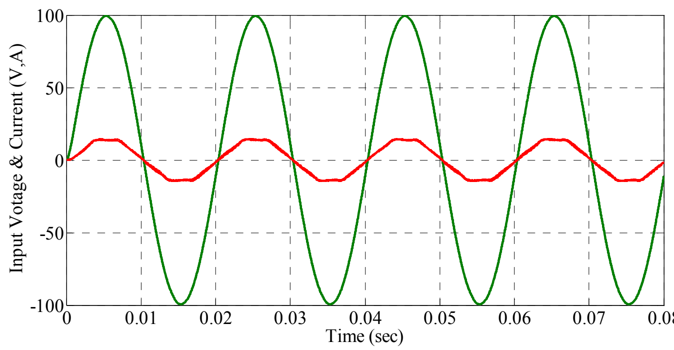

Fig. 6.36. Input side waveforms of 3 to 7-phase Matrix Converter: Voltage and current with input side over-modulation.

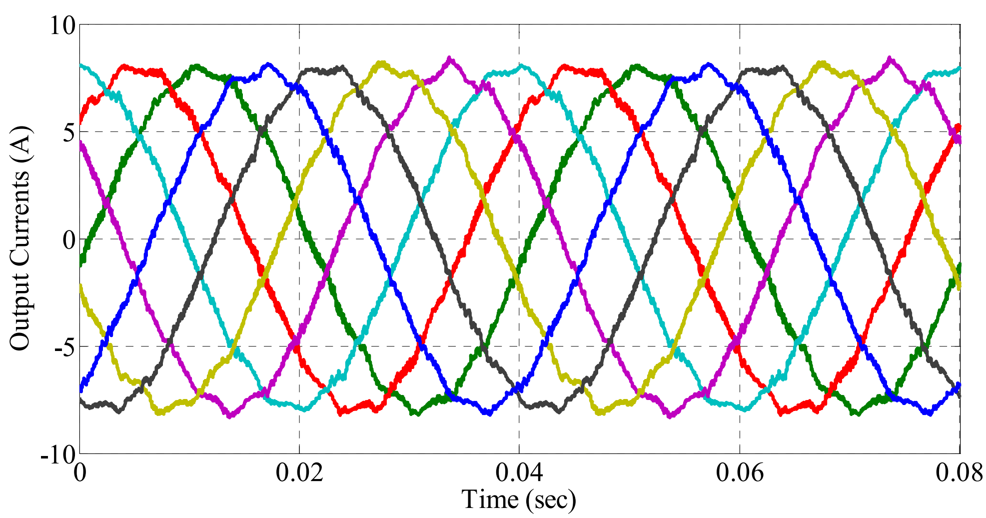

Fig. 6.37. Output side current waveforms of 3 to 7-phase Matrix Converter with input side over-modulation.

The THD output current with and without over modulation are 2.82% and 2%, respectively. While the THD of the input current with and without over modulation are 7.53% and 1.65%, respectively.

6.8 Seven-Phase Series Connected Three-Motor Drive System

The three-motor drive, used in the reference [6.8], is shown in Figure 6.38. Stator windings of the three machines are connected in series with appropriate phase transposition. The seven-phase machine has the spatial displacement between any two consecutive stator phases of (i.e. $\alpha = 2\pi/7$). It is to be noted here that the proposed PWM scheme is equally valid for series connection as well as parallel connection; however, only series-connected drive is elaborated here.

When the phase variable equations are transformed using decoupling matrix, four sets of equations are obtained, namely *d-q*, x_1-y_1, x_2-y_2 and zero sequence. In single seven-phase motor drive, the *d-q* components are involved in actual electromagnetic energy conversion while the x_1-y_1 and x_2-y_2 components increase the thermal loading of the machine. However, the extra set of current components (x_1-y_1 and x_2-y_2) available in a seven-phase system is effectively utilised in independently controlling two additional seven-phase machines when the stator windings of three seven-phase machines are connected in series and are supplied from a single seven-phase VSI. Reference currents/voltages generated by three independent vector controllers, are summed up as per the transposition rules and are supplied to the series-connected connected seven-phase machines. Block diagram of the three-motor drive systems is illustrated in Fig. 6.38 for series connection and the connectivity matrix is in Table 6.2.

Table 6.2. Connectivity matrix for the seven-phase series connected three-motor case**.**

	A	B	C	D	E	F	G
M1	1	2	3	4	5	6	7
M2	1	3	5	7	2	4	6
M3	1	4	7	3	6	2	5

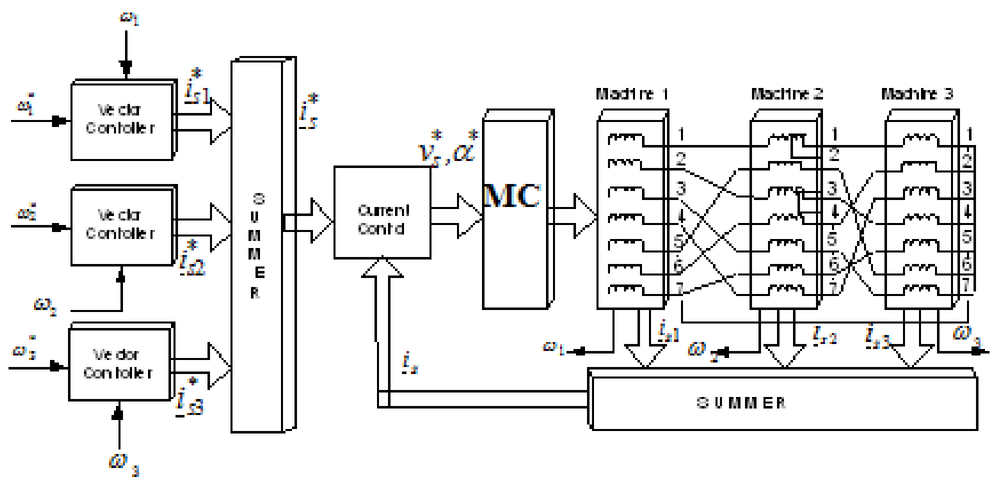

Fig. 6.38. Seven-phase series-connected three-motor drive structure.

The scheme of series-connected seven-phase three-motor drive discussed in the reference [6.8] utilizes current control in the stationary reference frame. However, if current control in the rotating reference frame is to be utilized, appropriate PWM scheme for seven-phase VSI needs to be developed to generate voltage references instead of current references.

6.8a Carrier-Based Pulse Width Modulation Technique

Carrier-based PWM scheme developed in this section follows the similar concept presented in reference [6.5]. Since the Matrix Converter output voltages with frequency decoupled from the input voltages, the duty ratios of the switches are to be calculated accordingly. The seven-phase output voltage duty ratios should be calculated in such a way that output voltages remain independent of input frequency. In a different way the seven-phase output voltages can be considered in synchronous reference frame and the three-phase input voltages can be considered to be in stationary reference frame, so that the input frequency term will be absent in output voltages. Considering the above points duty ratios of output phase j where are chosen as:

$$\begin{aligned} \delta_{ak} &= k_j \cos(\omega t - \rho), \\ \delta_{bk} &= k_j \cos(\omega t - 2\pi/3 - \rho), \\ \delta_{ck} &= k_j \cos(\omega t - 4\pi/3 - \rho) \end{aligned} \tag{6.79}$$

Therefore the phase A output voltage can be obtained by using the above duty ratios as:

$$\begin{aligned} v_A = k_A \vec{V}[&\cos(\omega t) \bullet \cos(\omega t - \rho) \\ &+ \cos(\omega t - 2\pi/3) \bullet \cos(\omega t - 2\pi/3 - \rho) \\ &+ \cos(\omega t - 4\pi/3) \bullet \cos(\omega t - 4\pi/3 - \rho)] \end{aligned} \tag{6.80}$$

The individual references of three machines are considered as:

$$\begin{aligned}
k_{A1} &= m_1 \cos(\omega_o t), \\
k_{B1} &= m_1 \cos(\omega_o t - 2\pi/7), \\
k_{C1} &= m_1 \cos(\omega_o t - 4\pi/7), \\
k_{D1} &= m_1 \cos(\omega_o t - 6\pi/7), \\
k_{E1} &= m_1 \cos(\omega_o t - 8\pi/7), \\
k_{F1} &= m_1 \cos(\omega_o t - 10\pi/7), \\
k_{G1} &= m_1 \cos(\omega_o t - 12\pi/7),
\end{aligned} \tag{6.81}$$

$$\begin{aligned}
k_{A2} &= m_2 \cos(\omega_o t + \vartheta), \\
k_{B2} &= m_2 \cos(\omega_o t - 2\pi/7 + \vartheta), \\
k_{C2} &= m_2 \cos(\omega_o t - 4\pi/7 + \vartheta), \\
k_{D2} &= m_2 \cos(\omega_o t - 6\pi/7 + \vartheta), \\
k_{E2} &= m_2 \cos(\omega_o t - 8\pi/7 + \vartheta), \\
k_{F2} &= m_2 \cos(\omega_o t - 10\pi/7 + \vartheta), \\
k_{G2} &= m_2 \cos(\omega_o t - 12\pi/7 + \vartheta),
\end{aligned} \tag{6.82}$$

$$\begin{aligned}
k_{A3} &= m_3 \cos(\omega_o t + \varphi), \\
k_{B3} &= m_3 \cos(\omega_o t - 2\pi/7 + \varphi), \\
k_{C3} &= m_3 \cos(\omega_o t - 4\pi/7 + \varphi), \\
k_{D3} &= m_3 \cos(\omega_o t - 6\pi/7 + \varphi), \\
k_{E3} &= m_3 \cos(\omega_o t - 8\pi/7 + \varphi), \\
k_{F3} &= m_3 \cos(\omega_o t - 10\pi/7 + \varphi), \\
k_{G3} &= m_3 \cos(\omega_o t - 12\pi/7 + \varphi),
\end{aligned} \tag{6.83}$$

Since the three machines are connected in series with phase transposition, the references should also be created accordingly as given in the following equation:

$$\begin{aligned}
k_A &= k_{A1} + k_{A2} + k_{A3} \\
k_B &= k_{B1} + k_{C2} + k_{D3} \\
k_C &= k_{C1} + k_{E2} + k_{G3} \\
k_D &= k_{D1} + k_{G2} + k_{C3} \\
k_E &= k_{E1} + k_{B2} + k_{F3} \\
k_F &= k_{F1} + k_{D2} + k_{B3} \\
k_G &= k_{G1} + k_{F2} + k_{E3}
\end{aligned} \tag{6.84}$$

The output voltage in phase-A is:

$$v_A = \left[\frac{3}{2} k_A \vec{V} \cos(\rho)\right]\left(\cos\left(\omega_{o1} t\right) + \cos\left(\omega_{o2} t + \vartheta\right) + \cos\left(\omega_{o3} t + \varphi\right)\right) \tag{6.85}$$

Similarly, the relationship for other six phases can be written. For the switches connected to output phase-A, at any instant, the condition $0 \le \delta_{aA}, \delta_{bA}, \delta_{cA} \le 1$ should be valid. Therefore, offset duty ratios should to be added to the existing duty-ratios, so that the net resultant duty-ratios of individual switches are always positive. Furthermore, the offset duty-ratios should be added equally to all the output phases to ensure that the effect of resultant output voltage vector produced by the offset duty-ratios is null in the load. That is, the offset duty-ratios can only add the common-mode voltages in the output. Considering the case of output phase-A:

$$\begin{aligned} \delta_{aA} + \delta_{bA} + \delta_{cA} &= k_A \cos(\omega t - \rho) + k_A \cos\left(\omega t - \frac{2\pi}{3} - \rho\right) \\ &+ k_A \cos\left(\omega t - \frac{4\pi}{3} - \rho\right) = 0 \end{aligned} \tag{6.86}$$

Absolute values of the duty-ratios are added to cancel the negative components from individual duty ratios. Thus the minimum individual offset duty ratios should be

$$\begin{aligned} & D_a(t) = \left|k_A \cos(\omega t - \rho)\right|, D_b(t) = \left|k_A \cos(\omega t - 2\pi/3 - \rho)\right| \\ & and \ldots D_c(t) = \left|k_A \cos(\omega t - 4\pi/3 - \rho)\right| \end{aligned} \tag{6.87}$$

The effective duty ratios are $\delta_{aA} + D_a(t), \delta_{bA} + D_b(t), \delta_{cA} + D_c(t)$, Other output phases can be written similarly. The net duty ratio $\delta_{aA} + D_a(t)$ should be accommodated within a range of 0 to 1. Therefore $0 \le \delta_{aA} + D_a(t) \le 1$ can be written as $0 \le k_A \cos(\omega t - \rho) + \left|k_A \cos(\omega t - \rho)\right| \le 1$

The maximum value of k_A is equal to 0.5. Hence the offset duty-ratios corresponding to the three input phases are chosen as:

$$\begin{aligned} & D_a(t) = \left|0.5\cos(\omega t - \rho)\right|, \\ & D_b(t) = \left|0.5\cos(\omega t - 2\pi/3 - \rho)\right| \\ & and \ldots D_c(t) = \left|0.5\cos(\omega t - 4\pi/3 - \rho)\right| \end{aligned} \tag{6.88}$$

The modified duty ratios for output phase A are

$$\begin{aligned} & \delta_{aA} = D_a(t) + k_A \cos(\omega t - \rho), \\ & \delta_{bA} = D_b(t) + k_A \cos(\omega t - 2\pi/3 - \rho), \\ & \delta_{cA} = D_c(t) + k_A \cos(\omega t - 4\pi/3 - \rho) \end{aligned} \tag{6.89}$$

In any switching cycle the output phase has to be connected to any of the input phases. The summation of the duty ratios in equation (6.89) must equal to unity. But the summation

$D_a(t)+D_b(t)+D_c(t)$ is less than or equal to unity. Hence another offset duty-ratio $[1-\{D_a(t)+D_b(t)+D_c(t)\}]/3$ is added to $D_a(t),\ D_b(t)\ and\ D_c(t)$ in equation (6.89). The addition of this offset duty-ratio in all switches will maintain the output voltages and input currents unaffected. Similarly, the duty-ratios are calculated for the other output phases.

If $k_A, k_B, k_C, k_D, k_E, k_F, k_G$ are chosen to be 7-phase sinusoidal references as given in equation (6.85), the input voltage capability is not fully utilized for output voltage generation. To overcome this, an additional common mode term equal to $\{\max(k_A,k_B,k_C,k_D,k_E,k_F,k_G)+\min(k_A,k_B,k_C,k_D,k_E,k_F,k_G)\}/2]$ is added as in the carrier-based space-vector PWM principle as implemented in two-level inverters. Thus the amplitude of $(k_A,k_B,k_C,k_D,k_E,k_F,k_G)$ can be enhanced from 0.5 with 0.5129.

The duty ratio for output phase A can be written as:

$$\begin{aligned}
&\delta_{aA} = D_a(t) + (1-\{D_a(t)+D_b(t)+D_c(t)\})/3 \\
&+[k_A - \{\max(k_A,k_B,k_C,k_D,k_E,k_F,k_G)+ \\
&\min(k_A,k_B,k_C,k_D,k_E,k_F,k_G)\}/2]\times\cos(\omega t-\rho) \\
&\delta_{bA} = D_a(t) + (1-\{D_a(t)+D_b(t)+D_c(t)\})/3 \\
&+[k_A - \{\max(k_A,k_B,k_C,k_D,k_E,k_F,k_G)+ \\
&\min(k_A,k_B,k_C,k_D,k_E,k_F,k_G)\}/2]\times\cos(\omega t-2\pi/3-\rho) \\
&\delta_{cA} = D_a(t) + (1-\{D_a(t)+D_b(t)+D_c(t)\})/3 \\
&+[k_A - \{\max(k_A,k_B,k_C,k_D,k_E,k_F,k_G)+ \\
&\min(k_A,k_B,k_C,k_D,k_E,k_F,k_G)\}/2]\times\cos(\omega t-4\pi/3-\rho)
\end{aligned} \tag{6.90}$$

where

$$\begin{aligned}
D_a(t) &= |0.5\cos(\omega t-\rho)| \\
D_b(t) &= |0.5\cos(\omega t-2\pi/3-\rho)| \\
D_b(t) &= |0.5\cos(\omega t-4\pi/3-\rho)|
\end{aligned} \tag{6.91}$$

6.8b Simulation Results

MATLAB/SIMULINK model is developed for the proposed Matrix Converter control. The input voltage is fixed at 100 V to show the ratio of output to input voltage gain. The switching frequency of the devices is chosen as 6 kHz. The purpose here is to show three fundamental components of current/voltage produced by the seven-phase Matrix Converter. These voltage components are independent from each other and thus can independently control the three machines whose stator windings are connected in series. The results shown here is only limited to the production of the appropriate voltage components. The motor behavior is not discussed here. The objective of controlling three machines will be accomplished if three independent voltages with different frequency components are generated.

6.8c Independent Control at Identical Frequencies

It is assumed, that the three supplied machines operate at same speeds. To fulfil such requirement, Matrix Converter needs to generate three independent frequency output in the output voltage waveforms. To prove the concept of decoupled control, simple R-L load is considered. The requirement imposed on the Matrix Converter, is the generation of three independent frequency component in three orthogonal planes (i.e. in *d-q, x1-y1* and *x2-y2*). The fundamental frequency is chosen as 50 Hz for all the three motors. For the simulation purpose a R-L load is connected with R = 10 Ω and L = 10 mH. Simulation results are shown for the modulation with common mode voltage addition in the output target voltage. Thus the maximum output of the Matrix Converter is limited to 75 V as the input is 100 V.

The resulting waveforms are presented in Figs. 6.39 to 6.41. The input source side voltage and currents waveforms are presented in Fig. 6.39. The result waveforms show unity power factor operation of the Matrix Converter. The output side filtered voltages are given in Fig. 6.40 The spectrum of the output PWM signal voltages are presented in Fig. 6.41. The spectrum of phase ‘A’ voltage is clearly evident that the phase ‘A’ voltage contains three fundamental components at 50 Hz (i.e. the sum of the three voltages at the same frequency). These voltages are then transformed to show in *d-q* plane (50 Hz), *x1-y1* plane (50 Hz) and *x2-y2* plane (50 Hz).

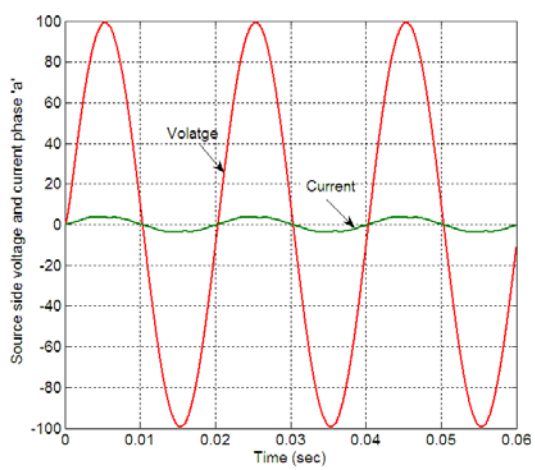

Fig. 6.39. Input side waveforms of 3 to 7-phase Matrix Converter.

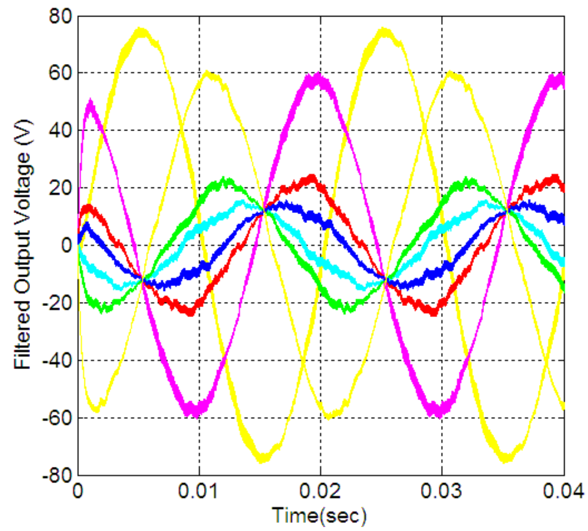

Fig. 6.40. Output waveforms, filtered output voltages.

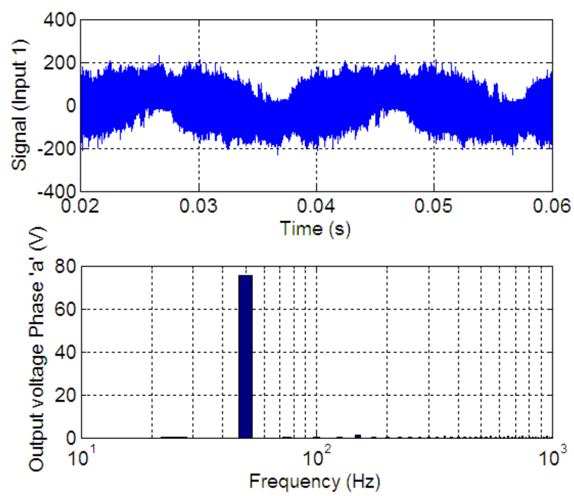

a.

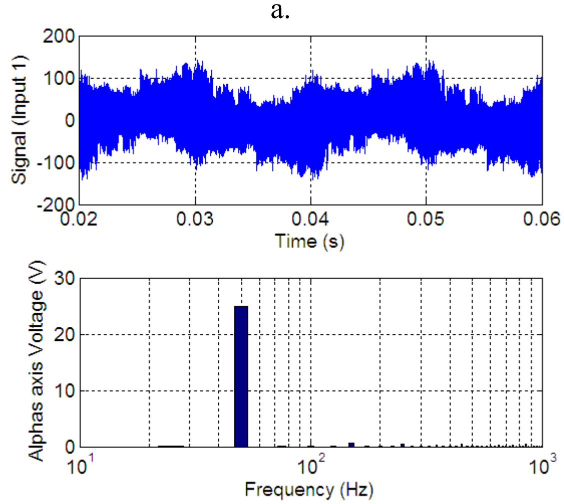

b.

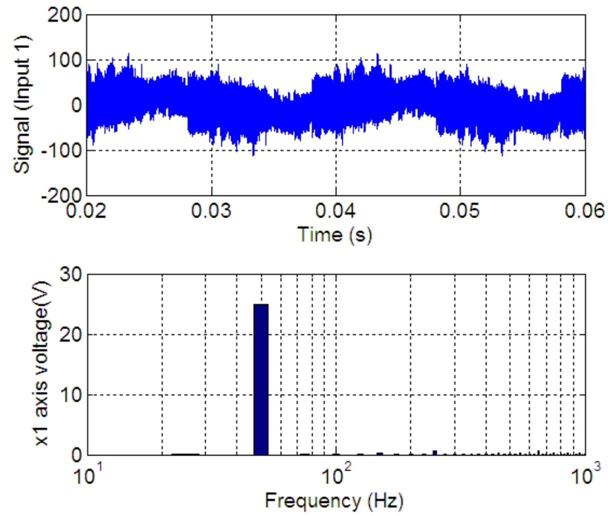

c.

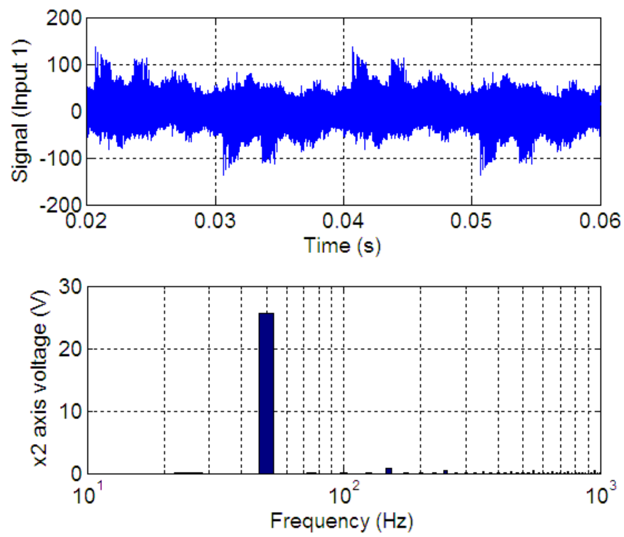

d.

Fig. 6.24. Spectrum of output voltages; a. phase ‘A’, b. α-axis voltage c. x1-axis voltage, d. x2-axis voltage.

Two more performance indices for comparison purpose are considered namely Total Harmonic Distortion (THD) and Weighted Total Harmonic Distortion (WTHD). The method of comparing the effectiveness of modulation is by comparing the unwanted components i.e. the distortion in the output voltage or current waveform, relative to that of an ideal sine wave, it can be assumed that by proper control, the positive and negative portions of the output are symmetrical (no DC or even harmonics).

Normalizing this expression of THD with respect to the quantity (V_1) i.e. fundamental, the weighted total harmonic distortion (WTHD) becomes defined as

$$WTHD = \frac{\sqrt{\sum_{n=3,5,7..}^{\infty}\left(\frac{V_n}{n}\right)^2}}{V_1} \tag{6.92}$$

For d-axis output voltage having a single component at 50 Hz frequency of magnitude 24.96 V and has THD = 4.38% of the fundamental and WTHD = 2.46% of the fundamental. For x1-axis output voltage having a single component at 50 Hz frequency of magnitude 24.96 V and has THD = 4.30% of the fundamental and WTHD = 1.93% of the fundamental. For x2-axis output voltage having a single component at 50 Hz frequency of magnitude 25.55Vand has THD = 4.64% of the fundamental and WTHD = 2.63 % of the fundamental. It shows that the output voltage is nearly equal to the sinusoidal value. Thus aim of the control is achieved.

6.8d Independent Control at Three Different Frequencies

It is assumed that one machine is running at rated speed and the second machine at half of the rated and third at one fourth of the rated. One voltage component has frequency of 12.5 Hz, second voltage component has frequency of 25 Hz and third voltage component has 50 Hz. To respect the *v/f*=constant control the voltage magnitude of the lower frequency component has compared to the higher frequency component with appropriate ratio.

The resulting waveforms are presented in Figs. 6.42 to 6.43. The spectrum of the output PWM signal of phase 'A' voltage and the transformed voltage are given in Fig. 6.42. It is clearly evident that the phase 'A' voltage contains three fundamental components at 12.5 Hz, 25 Hz and 50 Hz. These voltages are then decoupled and appear in α-β plane (12.5 Hz), x1-y1 plane (50 Hz) and x2-y2 plane (25 Hz). This shows independent control or decoupled control.

The Matrix Converter alpha-axis phase 'A' voltage in Fig. 6.42a. shows that it contains a single component at 12.5 Hz frequency with a magnitude of 5.49 V and has THD = 4.80% of the fundamental and WTHD = 4.10 % of the fundamental. Fig. 6.38(c) shows single component at 50 Hz frequency with a magnitude of 28.26 V in x_1-y_1 axis and has THD = 1.84 % of the fundamental and WTHD = 1.36 % of the fundamental. and Fig. 6.38(d) shows single component at 25 Hz frequency with a magnitude of 17.34 V in x_2-y_2 axis and has THD = 4.31% of the fundamental and WTHD = 4.20 % of the fundamental.

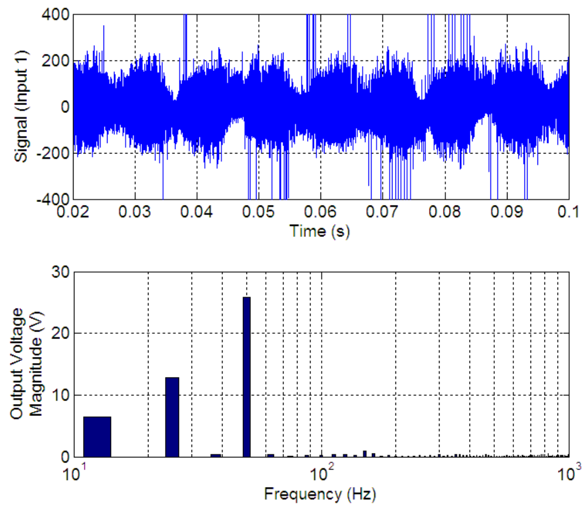
Signal (Input 1)
Time (s)
Output Voltage Magnitude (V)
Frequency (Hz)
a.

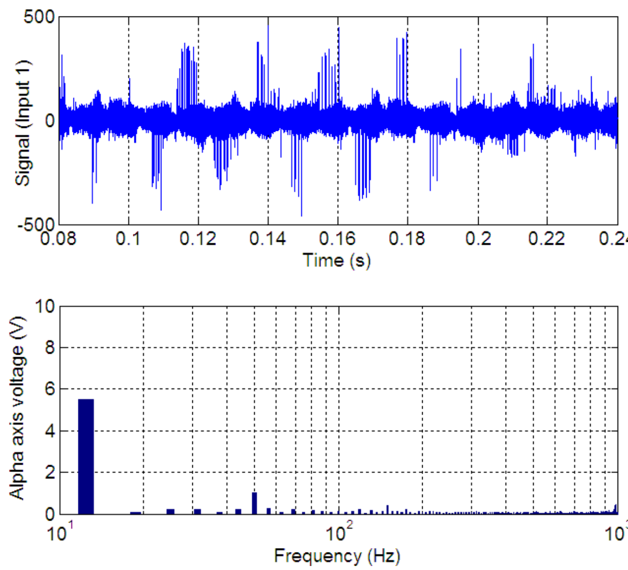
Signal (Input 1)
Time (s)
Alpha axis voltage (V)
Frequency (Hz)
b.

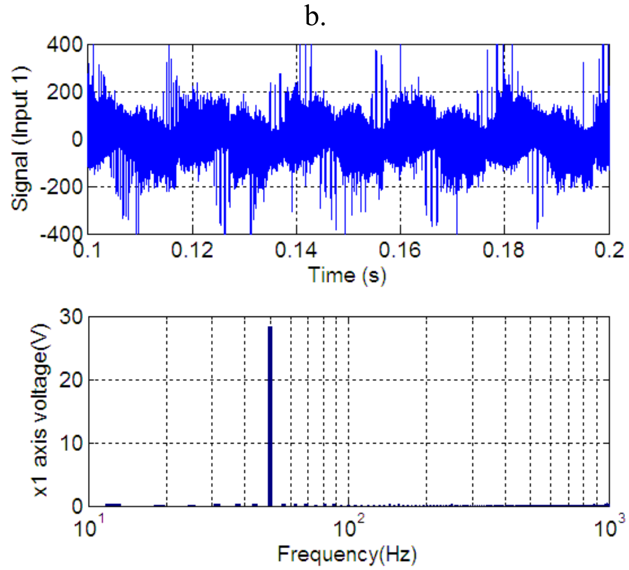
Signal (Input 1)
Time (s)
x1 axis voltage(V)
Frequency(Hz)
c.

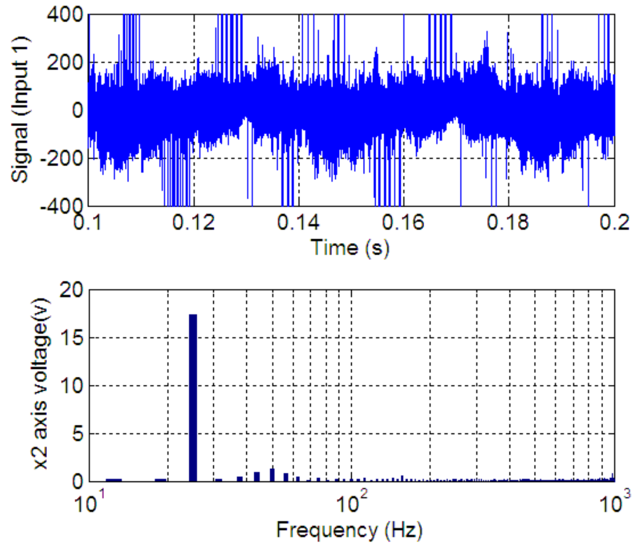

d.

Fig. 6.42. Spectrum of output voltages; a). phase ‘A’, b). α-axis voltage c). x1-axis voltage d). x2 - axis voltage.

Fig. 6.43 is showing the filtered output phase ‘a’ volatge of the seven phases after connecteing RL load at the output terminals.

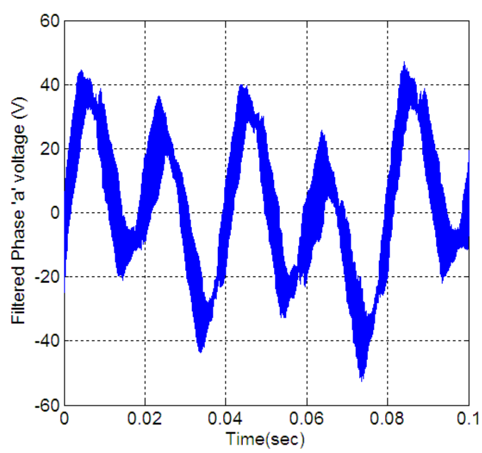

Fig. 6.25. Output waveforms, filtered output phase ‘a’ voltage.

6.9 Experimental Investigation

This section describes the experimental set-up that is developed for the validation of the simulation results and also the experimental results are shown.

6.9a Experimental Set-up

A prototype three-phase to nine-phase Matrix Converter is developed where input is three-phase and the output can be configured from single to nine phases. This is done in order to develop a modular multi-phase Matrix Converter where variety of experiments can be conducted. The set-up consists of hardware and software part. Hardware is related to the power switching devices that are arranged in the 3 x 9 array with associated auxiliaries such as input side filter and clamp circuit for protection. To control this Matrix Converter, control platform based on DSP/FPGA combination is developed. Since the DSP solution alone cannot be used for this application due to limited number of available PWM channels in a DSP chip. Hence, a solution is developed that is based on the integration of DSP and FPGA chip, where the processing is done in DSP core while the PWM is generated from FPGA. This is the most suitable control platform that can be developed for such complex system. The DSP/FPGA can be coded either in C++ using code compose studio compiler or in system generator from Xilinx. The DSP/FPGA board is interfaced with the PC using JTag emulator.

The proposed carrier based modulation scheme and direct duty ratio based PWM are implemented for three to five- phase and three-to-six phase in quasi configuration Matrix Converter for single and two-frequency output. The results of carrier-based scheme are shown in this chapter while the results of direct duty ratio based PWM is reported in Chapter 7.

The overall block schematic of the experimental set-up is presented in Fig. 6.44. The block diagram of the power module (3 x 9 phase Matrix Converter) is presented in Fig. 6.45 and detailed drawing is shown in Fig. 6.46. The pictorial views of different components are given in Fig. 6.47.

The power module is bi-directional switch FIO 50-12BD from IXYS and is composed of a diagonal IGBT and fast diode bridge in ISOPLUS i4-PAC™as shown in Fig. 6.48. The voltage blocking capability of the device is 1200 V and the current capacity is 50A. It controls bi-directional current flow by a single control signal. This comes in single chip with five output pins; four for the diode bridge and one for the gate drive of the IGBT. The advantage of this bi-directional power switch is the decreased number of IGBTs which is a major issue for multi-phase operation, but the major disadvantage is the higher conduction losses and the two-step commutation. The Matrix Converter consists of eighteen such bi-directional power switches.

Extra line inductances are used for safe operation during the overlapping of current commutation. Dead-time compensation is done along with snubbers and clamping circuit.

Input filter are used to reduce the switching frequency harmonics present in the input current. This filter circuit frequency does not need to store energy coming from the load. Simple LC filters used for this purpose.

Requirements of LC filter are

* Cut-off frequency lower than the switching frequency of Matrix Converter.

* Minimal reactive power at grid frequency.

* Minimal volume and weight.

* Minimal filter inductance voltage drop at rated current in order to avoid reduction in voltage transfer ratio.

Careful filter design is necessary else it will affect both the input and output currents of the converter. Block diagram of the input filter is shown in Fig. 6.50.

The control platform used is Spartan 3-A DSP controller and Xilinx XC3SD1800A FPGA as shown in Fig.6.49. The modulation code is written in C++ and is processed in the DSP. The logical tasks such as A/D and D/A conversion, gate drive signal generation etc are accomplished by the powerful FPGA board. The FPGA board is able to handle upto 50 PWM signals.

In a Matrix Converter, over voltages can appear from the input side, caused due to line perturbations over voltages can also appear from output side caused due to an over current fault. When switches are turned OFF, the current in the load is suddenly interrupted. The energy stored in the motor inductance has to be discharged without creating over-voltages. A clamp circuit is the common solution to avoid both input and output over voltages. This clamp circuit has 24 fast-recovery diode to connect capacitor to input and output terminals. Block diagram of the clamp circuit used in the set-up is presented in Fig. 6.52.

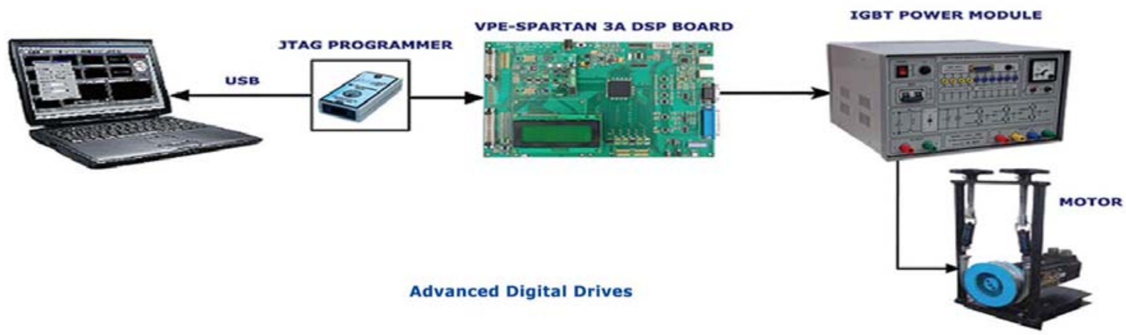

Fig. 6.44. Overall block schematic of the experimental set-up.

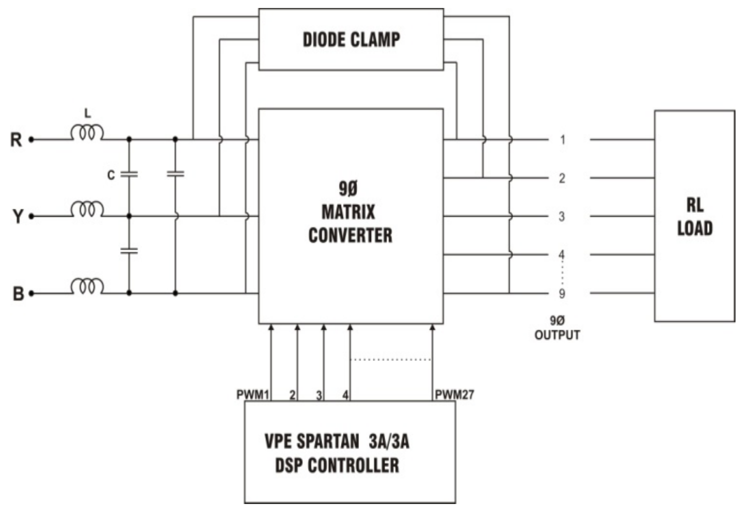

Fig. 6.45. Block schematic of experimental set-up of three-phase to Nine-phase Matrix Converter.

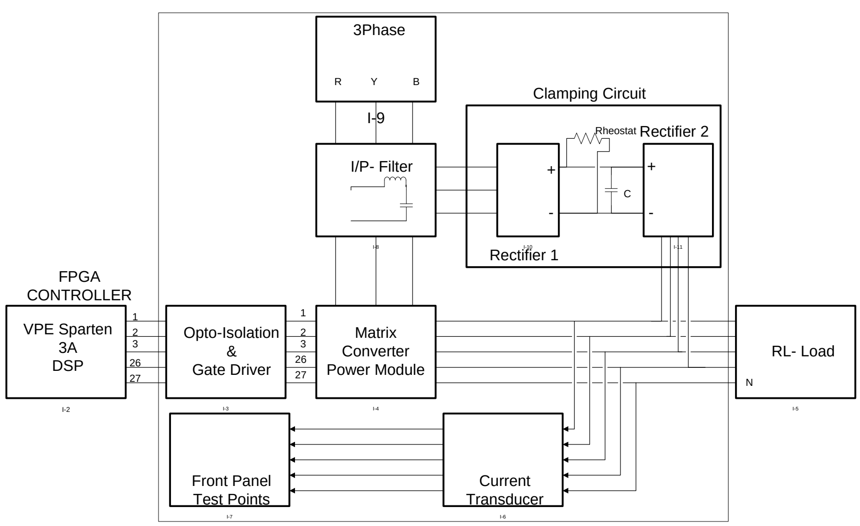

Fig. 6.46. Detailed drawing of the experimental set-up.

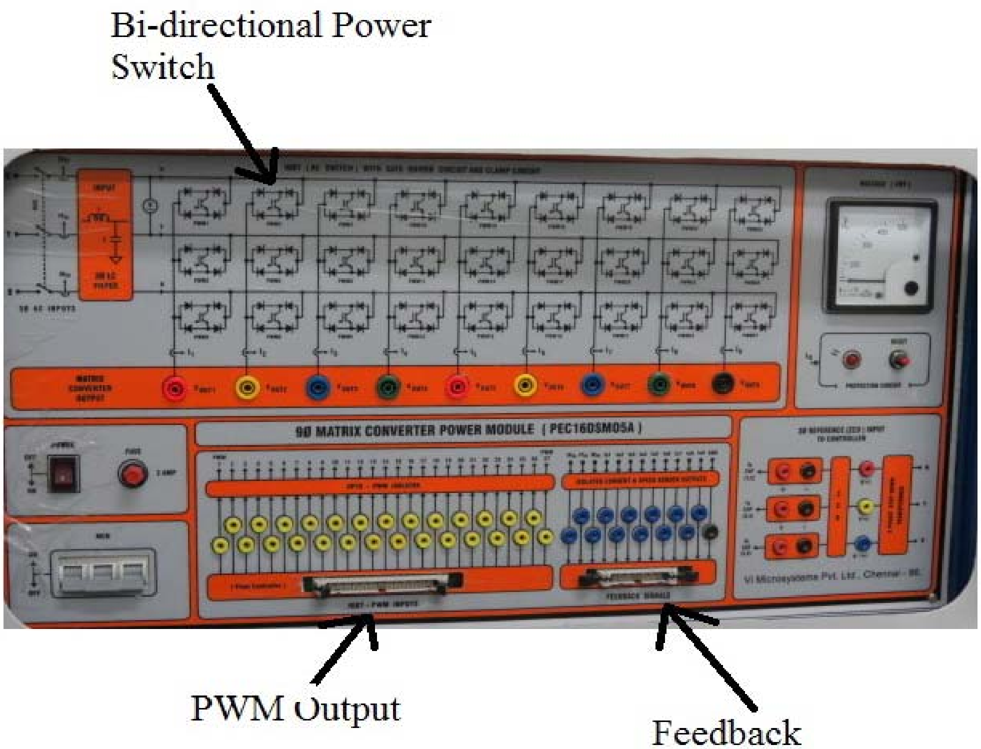

Fig. 6.47. An experimental setup photo graph (main power circuit).

Fig. 6.48. Nine units of Matrix Converter.

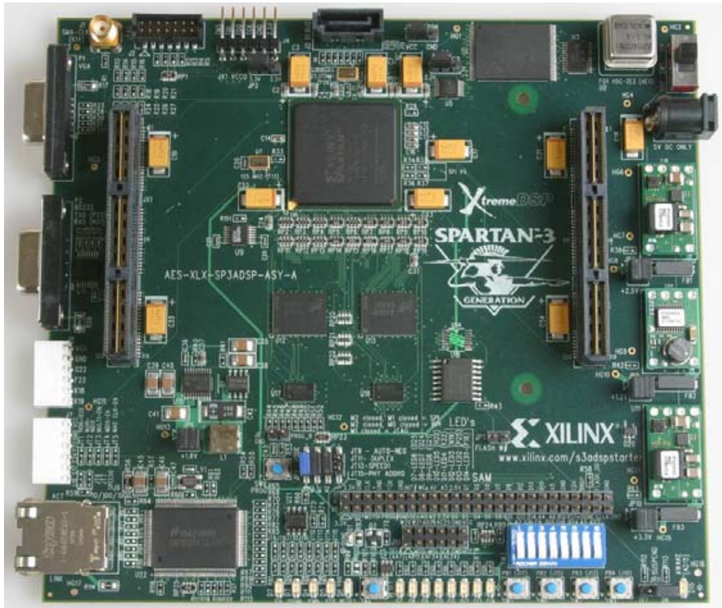

Fig. 6.49. Spartan DSP 3A evaluation board.

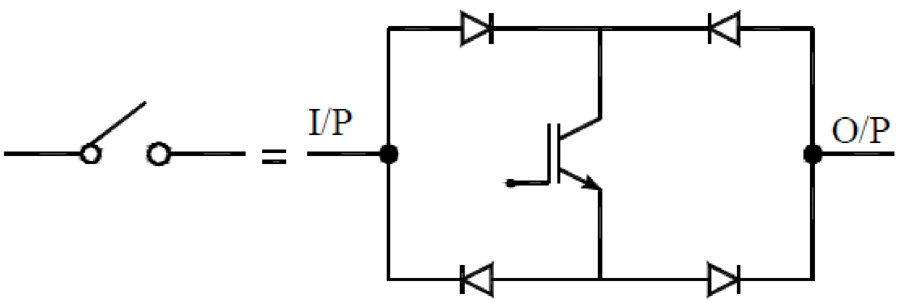

Fig. 6.50. Bi-directional switching arrangement.

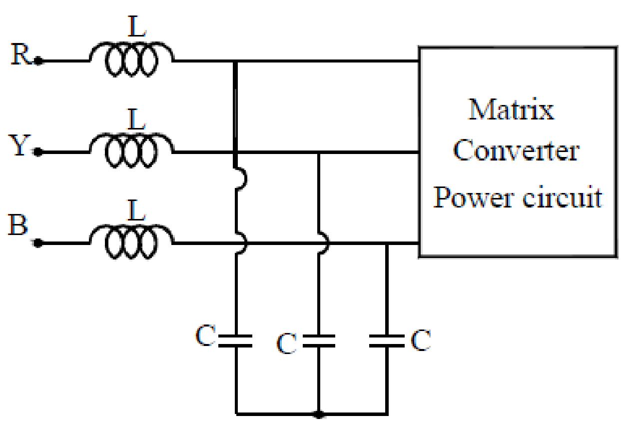

Fig. 6.51. Input filter structure.

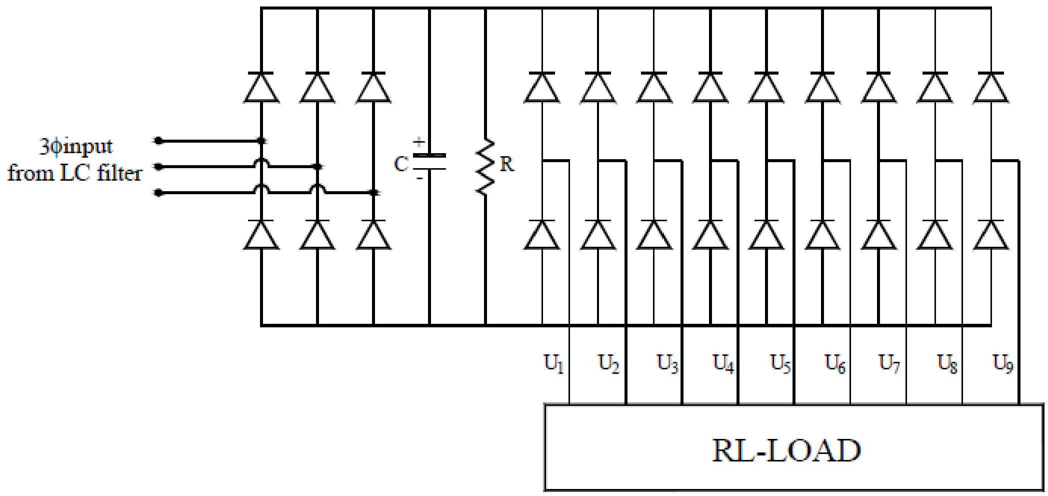

Fig. 6.52. Clamp circuit.

At the input side, an isolation transformer is required. An isolation transformer is a transformer, often with symmetrical windings, which is used to decouple two circuits. An isolation transformer allows an AC signal or power to be taken from one device and fed into another without electrically connecting the two circuits. Isolation transformers block transmission of DC signals from one circuit to the other, but allow AC signals to pass. They also block interference caused by ground loops. Isolation transformers with electrostatic shields are used for power supplies for sensitive equipment such as computers or laboratory instruments.

Isolation transformers are commonly designed with careful attention to capacitive coupling between the two windings. This is necessary because excessive capacitance could also couple AC current from the primary to the secondary. A grounded shield is commonly interposed between the primary and the secondary. Any remaining capacitive coupling between the secondary and ground simply causes the secondary to become balanced about the ground potential.

Overall block diagram of the Matrix Converter connection for experimental investigation is shown in Fig. 6.53. A Matrix Converter is implemented by a matrix module which consists of 9 bi-directional switches. The 3-phase input supply voltage is stepped down. The zero crossing of the input voltage is detected by the ZCD. ZCD output is given to the processor through the capture unit of Micro- 2812. In the processor sine PWM signal is generated. This signal is compared with the ZCD signal and a PWM signal is generated. This generated PWM is applied to the IGBT gate terminal. The PWM signal width is controlled by the I/O port key.

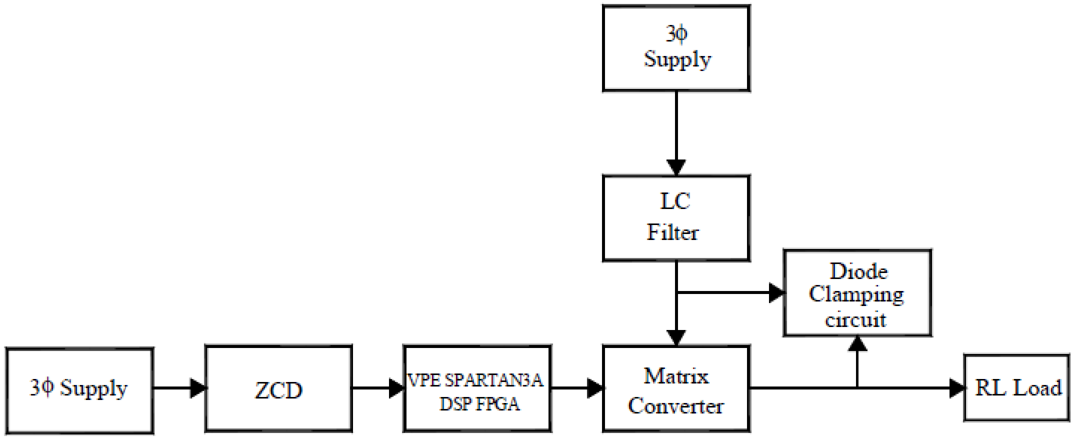

Fig. 6.53. Matrix Converter connection diagram.

Input supply is given from an auto-transformer and is fixed at 100 V rms, 50 Hz. The switching frequency of the bi-directional power switch of the Matrix Converter is fixed at 8 kHz. The developed Matrix Converter is tested for wide range of output frequencies for as low as 5 Hz fundamental. Multi-phase R-L load (R = 10 Ω, L = 10 mH) is connected at the output terminals of the Matrix Converter. The voltage probe is used with voltage scaling of 1/20. The current is measured with a scaling factor of 2A/V. Horizontal scale used for measuring the output waveform is 10 msec/div. Source side current waveform is measured with a horizontal scale of 5 msec/div. The resulting output waveform for fundamental frequency of 25 Hz and five-phase operation is presented fig. 6.54. Input current results with both linear and over modulation strategy are shown simultaneously in the fig. 6.55. The output voltage and current offers good results with sinusoidal waveform. This proves the viability of the proposed modulation scheme for three to five-phase Matrix Converter.

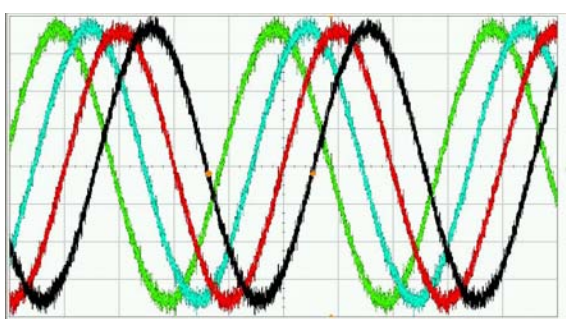

a.

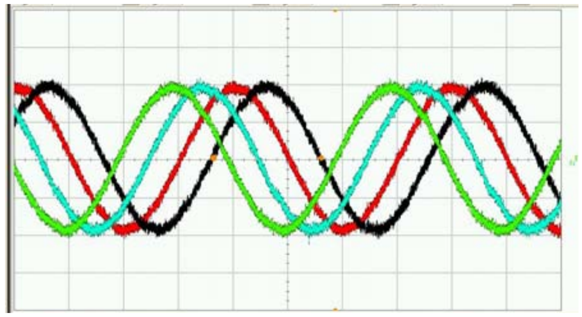

b.

Fig. 6.54. Output side five-phase waveform for 25 Hz; a. Output filtered phase voltages (20V/div) b. Output currents (4A/div). Time scale is 10 ms/div.

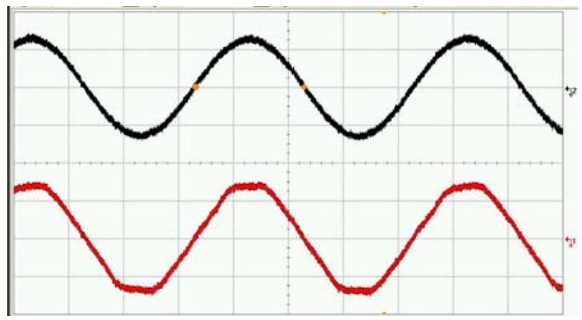

Fig. 6.55. Input current using linear modulation scheme as well as input side over modulation strategy (10A/div). Time scale 10 msec/div.

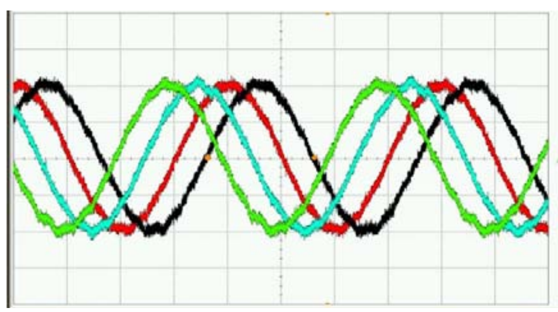

Fig.6.56. Output side waveform for 25 Hz using input side over-modulation strategy; Output currents (4A/div). Time scale 10 msec/div.

6.9b Experimental Investigation of two motor supply

Same experimental setup is utilised for three-phase to five-phase two motor supply, results obtained are reported in Figs. 6.57 -6.58. The Matrix Converter is connected to a five-phase R-L load and input voltage of 200 V is supplied. The output of the Matrix Converter contains two frequency components, one with 50 Hz and one with 25 Hz. One output voltage frequency component is intended to control one machine and the second frequency component controls the second machine. The experimental results is intended to show the successful generation of two decoupled frequency component at the output of the Matrix Converter. The obtained results matches very closely to simulation results.

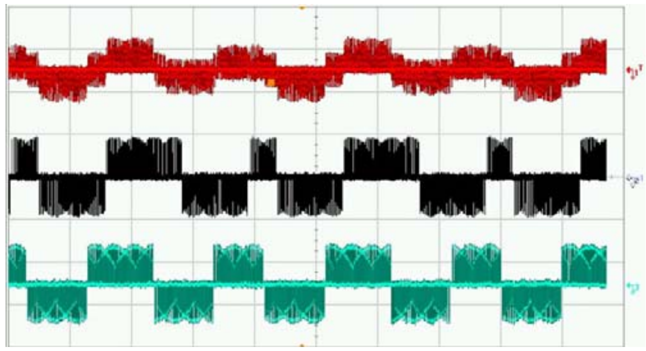

Fig. 6.57. Experimental results: tope trace, phase Voltage, middle trace adjacent line Voltage, and the bottom trace, non-adjacent line Voltage (y-axis: 200V/div, x-axis: 10 msec/div)

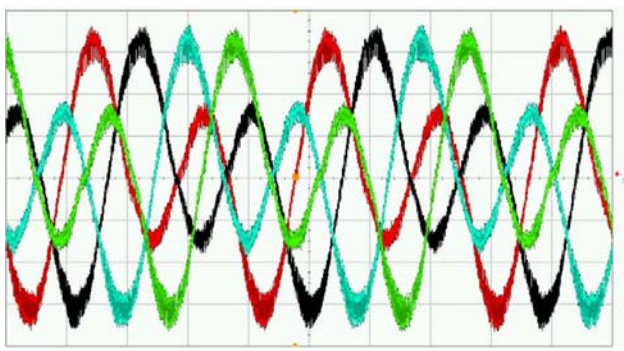

Fig.6.58. Experimental results: output currents, (y-axis 4 amp/div, x-axis: 10 msec/div)

6.9c Experimental investigation on 3x6 phase matrixconverter

Input supply is given from an autotransformer and is fixed at 100 V rms, 50 Hz. The switching frequency of the bi-directional power switch of the matrix converter is fixed at 6 kHz. The developed Matrix Converter is tested for wide range of output frequencies for as low as 5 Hz fundamental. Six-phase R-L load is connected at the output terminals of the matrix converter. The modulation code uses harmonic injection method. The resulting input and output side waveforms for output fundamental frequency of 25 Hz are presented in Fig.6.59 and 6.60, respectively. The top trace (Fig. 6.59a) shows all the three applied voltages and one phase converter input side current. To further illustrate the unity input power factor, phase ‘a’ voltage and phase ‘a’ currents are depicted in Fig. 6.59b. The current drawn from the three-phase grid is completely sinusoidal as illustrated in Fig. 6.59c which shows converter side and source side current in one trace.

The unfiltered output phase voltages of four different phases are presented in Fig. 6.60a and filtered output voltages are depicted in Fig. 6.60b. The output filtered phase voltages and load currents are shown in Fig. 6.60c. The output voltage and current offers good results with sinusoidal waveform. This proves the viability of the proposed modulation scheme for three to quasi six-phase matrixconverter.

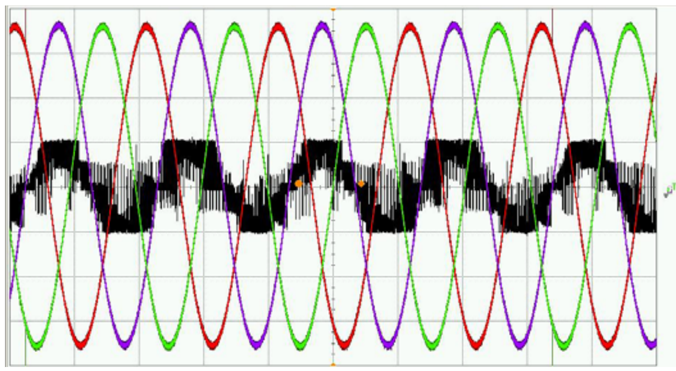

[40 V/div. and 10 A/div.]

a.

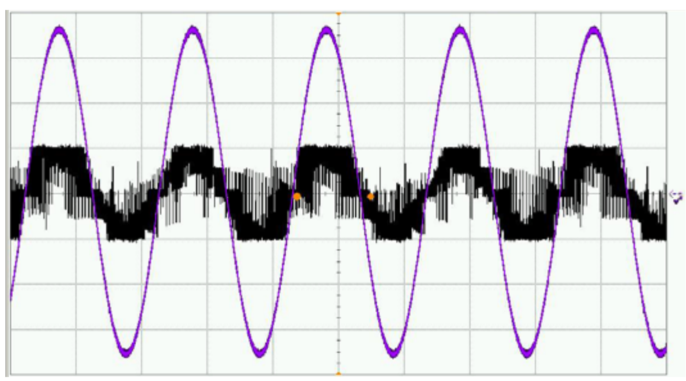

[40 V/div. and 10 A/div.]

b.

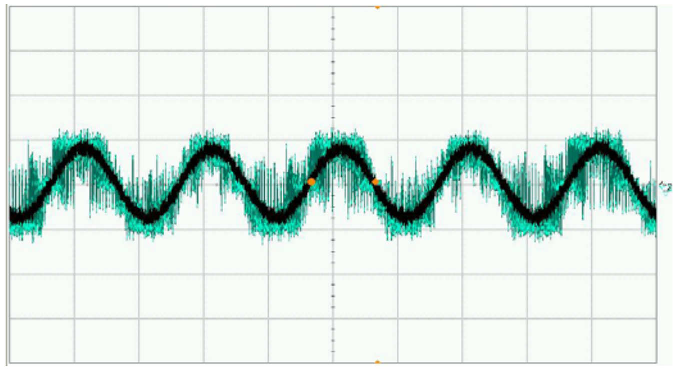

[10 A/div]

c.

Fig. 6.59. Experimental results of a 3 to quasi 6 phase matrix converter, a. input side voltages and current, b. phase 'a' voltage and phase 'a' converter side current, c. converter side and source side currents. Time scale (10 msec/div).

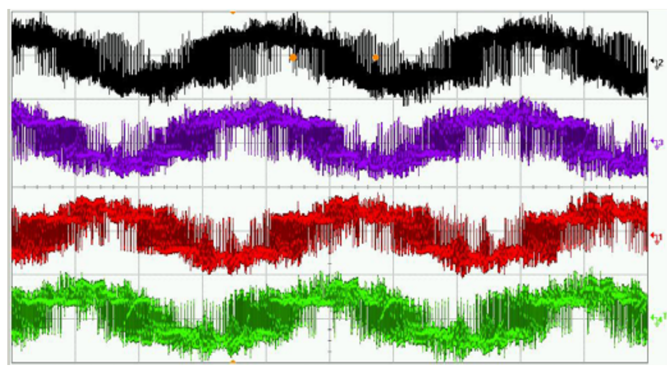

[150 V/div.]

a.

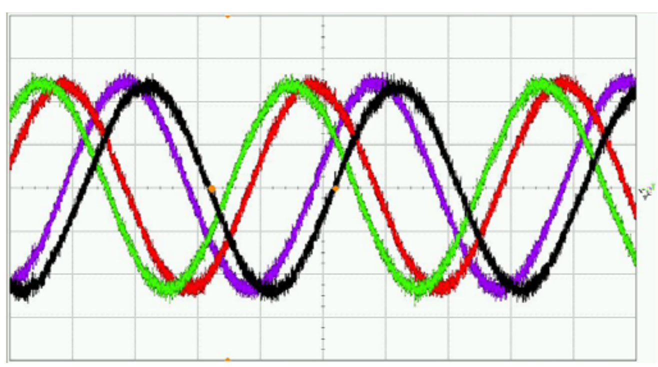

[40 V/div.]

b.

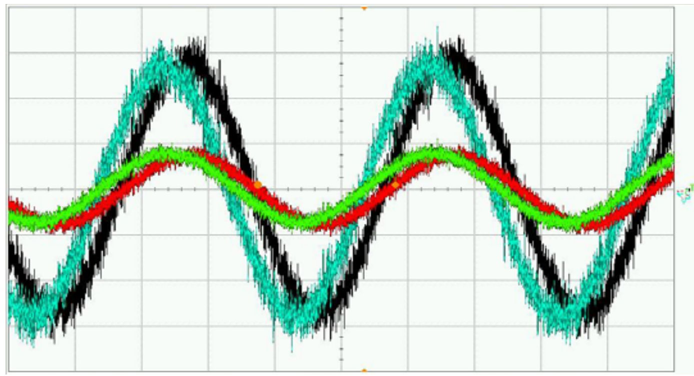

[40 V/div. and 10 A/div.]

c.

Fig. 6.60. Output side six-phase waveform for 25 Hz; a. Output unfiltered phase voltage, b. Output filtered phase voltage, c. output filtered voltage and currents. (10 msec/div**).**

6.10 Summary

This chapter focused on the development of simple control algorithms for multi-phase multi-motor drive system. Carrier-based sinusoidal PWM control is a generic method in a voltage source inverter. However, the same method when applied to a Matrix Converter need appropriate modification. This chapter elaborated the carrier-based PWM for a three-phase input to five-phase matrix converter supplying a five-phase series-connected/parallel-connected two-motor drive. Further carrier-based PWM for a three-phase input to six-phase output Matrix Converter supplying a series-connected/parallel-connected six-phase machine and three-phase machine is discussed. Additionally carrier-based PWM for a three-phase input to seven-phase output Matrix Converter supplying series-connected/parallel-connected three-motor drive system is discussed. It is seen that the major shortcoming is the lower output voltage of matrix converters. Since the overall output voltage is small, the series-connected and parallel-connected machines will be able to run at lower speeds only.

References

[6.1] Young-Doo Yoon, Seung-Ki Sul, “Carrier-based modulation technique for Matrix Converter,” IEEE Trans. Power Elect., vol. 21, no. 6, pp. 1691–1703, November 2006.

[6.2] Poh C. Loh, R. Rong, F. Blaabjerg, P. Wang, “Digital carrier Modulation and Sampling Issues of Matrix Converter,” IEEE Trans. On Power Elect., vol. 24, no. 7, July 2009.

[6.3] T. Satish, K.K. Mohapatra, N. Mohan, “Carrier-based control of matrixconverter in Linear and over-modulation modes,” Proc. of the 2007 summer computer simulation conf., San Diago, California, pp. 98-105, 2007.

[6.4] SK. M. Ahmed, A. Iqbal, H. Abu-Rub, “Carrier based PWM techniques for a three-to-five phase Matrix Converter,” PCIM 2010, 4-6 May 2010,Nuremberg, Germany, pp. 998-1003.
[6.5] A. Iqbal, “Modeling and Control of Five-phase and Six-phase Series-connected Two-motor drive system,” *PhD Thesis*, Liverpool John Moores University, UK, 2006.
[6.6] A. Iqbal, E. Levi, M. Jones, S.N. Vukosavic, “Generalised Sinusoidal PWM with harmonic injection for multi-phase VSIs,” IEEE 37th Power Electronics Specialist conf. (PESC) Jeju, Korea, 18-22 June 2006, CD_ROM paper No. ThB2-3, pp. 2871-2877.
[6.7] M. Jones, S.N. Vukosavic, E. Levi, A. Iqbal, “A six-phase series connected two-motor drive with decoupled dynamic control,” IEEE Trans. On Industry Application, vol. 41, no. 4, pp. 1056-1066, July/Aug, 2005.
[6.8] M. Jones, E. Levi, S.N. Vukosavic, H.A. Toliyat, “Independent vector control of a seven-phase three-motor drive system supplied by a single voltage source inverter,” Proc. 34th IEEE PESC, vol. 4, pp. 1865-1870, 2003.

Chapter 7
Direct Duty Ratio Based Pulse Width Modulation of Multi-phase Matrix Converter

7.1 Introduction

In this chapter, a PWM strategy based on direct duty ratio calculation approach is presented. At first generalized direct duty ratio based PWM (DDPM) is developed for three-phase to n-phase Matrix Converter. This approach does not rely on the discontinuous offset rather a continuous triangular carrier waveform is employed for the purpose of generating the switching signals. When the desired output phase voltage references are given, each of them can be synthesized by utilizing input phase voltages based on per-phase output concept. In addition, by changing simply the slope of the carrier, the input power factor can also be controlled, maintaining the sinusoidal input currents. The output voltage is limited to 78.86% of the input voltage magnitude in case of a three-phase input and five-phase output configuration. Theoretically this is the maximum output magnitude that can be obtained in this Matrix Converter configuration in the linear modulation region. Analytical approach is used to develop and analyse the proposed modulation techniques and are further supported by simulation results. The major aim of the modulation is to produce two fundamental frequency output from the Matrix Converter that can be used to control two series/parallel connected five-phase machines.

Major advantages of the presented scheme (direct duty ratio based PWM) are that it is highly intuitive and flexible. The output voltage limit is reached by simply adding a third harmonic component corresponding to the input frequency and the n^{th} harmonic corresponding to the output frequency with n number of output phase, into the output voltage references. The output voltage limit has different values for different output number of phases. The proposed control algorithm is modular in nature and can be extended to any number of input and output phases. The presented scheme can be employed effectively in variable speed multi-phase motor drive applications.

7.2 Direct Duty Ratio based PWM Technique for a Three-phase to n-phase Matrix Converter for Single-motor drive system

In this section the PWM is discussed based on duty ratio calculation in conjunction with the generalized three-to *n*-phase topology of a Matrix Converter. The duty ratio based PWM is developed by using the concept of per-phase output average over one switching period as shown in reference [7.1].The developed scheme is modular in nature and therefore, it is applicable to the generalized converter circuit topology.

A switching period T_s of the carrier wave consists of two sub-intervals, T_1 (rising slope of the triangular carrier) and T_2 (falling slope of the triangular carrier). When the carrier changes from zero to the peak value, the sub-interval is called T_1; however, when the carrier changes from peak to the zero value it is termed as sub-interval T_2. The input three-phase sinusoidal waveform can assume different values at different instants of times. The maximum among the three input signals is termed as *Max*, the medium amplitude among three input signals is termed as *Mid,* and the smallest magnitude is represented as *Min.* During interval T_1 (positive slope of the carrier), the line-to-line voltage between *Max* and *Min* ($Max\{v_A, v_B, v_C\} - Min\{v_A, v_B, v_C\}$) phases is used for the calculation of duty ratio. No consideration is given to the medium amplitude of input signal. The output voltage should initially follow the *Max* signal of the input and then should follow the *Min* signal of the input. During interval T_2, the two line voltages between *Max* and *Mid* ($Max\{v_A, v_B, v_C\} - Mid\{v_A, v_B, v_C\}$) and *Mid* and *Min* ($Mid\{v_A, v_B, v_C\} - Min\{v_A, v_B, v_C\}$) are calculated first. The largest among the two is used for the calculation of the duty ratio. This is done to balance the volt-second principle. Two different cases can arise in time interval T_2 depending upon the relative magnitude of the input voltages. If *Max-Mid >Mid-Min*, the output should follow *Max* for a certain time period and then follow *Mid* for a certain time period. This situation is termed as Case I. Similarly, if (*Max-Mid)* < (*Mid-Min)*, the output should follow at first *Mid* of the input signal and then *Min* of the input signal: this is termed as Case II. Thus the DPWM approach uses two out of the three line-to-line input voltages to synthesis output voltages, and all the three input phases are utilized to conduct current during each switching period. Case I and II and the generation of gating signals are further elaborated in the next section.

Case-I:

For condition (*Max-Mid)* ≥ *(Mid-Min),* the generation of gating pattern for the n^{th} output phase is illustrated in Fig. 7.1 for one switching period. To generate the pattern, at first the duty ratio $D_{k1}, n \in a,b,c.......$, is calculated and then compared with high frequency triangular carrier signal to generate the n^{th} output phase pattern. The gating pattern for the n^{th} leg of the Matrix Converter is directly derived from the output pattern. The switching pattern is drawn assuming that the *Max* is the phase 'A' of the input, *Mid* is the phase 'B', and *Min* is the phase 'C'. The switching pattern changes in accordance with the variation in the relative magnitude of the input phases. The output follows *Min* of the input signal, if the magnitude of the duty ratio is more than the magnitude of the carrier and the slope of the carrier is positive. The output follows the *Max* of the input signal if the magnitude of the carrier is greater than the magnitude of the duty ratio irrespective of the slope of the carrier. Finally, the output tracks *Mid* if the magnitude of the carrier signal is less than the magnitude of the duty ratio and the slope of the carrier is negative. Thus, the resulting output phase voltage changes like *Min→Max→Max→Mid*. These transition periods are termed as, t_{n1}, t_{n2}, t_{n3} and t_{n4} and these four sub-intervals can be expressed as in reference [7.1]:

$$\begin{aligned} t_{n1} &= D_{n1}\delta T_s \\ t_{n2} &= (1-D_{n1})\delta T_s \\ t_{n3} &= (1-D_{n1})(1-\delta)T_s \\ t_{n4} &= D_{n1}(1-\delta)T_s \\ T_s &= t_{n1}+t_{n2}+t_{n3}+t_{n4} \end{aligned} \tag{7.1}$$

where D_{n1} is the n^{th} phase duty ratio value, when Case I is under consideration and δis defined by $\delta = \frac{T_1}{T_s}$, which refers to the fraction of the slope of the carrier. Now, by using the volt-second principle of the PWM control, the following equation can be written:

$$v_{on}^{*}T_s = \int_0^{T_s} v_{on}dt = Min\{v_A, v_B, v_C\}.t_{n1} + Max\{v_A, v_B, v_C\}.(t_{n2}+t_{n3}) + Mid\{v_A, v_B, v_C\}.t_{n4}$$

(7.2)

Substituting the time intervals expressions from equations (7.1) into (7.2), yields

$$v_{on}^{*} = \frac{1}{T_s}\int_0^{T_s} v_{on}dt = D_{n1}\begin{pmatrix} \delta.Min\{v_A, v_B, v_C\} - \delta.Mid\{v_A, v_B, v_C\} + \\ Mid\{v_A, v_B, v_C\} - Max\{v_A, v_B, v_C\} \end{pmatrix} Max\{v_A, v_B, v_C\} \tag{7.3}$$

Where T_s is the sampling period, v_{on}^{*}, v_{on} are the reference and actual average output voltage of phase '*n*', respectively and v_A, v_B, v_C are the input side three-phase voltages. *Max, Mid* and

Min refer to the maximum, medium and minimum values, D_n represents the duty ratio of the power switch.

The duty ratio is obtained from equation (7.3) as:

$$D_{n1} = \frac{Max\{v_A, v_B, v_C\} - v_{on}^{*}}{\Delta + \delta\left(Mid\{v_A, v_B, v_C\} - Min\{v_A, v_B, v_C\}\right)} \tag{7.4}$$

where $\Delta = \left(Max\{v_A, v_B, v_C\} - Mid\{v_A, v_B, v_C\}\right)$

Similarly, the duty ratios of other output phases can be obtained and can subsequently be used for implementation of the PWM scheme.

B. *Case-II*:

Now considering another situation of (*Max-Mid)* < (*Mid-Min).* The output and the switching patterns can be derived once again following the same principle laid down in the previous sub section. Fig. 7.2 shows the output and switching pattern for the n^{th} output phase. Here once again a high frequency triangular carrier wave is compared with the duty ratio value, D_{n2} to generate the switching pattern. The only difference in this case compared to the previous case is that the interval when the magnitude of the carrier signal is greater than the magnitude of the duty ratio and the slope is negative, then, the output should follow *Mid* instead of *Max*. Contrary to Case I, for this situation the output must follow *Max* of the input. The time intervals t_{n1}, t_{n2}, t_{n3} and t_{n4} are the same as in equation (7.1) and now the output phase voltage is changed with the sequence of *Min→Max→Mid→Min*. The volt-second principle is now applied to derive the equation for the duty ratio. The volt-second principle equation can be written as;

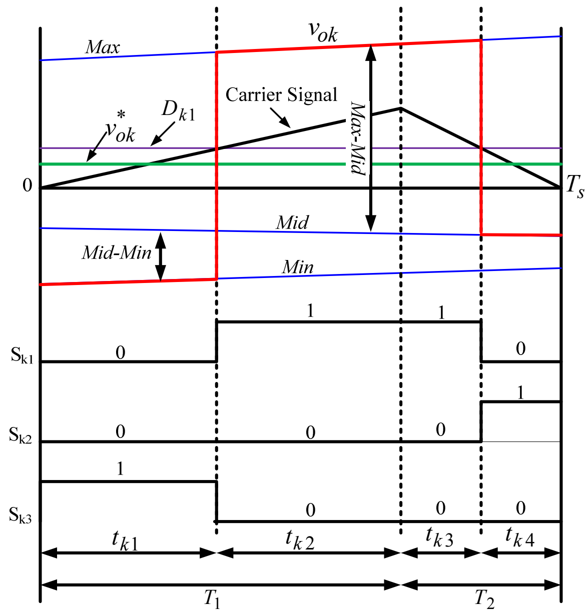

Fig. 7.1. Output and Switching pattern for n[th] phase in the Case I.

$$v_{on}^* T_s = \int_0^{T_s} v_{on} dt = Min\{v_A, v_B, v_C\}.(t_{n1} + t_{n4}) + Max\{v_A, v_B, v_C\}.t_{n2} + Mid\{v_A, v_B, v_C\}.t_{n3} \tag{7.5}$$

Now once again substituting the time expression from equation (7.1) into equation (7.5), one obtains:

$$v_{on}^* = \frac{1}{T_s}\int_0^{T_s} v_{on} dt = D_{n2}\begin{pmatrix} Min\{v_A, v_B, v_C\} - \delta.Max\{v_A, v_B, v_C\} - \\ Mid\{v_A, v_B, v_C\} + \delta.Mid\{v_A, v_B, v_C\} \end{pmatrix} + \delta.Max\{v_A, v_B, v_C\} - \delta.Mid\{v_A, v_B, v_C\} + Mid\{v_A, v_B, v_C\} \tag{7.6}$$

The duty ratio can now be obtained as:

$$D_{n2} = \frac{\delta.\Delta + \left(Mid\{v_A, v_B, v_C\} - v_{ok}^*\right)}{\delta.\Delta + \left(Mid\{v_A, v_B, v_C\} - Min\{v_A, v_B, v_C\}\right)} \tag{7.7}$$

The switching signals for the bi-directional power switching devices can be generated by considering the switching states of Figs. 7.1 and 7.2. Depending upon the output pattern, the gating signals are derived. If the output pattern of phase "*n*" is *Max* (or *Mid*, *Min*), then the output phase "*n*" is connected to the input phase whose voltage is *Max* (or *Mid*, *Min*). The pulse width modulation algorithm can be explained by the block diagram given in Fig. 7.3.

The input voltages are at first examined for their relative magnitudes and the phases with maximum, medium, and minimum values are determined. The information about their relative magnitudes are given to the next computation block along with the commanded output phase voltages. The computation block either uses equation (7.4) or equation (7.7) to generate the duty ratios depending upon the relative magnitude of the input voltages. The duty ratio obtained goes to the PWM block. The PWM block calculates the time sub-interval using equation (7.1). The gating pattern is then derived accordingly and given to the Matrix Converter.

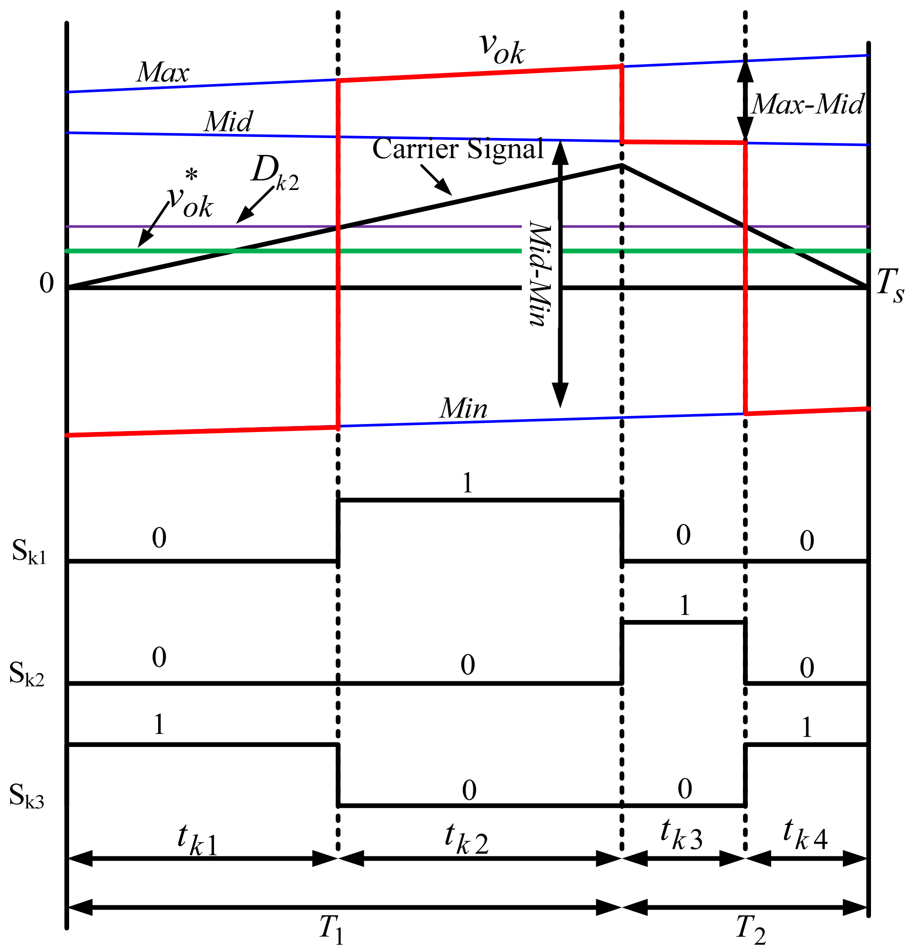

Fig. 7.2. Output and Switching pattern for nth phase in the Case II.

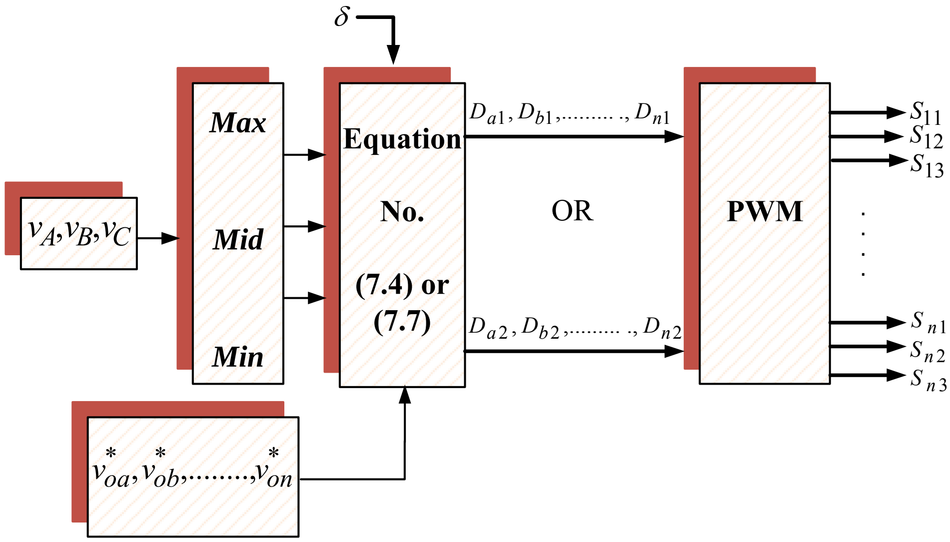

Fig. 7.3. General Implementation diagram of 3 to k phase Matrix Converter.

7.3 Direct Duty Ratio Based PWM for 3-phase to 5-phase Matrix Converter

A specific case of three-to-five phase Matrix Converter is consodered and DDPWM is developed. This topology was presented in reference [7.2] where simple carrier based PWM technique were used and simulation results were obtained. Section (7.3) describes the use of direct duty ratio PWM for the same topology. The input to the Matrix Converter is three-phase supply from the grid and the output will be five-phase with varaible voltage and variable frequency. This type of supply is required for five-phase machine drives. At first the output pattern is elaborated for one sampling interval. For a particular switching period the output pattern of phases *a,b,c,d & e,* are shown in Figs. 7.4 to 7.8, considering only Case I. Since Case II is similar to Case I with only minor modification, the output pattern and subsequently the switching pattern can also be derived; however it will not be shown here. The switching pattern is direclty related to the output patterns as described in section III and are thus not shown in the Figures 7.4 to 7.8.

The major advantage of the proposed PWM control is it is modular in nature; hence each phase of the outputs can be modulated separately to follow their references. Depending upon how the reference or target output voltages are created, two methods are evolved. One method is termed as 'without harmonic injection' and the other is called 'with harmonic injection'. The maximum output voltage reaches half of the input voltage if simple sinusoidal reference voltages are assumed. It is shown in reference [7.3] that the magnitude of the output voltages can be enhanced by subtracting the common mode third harmonic of the input phase voltages from the input phase voltages. The optimum value of the injected harmonic is obtained as one fourth of the input maximum magnitude. Thus by adopting the harmonic injection scheme, the output voltage magnitude reaches 0.75 of the input voltage value. Further enhancement in the output voltage is achieved by injecting the third harmonic of the output frequency in the reference output voltage. Thus by injecting one sixth of the magnitude of the third harmonic, the voltage transfer ratio goes up to 0.866 in the case of a three-to-three phase Matrix Converter. This is a 15.5% increase compared to the harmonic injection in the input side voltage only. It is important to note that the value 15.5% is same as the amount of enhancement of the modulation index in the case of a three-phase voltage source inverter, which is achieved by harmonic injection when compared to simple carrier-based scheme.

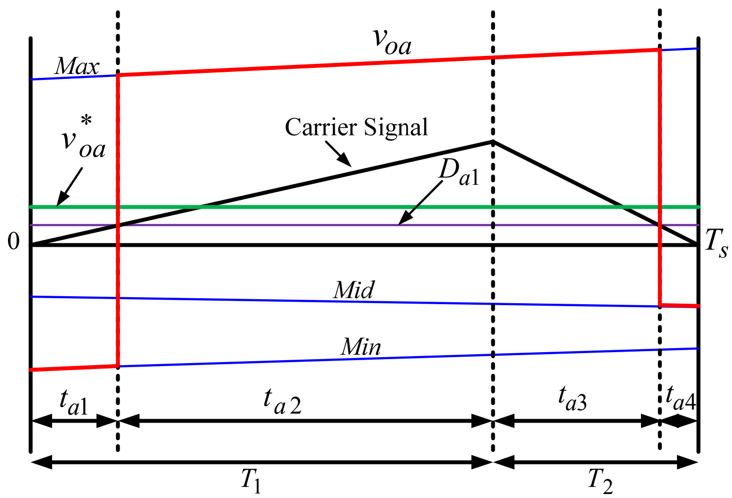

Fig. 7.4. Output pattern of phase ‘a’.

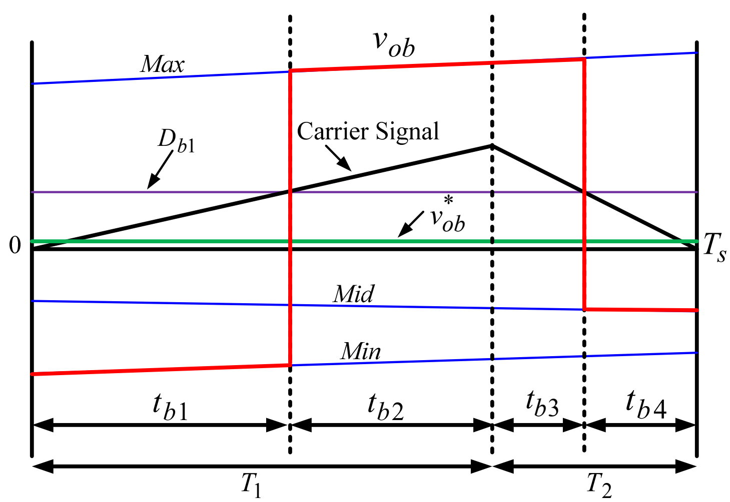

Fig. 7.5. Output pattern of Phase ‘b’.

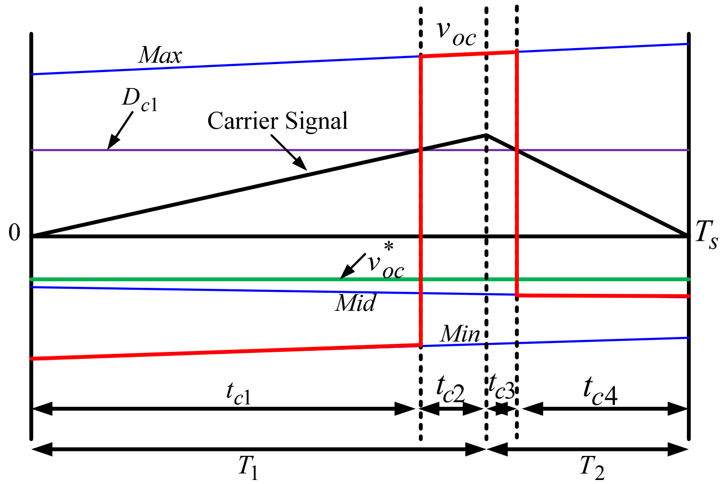

Fig. 7.6. Output pattern of phase ‘c’.

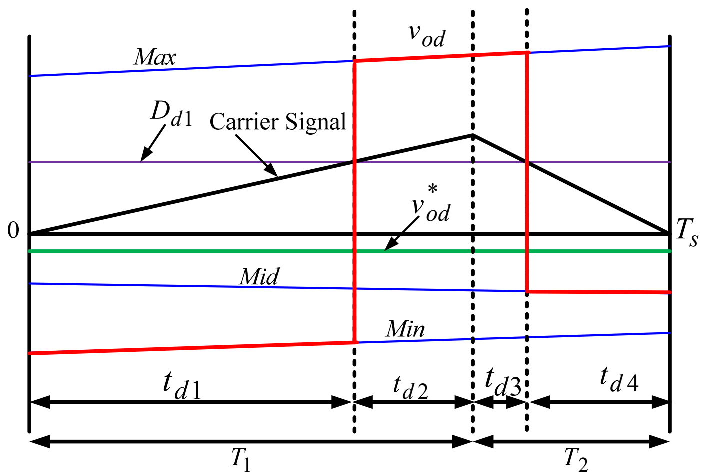

Fig. 7.7. Output pattern of phase ‘d’.

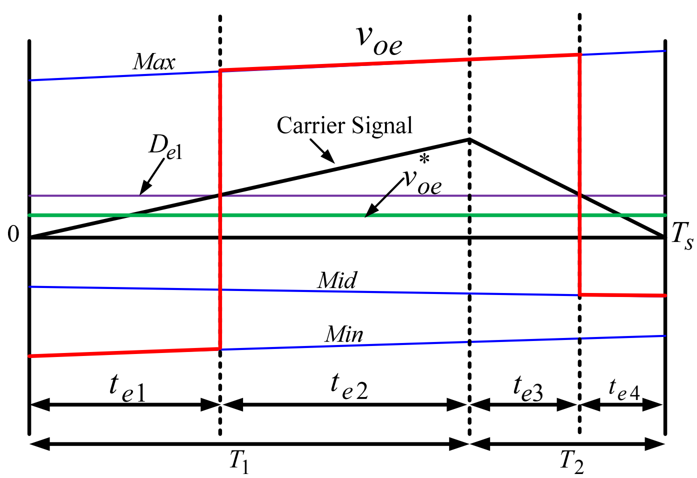

Fig. 7.8. Output pattern of phase ‘e’.

In the case of multi-phase voltage source inverter, a similar concept of the n^{th} harmonic injection was proposed in reference [7.4] for enhancement of the modulation index. It was shown that by injecting n^{th} harmonic of magnitude $M_n = -M_1 \sin\left(\frac{\pi}{2n}\right)/n$, where n is the number of phases, the output voltage increases by $1/\cos\left(\frac{\pi}{2n}\right)$. A similar approach is thus used in this thesis to enhance the output voltage magnitude as discussed in the section (7.4).

7.4 Simulation Results for Five-phase Single-motor Drive

Modulation without harmonic injection

Simulation is carried out to study the operation of a three to five-phase Matrix Converter using the modulation scheme that is elaborated in the section (7.3) known as direct duty ratio PWM [7.5]. The simulation model is developed in the MATLAB/SIMULINK platform by using 'simpowersystem' block set library.

The output reference voltages are given as:

$$
\begin{aligned}
v_{oa}^* &= \sqrt{\frac{2}{5}} q V_{in-rms} \cos(\omega_o t) \\
v_{ob}^* &= \sqrt{\frac{2}{5}} q V_{in-rms} \cos\left(\omega_o t - 2\frac{\pi}{5}\right) \\
v_{oc}^* &= \sqrt{\frac{2}{5}} q V_{in-rms} \cos\left(\omega_o t - 4\frac{\pi}{5}\right) \\
v_{od}^* &= \sqrt{\frac{2}{5}} q V_{in-rms} \cos\left(\omega_o t + 4\frac{\pi}{5}\right) \\
v_{oe}^* &= \sqrt{\frac{2}{5}} q V_{in-rms} \cos\left(\omega_o t + 2\frac{\pi}{5}\right)
\end{aligned}
\tag{7.8}
$$

where the factor $q<=0.5$ and $V_{in\text{-}rms}$ are the input phase voltage RMS value. The implementation block diagram of the proposed PWM scheme is illustrated in Fig. 7.9.

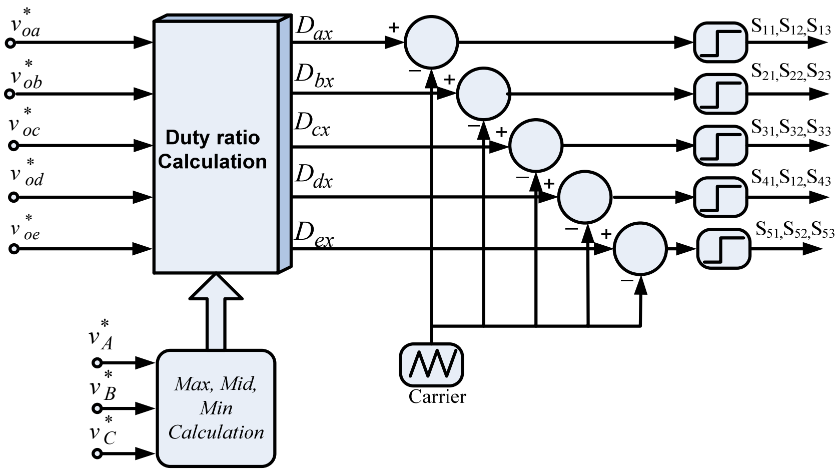

Fig. 7.9. DPWM implementation block without harmonic injection.

The output target voltage and the maximum, minimum, and medium of the input are given to the duty ratio calculation block. The duty ratios thus generated $\left(D_{ax}, D_{bx}, D_{cx}, D_{dx}, D_{ex}, x = 1\, or\ 2\right)$ are compared with the high frequency carrier signal. The output pattern is then generated as per the control law discussed in the previous section. The gate drive signals are then derived directly from the output voltage pattern. The maximum output voltage is limited to half the input voltage value (in this case as no common mode voltages are added to the input or output references). The simulation is done for the whole range of operation of the Matrix Converter and is tested for wide range of output frequencies. The proposed modulation scheme and the Matrix Converter topology offer excellent performance with a completely sinusoidal output and minimal simulation effort. A sample result is presented here for input frequency of 50 Hz, the output frequency is kept at 25 Hz and the modulation index is kept at a maximum of 0.5. The switching frequency of the Matrix Converter is kept at 10 kHz and the simulation step size is fixed at 10 μsec. The input voltage magnitude is fixed at 100 V and a R-L load is connected at the output of the Matrix Converter with R= 10 Ω and L = 1 mH. The modulation code is written using the Embedded MATLAB function. A suitable discrete filter is designed to be used in the simulation. The resulting waveforms are depicted for input quantities and output quantities in Figs. 7.10 and 7.11, respectively. Output and input voltages are also depicted on the same plot in Fig. 7.12 to show the maximum modulation index. The output voltage shows a 25 Hz signal and the input voltage is 50 Hz with output being half the magnitude compared to the input voltage.

It is seen from Fig. 7.10a that the input is controlled at unity p.f. and is independent of the output power factor. The input current spectrum is completely sinusoidal with magnitude equal to 4.3 Amp, as seen from Fig. 7.10b and from the locus of the α-β axis input current of Fig. 7.10c. The total harmonic distortion (THD) in the input current is calculated for up to the 20^{th} harmonic and is found to be only 3.78%, which is well under the prescribed limit of IEEE 519-1999 standard.

The output voltage waveform of Fig. 7.11a shows the successful conversion of three-phase input to the five-phase output voltages. The spectrum of filtered voltage (Fig. 7.11b) clearly indicates the sinusoidal output with a total harmonic distortion of 1.25%, which is well under the prescribed limit. The THD is once again calculated for low order harmonics upto 20. The locus of the transformed currents shows that the current component in *x-y* axis is minimal and the entire current remains in the α-β axis (Figs. 7.11c and 7.11d). This shows the effectiveness of the modulation technique since it is successfully eliminating the unwanted *x-y* components.

Modulation with harmonic injection

The output voltage is limited to half of the input voltage. Thus this section develops a scheme to enhance the output voltage magnitude by injecting common mode third and fifth harmonic into the output voltage references. Third harmonic corresponds to the input voltage frequency while the fifth harmonic voltages correspond to the output voltage reference frequency. The optimum amount of third harmonic and fifth harmonic are obtained as $\frac{\sqrt{6}}{12}V_{in-rms}$ and $\frac{\sqrt{6}}{48.5}qV_{in-rms}$, respectively. The input voltage magnitude is assumed fixed and the output is variable, hence the output term is multiplied with the modulation index term *q,* where $0 \le q \le 0.7886$.

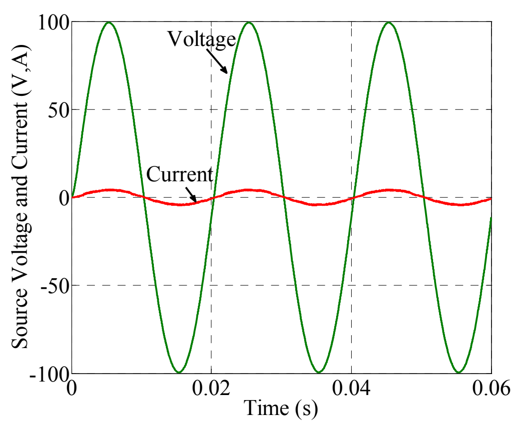

a.

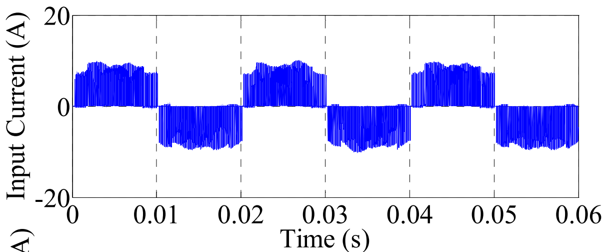

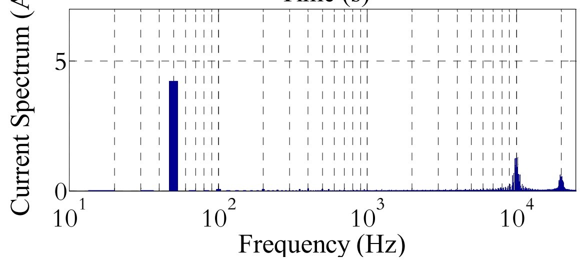

b.

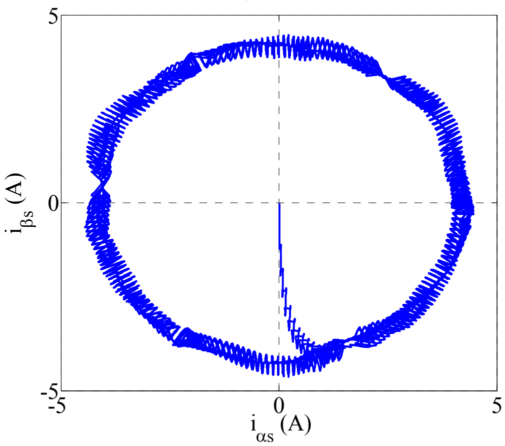

c.

Fig. 7.10. Input side waveforms of 3 to 5-phase Matrix Converter: a. Input voltage and input filtered current b. Spectrum input current, c. Input phase current locus.

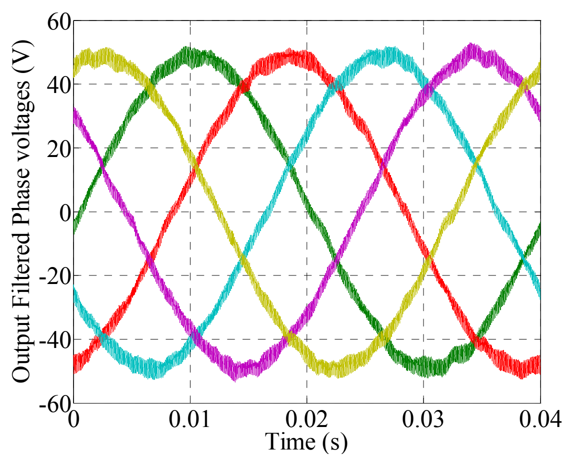

a.

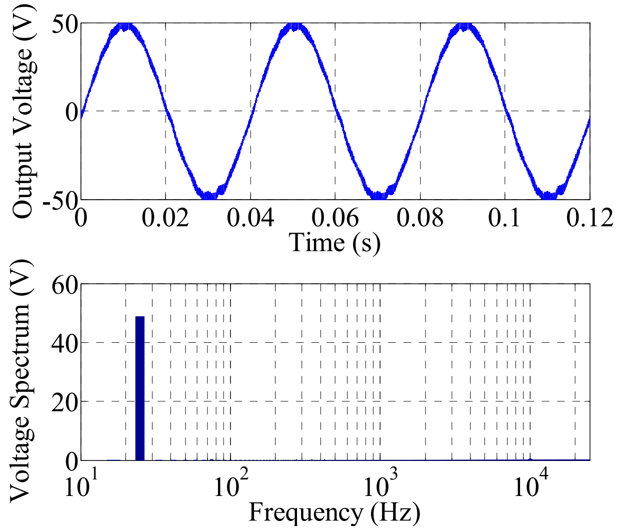
Output Voltage (V)
Time (s)
Voltage Spectrum (V)
Frequency (Hz)

b.

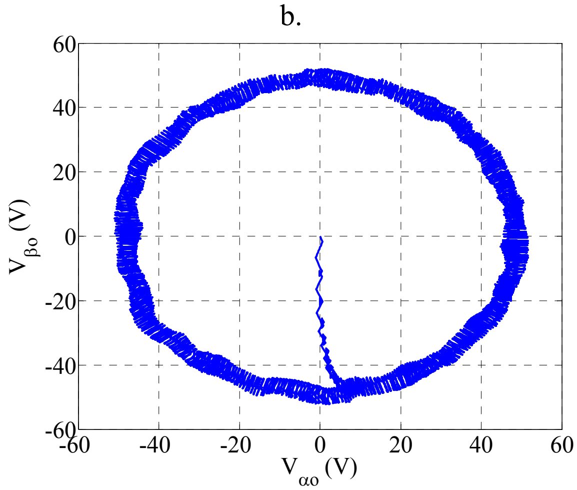
$V_{\beta o}$ (V)
$V_{\alpha o}$ (V)

c.

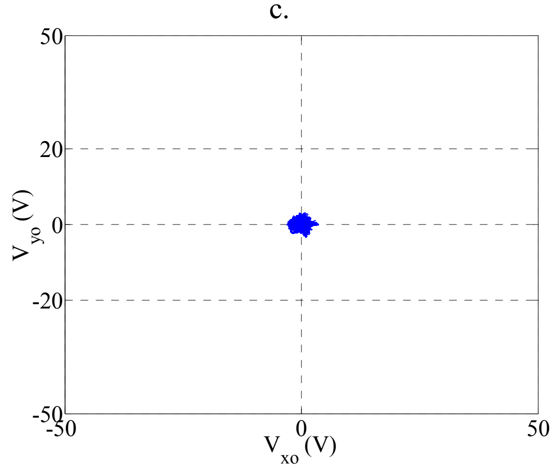
V_{yo} (V)
V_{xo} (V)

d.

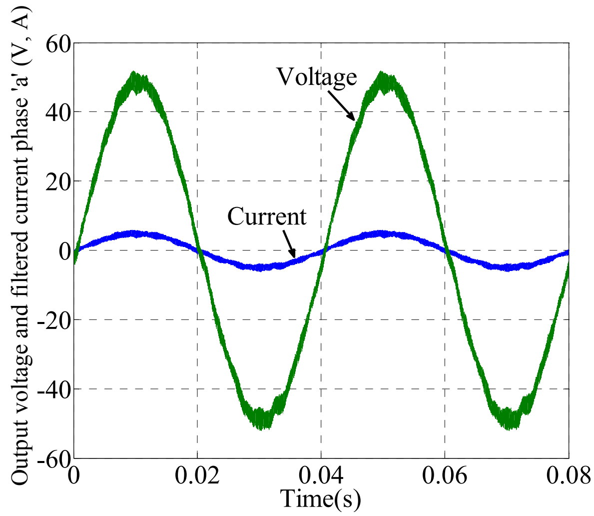

e.

Fig. 7.11. Output side waveforms of 3 to 5-phase Matrix Converter: a. Five-phase output filtered phase voltages b. Spectrum output filtered voltage, c. locus of α-β axis output voltage, d. locus of x-y axis output voltage, and e. output voltage and current phase 'a'.

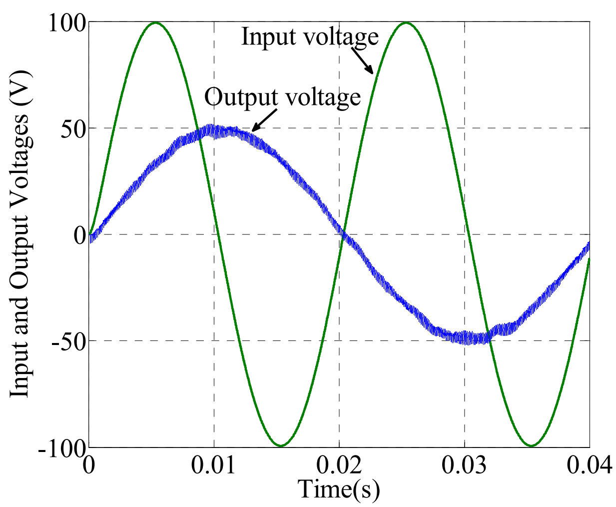

Fig. 7.12. Input and output voltage waveforms for a 3 to 5-phase Matrix Converter.

It is observed that by injecting only the 3rd harmonic, the output voltage becomes 0.75 of the input voltage. This increase is same as the one achieved in the three to three-phase Matrix Converter. Now in the case of three to five-phase Matrix Converter, the 3rd harmonic of output cannot be injected, hence the 5th harmonic of the output frequency is injected. The output voltage magnitude thus reaches 0.7886 of the input voltage magnitude by injecting both 3rd and 5th harmonics. Hence, the overall gain in the output is 5.15%. It is to be noted here that the same amount of enhancement is achieved by the 5th harmonic injection in a five-phase voltage source inverter [7.4]. The output voltage reference is given as:

$$v_{oa}^{*}=\sqrt{\frac{2}{5}}qV_{in-rms}\cos(\omega_o t)-\phi(t)$$
$$v_{ob}^{*}=\sqrt{\frac{2}{5}}qV_{in-rms}\cos\left(\omega_o t-2\frac{\pi}{5}\right)-\phi(t)$$
$$v_{oc}^{*}=\sqrt{\frac{2}{5}}qV_{in-rms}\cos\left(\omega_o t-4\frac{\pi}{5}\right)-\phi(t) \tag{7.9}$$
$$v_{od}^{*}=\sqrt{\frac{2}{5}}qV_{in-rms}\cos\left(\omega_o t+4\frac{\pi}{5}\right)-\phi(t)$$
$$v_{oe}^{*}=\sqrt{\frac{2}{5}}qV_{in-rms}\cos\left(\omega_o t+2\frac{\pi}{5}\right)-\phi(t)$$

The output reference is now the sum of the fundamental and the 3^{rd} and 5^{th} harmonic components, where the sinusoidal output references ride on a common mode voltage $\phi(t)$, which is:

$$\phi(t)=\frac{\sqrt{6}}{12}V_{in-rms}\cos(3\omega_i t)+\frac{\sqrt{6}}{48.5}qV_{in-rms}\cos(5\omega_o t) \tag{7.10}$$

The ω_i,ω_o are the input and output frequencies, respectively. The implementation block diagram of the proposed method of the PWM is shown in Fig. 7.13. The input and output references, along with their common mode voltages and the relative magnitude of the input voltages, are fed to the 'duty ratio calculation' block.

The outputs $(D_{ax},D_{bx},D_{cx},D_{dx},D_{ex},x=1\,or\,2)$ are compared with a high frequency carrier signal to generate the output voltage pattern. The gate signals are then derived directly from the generated output voltage patterns.

The simulation is carried out for the reference voltage generation using harmonic injection. The parameters used in the model are: input frequency = 50 Hz; output frequency = 25 Hz; Load resistance=10 Ω; Load inductance=1 mH; Filter inductance=500 µH; Filter Capacitance=50 µF; Carrier frequency=10 KHz; $V_{in-rms}=100$ V $V_{\text{in-rms}} = 100\text{V}$. The simulation results are provided for the maximum input to output voltage ratio of 78.8%. The resulting input and output waveforms are illustrated in Figs. 7.14 and 7.15, respectively. Output and input voltages are also depicted on the same plot shown in Fig. 7.16 to show the maximum achievable output voltage.

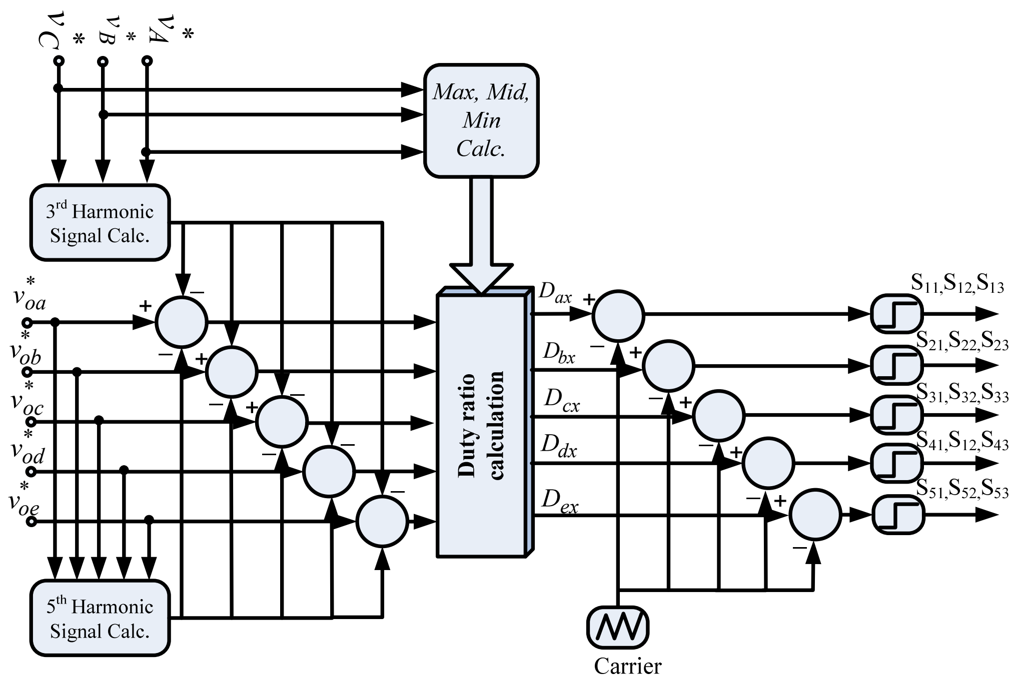

Fig. 7.13. Modulation Implementation block using harmonic injection.

The unity power factor of the input current is evident from the Fig. 7.14a, and this can be controlled independently of the load power factor. The input current remains sinusoidal with magnitude of 10.05 Amp, as seen from Figs. 7.14b and 7.14c. The THD in the input current is limited to 1.08% and is slightly better than the previous case without harmonic injection in the target output. The input current is slightly increased when compared to the previous case due to the higher output voltage of the Matrix Converter and is reflected at the input side as well.

The output voltage magnitude is increased when compared to output of modulation without harmonic injection, preserving its sinusoidal nature. The output voltage spectrum is completely sinusoidal. The locus of the output current remains entirely on the *α*-*β* axis and the *x*-*y* components are almost negligible. This proves the effectiveness of the modulation scheme in eliminating the unwanted low-order harmonics. Once again it is seen that the proposed Matrix Converter is capable of producing the output of any frequency and magnitude from zero to 78.86% of the input.

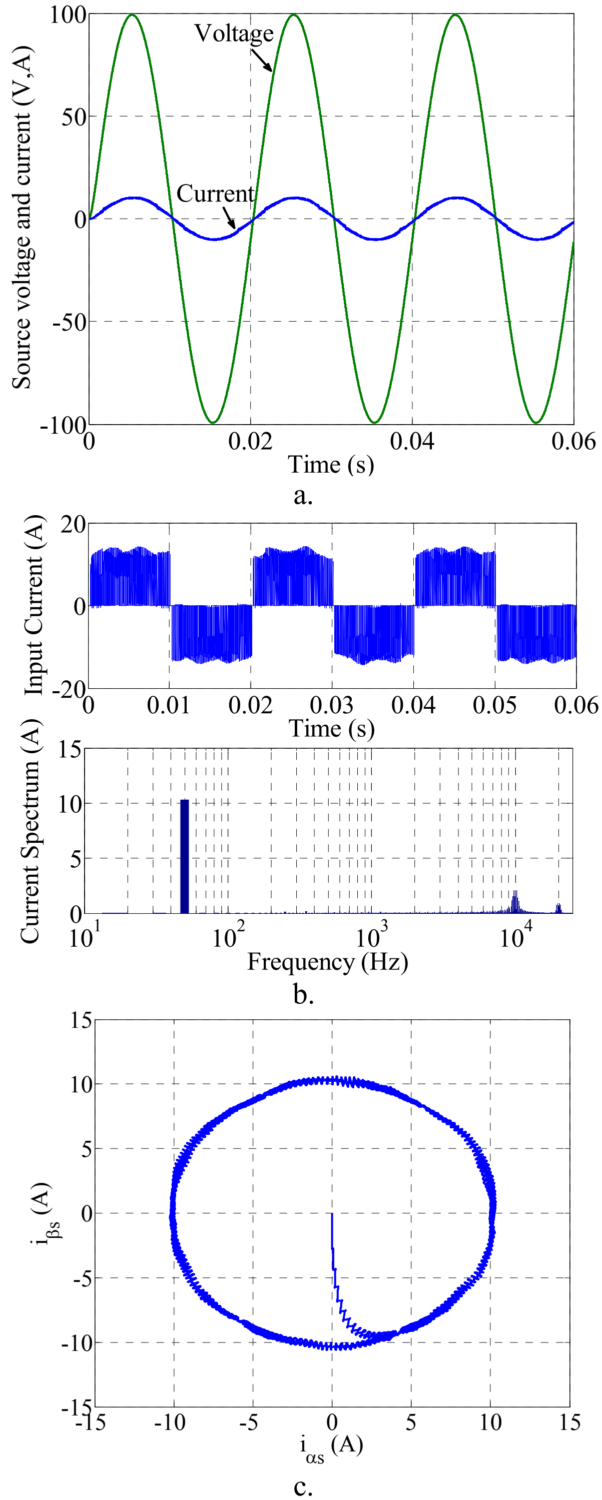

Fig. 7.14. Input side waveforms of 3 to 5-phase Matrix Converter: a. Input voltage and current, b. Spectrum input current, c. Input phase current locus.

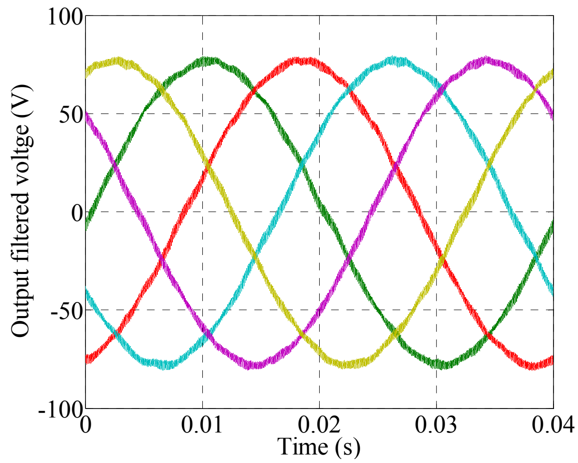
100
50
0
-50
-100
0
0.01
0.02
0.03
0.04
Output filtered voltge (V)
Time (s)
a.

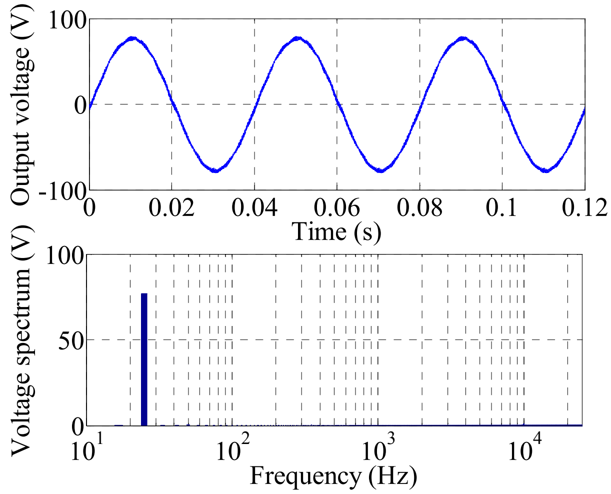
100
0
-100
0
0.02
0.04
0.06
0.08
0.1
0.12
Output voltage (V)
Time (s)
100
50
0
10^1
10^2
10^3
10^4
Voltage spectrum (V)
Frequency (Hz)
b.

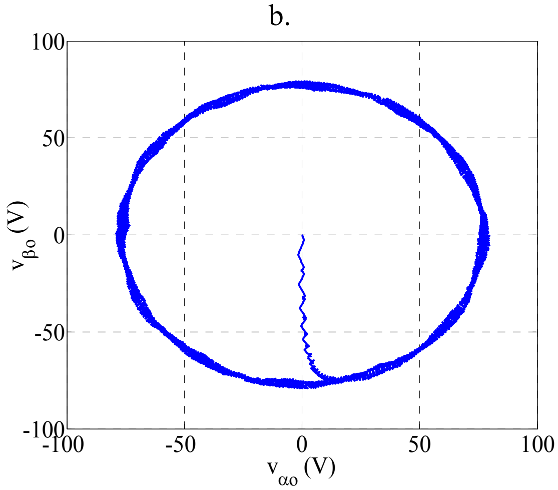
100
50
0
-50
-100
-100
-50
0
50
100
$v_{\beta o}$ (V)
$v_{\alpha o}$ (V)
c.

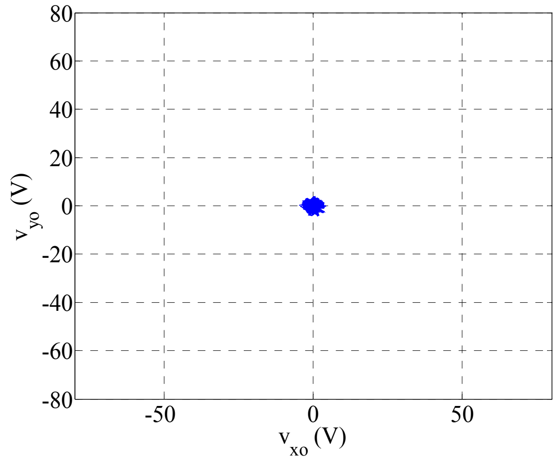

d.

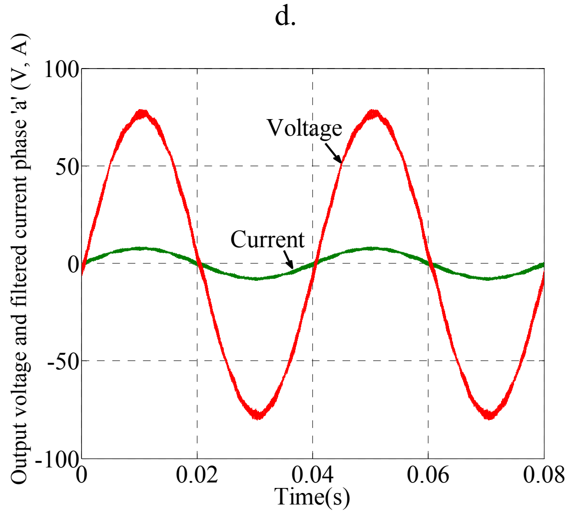

e.

Fig. 7.15. Output waveforms of 3 to 5-phase Matrix Converter: a. Five-phase output filtered voltages, b. Spectrum output voltage, c. locus of *α-β* axis output voltage, d. locus of *x-y* axis output voltage and e. Phase 'a' voltage and current.

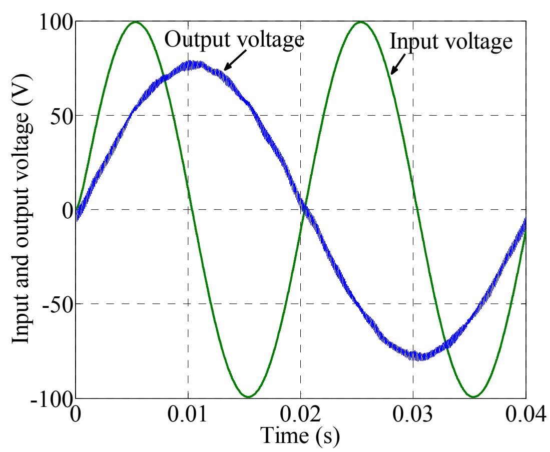

Fig. 7.16. Input and output voltage waveforms for a 3 to 5-phase Matrix Converter with harmonic injection.

7.4 DDPWM of three-to-fivephase Matrix Converters for five-phase two-motor drive

The direct duty ratio based PWM (DDPWM) technique for multi-phase Matrix Converter is elaborated in the Section 7.2 that is applicable to single-motor drive system (produces one fundamental frequency component, that can control one machine/load). For controlling two machines supplied by only one Matrix Converter, the output of the Matrix Converter should contain two fundamental frequencies.

As discussed in Section 7.2, two different cases can arise in time period T_2 depending upon the relative magnitude of the input voltages. If (*Max-Mid)* > (*Med-Min)*, the output should follow *Max* for a certain time period and then follow *Med* for ascertain time period. This situation is termed as Case I. Similarly, if (*Max-Med)* < (*Med-Min)*, the output should follow at first *Med* of the input signal and then *Min* of the input signal; this is termed as Case II. Thus the DDPWM approach uses two out of the three line-to-line input voltages to synthesise output voltages, and all the three input phases are utilized to conduct current during each switching period.

The duty ratio obtained for case I is:

$$D_{k1} = \frac{Max\{v_A, v_B, v_C\} - v_{ok}^*}{\Delta + \delta\left(Med\{v_A, v_B, v_C\} - Min\{v_A, v_B, v_C\}\right)} \tag{7.11}$$

where $\Delta = \left(Max\{v_A, v_B, v_C\} - Med\{v_A, v_B, v_C\}\right)$

The duty ratio obtained for case II is:

$$D_{K2} = \frac{\delta.\Delta + \left(Med\{v_A, v_B, v_C\} - v_{ok}^*\right)}{\delta.\Delta + \left(Med\{v_A, v_B, v_C\} - Min\{v_A, v_B, v_C\}\right)} \tag{7.12}$$

Depending upon the output pattern, the gating signals are derived. If the output pattern of phase "*k*" is *Max* (or *Med*, *Min*), then the output phase "*k*" is connected to the input phase whose voltage is *Max* (or *Med*, *Min*). The only difference between single-motor drive and two-motor drive is the generation of reference output voltage v_{ok}^*. The output voltage reference in case of two-motor drive is the sum of the individual five-phase voltage references corresponding to the operating conditions of the two motors and summed according to the phase transposition rule as discussed in Chapter 3.

The PWM algorithm can be explained by the block diagram given in Fig. 7.17.

The input voltages are at first examined for their relative magnitudes and the phases with maximum, medium, and minimum values are determined. The information about their relative magnitudes are given in the next computation block along with the commanded output phase voltages. The computation block generate the duty ratios depending upon the relative magnitude of the input voltages. The duty ratio obtained goes to the PWM block. The PWM block calculates the time sub-interval using equation (7.1). The gating pattern is then derived accordingly and given to the Matrix Converter.

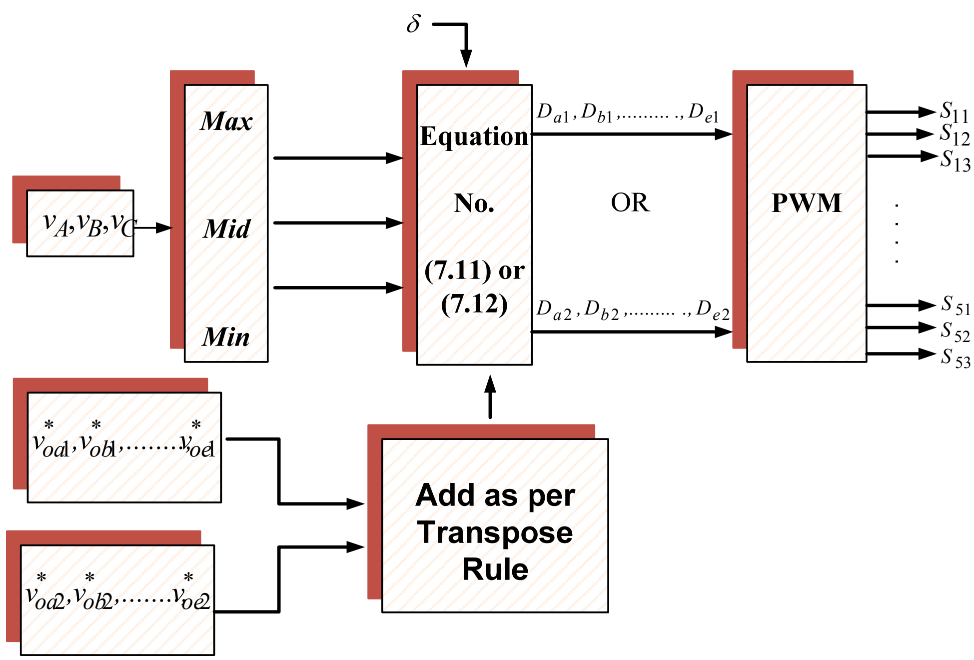

Fig. 7.17 General Implementation diagram of 3 to 5phase Matrix Converter.

In the case of multi-phase voltage source inverter, a concept of the n^{th} harmonic injection was proposed in reference [7.4] for enhancement of the modulation index. It was shown that by injecting n^{th} harmonic of magnitude $M_n = -M_1 \sin\left(\frac{\pi}{2n}\right)/n$, where n is the number of phases, the output voltage increases by $1/\cos\left(\frac{\pi}{2n}\right)$. A similar approach is thus used in this thesis to enhance the output voltage magnitude. Overall block schematic of the PWM for two-motor drive system is presented in Fig. 7.18.

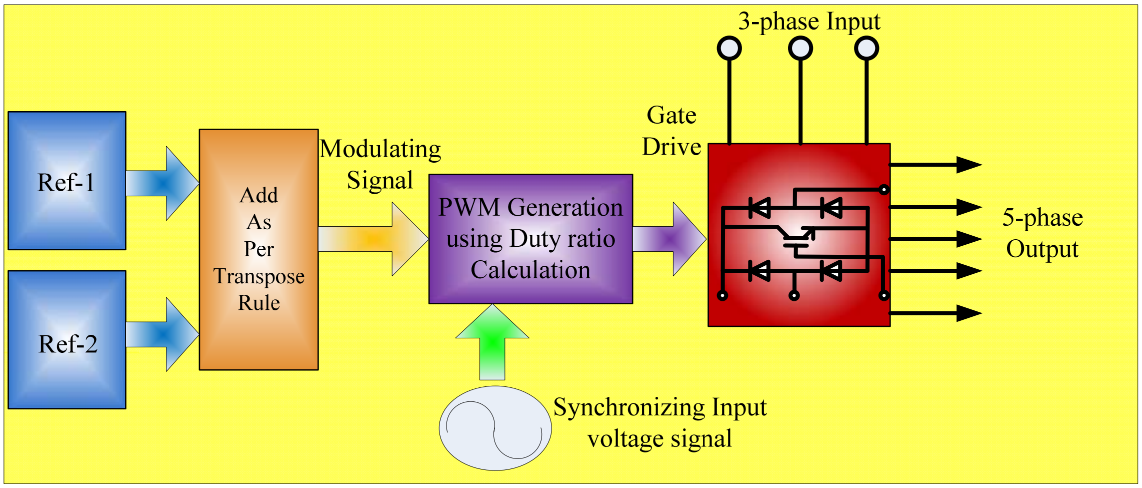

Fig. 7.18. General Block diagram of PWM for two frequency output.

It is observed that by injecting only 3rd harmonic the output becomes 0.75 of the input. Now in case of three to five-phase Matrix Converter, 3rd harmonic of output cannot be injected hence 5th harmonic of the output frequency is injected. For two frequency output, the injection for both input and output frequency should be proportionally distributed among the two output frequencies term according to *v/f* control scheme. The output voltage magnitude reaches 0.7886 of the input voltage magnitude by injecting both 3rd and 5th harmonic. Thus the overall gain in the output is 5.15% similar to that of in the reference [7.3]. It is to be noted here that the same amount of enhancement is achieved by 5th harmonic injection in a five-phase voltage source inverter. The output voltage reference for the two frequency output is give as:

$$
\begin{aligned}
v_{oa}^{*} &= \sqrt{\frac{2}{5}}\frac{q}{3}V_{in-rms}\cos(\omega_o t)-\phi_1(t)+\sqrt{\frac{2}{5}}\left(\frac{2*q}{3}\right)V_{in-rms}\cos(2*\omega_o t)-\phi_2(t)\\
v_{ob}^{*} &= \sqrt{\frac{2}{5}}\frac{q}{3}V_{in-rms}\cos\left(\omega_o t-2\frac{\pi}{5}\right)-\phi_1(t)+\sqrt{\frac{2}{5}}\left(\frac{2*q}{3}\right)V_{in-rms}\cos\left(2*\omega_o t-2\frac{\pi}{5}\right)-\phi_2(t)\\
v_{oc}^{*} &= \sqrt{\frac{2}{5}}\frac{q}{3}V_{in-rms}\cos\left(\omega_o t-4\frac{\pi}{5}\right)-\phi_1(t)+\sqrt{\frac{2}{5}}\left(\frac{2*q}{3}\right)V_{in-rms}\cos\left(2*\omega_o t-4\frac{\pi}{5}\right)-\phi_2(t)\\
v_{od}^{*} &= \sqrt{\frac{2}{5}}\frac{q}{3}V_{in-rms}\cos\left(\omega_o t+4\frac{\pi}{5}\right)-\phi_1(t)+\sqrt{\frac{2}{5}}\left(\frac{2*q}{3}\right)V_{in-rms}\cos\left(2*\omega_o t+4\frac{\pi}{5}\right)-\phi_2(t)\\
v_{oe}^{*} &= \sqrt{\frac{2}{5}}\frac{q}{3}V_{in-rms}\cos\left(\omega_o t+2\frac{\pi}{5}\right)-\phi_1(t)+\sqrt{\frac{2}{5}}\left(\frac{2*q}{3}\right)V_{in-rms}\cos\left(2*\omega_o t+2\frac{\pi}{5}\right)-\phi_2(t)
\end{aligned}
\tag{7.13}
$$

The sinusoidal output references ride on a common mode voltage $\phi_1(t)$ and $\phi_2(t)$, which are:

$$
h(t) = -\frac{\sqrt{6}}{12}V_{s\text{-}rms}.\sin(6\pi f_i t) - \frac{\sqrt{6}}{48.5}.q.V_{s\text{-}rms}.\sin(10\pi f_o t)
$$

$$\phi_2(t)=\frac{\sqrt{6}}{24}V_{in-rms}\cos(3\omega_i t)+\frac{\sqrt{6}}{48.5}\left(\frac{2*q}{3}\right)V_{in-rms}\cos(5*2*\omega_o t) \tag{7.14}$$

The first term of equation (7.14) is related to the input side and the second term is for the output side.

7.5 Simulation Results for Two-motor drive system

MATLAB/SIMULINK model is developed for the proposed Matrix Converter control. The input voltage is fixed at 100 V to show the exact gain at the output side. The switching frequency of the devices is kept at 10 kHz., Load resistance = 4 Ω; Load inductance =1 mH; Filter inductance = 500 μH; Filter Capacitance = 50 μF.

The input is three phase ac source and the output is five phase. The output is a combination of two frequencies controlled by the direct duty ratio PWM scheme. The output loads are connected in series with phase transposition so that the *d-q* and *x-y* components of the output five phases can be utilized. DDPWM scheme needs the reference values of input three phases and output five phases. Time is given as the third input for the direct duty ratio PWM block sub system.

The purpose here is to show two decoupled fundamental components of voltages produced by the Matrix Converter. The load to the Matrix Converter can be two series/parallel-connected five-phase machines. These voltage components produced by the Matrix Converter are decoupled from each other and thus can independently control the two machines. The results shown here is only limited to the production of the appropriate voltage components. The motor behaviour is not discussed in this thesis. It is assumed that one voltage component has frequency of 25 Hz (750 rpm of the motor) and second voltage component has 50 Hz (1500 rpm of the motor). To respect the *v/f* = constant control the voltage magnitude of the lower frequency component is half compared to the higher frequency component. Simulation results are shown for the modulation with common mode voltage addition in the output target voltage to obtain the maximum possible voltage at the output of the Matrix Converter. Thus the maximum output of the Matrix Converter is limited to 78.8 V as the input is 100 V. Two voltage references are generated corresponding to the two operating speeds of the motors (25 Hz and 50 Hz in this case) and are added as per the transposition rule. The voltage references thus generated are the modulating signals. The duty ratios are then calculated and used further to generate the switching signals for the bi-directional power switches of the Matrix Converter.

The resulting waveforms are presented in Figs. 7.19 to 7.21. The input source side (at the three-phase supply) and converter side (Matrix Converter input side after the filter) waveforms are presented in Fig. 7.19. The results clearly show unity power factor at the input side. The converter side current shows PWM signals while the source side currents are sinusoidal. Thus the input filter design is satisfactory to eliminate the switching harmonics from the PWM signals. The lower-order harmonics are not present in the converter side or source side currents. This is the special feature of the Matrix Converter as the input currents from the source are sinusoidal.

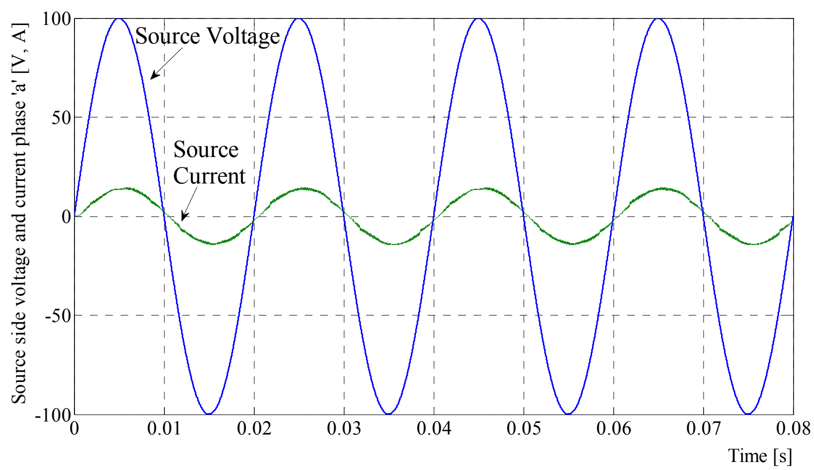

a.

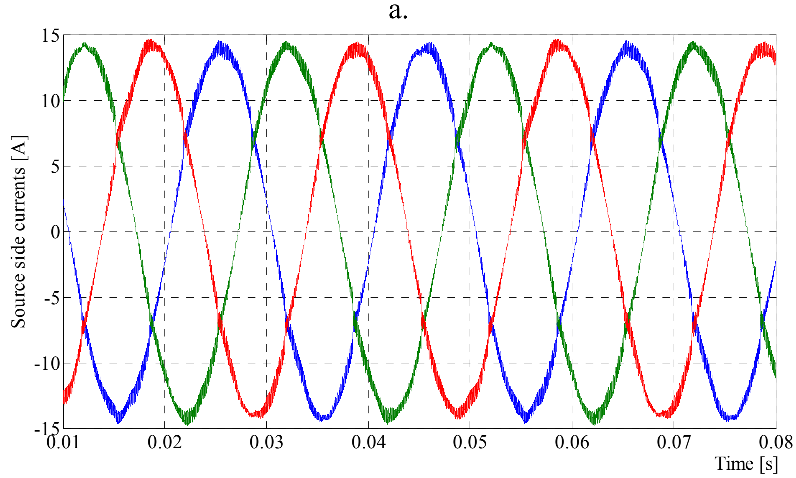

b.

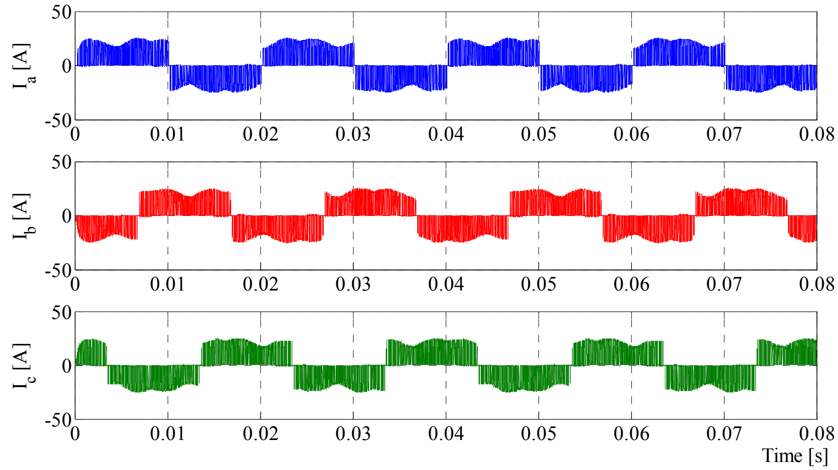

c.

Fig. 7.19. The input side waveforms; a. source side voltage and current for phase 'a', b. source side three-phase currents, c. converter side three-phase currents.

The output side waveforms are depicted in Fig. 7.20a and the spectrums are shown in Fig. 7.20b. Two system of line voltages exist in a five-phase system adjacent line voltages (V_{ab}, V_{bc}, V_{cd}, V_{de}) and non-adjacent voltages (V_{ac}, V_{bd}, V_{ce}, V_{db}). One phase voltage, V_a, one adjacent line voltage, V_{ab} and one non-adjacent line voltage V_{ac} are depicted in Fig. 7.20a. The filtered five-phase voltages are presented in Fig. 7.20b, that shows the combination of fundamental and its second harmonic voltages. The output inverter currents are presented in Fig. 7.20c that also shows two components.

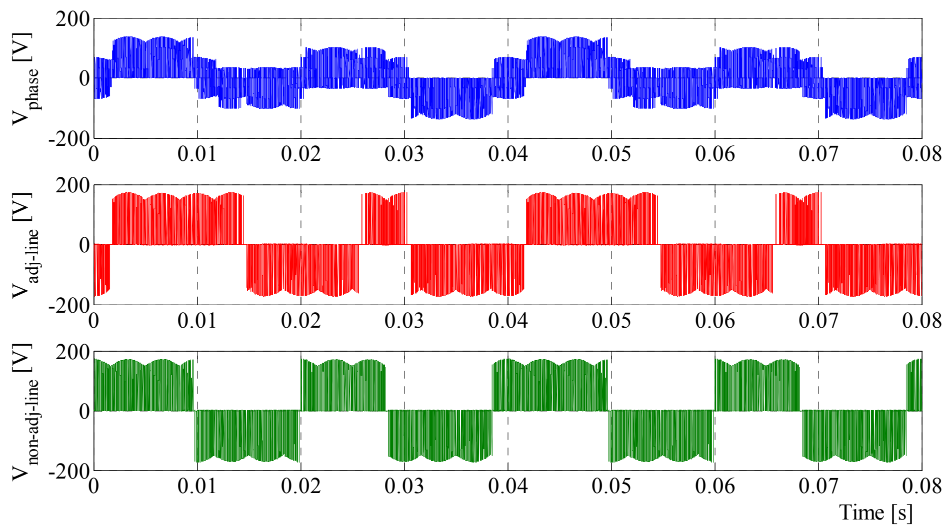

a.

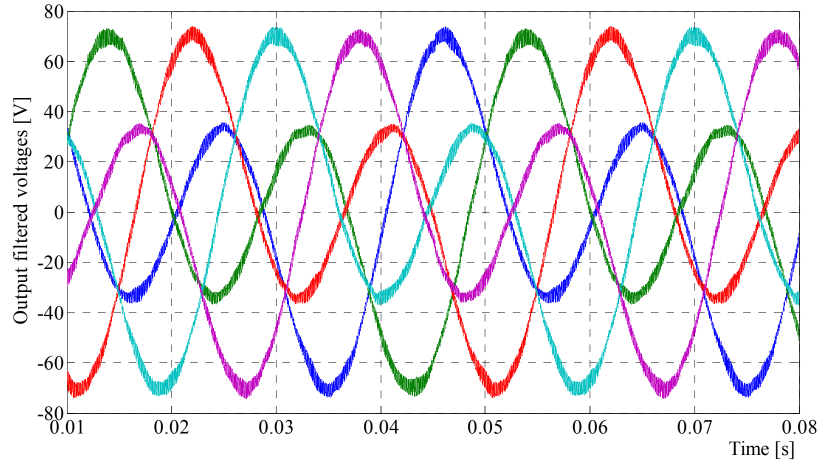

b.

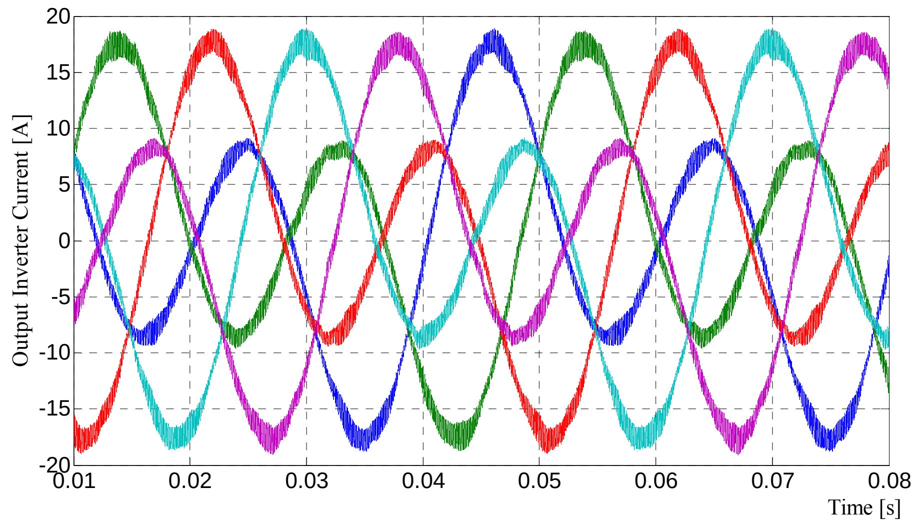

c.

Fig. 7.20. The output side waveform; a. Phase, adjacent and non-adjacent voltages, b. filtered output phase voltages, c. five-phase inverter currents.

The output filtered phase voltage of the Matrix Converter is transformed in the stationary reference frame into two orthogonal components namely $V_{\alpha\beta}$ and V_{xy} and are shown in Fig. 7.21. The $V_{\alpha\beta}$ components control one machine which operates at 25 Hz and the other components V_{xy} control the other machine that operate at 50 Hz. The peak voltage of the $V_{\alpha\beta}$ component is half that of the V_{xy} component as the frequency of operation is half and thus *v/f* = constant principle is maintained. It is evident that both the componens of voltages are independent and sinuosoidal.

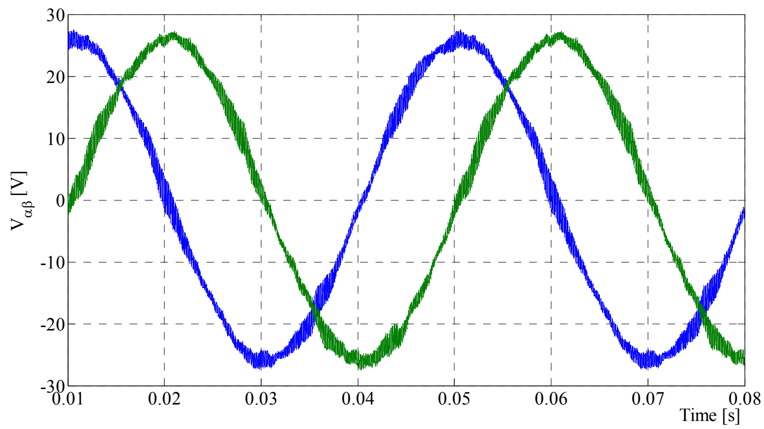

a.

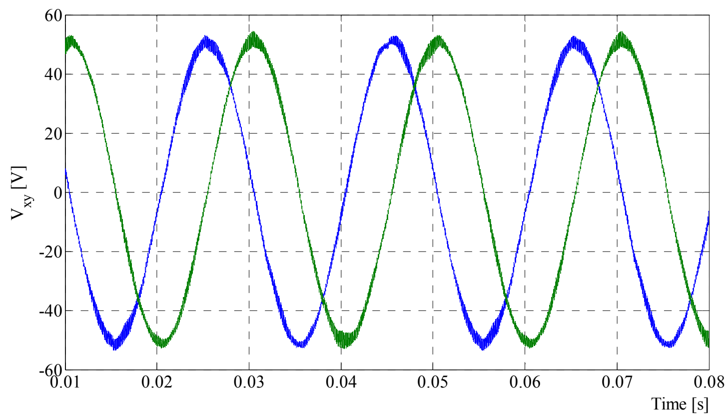

b.

Fig. 7.21. The transformed voltage of the output phase voltages: a. and b. V_{xy}.

The FFT analyis is further carried out for the phase voltage and the transformed voltages to prove the decoupled components of the voltages. The resulting time domain and frequency domain voltages are depicted in Fig. 7.22. The phase 'a' voltage shows two component of voltages at the fundamental frequencies of 25 Hz and 50 Hz. The 25 Hz component is taken as the first fundamental voltage and has 100% magnitude of 25.9 V, while the 50 Hz component shows the magnitude of 200% i.e. 25.9 x 2 = 51.8 V. The sum of these two voltages are (51.8 + 25.9 = 77.7 V) which is slighlty smaller than the therotecial value of 78.7 V and this is due to the numerical error in the computation and the sampling time of the simulation model. The transformed voltage are further shown in Figs. 7.22b and 7.22c and these two components shows peaks at 25 Hz and 50 Hz. Hence, it is evident that the two components are independent of each other and will subsequently control the two machines independently. Thus the proposed PWM control of the Matrix Converter succefully produces two independent voltage components.

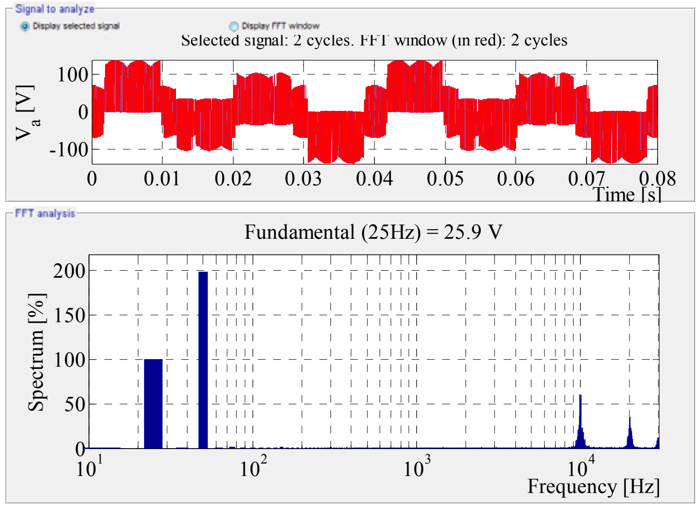

a.

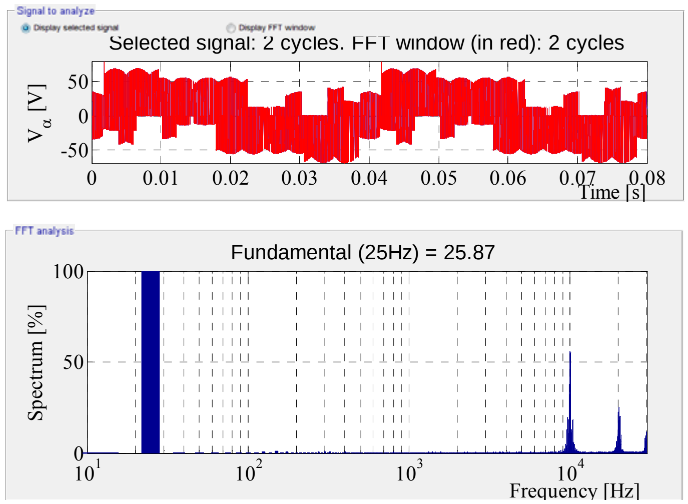

b.

c.

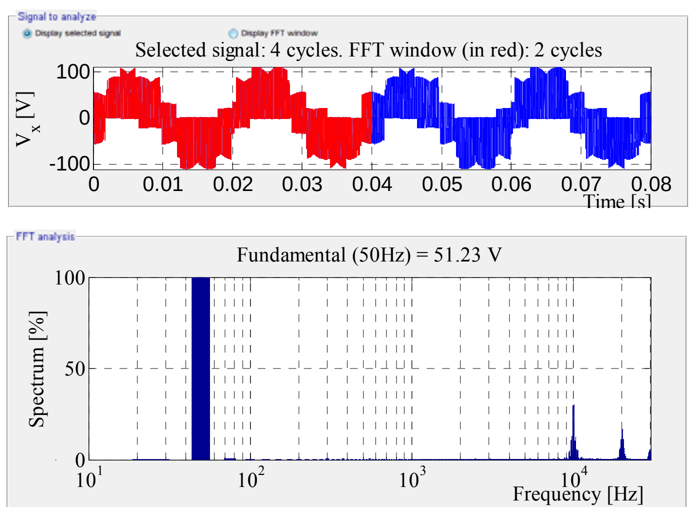

Fig. 7.22**.** Time domain and frequency domain waveforms: a. Phase 'a' voltage, b.   voltage and c. V_x voltage**.**

The output side filtered voltages are given in Fig. 7.19 and the spectrum of the output PWM signal voltages are presented in Fig.7.21. The output filtered phase voltages shows superimposed fundamental and second harmonic components. The spectrum of phase 'A' voltage and the transformed voltage are given in Fig. 7.21. It is clearly evident that the phase 'A' voltage contains two fundamental components at 25 Hz and 50 Hz. These voltages are then decoupled and appear in α-β plane (50 Hz) and x-y plane (25 Hz). Thus the aim of the control is achieved. Also the magnitude of the two voltages follows *v/f* = constant rule.

7.6 Experimental Results

The Matrix Converter is connected to a five-phase R-L load and input voltage of 200 V is supplied. The output of the Matrix Converter contains two frequency components, one with 50 Hz and one with 25 Hz. One output voltage frequency component is intended to control one machine and the second frequency component will control the second machine. The experimental results is intended to show the successful generation of two decoupled frequency component at the output of the Matrix Converter. The obtained results matches very closely the simulation results. The experimental results are shown in figs.7.23-7.24

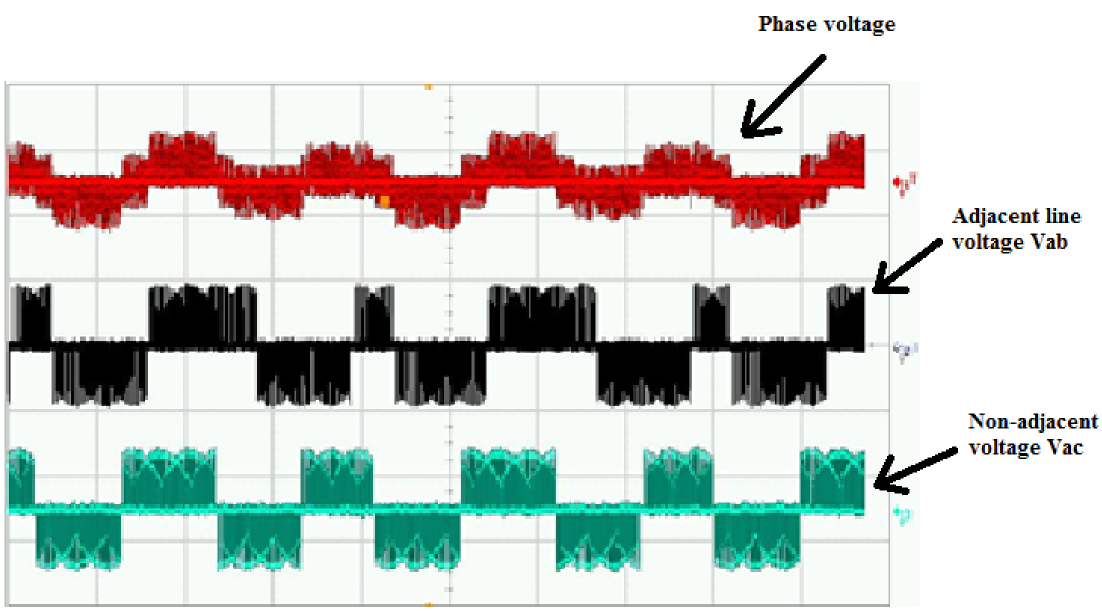

Fig. 7.23a . Experimental results: tope trace, phase Voltage, middle trace adjacent line Voltage, and the bottom trace, non-adjacent line Voltage (y-axis: 200V/div, x-axis: 10 msec/div).

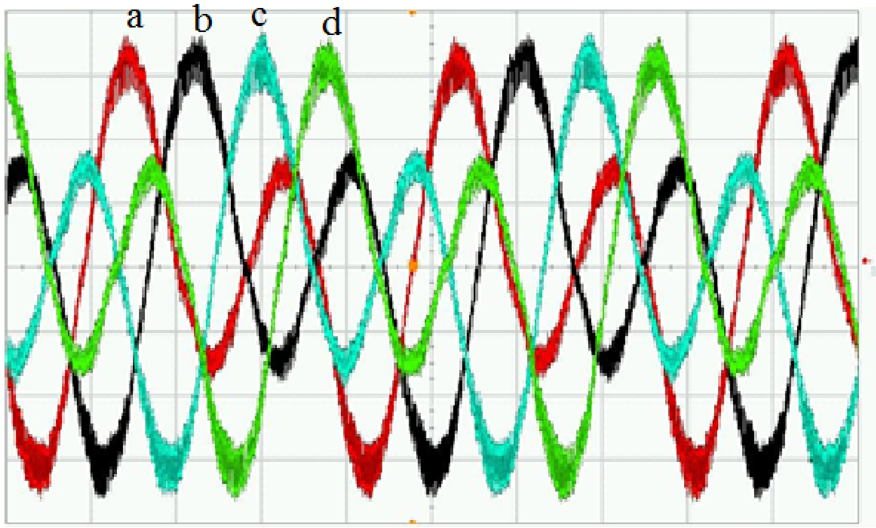

Fig. 7.23b. Experimental results: output currents, (y-axis 4 amp/div, x-axis: 10 msec/div)

7.7 Summary

This chapter present direct duty ratio based PWM for a three-phase to five-phase Matrix Converter supplying series-connected/parallel-connected five-phase two-motor drive system. The presented PWM is different from carrier-based and space vector methods. The presented scheme is modular in nature and can be applied to any number of output phases of Matrix Converter. The output limit is same as that of obtainable using carrier-based and space vector PWMs. However, the simplicity of approach is the major attraction of direct duty ratio based PWM methods.

References

[7.1] Yulong Li, Nam-Sup Choi, Byung-Moon Han, Kyung Min Kim, Buhm Lee and Jun-Hyub Park, "Direct duty ratio pulse width modulation method for Matrix Converter," Int. Journal of Control Automation and Systems, vol. 6, no. 5, pp. 660-669, Oct. 2008.

[7.2] A. Iqbal, Sk. M. Ahmad, H. Abu-Rub and M.R. Khan, "Carrier based PWM technique for a novel three-to-five phase Matrix Converter," Proc. European PCIM, CD-Rom paper no. 173, 2-6 May Nuremberg, Germany, 2010.

[7.3] M.P. Kazmierkowaski, R. Krishnan and F. Blaabjerg, "*Control in Power Electronics-Selected problems,*" Academic Press, USA, 2002.

[7.4] A. Iqbal, E. Levi, M. Jones, S.N. Vukosavic, "Generalised Sinusoidal PWM with harmonic injection for multi-phase VSIs," IEEE 37th Power Electronics Specialist conf. (PESC) Jeju, Korea, 2006, CD_ROM paper No. ThB2-3, pp. 2871-2877, 2006.

[7.5] B. Wang, G. Venkataramanan, "A carrier-based PWM algorithm for indirect Matrix Converters," in Proc. IEEE-PESC 2006, pp. 2780–2787, 2006.

Chapter 8
Conclusions and Future Work

8.1 Conclusions

Research on variable speed multi-phase motor drive systems has seen a significant growth in recent years. The main driving force behind the accelerated research input is the advent of cheap and reliable semiconductor power switching devices and fast and efficient Digital Signal Processors/Field programmable gate arrays/Microcontroller/Embedded controllers etc. Thus more complex control algorithm can be implemented in real time more efficiently. The development in power electronic converter technology has also enabled the number of phases to be considered as an additional design parameter. Multi-phase (more than three phases) machines offer some major advantages over three-phase ones, such as reduced torque pulsation and pulsation at higher frequency, higher fault tolerance, lower per-phase power handling requirements, enhanced modularity, lower DC link harmonics and improved noise characteristics. In spite, notable advantages of multi-phase machines, 'off the shelf availability' of three-phase machines still limits the application of multi-phase machine to specialized applications, for which three-phase drives are either not readily available or do not satisfy the specification. One of the important application areas due to the high fault tolerance of multi-phase drives, is in aerospace, predominantly in conjunction with multi-phase Permanent Magnet machines. Applications of multi-phase machines in electric and hybrid electric vehicles for propulsion and power steering are also feasible. Ship propulsion is considered as one of the main areas of application formulation-phase drives. Multi-phase Wind turbine generators are also considered for remote offshore applications especially using six-phase configuration. The multi-phase output generated by wind generator is rectified to DC and the power is transferred to shore using HVDC.

Multi-motor drive system (series-connected/parallel-connected) supplied by a single power converter is an attractive features of multi-phase system. Stator windings of two or more machines (depending upon the number of phases) can be connected in series/parallel and supplied by one variable voltage and variable frequency source and controlled using field oriented control principle, can independently control the machines. The major advantage of this drive configuration is the saving in the number of converter legs. The major application areas for multi-motor drive system could be in ship propulsion (main propeller and auxiliary functions), mining (due to space restriction), winder application (two machines runs to wind and unwind finished product) etc.

The multi-phase multi-motor drive system is readily supplied by current controlled pulse width modulated inverters. In this thesis, alternative power supply solution is explored and a direct Matrix Converter is considered.

This thesis is thus aimed at development of modeling and control algorithms for multi-phase direct Matrix Converter. The Matrix Converter topology investigated in this thesis has three-phase input and multi-phase output. The most common power converter supplying a multi-phase motor drive for variable speed applications is a voltage source inverter. However, the major drawback of a voltage source inverter is the presence of bulky DC link capacitors. Further, the quality of source side current (utility grid side) in terms of high total harmonic distortion is poor, due to presence of diode based rectifier at the front end. Moreover, the power factor at the source side in not controllable. The alternative to this topology is voltage source inverter with active front end rectifier, also called back-to-back converter. This topology offers controllable source side power factor, bi-directional power flow and sinusoidal source side (utility grid side) current. However, the DC link capacitor is unavoidable which add to the cost and volume. An alternative topology is a Matrix Converter.

In a general case, a Matrix Converter can be viewed as an array of $n \times k$ bi-directional power semiconductor switches that are able to transform n-phase input voltages into k-phase output voltages of variable magnitude, phase and frequency. The circuit configuration, typically has no energy storage element and eliminate the need of a DC-link circuit. The input side of the Matrix Converter is considered as voltage fed, while the output is a current fed system. For this reason a capacitive filter on the input and an inductive one on the output are necessary. The size of the filter is significantly lower in comparison to the equivalent voltage source inverter.

Since space vector approach offers more generic method of modeling, it is adopted in the thesis for modeling a five-phase, six-phase and a seven-phase direct Matrix Converter. This is followed by development of various control algorithms. For the considered 3-phase (input) to k-phase (output) configuration, the theoretical number of switching states amounts to $2^{3 \cdot k}$, out of which some are not useful for implementing modulation algorithms. Considering the nature of the two sides of the converter, the constraints are that two phases of the input should never be short circuited and the output current should not be interrupted. As a result, exactly one switch should conduct in each output phase in every instant. This makes the number of usable switching states 3^k. The complete set of switching states and usable vectors are given in the thesis.

In case of a voltage source inverter, the output voltage level is fixed such as 2-level, 3-level etc. However, in case of a Matrix Converter, the number of output voltage level can be of any value by using any of the values of the voltages of the input 3 phases. The result is a complex switching logic in a Matrix Converter, however, the availability of desired voltage level at the output side is a significant advantage of a Matrix Converter. The basic operating principle of a Matrix Converter, is to piece together an output voltage waveform with the desired fundamental component from selected segments of the input voltage waveforms. For safe operation of a Matrix Converter, an adequate clamping circuit is usually added to it that allow output current free-wheeling path. This clamping circuit usually incorporates a capacitance which is significantly smaller than the one used in counterpart Voltage Source Inverters.

The multi-phase Matrix Converters (multi-phase refers to three-phase input and more than three-phase output) use the same bi-directional power semiconductor switching device and apply the same switching strategies as in the three-phase case. Multi-phase Matrix Converters represent a significant challenge when developing suitable modulation methods. This challenge is even more pronounced than in the case of the multi-phase VSIs, due to the higher number of possible switching states in Matrix Converters.

The modulation strategies considered in this thesis are;

- Carrier-based PWM, and
- Direct-duty ration based PWM

Carrier-based modulation methods, have been used for three-to-five, three-to-six and three-to-seven phase topologies in. The duty ratios obtained using analytical method represent sinusoidal functions, similar to the coefficients of a rotational transformation to the synchronous reference frame, allowing the resulting voltage to be independent of the three-phase supply frequency. This is a critical requirement of modulation of a Matrix Converter using carrier-based scheme. The change of the phase shift and magnitudes of these coefficients results in the alteration of the phase shift and magnitude of the output voltages. Thus the carrier-based PWM scheme used to independently control multi-phase multi-motor drive system (five-phase, six-phase and seven-phase) can effectively control the series/parallel-connected machines. The source side current is sinusoidal with controllable power factor.

In direct duty ratio based PWM, duty ratios is calculated for each switch, and is compared to a carrier signal. It applies to each output phase independently and therefore, can be used to supply multi-phase loads. The input number of phases is restricted to three, since the modulation requires identification of the values of the input voltages as the highest, medium and the lowest. Once again independence of control is achieved for a five-phase series/parallel-connected two-motor drive system. The source side current is sinusoidal with unity power factor. The output voltage shows two fundamental frequencies that are used to control two machines independently. This is a modular approach and can be used for any number of phases. By changing the slope of carrier the power factor of the source can be varied.

The voltage transfer ratio between the output voltage to input voltage magnitude for different phase numbers is obtained as (first column given the number of input phase number which is 3 and the second to 5th column shows the output phase number);

Input phase/Output phase	3	5	6	7
3	86.6%	78.8%	75%	76.9%

It is observed that the output voltage magnitude reduces as the number of output phases increases. In case of series/parallel-connected multi-phase multi-motor drive system, this voltage has to be appropriately distributed among different machines. Since the output of a Matrix Converter voltage is lower, supplying more than one machine, is difficult and voltage reserve issue may arise. Either using lower rated voltage machines or using boost in the Matrix Converter (AC chopper) is seen as possible solution. However, this is not considered in the thesis. The major aim of the thesis is to investigate the possibility of generating more than one independent fundamental frequency components and this is successfully achieved.

8.2 Future Work

The work carried out in thesis is limited to the modelling and control of a five-phase, six-phase and seven-phase inverter with resistive (R) and resistive and inductive (R-L) load in open-loop mode. However, there is still a huge scope of further research on this topic. The motor drive supplied using the developed schemes have not yet been taken up. Hence performance evaluation of multi-phase motors fed using multi-phase Matrix Converter with the proposed control algorithms could be a direction of further research.

The multi-phase Matrix Converters provide improvements compared to the three-phase counterparts. In this respect, converters with multi-phase input or output phase number can be considered separately. When the number of input phases is higher than the output, the likely applications would be wind generation interface system. This configuration of Matrix Converter potentially provides higher resolution in the achievement of the output voltage and also a higher achievable output voltage. There exists huge scope in further research in this direction.

However, if the Matrix Converters are considered as multi-level inverters with their DC bus potentials being variable, such a topology can be considered quite promising. This can also be taken up in future research.

The effect of input side disturbances in terms of voltage variation, waveform distortion and change in grid frequency, can be taken up for investigation in future work.

Multi-phase multi-level Matrix Converter can also be investigated and this is a good leading direction of research. Voltage boost using impedance network at the source side or AC chopper at the output side could be considered as a potential direction of research.